

ศิลปวรรณาน่าอ่านและลำดับชั้นหินที่เกี่ยวข้องในบริเวณตอนกลางของแอ่งแม่เมาะ จังหวัดลำปาง



บทคัดย่อและแฟ้มข้อมูลฉบับเต็มของวิทยานิพนธ์ตั้งแต่ปีการศึกษา 2554 ที่ให้บริการในคลังปัญญาจุฬาฯ (CUIR)
เป็นแฟ้มข้อมูลของนิสิตเจ้าของวิทยานิพนธ์ ที่ส่งผ่านทางบัณฑิตวิทยาลัย

The abstract and full text of theses from the academic year 2011 in Chulalongkorn University Intellectual Repository (CUIR)
are the thesis authors' files submitted through the University Graduate School.

วิทยานิพนธ์นี้เป็นส่วนหนึ่งของการศึกษาตามหลักสูตรปริญญาวิทยาศาสตรมหาบัณฑิต
สาขาวิชาธรณีวิทยา ภาควิชาธรณีวิทยา
คณะวิทยาศาสตร์ จุฬาลงกรณ์มหาวิทยาลัย
ปีการศึกษา 2559
ลิขสิทธิ์ของจุฬาลงกรณ์มหาวิทยาลัย

COAL PETROGRAPHY AND ASSOCIATED
STRATIGRAPHY IN CENTRAL PART OF MAE MOH BASIN, CHANGWAT LAMPANG

Miss Kunwatoe Rittidate



A Thesis Submitted in Partial Fulfillment of the Requirements
for the Degree of Master of Science Program in Geology

Department of Geology

Faculty of Science

Chulalongkorn University

Academic Year 2016

Copyright of Chulalongkorn University

Thesis Title	COAL PETROGRAPHY AND ASSOCIATED STRATIGRAPHY IN CENTRAL PART OF MAE MOH BASIN, CHANGWAT LAMPANG
By	Miss Kunwattoo Rittidate
Field of Study	Geology
Thesis Advisor	Associate Professor Punya Charusiri, Ph.D.
Thesis Co-Advisor	Associate Professor Benjavun Ratanasthien, Ph.D.

Accepted by the Faculty of Science, Chulalongkorn University in Partial Fulfillment of the Requirements for the Master's Degree

.....Dean of the Faculty of Science
(Associate Professor Polkit Sangvanich, Ph.D.)

THESIS COMMITTEE

.....Chairman
(Assistant Professor Thasinee Charoentirat, Ph.D.)

.....Thesis Advisor
(Associate Professor Punya Charusiri, Ph.D.)

.....Thesis Co-Advisor
(Associate Professor Benjavun Ratanasthien, Ph.D.)

.....Examiner
(Assistant Professor Vichai Chutakositkanon, Ph.D.)

.....External Examiner
(Pramote Laoprapaipan, Ph.D.)

กุลวธู ฤทธิเดช : ศิลาวรรณนาถ่านหินและลำดับชั้นหินที่เกี่ยวข้องในบริเวณตอนกลางของ
แอ่งแม่เมาะ จังหวัดลำปาง (COAL PETROGRAPHY AND ASSOCIATED
STRATIGRAPHY IN CENTRAL PART OF MAE MOH BASIN, CHANGWAT LAMPANG)
อ.ที่ปรึกษาวิทยานิพนธ์หลัก: รศ. ดร.ปัญญา จารุศิริ, อ.ที่ปรึกษาวิทยานิพนธ์ร่วม: รศ. ดร.
เบ็ญจวรรณ รัตนเสถียร, 178 หน้า.

ถ่านหินทั้ง 35 ตัวอย่าง จากหลุมเจาะสำรวจ 3 หลุมบริเวณตอนกลางของแอ่งแม่เมาะ ได้
ถูกนำมาศึกษาลำดับชั้นหิน ศิลาวรรณนา และธรณีเคมี ลำดับชั้นหินที่ศึกษาอยู่ในกลุ่มหินแม่เมาะ
หมวดหินนาแวม ประกอบด้วยตะกอนละเอียดสีเทาขนาดหินเคลย์และหินเคลย์ปนทรายแป้ง สละสม
ตัวแทรกสลับกับชั้นถ่านหินสีเทาดำถึงดำชั้นหนาถึงบาง เรียงจากด้านล่างขึ้นบน ดังนี้ ถ่านหินชั้น Q
ชั้น K และชั้น J สภาพแวดล้อมการสะสมตัวของหมวดหินชุดนี้ แสดงลักษณะการสะสมแบบ
ทะเลสาบสลับกับป่าพรุ หมวดหินนาแวมปิดทับด้วยหมวดหินห้วยหลวง ตะกอนละเอียดเนื้อหินเคลย์
สีแดงชั้นหนาและพบตะกอนหยาบขนาดหินทราย แทรกเป็นชั้น พบถ่านหินชั้น I สละสมตัวเป็นชั้นบาง
ตะกอนในหมวดหินนี้สละสมตัวโดยได้รับอิทธิพลจากทางน้ำ ศิลาวรรณนาของถ่านหินที่ศึกษาพบ
ปริมาณแร่อินทรีย์ มาซิรอล มากกว่า 70 % และแร่อนินทรีย์น้อยกว่า 30 % โดยมากพบแร่อินทรีย์
กลุ่มฮิวมิไนต์ 43-68% ชนิดเจลลิไนต์ เดนซิไนต์ และเทคโทลูไลไนต์ รองลงมาคือแร่อินทรีย์กลุ่ม
ลิปทิไนต์ 5-30% ชนิดลิบโดเตทริไนต์ สปอริไนต์ คิวติไนต์ อัลจีไนต์ และ เอกซุดาติไนต์ แร่อินทรีย์ใน
กลุ่ม อินเนอร์ติไนต์ ส่วนน้อย 4-15% ชนิด ฟิวซิไนต์ เซมิฟิวซิไนต์ และ สเคอโรติไนต์ แร่อินทรีย์ 8-
30% เป็นไดอะตอมไมต์จำนวนมาก พบแร่ดิน เฟรมบอยดอลไฟไรต์ ซิลิกา คาร์บอนเนต และบางครั้ง
พบแก้วภูเขาไฟ นำปริมาณของแร่อินทรีย์ไปหาค่า TPI (Tissue Preservation Index) และ GI
(Gelification Index) พบว่า TPI มีค่าต่ำ (0.11-0.52) GI ปานกลางถึงสูง (3.67-13.50) เมื่อพลอตลง
ใน Diessel's diagram(1986) ซึ่งแสดงความสัมพันธ์ระหว่างค่า TPI และ GI สามารถบ่งชี้
สภาพแวดล้อมการสะสมตัวของถ่านหิน พบว่าถ่านหินในพื้นที่ศึกษาเกิดในสภาพแวดล้อมแบบ
ทะเลสาบ พีชที่เป็นต้นกำเนิดของถ่านหินเกิดและเติบโตในบึงและป่าพรุ และจากผลการศึกษารณี
เคมีสามารถจำแนกลำดับชั้นการกลายเป็นถ่านหิน ถ่านหินในพื้นที่ศึกษาอยู่ในชั้น ลิกไนต์เอ ถึง ซับปี
ทูนีสปี จัดเป็นถ่านหินชั้นต่ำ คุณภาพไม่ดี เนื่องจากมีปริมาณซัลเฟอร์สูง

ภาควิชา	ธรณีวิทยา	ลายมือชื่อนิสิต
สาขาวิชา	ธรณีวิทยา	ลายมือชื่อ อ.ที่ปรึกษาหลัก
ปีการศึกษา	2559	ลายมือชื่อ อ.ที่ปรึกษาร่วม

5572220423 : MAJOR GEOLOGY

KEYWORDS: COAL PETROGRAPHY / STRATIGRAPHY / MACERAL / LACUSTRINE / SWAMP
/ MAE MOH BASIN / NORTHERN THAILAND

KUNWATOO RITTIDATE: COAL PETROGRAPHY AND ASSOCIATED
STRATIGRAPHY IN CENTRAL PART OF MAE MOH BASIN, CHANGWAT LAMPANG.
ADVISOR: ASSOC. PROF. PUNYA CHARUSIRI, Ph.D., CO-ADVISOR: ASSOC. PROF.
BENJAVUN RATANASTHIEN, Ph.D., 178 pp.

35 coal samples from 3 boreholes in the central part of Mae Moh basin have been investigated for stratigraphy, petrography, and geochemical analyses. Lithostratigraphic of studied boreholes is Na Khaem formation in Mae Moh group, characterized by fine grained sediments with thin to thick coals from bottom to top as Q-, K- and J seams. The Na Khaem formation has been formed by the sedimentation under the alternation of lacustrine and swamp. Na khaem formation is overlaid by Huai Luang formation mainly of fine to coarse grained sediments with thin coal as I seam interbedded, indicated fluvial environment. Detailed petrographic of individual seam reveals the studied coals consist largely of macerals >70% with small amount of inorganic materials <30%. Huminite group (43-68%) is characterized by gelinite, densinite, and some textolinite. Liptinite group (5-30%) is composed of liptodetrinite, sporinite, cutinite, alginite, and exsudatinite. Inertinite group (4-15%) is fusinite, semifusinite and sclerotinite. The inorganic material (8-30%) is characterized by diatomite, clay mineral, framboidal pyrite, silicate, carbonate, and some volcanic ash in place. Mae Moh coals were plotted in the Diessel's diagram (1986) with TPI (Tissue Preservation Index) and GI (Gelification Index) base on maceral assemblage. The results are low TPI values (0.11-0.52) and moderate to high GI value (3.67-13.50); suggesting coals have originated under limnic condition (lacustrine) of peat formation with vegetation characteristics of marsh and wet forest swamp. Based upon the geochemical analyses, the studied coals can be classified as low rank (lignite A to subbituminous B) and low quality due to high ash and sulphur contents.

Department: Geology

Student's Signature

Field of Study: Geology

Advisor's Signature

Academic Year: 2016

Co-Advisor's Signature

ACKNOWLEDGEMENTS

I would like to express my profoundly sincere gratitude and appreciation to my thesis advisor, Associate Professor Dr. Punya Charusiri and thesis co-advisor Associate Professor Dr. Benjavun Ratanasthien for their guidance, encouragement as well as the reading the constructive criticism of the manuscript.

Great thanks to my thesis committee, Dr. Pramote Laoprapaipan, Assistant Professor Dr. Thasinee Charoentitirat and Assistant Professor Dr. Vichai Chutakositkanon for constructive comments and approval of this thesis.

I am highly indebted to the Graduated School of Chulalongkorn University, 90th Year Chulalongkorn Scholarship, for the financial support.

I would also like to acknowledge Department of Geology, Chulalongkorn University and Chiang Mai University for all academic facilities throughout the research. I am grateful to the Mae Moh Mine under Electricity Generating Authority of Thailand (EGAT), for permission to assess some information of the Mae Moh basin and provide other supports. Special recognition and thanks are due to the EGAT managements of Mae Moh Mine, Mr. Pramote Pornrattapitak, Mr. Manote Chuchartvanakul and Mr. Visut Bunthai for their valuable comments. Acknowledgement is also extending to Mr.Pankant Permsook, Head of Drilling Exploration Section for providing core samples and geophysical logging data, Dr.Kanitta Wongyai, Head of Laboratory Section, for geochemistry data acquirement.

Finally, I would like to thank Mr. Niphan Donmuang and Mr. Nattapol Srinak for assistance throughout the preparation of this thesis. They are as the second reader of this thesis, and I am gratefully indebted to them for very valuable comments which are greatly improved the manuscript. No thesis can be completed without the help and encouragement of my parents, friends and Mr. Weerayut Wilaikeaw who put up so much effort to me as well.

CONTENTS

	Page
THAI ABSTRACT	iv
ENGLISH ABSTRACT	v
ACKNOWLEDGEMENTS	vi
CONTENTS	vii
LIST OF TABLES	x
LIST OF FIGURES	xi
Chapter 1.....	1
1. Introduction	1
1.1 The study area.....	3
1.2 Objectives	5
1.3 Scope of work and Methodology	6
1.4 Literature reviews.....	7
Chapter 2.....	11
2. Geologic setting.....	11
2.1 General tectonic setting.....	11
2.2 General structure geology	17
2.3 General stratigraphy.....	19
2.3.1 Triassic Lampang group	19
2.3.2 Mae Moh group	19
2.3.3 Pleistocene - Present	24
Chapter 3.....	27
3. Sample collection and analytical method.....	27

	Page
3.1 Sample collection.....	27
3.1.1 Sample description.....	36
3.2 Analytical method.....	53
3.2.1 Petrographic analysis.....	53
3.2.2 Geochemical analysis.....	55
Chapter 4.....	59
4. Results.....	59
4.1 Lithostratigraphy.....	59
4.1.1 Borehole no. MMC-1.....	60
4.1.2 Borehole no. MMC-2.....	65
4.1.3 Borehole no. MMC-3.....	70
4.2 Geochemical results.....	75
4.3 Petrographic results.....	87
4.3.1 Petrographic determination.....	87
4.3.2 Vitrinite reflectance measurement.....	117
Chapter 5.....	119
5. Discussion.....	119
5.1 Depositional paleo environment.....	119
5.2 Coalification rank.....	133
5.3 Evolution.....	146
Chapter 6.....	153
6. Conclusion.....	153
REFERENCES.....	157

	Page
APPENDIX.....	162
Appendix A.....	163
Appendix B.....	175
VITA.....	178



LIST OF TABLES

Table 4.1 Classification of macerals into subgroups and groups, based on the International Committee for Coal and Organic Petrology (1998 and 2001), the Australian Standard system of nomenclature (AS, 1995), and the American Society for Testing and Materials (ASTM, 1996).....	88
Table 4.2 The average percentage of maceral and mineral matter and calculated facies indices of coals in central part of Mae Moh basin.....	90
Table 5.1 Comparison the vitrinite reflectance measurements between the study coals and oversea coals.....	145



LIST OF FIGURES

Figure 1.1 Index map of Thailand showing location of Mae Moh Mine in northern Thailand (modified from (Map.google.com)).....	2
Figure 1.2 Topographic map showing the shape of Mae Moh basin (modified after(Dame and Moore, 1996))......	4
Figure 1.3 Aerial photo showing the mining area and the study area, located in central part of the Mae Moh basin (modified from (Map.google.com)).....	5
Figure 1.4 Schematic diagram showing sequences of work under this study.....	10
Figure 2.1 Tectonic map of Thailand has been controlled, to some extent, by the interaction of Australia-India, Burma, and the SE Asian plated sine early to middle Tertiary (Charusiri and Pum-Im, 2009).	12
Figure 2.2 The distribution of major Cenozoic basins in Thailand	13
Figure 2.3 Geological map of the Mae Moh region and Mae Moh basin divisible into the western, northern, central and southern subbasins and an intervening central ridge (modified after Dame and Moore,1996).....	15
Figure 2.4 Descriptive symbols of geological map of the Mae Moh region and Mae Moh basin (modified after Dame and Moore,1996).	16
Figure 2.5 Structural map of Mae Moh basin showing North-South trending faults	18
Figure 2.6 Stratigraphy of Mae Moh basin, Lampang province (modified after (Sompong et al., 1996).	26
Figure 3.1 Map of the Mae Moh basin showing location of the study boreholes basin (modified after Dame and Moore, 1996).....	28
Figure 3.2 Descriptive symbols of geological map of the Mae Moh region and Mae Moh basin (modified after Dame and Moore, 1996).	29
Figure 3.3 The geophysical responses of borehole no. MMC-1.....	30
Figure 3.4 The sample descriptions of borehole no. MMC-1.	31

Figure 3.5 The geophysical responses of borehole no. MMC-2.....	32
Figure 3.6 The sample descriptions of borehole no. MMC-2.	33
Figure 3.7 The geophysical responses of borehole no. MMC-3.....	34
Figure 3.8 The sample descriptions of borehole no. MMC-3.	35
Figure 3.9 Sample descriptions of Q seam coal.....	38
Figure 3.10 Sample descriptions of K seam coal.....	39
Figure 3.11 Sample descriptions of J seam coal.....	40
Figure 3.12 Sample descriptions of I seam coal.....	41
Figure 3.13 Mesoscopic of Q4 subseam - grayish black to black, dull, brittle to hard, sub-conchoidal to conchoidal fracture.	42
Figure 3.14 Mesoscopic of Q3 subseam - grayish black to black, dull, brittle to hard, sub-conchoidal to conchoidal fracture and plant remains.....	43
Figure 3.15 Mesoscopic of Q2 subseam - brownish black to grayish black, dull, brittle to slightly hard, sub-conchoidal fracture, claystone fragments, calcareous white spot and plant remains.....	44
Figure 3.16 Mesoscopic of Q1 subseam - grayish black to black, dull to brighten banded, brittle to hard, sub-conchoidal to conchoidal fracture.	45
Figure 3.17 Mesoscopic of K3 subseam - grayish black to black, dull to slight bright in part, brittle to hard, sub-conchoidal to conchoidal fracture, gastropod fossils (<i>Planorbis</i> sp.), and white spots of calcareous.	46
Figure 3.18 Mesoscopic of K2 subseam - grayish black, dull, brittle to slightly hard, sub-conchoidal to conchoidal fracture, layers of diatomite and plant remains.	47
Figure 3.19 Mesoscopic of K1 subseam - grayish black to black dull to slight bright in black band, brittle to slightly hard, sub-conchoidal to conchoidal fracture, rough core surface.....	48

Figure 3.20 Mesoscopic of J6 subseam - brownish black to grayish black, dull, brittle, and gastropods remain (<i>Melanoides sp.</i>).....	49
Figure 3.21 Mesoscopic of J5 subseam - brownish black to grayish black, dull, white spots of fossil fragments, mudstone fragments and volcanic debris?	50
Figure 3.22 Mesoscopic of J4 subseam - brownish black, dull, white spots of calcareous and siliceous, mudstone banded and volcanic debris?.	51
Figure 3.23 Mesoscopic of J3 subseam - brownish black, dull, white spots of fossils fragments, with mudstone clasts.	52
Figure 3.24 The polished section of coal for petrographic microscope study.	54
Figure 3.25 Polarizing microscope with UV Excitation at Geology department, Chiangmai University.....	54
Figure 3.26 Proximate analyzer (LECO TGA-701) at Laboratory Section, Mae Moh Mine.....	56
Figure 3.27 CHN determinator (LECO TRuSpec CHN) for carbon, hydrogen and nitrogen contents at Laboratory Section, Mae Moh Mine.	57
Figure 3.28 S determinator (LECO SC632) for sulphur contents at Laboratory Section, Mae Moh Mine.....	57
Figure 3.29 Bomb calorimeters (LECO AC600) at Laboratory Section, Mae Moh Mine.....	58
Figure 4.1 Geological cross section of mine grid line N17 in central part of Mae Moh basin (unpublished cross section from EGAT, 2016).....	63
Figure 4.2 Lithostratigraphic column of borehole no. MMC-1	64
Figure 4.3 Geological cross section of mine grid line N8 in central part of Mae Moh basin (unpublished cross section from EGAT, 2016).	68
Figure 4.4 Lithostratigraphic column of borehole no. MMC-2.....	69
Figure 4.5 Geological cross section of mine grid line N0 in central part of Mae Moh basin (unpublished cross section from EGAT, 2016).	72

Figure 4.6 Lithostratigraphic column of borehole no. MMC-3.....	73
Figure 4.7 Composite stratigraphy of study area.....	74
Figure 4.8 Graph showing fixed carbon variations (<i>on as received basis</i> , weight %) within the coal sequence, in central part of Mae Moh basin.	76
Figure 4.9 Graph showing volatile matter variations (<i>on as received basis</i> , weight %) within the coal sequence, in central part of Mae Moh basin.	77
Figure 4.10 Graph showing ash variations (<i>on as received basis</i> , weight %) within the coal sequence, in central part of Mae Moh basin.	78
Figure 4.11 Graph showing moisture variations (<i>on as received basis</i> , weight %) within the coal sequence, in central part of Mae Moh basin.	79
Figure 4.12 Graph showing carbon content variations (<i>on dry basis</i> , weight %) within the coal sequence, in central part of Mae Moh basin.	81
Figure 4.13 Graph showing hydrogen content variations (<i>on dry basis</i> , weight %) within the coal sequence, in central part of Mae Moh basin.	82
Figure 4.14 Graph showing nitrogen content variations (<i>on dry basis</i> , weight %) within the coal sequence, in central part of Mae Moh basin.	83
Figure 4.15 Graph showing oxygen content variations (<i>on dry basis</i> , weight %) within the coal sequence, in central part of Mae Moh basin.	84
Figure 4.16 Graph showing sulphur content variations (<i>on dry basis</i> , weight %) within the coal sequence, in central part of Mae Moh basin.	85
Figure 4.17 Graph showing calorific value variations (<i>on as received basis</i> , Kcal/kg.) within the coal sequence, in central part of Mae Moh basin.	86
Figure 4.18 Graph showing huminite contents (%) within the coal sequence, in central part of Mae Moh basin.	91
Figure 4.19 Graph showing liptinite contents (%) within the coal sequence, in central part of Mae Moh basin.	92

- Figure 4.20 Graph showing inertinite contents (%) within the coal sequence, in central part of Mae Moh basin. 93
- Figure 4.21 Graph showing mineral matter contents (%) within the coal sequence, in central part of Mae Moh basin..... 94
- Figure 4.22 photomicrographs of highly reflecting fusinite band under plane polarize light (A), bright yellow serrated linear of cutinite, bright yellow various shape of sporinite, bright yellowish green of alginite stand out in the groundmass, and common pale yellow to pale green small fragment of liptodetrinite under fluorescence light (C) in groundmass of densinite; Q4 subseam. 96
- Figure 4.23 photomicrographs of bright yellow serrated linear of cutinite, bright yellow various shape of sporinite under fluorescence light (C) in the groundmass of densinite with abundant pyrite; Q4 subseam..... 97
- Figure 4.24 photomicrographs of texto-ulminite including highly reflecting round shape of sclerotinite which derived from fungal material and considered being an oxidation product of resin; Q3 subseam. 98
- Figure 4.25 photomicrographs of dark stringer cutinite, which running across (thin-walled cutinite) under plane polarize light (A), bright yellowish green round shape of sporinite and some exsudatinites filled into crack in groundmass of densinite, under cross polarized light (C); Q2 subseam..... 99
- Figure 4.26 photomicrographs of intermediate reflecting of semifusinite, which partially visible cellular structure under plane polarize light (A), discrete small fragment of liptodetrinite, amorphous shape of amorphinite under fluorescence light (C) in the groundmass of densinite; Q1 subseam..... 100
- Figure 4.27 photomicrographs of yellowish green fluorescing of alginite, yellowish brown fluorescing of sporinite, associated with yellowish green serrated linear fluorescing of cutinite in groundmass of densinite; K3 subseam. 102
- Figure 4.28 photomicrographs of bright linear yellow fluorescing of alginite in type of *Lamalginite?*, abundant yellowish green various shape of sporinite under

fluorescence light (C) in the groundmass of densinite with abundant pyrite; K3 subseam.	103
Figure 4.29 photomicrographs of texto-ulminite, represent intact fragments of plant matter; presence of remnant cell structure, filled with mineral matter under cross polarized light (B); K2 subseam.	104
Figure 4.30 photomicrographs of bright yellow to yellowish green round shape of alginite in type of <i>Botryococcus sp.?</i> stand out under fluorescence light (C), associated with diatomite and mineral matter; K2 subseam.	105
Figure 4.31 photomicrographs of diatomite, yellow various shapes of sporinite, associated with yellowish green serrated linear fluorescing of cutinite under fluorescence light (C) in the groundmass of densinite and gelinite; K1 subseam.	106
Figure 4.32 photomicrographs of gelified material of gelinite and individual small fragment of densinite, including yellow fluorescing crenulation on some surface of cutinite, bright yellow of alginite stand out under fluorescence light (C), associated with mass of mineral matters mainly pyrite; J6 subseam.	108
Figure 4.33 photomicrographs of bright yellow appendage of cutinite, bright yellowish green various shapes of sporinite, yellow discrete small fragment of liptodetrinite under fluorescence light (C), associated with pyrite in form of framboidal pyrite (round shape) brighten under plane polarize light (A) in groundmass of densinite and gelinite; J5 subseam.	109
Figure 4.34 photomicrographs of gelified material layer of gelinite and individual small fragment of densinite, associated with discrete small fragment of liptodetrinite, amorphous shape of amorphinite, and fossil remains (fish fragments?); J4 subseam.	110
Figure 4.35 photomicrographs of gelified material layer of gelinite and individual small fragments of densinites, including bright yellowish green various shape of sporinite, discrete small fragment of liptodetrinite under fluorescence light (C), associated with brighten pyrite in form of framboidal pyrite (round shape) under plane polarize light (A); J3 subseam.	111

Figure 4.36 photomicrographs of gelified material layer of gelinite, including bright yellow fluorescing alginite, bright yellow various shape of sporinite, yellow discrete small fragment of liptodetrinite under fluorescence light (C), associated with mass of mineral matter mainly quartz and pyrite; I seam.	113
Figure 4.37 photomicrographs of brighten pyrite in form of framboidal pyrite (round shape) under plane polarize light (A) and bright yellow under cross polarized light (B) in the groundmass of gelinite; I seam.....	114
Figure 5.1 Depositional environment interpretation of study area in central part of Mae Moh basin.....	124
Figure 5.2 Ternary diagram suggesting peat-forming environments for Mae Moh coals, based on maceral assemblages (modified after (Mukhopadhyay, 1986)).....	126
Figure 5.3 The study coal facies depicted from the Gelification Index (GI) and Tissue Preservation Index (TPI) in relation to depositional setting and type of mire (modified after (Diessel, 1986))......	128
Figure 5.4 Comparisons of maceral contents (%) related to depositional environment of the study coals in Mae Moh basin and other basins.	131
Figure 5.5 Diagram of TPI versus GI showing the depositional paleo environment of the peat mires (modified after (Diessel, 1986)), compare between the study coals in Mae Moh basin and oversea coals basin.	132
Figure 5.6 The Mae Moh coal samples plotted on H/C versus O/C atomic ratio diagram (modified after (Krevelen, 1993)).	135
Figure 5.7 Graph showing coal rank related to coal seams by using the ASTM standard (D388), which described by the fixed carbon on dry, mineral matter free basis.....	136
Figure 5.8 Graph showing coal rank related to coal seams by the ASTM standard (D388), which described by the volatile matter on dry, mineral matter free basis. ...	137

Figure 5.9 Graph showing coal rank related to coal seams by using the the ASTM standard (D388), which described by calorific value on moist, mineral matter free basis.....	138
Figure 5.10 Graph showing fixed carbon (on dry, mineral matter free basis, avg. %) compared between central part by this study and northeast part by Sompong et al. (1996) following ASTM D388.....	139
Figure 5.11 Graph showing volatile matter (on dry, mineral matter free basis, avg. %) compared between central part by this study and northeast part by Sompong et al. (1996) following ASTM D388.....	140
Figure 5.12 Graph showing gross calorific value (on moist, mineral matter free basis, avg. Btu/lb.) compared between central part by this study and northeast part by Sompong et al. (1996) following ASTM D388.....	141
Figure 5.13 Comparisons of the vitrinite reflectance (Ro %) of coals in central part of Mae Moh basin by this study and Singharajwarapan et al. (2014).....	143
Figure 5.14 Depositional environment of coal S seam.....	146
Figure 5.15 Depositional environment of coal R seam.....	147
Figure 5.16 Depositional environment of underburden.....	147
Figure 5.17 Depositional environment of coal Q seam.....	148
Figure 5.18 Depositional environment of interburden.....	149
Figure 5.19 Depositional environment of coal K seam.....	149
Figure 5.20 Depositional environment of overburden.....	150
Figure 5.21 Depositional environment of coal J seam.	151
Figure 5.22 Depositional environment of red bed.....	152
Figure 5.23 Depositional environment of coal I seam.....	152
Figure 6.1 The relation of petrographic study, geochemical analysis and depositional paleo environment.....	156

Chapter 1

1. Introduction

Mae Moh mine is located in Mae Moh basin, Mae Moh district, Lampang province in Thailand; about 630 kilometers north of Bangkok (figure 1.1). The Mae Moh basin measures some $16 \times 7 \text{ km}^2$, more than 900 meters deep, and is the site of the largest Tertiary coal mine in Southeast Asia. The opencast mines extract more than 50,000 tons per day to fuel ten coal fired power plants (unit 4 to unit 13) with a total capacity of 2,400 MW. This mine is operated by EGAT (Electricity Generating Authority of Thailand), and it is the largest open pit coal mine in Thailand. The total geological and economical coal reserves are approximately 1,040 million tons and 814 million tons, respectively. The annual production is about 16 million tons. Most of the coal produced from Mae Moh mine is supplied to the Mae Moh power plant that is providing 15% of the total electricity demand of Thailand. About 430 million tons of coal resources have been produced, and the remaining future coal reserves are approximately 384 million tons, located in the central area of the Mae Moh basin. EGAT will be replaced the existing three units (unit 4 to unit 7) of the Mae Moh power plant. They need the coal resources for supplying the new power plant. In the central area of Mae Moh basin have been sufficient coal reserves. This area hasn't been mined. Detailed of stratigraphy, petrography and geochemistry have been investigated in the core samples of boreholes from the central area. The results of this study can be interpreted coalification rank and their depositional of paleo environment in central area of Mae Moh basin. They are usefully for coal excavation and burden removal in mine operation and designing boilers of new coal fired power plants.



Figure 1.1 Index map of Thailand showing location of Mae Moh Mine in northern Thailand (modified from (Map.google.com)).

1.1 The study area

The current Mae Moh mine covers an area of $4 \times 7 \text{ km}^2$, divided into nine mine areas are as SB (Sub Basin), NE (North-East), BT (Buttress), SE (South-East), NW (North-West), SW (South-West), C1 (Central 1), C2 (Central 2) and C3 (Central 3). The study area is lower part of C1 and C2 which haven't been mined, located in the central area of Mae Moh basin covering approximately $1.5 \times 3 \text{ km}^2$. The boundaries of study defined in term of latitude and longitude grid reference as the follows: Latitude grid lines from $18^\circ 21' \text{N}$ to $18^\circ 18' 36'' \text{N}$ and Longitude grid lines from $99^\circ 42' 36'' \text{E}$ to $99^\circ 43' 43'' \text{E}$ (figure 1.2 and 1.3). The study area can be accessed by three ways. The first is using the Asian Highway No.2 from Bangkok passing Ayutthaya, Angthong, Singburi, Chainat, Nakhonsawan, Kamphaengphet, Tak to Lampang city, and turning right to Highway no.11, then turn left at Phalad intersection to road no.1348 to Mae Moh mine. The other ways by train to Mae Moh station of Amphoe Mae Moh, or by an airplane to Lampang Province.

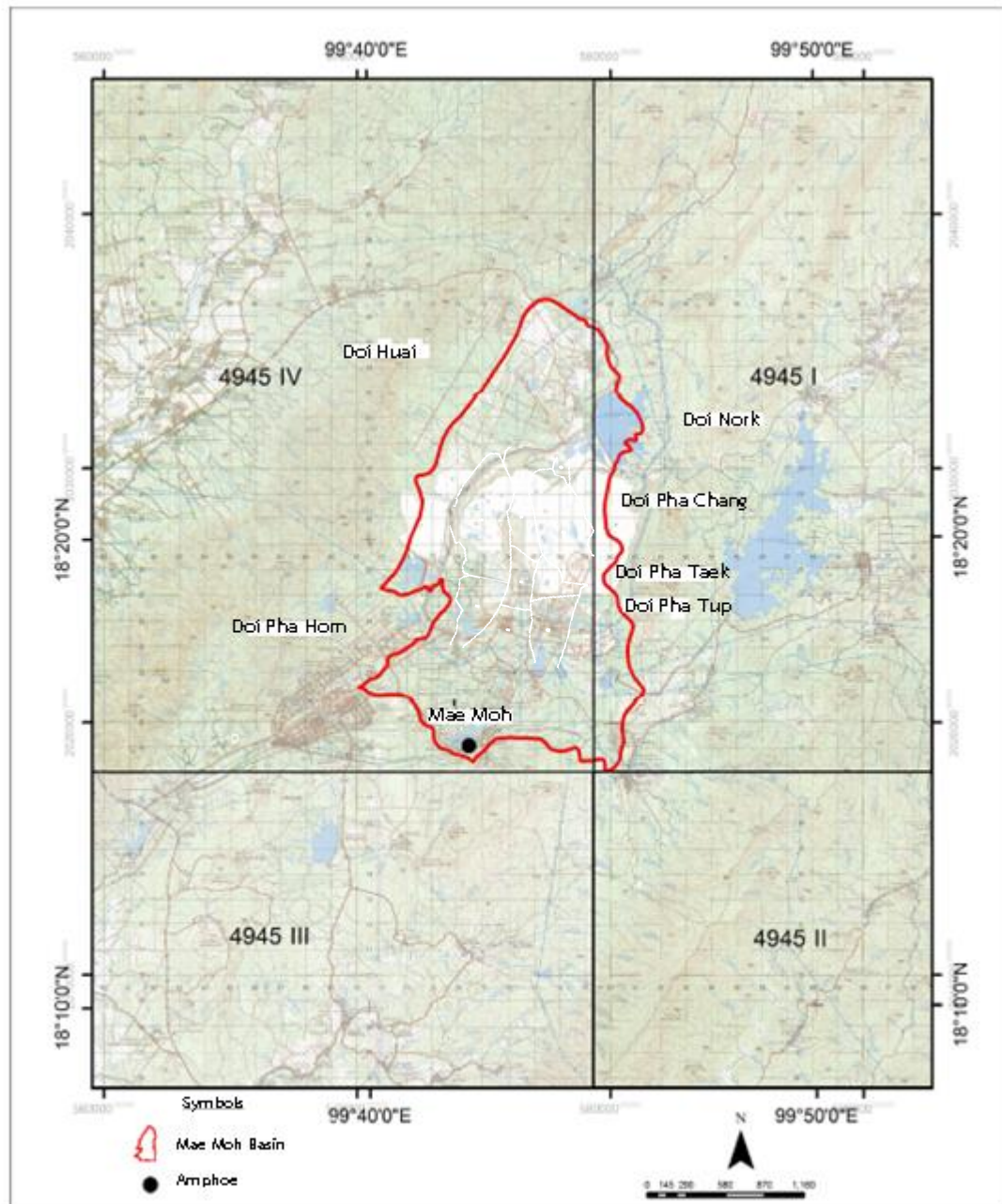


Figure 1.2 Topographic map showing the shape of Mae Moh basin (modified after(Dame and Moore, 1996)).



Figure 1.3 Aerial photo showing the mining area and the study area, located in central part of the Mae Moh basin (modified from (Map.google.com)).

1.2 Objectives

The objectives of this study are as follows:

1. To study stratigraphy of sediments and coals, located in the central part of Mae Moh basin;
2. To study petrography and geochemistry of coals, located in the central part of Mae Moh basin; and determine the coalification rank;
3. To interpret the depositional paleo environments.

1.3 Scope of work and Methodology

The scope of this study is coal petrography and associated stratigraphy in central part of Mae Moh basin, covers approximately $1.5 \times 3 \text{ km}^2$ in lower part of C1 and C2 mine area. In this study, 35 coal samples have been selected for petrographic and geochemical analysis. They were collected from main coal seams in Mae Moh group as J-, K- and Q seam of the Na Khaem formation, and minor coal seam as I seam of Huai Luang formation, were taken from the 3 boreholes and previous stratigraphy is used to interpret the sedimentary sequence along with the lithostratigraphic of study boreholes. The resulting can be used to determine for coalification rank and depositional paleo environment.

The petrographic study was performed using a coal petrographic microscope using white light and fluorescence excitation. Organic matter was examined and identified. Several standardized systems of nomenclature exist worldwide. The Australian Standard, AS3856-1986, (Australian Standards, 1995) and the ASTM Standard, (ASTM, 1996) are variations of the system used by the International Committee for Coal and Organic Petrology (1998 and 2001), which is continually reviewing their terminology and classification. This study was using the classification and properties of macerals, following the Australian Standard, AS3856-1986, (Australian Standards, 1995). The geochemistry studies on proximate; ultimate analyses and calorific values as well as coalification rank determination based on ASTM Standards.

Finally, interpretation, discussion and conclusion will be performed and resulted in the final thesis, presentation and manuscripts for a journal publication. The methodology was summarized as schematic diagram (figure 1.4). This thesis report is presented in 6 chapters as follows: Chapter 1: introduce the study area, objectives, scope of work, and methodology, and research background focusing on previous stratigraphy of Mae Moh basin and coal petrography in Tertiary basin.

Chapter 2: overview the geological setting of northern Thailand for Mae Moh coal deposit and stratigraphic sequence. Chapter 3: sample preparation and analytical method. Chapter 4: results of lithostratigraphy study which described the sedimentary sequence in the study area, and geochemical study, and coal petrography study which describes the macerals and vitrinite reflectance measurement. Chapter 5: discussion on deposition paleo environment, coalification rank by using petrography and geochemistry study. Chapter 6: conclusion of the resulting to identify and apply all data also implies that coal deposit.

1.4 Literature reviews

Ratanasthien et al. (1999) studied Liptinite in coal and oil source rocks in northern Thailand. Palynological study of northern Thailand coal and oil deposits indicates a similar palynological association to that of the Borneo region and can be referred to the *Florschuetzia trilobata* and *Magnastriatites howardii* zones as defined by Germeraad et al. (1968). Coal petrographic study shows variations in the liptinite maceral, especially alginite types. The oldest of these coal and oil deposits, which are of Late Oligocene to Early Miocene age, are dominated by *Botryococcus* sp. or *Botryococcus* related algae. Spore and pollen and thick walled lamaginite are found in some area. By contrast, in Late Middle Miocene is dominated by thin walled lamaginite. Resinite, suberinite, and cutinite are dominant in forest swamp coal deposits whereas alginite, cutinite and lycopodium spores are dominant in lacustrine environments. Exsudatinite is common even at early levels of maturation. These liptinite macerals can be major sources of oil and gas.

Iordanidis and Georgakopoulos (2003) studied Pliocene lignites from Apofysis mine, Amynteo basin, Northwestern Greece: petrographical characteristics and depositional environment. Coal petrological investigation along with geochemical analyses were undertaken to determine the petrographic characteristics and their

depositional environment. Eight samples (representing different lignite beds of the Apofysis deposit) were collected from a borehole. The Apofysis lignites have an Eulminite B reflectance of $R_r = 0.22\%$, and in terms of lithotype belong to matrix soft brown coals. Huminite is the most abundant maceral group and consists mostly of humodetrinite. Inertinite has relatively low percentages whereas liptinite concentrations are low in the lower lignite beds and higher in the upper ones. Ternary plots and facies indices were investigated the paleo environment. The depositional environment of the Apofysis lignites is not definitely ascribed to a forest swamp or a reed marsh environment. The high ash content of the analysed samples is a clear indication of a topogenous setting. Low tissue preservation index (TPI) and high gelification index (GI) values are observed. High alkalinity and strongly reducing conditions may be inferred from the presence of syngenetic (framboidal) pyrite, the low TPI values which indicate high bacterial activity, and thus high pH conditions, and the preservation of gastropod shells and chlorophyllinite. High GI indicates a constant influx of calcium-rich waters into the coal swamp. The Apofysis lignite deposit may be interpreted to be autochthonous to hypoautochthonous. The peat accumulation was governed by a high groundwater level (wet telmatic to limno-telmatic facies) and a moderate subsidence rate.

Sotirov and Kortenski (2004) studied Petrography of the coal from the Oranovo–Simitli basin, Bulgaria and indices of the coal facies. Petrographic analyses of 137 coal samples collected from an underground mine in the Oranovo–Simitli basin show vitrinite (huminite) reflectance ranged from 0.33% to 0.34%, which is consistent with the subbituminous C rank of these coals determined by Sotirov and Sokolov (1998). This middle Miocene age coal is mostly made of vitrinite (huminite), with about 10% liptinite and lesser amounts of inertinite. The inertinite group macerals are entirely funginite (sclerotinite) and inertodetrinite. The liptinite group macerals include fluorinite, which is identified for the first time in a Bulgarian coal. The abundant, degraded vitrinite group macerals result in a high gelification index

and a high tissue preservation index, which are consistent with a forested, continuously wet raised-bog depositional environment.

Sia and Abdullah (2012) studied Geochemical and petrographical characteristics of low rank Balingian coal from Sarawak, Malaysia: Its implications on depositional conditions and thermal maturity. Geochemical and coal petrographical analyses were undertaken on low rank upper Pliocene Balingian coal from Sarawak, Malaysia, in an attempt to reconstruct the conditions during peat accumulation and the subsequent coalification processes. Chemically, the coal in this study is characterized by high moisture, low ash yield and low sulphur content. The low ash yield and low sulphur content, together with the lack of epiclastic partings clearly indicate that it was deposited in ombrotrophic raised bogs. The coal was plotted in the Type III terrigenous kerogen zone of the van Krevelen diagram, with H/C value below 0.9. This shows that the coal was derived from plant materials of terrigenous origin and is still immature for petroleum generation. The petrographic study reveals, nonetheless, the expulsion of early generated hydrocarbons from the disintegration of suberinite, and also from phlobaphinite and cutinite. Petrographically, the coal is dominated by huminite, with low to moderate amounts of liptinite and low amounts of inertinite, pointing to predominantly anaerobic deposition conditions in the paleomires, with limited thermal and oxidative tissue destruction. Most of the studied samples are characterized by low TPI and high GI values, and are plotted on the marsh field of the Diessel's diagram, or it could also originate from decomposed wood in forested swamps. Nevertheless, coals originating from both these sources usually generate high ash yield, which is not the case for the studied coal. This shows that the interpretation as suggested by the Diessel's diagram is not valid for the studied coal. The coal has a mean random huminite reflectance between 0.26 and 0.35%, suggesting a lignite coal rank for the coal. Nevertheless, geochemical classification based on total moisture and calorific value suggests a subbituminous C rank.

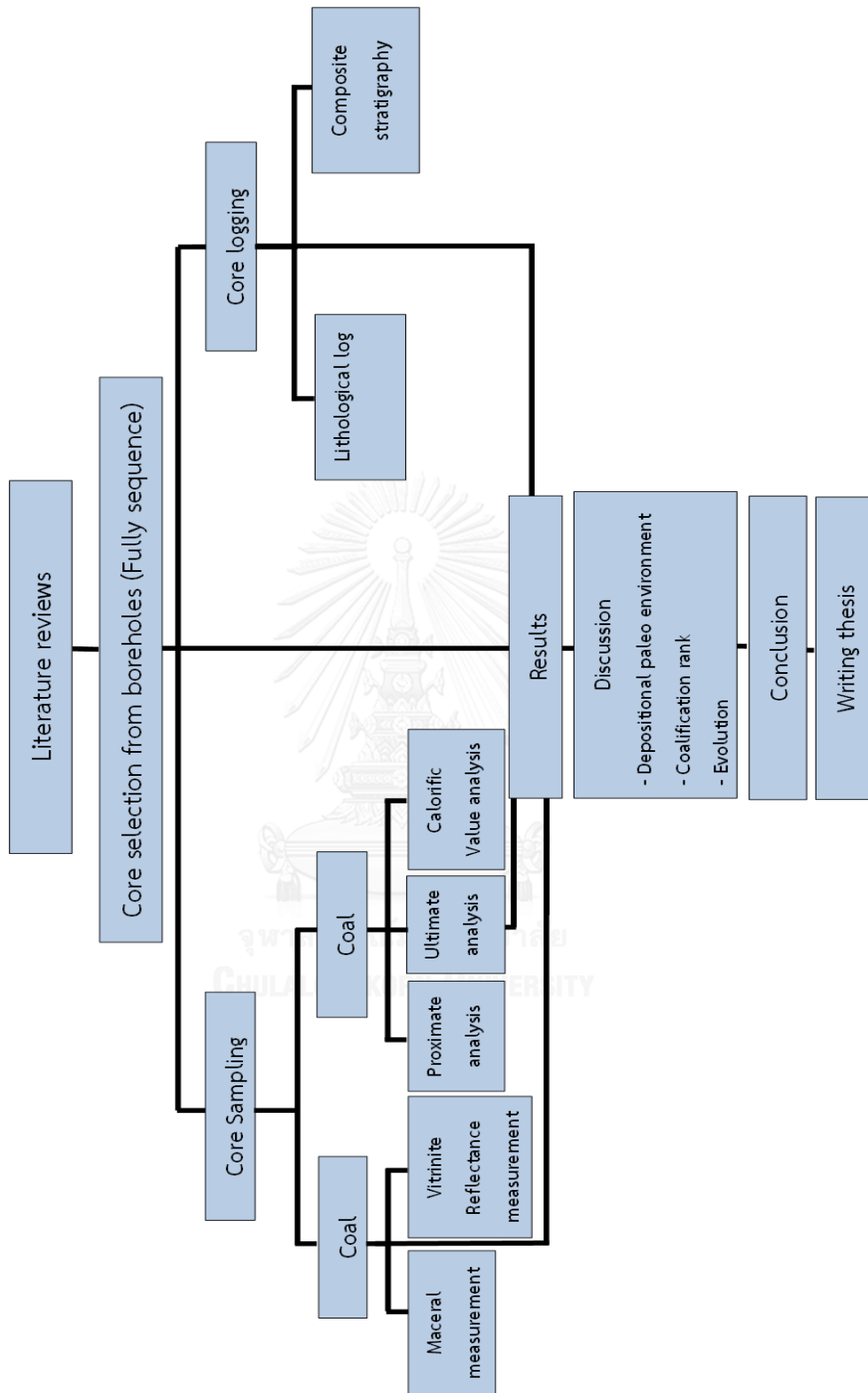


Figure 1.4 Schematic diagram showing sequences of work under this study.

Chapter 2

2. Geologic setting

2.1 General tectonic setting

Tertiary rift basins are elongated and N-S trending half grabens and grabens. Most geologists believed that basins are originated in Late Oligocene (Chinbunchorn et al., 1989).

Bunopas (1981) described basins as pure rift/back-arc basins while others proposed that they had probably been brought about by NW-SE and NNE-SSW trending conjugate strike-slip fault. The movement of the NW-SE trending faults was left lateral in the Tertiary.

In addition, Le Dain et al. (1984) and Tapponnier et al. (1986) believed that the movement of NW-SE and NNE-SSW trending faults changed (in the Late Miocene) from left to right lateral and right to left lateral respectively, based on the actual fault trend distribution, which suggested that all Tertiary basins in Thailand were probably developed as a result of the movements of the NW-SE trending right lateral fault and the NNE-SSW trending left lateral conjugate faults.

Charusiri and Pum-Im (2009) compiled the recent information about geomorphology, sequence stratigraphy, structure, geographical distribution and geotectonic evolution. They categorized the major Cenozoic basins in Thailand into 7 segments: Northern, Northwest-West, Central, Northeastern, Southern, Gulf, and Andaman group. Mae Moh basin is in the Northern segments. The evolution of basins developed from India plate moving to Asia plate. The change of direction of plate interaction from E-W to N-S, the tectonic changed from transgression to transtensional regimes. The India collision (45-55 Ma.) stopped the reactivation of fault movement. And then, the major faults changed the movement directions (35

Ma.) becoming right lateral movement for the NW-trending and left lateral movement for the NE-trending faults. Major basins occurred at that time. The South China plate anticlockwise rotation and the beginning of tectonic extrusion of SE Asian continental clock, southeastward between Red River and Mae Ping – Three Pagoda Faults developed the rift. The pull apart basin occurred and N-S trending faults bounded basin.

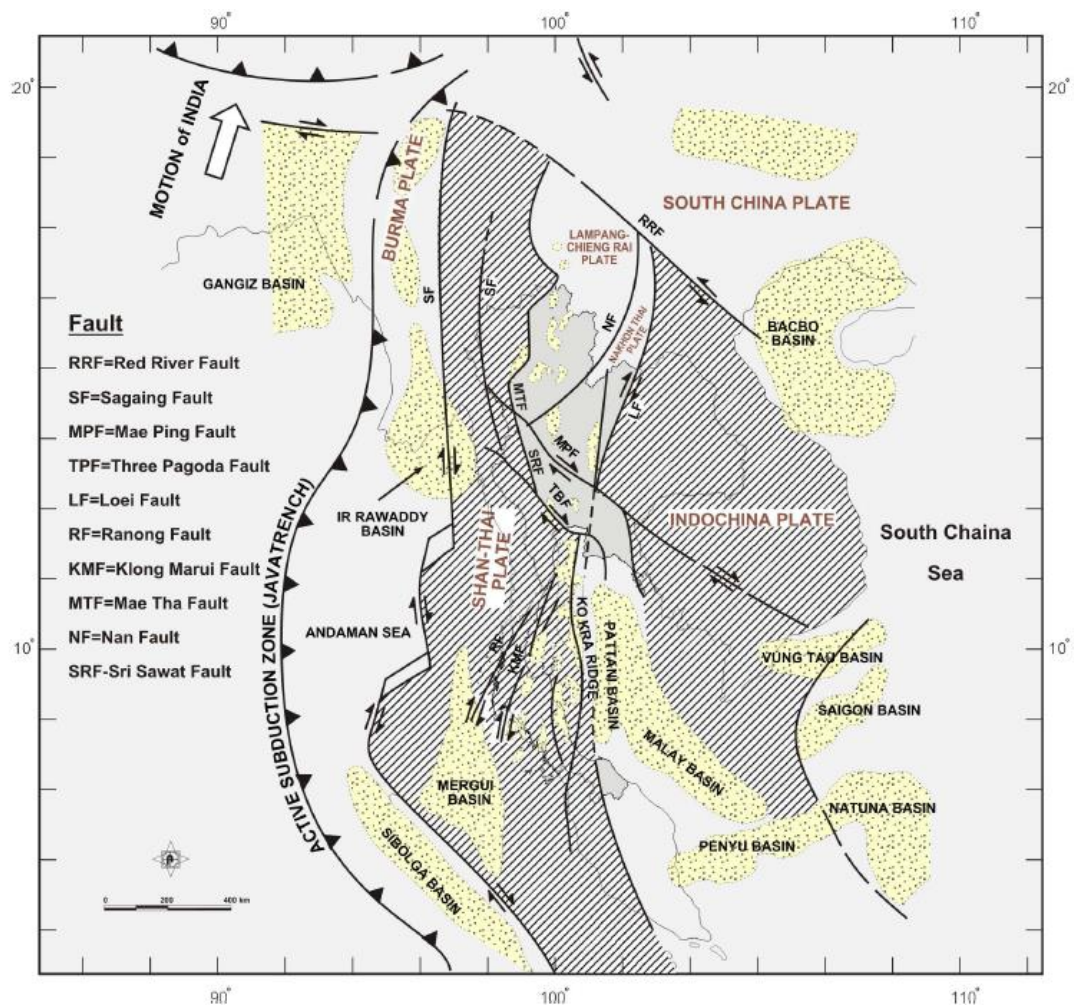
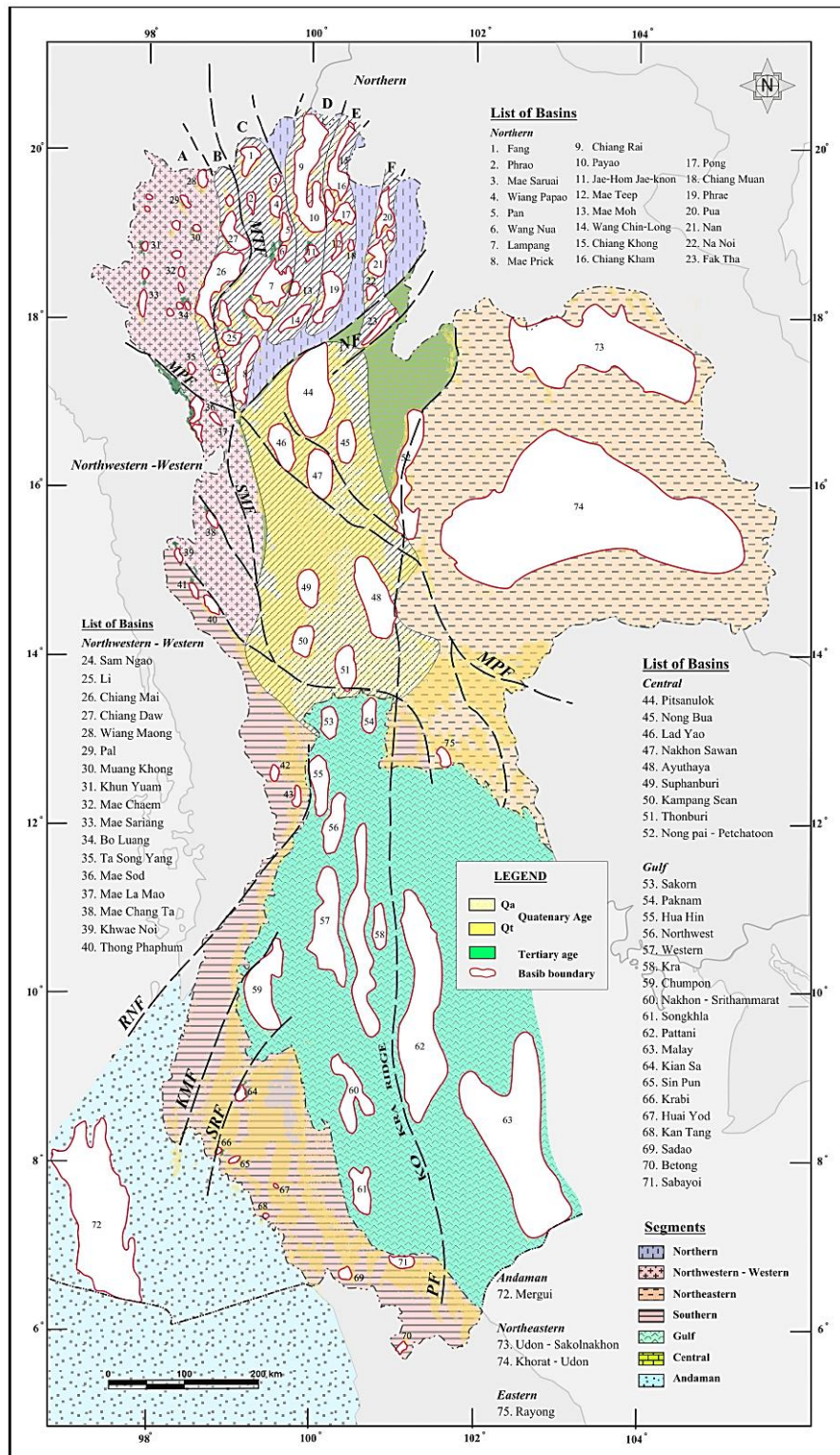


Figure 2.1 Tectonic map of Thailand has been controlled, to some extent, by the interaction of Australia-India, Burma, and the SE Asian plates since early to middle Tertiary (Charusiri and Pum-Im, 2009).



MPF = Mae Ping Fault, TPF = Three - Pagoda Fault, NF = Nan Fault, RNF = Ranong Fault, KMF = Klong Marui Fault, SWF = Sri Sawat Fault, MTF = Mae Tha Fault

Figure 2.2 The distribution of major Cenozoic basins in Thailand (Charusiri and Pum-Im, 2009).

According to Metcalfe (1993), Cenozoic modification of Southeast Asia involved substantial movements along, and rotations of strike-slip faults, rotation of continental blocks and the development and spreading of margin seas. These modifications were due to the combined effect of the interaction of the Eurasian, Pacific and Indo-Australian plates and the collision of India with Eurasia. Sundaland was not deformed as a coherent block. Strain was accommodated by movements on many strike slip faults and considerable block rotation. Clock-wise block rotation and strike slip faulting was significant at least as late as the Miocene. The corridor of fault-bounded Cenozoic basins in central Thailand that include the Mae Moh basin was created and deformed at this time. Later Neogene movements uplifted northern Thailand. In the process, the Mae Moh basin was subjected to erosion. The geology of the Mae Moh region was mapped by Dame and Moore (1996). The Mae Moh deposit lies within a north/northeast trending intermountain basin 16 kilometers long by 7 kilometers wide and more than 900 meters deep. The basin is divisible into the western, northern, central and southern subbasins and an intervening central ridge. Mining operations are restricted to the central subbasin where coal sub crops in an ovoid basin shape within an area about 8 kilometers long and 4.5 kilometers wide.

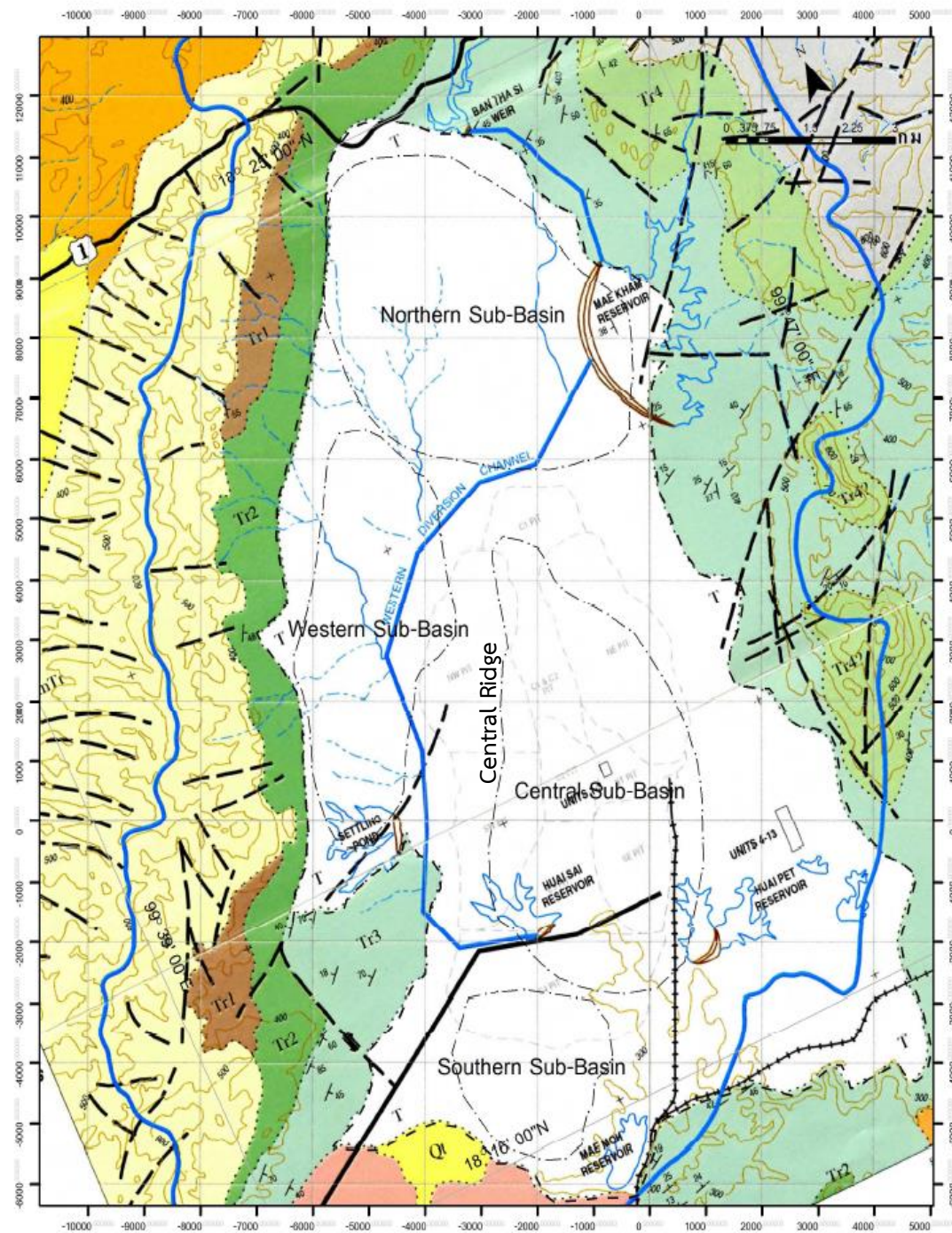


Figure 2.3 Geological map of the Mae Moh region and Mae Moh basin divisible into the western, northern, central and southern subbasins and an intervening central ridge (modified after (Dame and Moore, 1996)).

AGE	GROUP	FORMATION		DESCRIPTION
Sedimentary Rocks				
RECENT	MAE TAENG	QUATERNARY	Qa	RIVER GRAVEL, SAND, SILT, CLAY
PLEISTOCENE			Qt	TERRACE GRAVEL, SAND, SILT, CLAY
Unconformity				
PLIOCENE MIOCENE	MAE MOH	HUAI LUANG	T	CLAY, SILTY CLAY; REDDISH BROWN
		NA KHAEM		SILTY CLAYSTONE, LIGNITE; GREY
		HUAI KING		SILTY CLAY, CLAY, SILTY CLAYSTONE; RED, PURPLE, YELLOW AND GREY
Unconformity				
UPPER TRIASSIC		PHA DAENG	Tr5	SANDSTONE, SHALE, CONGLOMERATE, SILTSTONE; REDDISH BROWN, GREENISH GREY
MIDDLE TRIASSIC	LAM PANG	DOI LONG	Tr4	LIMESTONE, SHALE, CONGLOMERATE; GREY TO LIGHT GREY, MASSIVE
		HONG HOI	Tr3	SHALE, SANDSTONE, TUFFACEOUS SANDSTONE AND MINOR INTERBEDDED LIMESTONE; GREENISH GREY
		Pha Kan	Tr2	LIMESTONE, SHALE, SANDSTONE; DARK GREY TO MEDIUM GREY, GREYISH BROWN, WELL STRATIFIED, MASSIVE
LOWER TRIASSIC		PHRA THAT	Tr1	BASAL CONGLOMERATE, SANDSTONE, SILTSTONE, SHALE; RED TO REDDISH BROWN
Unconformity				
			Pm1	
			Pm2	
U. PERMIAN	RATBURI	HUAI THAK	Pm3	SHALE, LAMINATED SHALE AND SILICIFIED SHALE
Igneous Rocks				
PLEISTOCENE			Bs	BASALT, VESICULAR
PERMO-TRIASSIC			PmTr	RHYOLITE, RHYOLITIC TUFF, TUFF, AGGLOMERATE ANDESITE
SYMBOLS				
- - - -	GEOLOGICAL BOUNDARY	30°	BEDDING DIP	--- SUB-BASIN
- - - -	FAULT OR LINEAMENT		SYNCLINE	--- MAE MOH BASIN
	CATCHMENT AREA			

Figure 2.4 Descriptive symbols of geological map of the Mae Moh region and Mae Moh basin (modified after (Dame and Moore, 1996)).

2.2 General structure geology

The Mae Moh basin is a remnant of a once larger depositional basin. The present western flank of the basin is close to the original deposition margin, but the eastern flank is the product of structuring and erosion. The mining area is complex faulted syncline created by crustal collapse on a series of master faults both during and after the deposition of the Miocene. Erosion has removed at least 400 m of sediments from the flank of the basin and has exposed the coals in their present configuration. The basin was created by slippage on a series of north/south trending, east dipping listric faults within the Triassic. Block rotation upon the listric master fault controlled formations of the sub-basins and the central ridge. Families of synthetic and antithetic faults extend upwards through the Miocene from the master fault. The coal bearing central sub-basin is a north/northeast by south/southwest orientated depression. The axis plunges gently from the north and south at approximately 7 degrees and flattens centrally. Dips on the eastern and western margins are between 5 and 25 degrees. At its deepest the coal sequence is buried by up to 500 m of sediments. A series of broadly north/south trending faults have extensively deformed the Miocene sequence. Faulting is most intense in the north-west and least within the graben. As a consequence of faulting, block rotation is common and drag folding is often developed (Sompong et al., 1996).

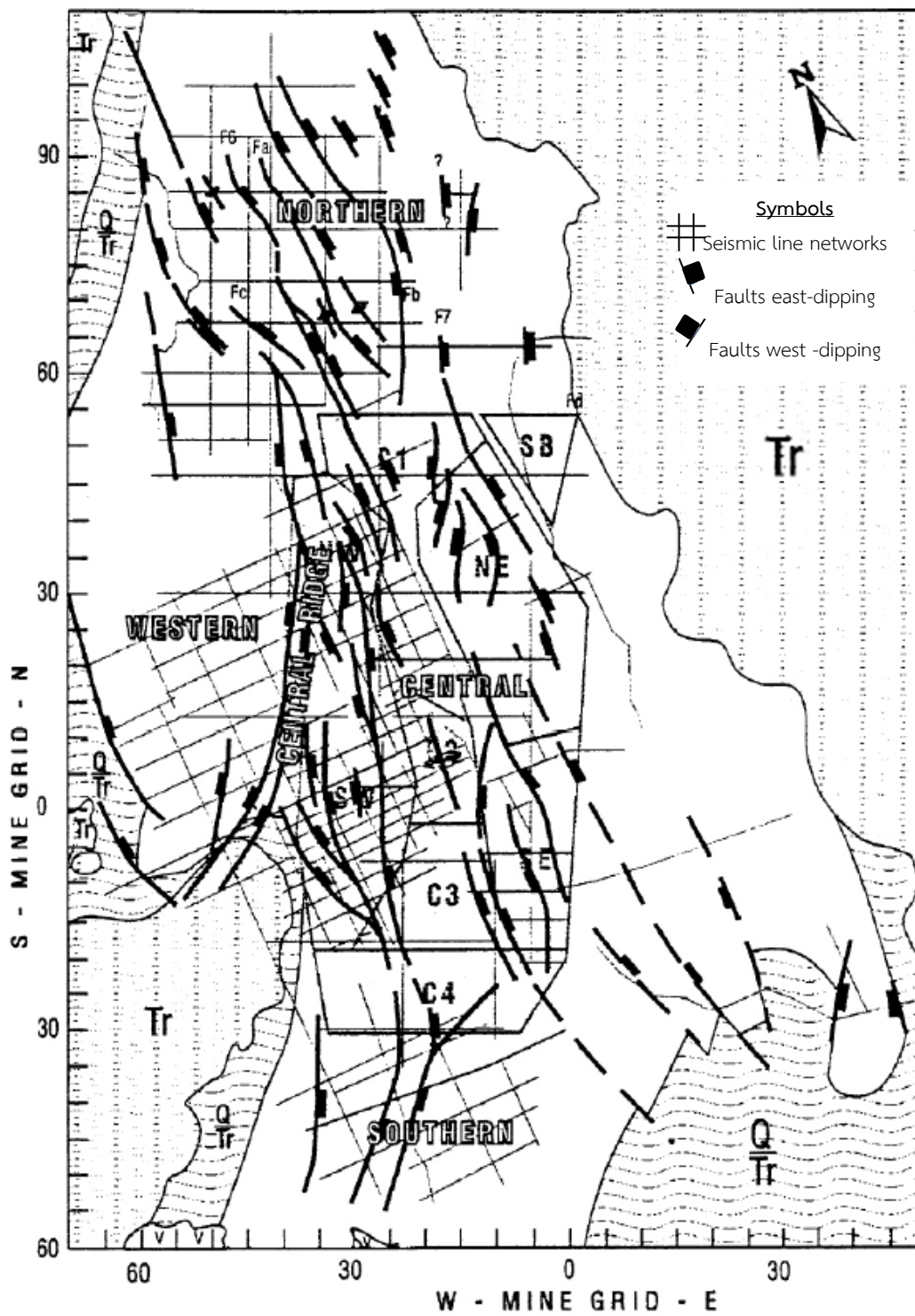


Figure 2.5 Structural map of Mae Moh basin showing North-South trending faults (modified after (Sompong et al., 1996)).

2.3 General stratigraphy

The Stratigraphic classification of Mae Moh basin has been described by several authors. Coal occurs in the Mae Moh group, a sequence of Early – Middle Miocene sediments exceeding 900 m thick that overlies a folded and faulted basement of the Triassic Lampang group.

2.3.1 Triassic Lampang group

Triassic Lampang group, consisting of five formations are recognized in the Triassic Lampang group, the Phra That formation (Tr1) at the base, consisting of claystone, siltstone, sandstone, conglomerate, breccia and limestone, the Pha Kan formation (Tr2), dominated by limestone, the Hong Hoi formation (Tr3), consisting of claystone, siltstone, sandstone, shale and conglomerate, the Doi Long formation (Tr4) of limestone and the Phae Daeng formation (Tr5) of red beds, consisting of claystone, siltstone, sandstone and conglomerate. The basement to the Mae Moh basin is principally shale and sandstone of the Hong Hoi formation, but there is a significant block of limestone in faulted beds below the northeast pit that is thought to be Doi Long formation. The Mae Moh basin is bounded mostly by marine Triassic rocks, with the exception of the southern part of the basin which is overlay by Quaternary basalt (Charoenprawat et al., 1995). Elsewhere across the basin the Tertiary sediment are overlain by unconsolidated Quaternary fluvial deposits (Jitapankul et al., 1985). The Tertiary sequence of the Mae Moh Basin has been named the Mae Moh group.

2.3.2 Mae Moh group

The Mae Moh group is divided into three formations each with distinctive lithology, sedimentary structure, degree of consolidation and fossil content. The succession is described from bottom to top in the following account:

2.3.2.1 Huai King formation

Huai King formation (Corsiri and Crouch, 1985), the oldest division of the Mae Moh group, the Huai King formation is a deposit of interbedded fluvial and alluvial sandstone, partially oxidized sandy claystone, and siltstone with calcrete layers at the base of the Mae Moh basin. The formation overall is a fining upwards sequence that culminates in a dominantly silty clay facies. Generally there are no macrofossils although, in the southern part of the basin, abundant *Viviparus* sp. is present in the lower part of the formation. Much of the basin contains no more than 20-40 m of the Huai King formation. In contrast, there are at least 300 m to the southeast of the central sub-basin. The formation is absent from parts of the central ridge, central sub-basin (below the northeast pit), and much of the northern sub-basin that were emergent during deposition. The lower part of the formation is mainly coarse grained. At the base are several individual sequences that grade upwards from fine conglomerate to sandstone, while the remainder consists of graded sequences of conglomeratic sandstone to clayey siltstone. The upper parts of the formation contain sequences of claystone or silty claystone. Individual fining upwards sequences grade from sandstone or conglomeratic sandstone to interbedded red and grey claystone or silty claystone. The sources of the sediments are varied. Basal breccias are locally derived. Basal conglomeratic facies are prominent adjacent to the central ridge. Sandstone in the middle of the formation is poorly sorted litharenite, consisting of angular to sub rounded quartz, rock fragments of quartzite, chert, shale, siltstone, schist and volcanic rocks, with some feldspar and siliceous cement (Chaodumrong, 1985) there is a significant pyroclastic contribution. The sand/shale ratio is highest in the center of the basin and diminishes to the southeast implying the source area was to the west. Permo-Triassic pyroclastic rocks to the west of the Mae Moh basin are therefore the likely source of much of the Huai King formation.

2.3.2.2 Na Khaem formation

Na Khaem formation (Corsiri and Crouch, 1985), a widespread suit of lacustrine, alluvial, and deltaic claystone, silty claystone, and minor thin sandstone beds up to 400 m thick, contains the three economically important coal bearing horizons (J-, K- and Q zones) and non-economically R and S zones. The claystone and silty claystone occasionally include thin concentrations of small invertebrates, mainly freshwater gastropods and ostracods. This formation was divided into three members, from bottom to top in the following account:

Member III (Underburden), this is a sequence of grey to greenish grey claystone and mudstone, calcareous, silty claystone, with the thin layer of coal of S and R zone. The top of the Member is placed at the gradational contact with coal of Q zone. Galloway (1989), the boundary between coal of S zone and the lacustrine sediments of Member III was a flooding surface. The beds are laminated to thick planar bedded, highly calcareous and in the upper part there are abundant gastropod beds (Songtham et al., 2005) referred to this member as *Paludina* sp., fish fragments, ostracods and plant rootlets. Intraformational conglomerate, invertebrate burrows and load casts are present. Member III below the R zone in the central sub-basin is about 100 m thick, but thickens to the southeast. It thins against and across the flank of the central ridge and towards the basement high below the northeast area. Without the presence of the key marker, the R zone, it is not possible to identify whether correlatives of this lower section of Member III are present in the northern and western sub-basins. In general, however, the data indicate that distribution of the sequence is similar to that of the underlying Huai King formation. The section above the R zone is the most extensive part of Member III. It is present across the entire basin, but reaches a maximum thickness of about 200 m in the Central sub-basin. Depositional of the Member III was a lake with a low-lying hinterland which probably lacked much vegetation.

Member II contains the economically coal sequence and was divided into three parts (in ascending order): the Q zone, interburden and the K zone, the each of

coal zone up to 30 m. thick, and separated by 10-30 m of claystone (the Interburden). The commercially viable coals of the K and Q zone are confined to the central sub-basin both zones split to the north and south of the sub-basin, where coal quality deteriorated and clastic parting thicken. The coals in the central sub-basin follow a west to east depositional axis and thicken to the southeast, reaching the maximum near the current eastern outcrop. There was uniform accumulation of peat over a north to south distance of about 4 km, with relatively rapid splitting and thinning at the depositional northern and southern extremities and gradual thinning to the west. The swamp clearly extended further east of the central sub-basin, from where it has been removed by subsequent uplift and erosion. Coals occur sporadically across the northern sub-basin. Correlatives of the Q zone are the most persistence and the K zone merges with fossiliferous shale. Similar changes occur across the western sub-basin. In the southern sub-basin sub-seams of both the K and Q zone are represented by well-spaced, thin coals horizons. Thin sands are associated with the K zone in place, and Q zone is represented by sandy clay. To the west and south of the area, sands substitute for coals. To the east, the K zone is represented by grey and brown clay and claystone.

The Q zone is brown to black, brittle to slightly hard; pyritized gastropods (*Viviparus* sp. and *Planobidae* sp.), diatoms and plants remain with mineral matters. It consists of interbedded light brown claystone and silty claystone about 30% of the section. The thickness of Q zone is 15-30 m. The Q zone divided into four subseams (Q1 to Q4) and their subdivisions in the mining area are distinguished largely by their mineral content, in turn identified by their geophysical responses.

Interburden is a persistent sequence of the fine grained sediments of brown, brownish gray, gray, green and greenish gray claystone, 10-30 m thick, and containing common coal flakes, fish remains, plant roots, rare ostracods and gastropods (*Viviparus* sp.). Intra formational conglomeratic texture is common low in the sequence, and load structures and micro slip planes are present. Locally in the

northern sub-basin the Interburden is sandy; in the southern sub-basin its correlatives are both sandy and shaly.

K zone is brownish black to black, brittle to slightly hard, interbedded with light yellowish gray to gray silty claystone. Gastropods (*Planorbis* sp., *Melanoides* sp.), diatoms, fish and plant remain are present. Variations in seam characteristics enable recognition of four subseams (K1 to K4), although the zone splits both to the north and south of the central mining area. Their subdivisions are distinguished largely by their mineral content, in turn identified by their geophysical responses. The thickness of K zone is 15-30 m.

Member I (Overburden), consists of claystone and mudstone with occasional siltstone, 60-100 m thick, highly calcareous, pyritic in part, and containing in its upper half a section about 40 m thick that included coal of J zone. A fossil gastropod, *Melanoides* sp. is common interbedded of the J zone. The J zone is of commercial significance, at least in the northern half of the mining area, where they are well developed. The upper most 15-20 m of top J zone is dominant of claystone, siltstone and silty claystone, with vary color. It marks the transition from the reducing environment of lacustrine deposition typical of the Na Khaem formation to the oxidizing condition characteristic of the alluvium deposits of the Huai Luang formation. The J zone is grouped into six subseams, J1 to J6. J1 to J2 consist of poor coal quality (high mineral content), interbedded with claystone and J3 to J6 are characterized by coal with a low mineral content interbedded with intra-formational conglomeratic mudstone. Correlatives of Member I occur throughout the basin. J zone lensing out southwards are replaced by clay and siltstone, and in the far south, by gravelly and sandy clay. In contrast, seams thickness to the north, then diminish to insignificance in the northern sub-basin, where they are largely replaced by fossiliferous lacustrine shale.

2.3.2.3 Huai Luang formation

Huai Luang formation (Corsiri and Crouch, 1985) is the uppermost division of the Mae Moh group, which is also commonly referred to as Red Beds. The thickness of this formation may be up to 400 m, consists of red to brownish-red, claystone, siltstone and mudstone with lenses of sandstone and conglomerate. Engineers (1981), the brownish red to red colors due to the oxidation of fine grained pyrite to hematite disseminated throughout certain layers of the formation. No macrofossils have been found but there are abundant gypsums and pyrites with rare roots and flame structures. Sandstone and gravel are rare. Proportionately more gravel is encountered in two horizons, one at the base, and the other near the middle of the formation. Gravels are particularly common in the west of the southern sub-basin, close to the central ridge. Local unconformities within the Huai Luang formation, particularly in the western subbasin, are expressions of contemporaneous movements on some of the major faults during subsidence and deposition. This formation contains non-economic coal of I zone, divided into two subseams as I1 and I2, the thickness each of subseam is up to 3 m., brownish black, soft to brittle, interbedded with gray silty claystone and abundant pyritized gastropods. Songtham et al. (2005) identified gastropods are *Margaya* sp. The sulphur isotope studied the red bed indicated sulphur source from aqueous sulphates, while the pyritized gastropods from I zone coal indicated bacterial reduction of sulphate to sulphide (Silaratana, 2005; Silaratana et al., 2004).

2.3.3 Pleistocene - Recent

Pleistocene - Recent, surficial alluviums consist of unconsolidated materials up to 30 m thick: top soils, clays, silts, sands and gravels, vary color: yellow, red, light to medium brown, extend across much of the area. The Mae Tha basalt also known as the Lampang Basalt (Barr et al., 1976), floors the valley to the south of the mine site. The basalts are massive and vesicular, dark grey to black, fine-grained, amygdaloidal, with recrystallized secondary minerals, and usually flowed as pahoehoe type. Two cones, likely to have been vents, are preserved near the

Lampang-Mae Moh mine road, to the north of Ban Pha Lad. Doi Pha Kok Jum Pa Dad, has a height of 120 m and diameter of 150 m. Pha Kok Hin Foo located 2 km to the south, has a height of 80 m and diameter of 200 m (Jungyusuk and Sirinawin, 1983). Sasada et al. (1987), using K-Ar methods, placed the age of samples from the basalt at 0.8 ± 0.2 million years.



Age	Formation		Lithology	Description
	Pleistocene - Recent			Alluvium deposits ; top soils, clays, silts, sands, gravels, massive and vesicular basalts, vary color: yellow, red, light to medium brown, dark gray to black. 1-30 m thick.
Miocene	Huai Luang 0-400 m	I zone 10-15 m		<p style="text-align: center;">Unconformity</p> <p>Red Beds; consists of red to brownish-red, claystone, siltstone and mudstone with lenses of sandstone and conglomerate, no macrofossils, abundant gypsums and pyrites with rare plant roots and flame structure, 0-400 m thick. This formation contains the coal of I zone, 10-15 m thick. Associated with the I-zone coal are abundant partly pyritized gastropods (<i>Margaya</i> sp.).</p> <p>The I zone is divided into two sub-seams as I1 and I2, the thickness each of sub-seam is up to 5 m., brownish black to black, soft to brittle, interbedded with gray silty claystone with pyrite and gypsum.</p>
				<p>The upper most 15-20 m of top J zone is dominant of claystone, siltstone, sandstone and silty claystone, with vary color. It marks the transition from the reducing environment of lacustrine deposition.</p> <p>Claystone and mudstone with occasional siltstone, 60-100 m thick, highly calcareous, pyritic in part, and containing in its upper half a section about 40 m thick that included coal of J zone. Gastropod (<i>Melanoides</i> sp.) is common interbedded of the J zone.</p> <p>The J zone is divided into six sub-seams as J1 to J6. J1 to J2 consist of poor coal quality (high mineral content), interbedded with claystone and J3 to J6 are characterized by coal with a low mineral content interbedded with intra-formational conglomeratic mudstone.</p>
	Na Kheam 300-400 m	Member I J zone 10-30 m		<p>The K zone is brownish black to black, brittle to slightly hard interbedded with light yellowish gray to gray silty claystone. Gastropods (<i>Planorbis</i> sp., <i>Melanoides</i> sp.), fish and plant remains are present. The thickness of K zone is 15-30 m.</p>
				<p>Fine-grained sediments of brown, brownish gray, gray, green and greenish gray claystone and containing common coal flakes, fish remains, plant roots, rare ostracods and common gastropods (<i>Viviparus</i> sp.). The thickness of K zone is 15-30 m.</p>
		Overburden		
	Member II K zone 15-30 m		<p>The Q zone is brownish to black, brittle to slightly hard and plants remain, and interbedded with light brown claystone and silty claystone. The thickness of Q zone is 15-30 m.</p>	
			Interburden	
Q zone 15-30 m				
Member III R zone 1-2 m		<p>Sequence of grey to greenish grey claystone and mudstone, calcareous, silty claystone. The beds are laminated to thick planar bedded, highly calcareous and in the upper part there are abundant gastropod beds (<i>Paludina</i> sp.), fish fragments, ostracods and plant rootlets. Intraformational conglomerate, invertebrate burrows and load casts are present.</p> <p>The R zone, brownish black to black, 1-2 m thick.</p>		
		S zone 1-2 m		
	Huai King 0-300 m			<p>The formation overall is a finding upwards sequence that culminates in a dominantly silty clay facies interbedded fluvial and alluvial sandstone, partially oxidized sandy claystone, and siltstone with calcrete layers at the base of the Mae Moh basin, no macrofossils, abundant gastropods (<i>Viviparus</i> sp.) is present in the lower part of the formation.</p>
Triassic	Basement Lampang Group			<p style="text-align: center;">Unconformity</p> <p>Triassic marine sediments; sandstone, mudstone, limestone, shale, conglomerate, tuffaceous sandstone, agglomerate and tuff.</p>

Figure 2.6 Stratigraphy of Mae Moh basin, Lampang province (modified after (Sompong et al., 1996)).

Chapter 3

3. Sample collection and analytical method

3.1 Sample collection

Coals are used to interpret depositional environment. Sediments are used to help interpreting by appearance characters. The coal samples were prepared as polished section for petrographic microscope study. Moreover, proximate analysis, and ultimate analysis, along with calorific analysis for geochemical study can assess the coalification rank as well as vitrinite reflectance measurement in petrographic study.

35 coal samples were collected from the 3 boreholes, which located in central part of Mae Moh basin (figure 3.1). Borehole no. MMC-1 contains 11 coal samples. Borehole no. MMC-2 contains 12 coal samples. Borehole no. MMC-3 contains 12 coal samples. The samples were collected by every subseam in a vertical succession of core from bottom to top, which identified by their geophysical responses (figure 3.3, 3.5, and 3.7) and lithological features (figure 3.4, 3.6, and 3.8).

Physical properties of coal bearing sequence have in general a lower density, a lower seismic velocity, a lower magnetic susceptibility, a higher electrical resistivity and low radioactivity compared with surrounding rocks in typical coal-bearing sequences. Gamma ray log can be displayed as counts per second (CPS). Radioactivity associated with shaliness and radioactive bed. Coal seam thickness can be interpreted by taking the point on the gamma ray curve one-third down from the high level of natural radiation. Density log can be displayed as counts per second (CPS). Formation density depends on lithology and porosity. Coal seam thickness can be interpreted by taking the point on the density curve one-third down from the high level of density. Neutron log can be displayed as counts per second (CPS). Neutron correlates on hydrogen content of formation and large shale response. Coal seam

thickness can be interpreted by taking the point on the neutron curve one-third down from the high level of neutron. This study was using the density, gamma ray and neutron logs to interpret the coal zones and coal subseams for the sample collection method.

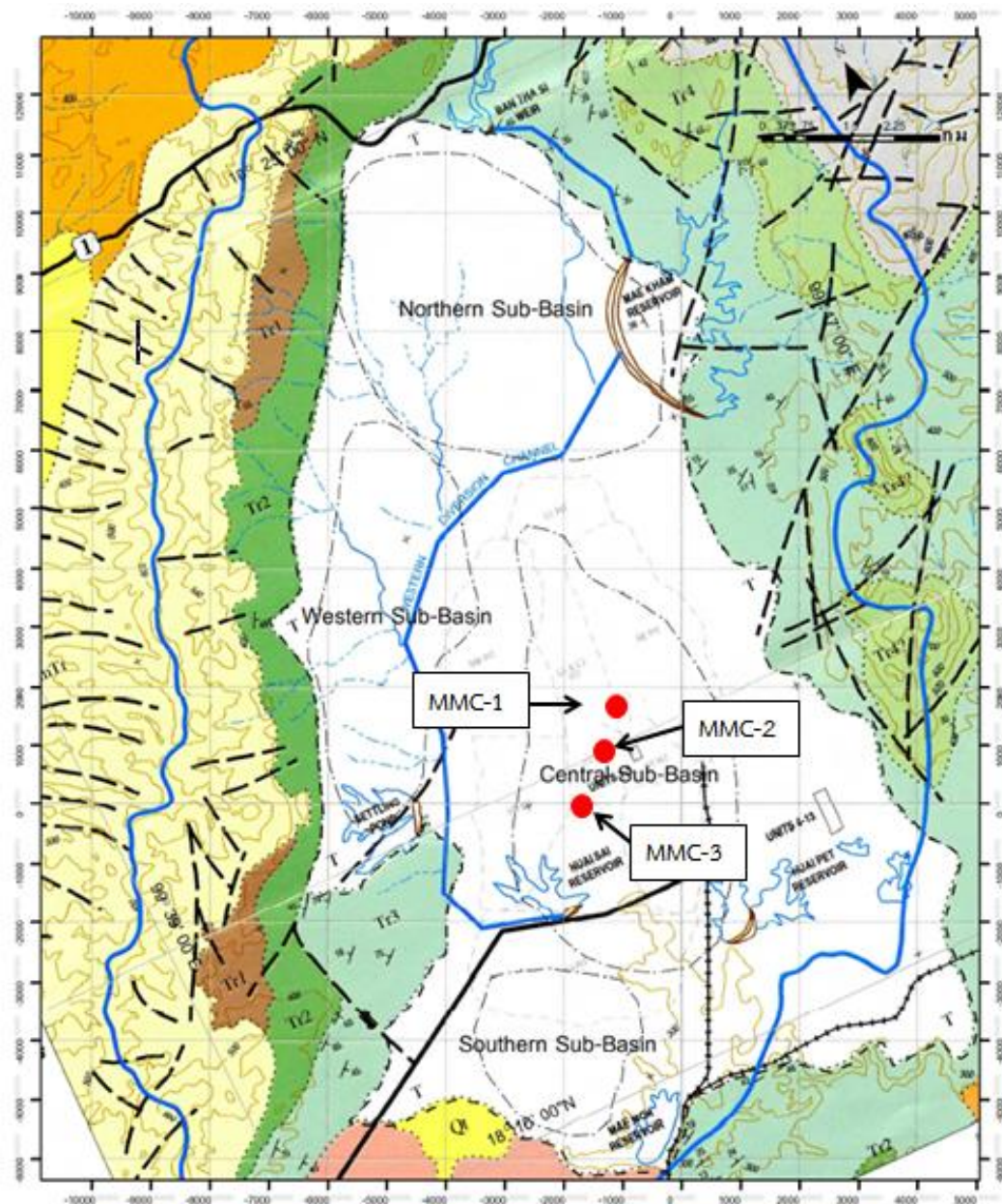


Figure 3.1 Map of the Mae Moh basin showing location of the study boreholes basin (modified after (Dame and Moore, 1996)).

AGE	GROUP	FORMATION		DESCRIPTION
RECENT PLEISTOCENE	MAE TAENG	QUATERNARY	Qa Qt	Sedimentary Rocks RIVER GRAVEL, SAND, SILT, CLAY TERRACE GRAVEL, SAND, SILT, CLAY
Unconformity				
PLIOCENE MIOCENE	MAE MOH	HUAI LUANG NA KHAEM HUAI KING	T	CLAY, SILTY CLAY; REDDISH BROWN SILTY CLAYSTONE, LIGNITE; GREY SILTY CLAY, CLAY, SILTY CLAYSTONE; RED, PURPLE, YELLOW AND GREY
Unconformity				
UPPER TRIASSIC		PHA DAENG	Tr5	SANDSTONE, SHALE, CONGLOMERATE, SILTSTONE; REDDISH BROWN, GREENISH GREY
MIDDLE TRIASSIC	LAM PANG	DOI LONG	Tr4	LIMESTONE, SHALE, CONGLOMERATE; GREY TO LIGHT GREY, MASSIVE
		HONG HOI	Tr3	SHALE, SANDSTONE, TUFFACEOUS SANDSTONE AND MINOR INTERBEDDED LIMESTONE; GREENISH GREY
		Pha Kan	Tr2	LIMESTONE, SHALE, SANDSTONE; DARK GREY TO MEDIUM GREY, GREYISH BROWN, WELL STRATIFIED, MASSIVE
LOWER TRIASSIC		PHRA THAT	Tr1	BASAL CONGLOMERATE, SANDSTONE, SILTSTONE, SHALE; RED TO REDDISH BROWN
Unconformity				
			Pm1 Pm2 Pm3	
U. PERMIAN	RATBURI	HUAI THAK		SHALE, LAMINATED SHALE AND SILICIFIED SHALE
Igneous Rocks				
PLEISTOCENE PERMO- TRIASSIC			Bs PmTr	BASALT, VESICULAR RHYOLITE, RHYOLITIC TUFF, TUFF, AGGLOMERATE ANDESITE
SYMBOLS				
.....	GEOLOGICAL BOUNDARY	30°	BEDDING DIP	--- SUB-BASIN
---	FAULT OR LINEAMENT		SYNCLINE	--- MAE MOH BASIN
---	CATCHMENT AREA			

Figure 3.2 Descriptive symbols of geological map of the Mae Moh region and Mae Moh basin (modified after (Dame and Moore, 1996)).

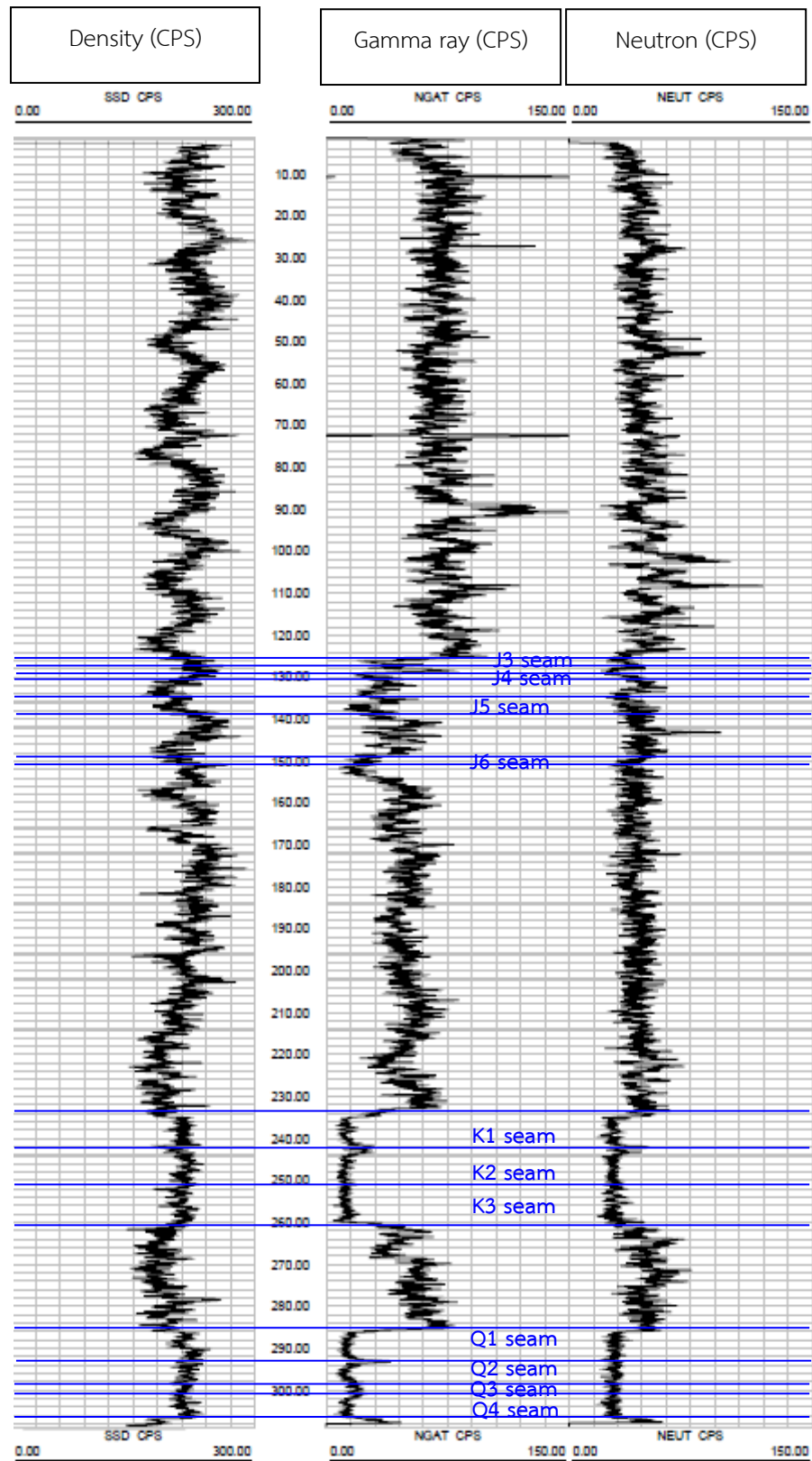


Figure 3.3 The geophysical responses of borehole no. MMC-1.

Bore Hole No: MMC-1		Location : North 17.04, West 13.96	
Total Depth Drilled :317 m.		Elevation :+211 m.	
Log by :Kunwato Rittidate			
Depth (meters)	Lithology	Sample descriptions	Sample id
50		Claystone, mudstone and siltstone: red to brownish-red, with lenses of sandstone, and gray silty claystone with red brown mottled in the lower part.	
100		Coal (J3 subseam): brownish black, dull, crumbly, gypsum and pyrite disseminated.	MMC-1-2-J3
		Coal (J4 subseam): brownish black, dull, crumbly, gastropod fragments, gypsum and pyrite disseminated.	MMC-1-3-J4
		Coal (J5 subseam): brownish black, dull, brittle, gypsum and pyrite disseminated.	MMC-1-4-J5
		Coal (J6 subseam): brownish black, dull, brittle, gastropod fragments, gypsum and pyrite disseminated.	MMC-1-5-J6
150		Overburden: claystone and mudstone with occasional siltstone, brownish gray, gastropods (<i>Melanoides sp.</i>) remain.	
200		Coal (K1 subseam): grayish black to black banded, dull to brighten banded, brittle to hard, pyrite disseminated and plants remain.	MMC-1-6-K1
		Coal (K2 subseam): brownish black to grayish black, dull, brittle to hard, pyrite disseminated, gastropod fossil (<i>Planorbis sp.</i>) and plants remain.	MMC-1-7-K2
250		Coal (K3 subseam): grayish black to black banded, dull to brighten banded, brittle to hard, gastropod fragments, and plants remain.	MMC-1-8-K3
		Interburden: brown, brownish gray, gray, green and greenish gray claystone contains common coal flakes, gastropods and rare ostracods.	
300		Coal (Q1 subseam): brownish black to grayish black, dull to brighten banded, brittle to hard, dull, plants remain.	MMC-1-9-Q1
		Coal (Q2 subseam): brownish black to grayish black, dull to brighten banded, brittle to slightly hard, plant remains.	MMC-1-10-Q2
350		Coal (Q3 subseam): grayish black to black, dull to brighten banded, brittle to hard, pyrite disseminate, plants remain.	MMC-1-11-Q3
		Coal (Q4 subseam): grayish black to black, dull to brighten banded, soft to brittle in a top part and hard in a bottom part.	MMC-1-12-Q4
400		Underburden: claystone, mudstone and silty claystone, grey to greenish grey.	

● location of selected sample

Figure 3.4 The sample descriptions of borehole no. MMC-1.

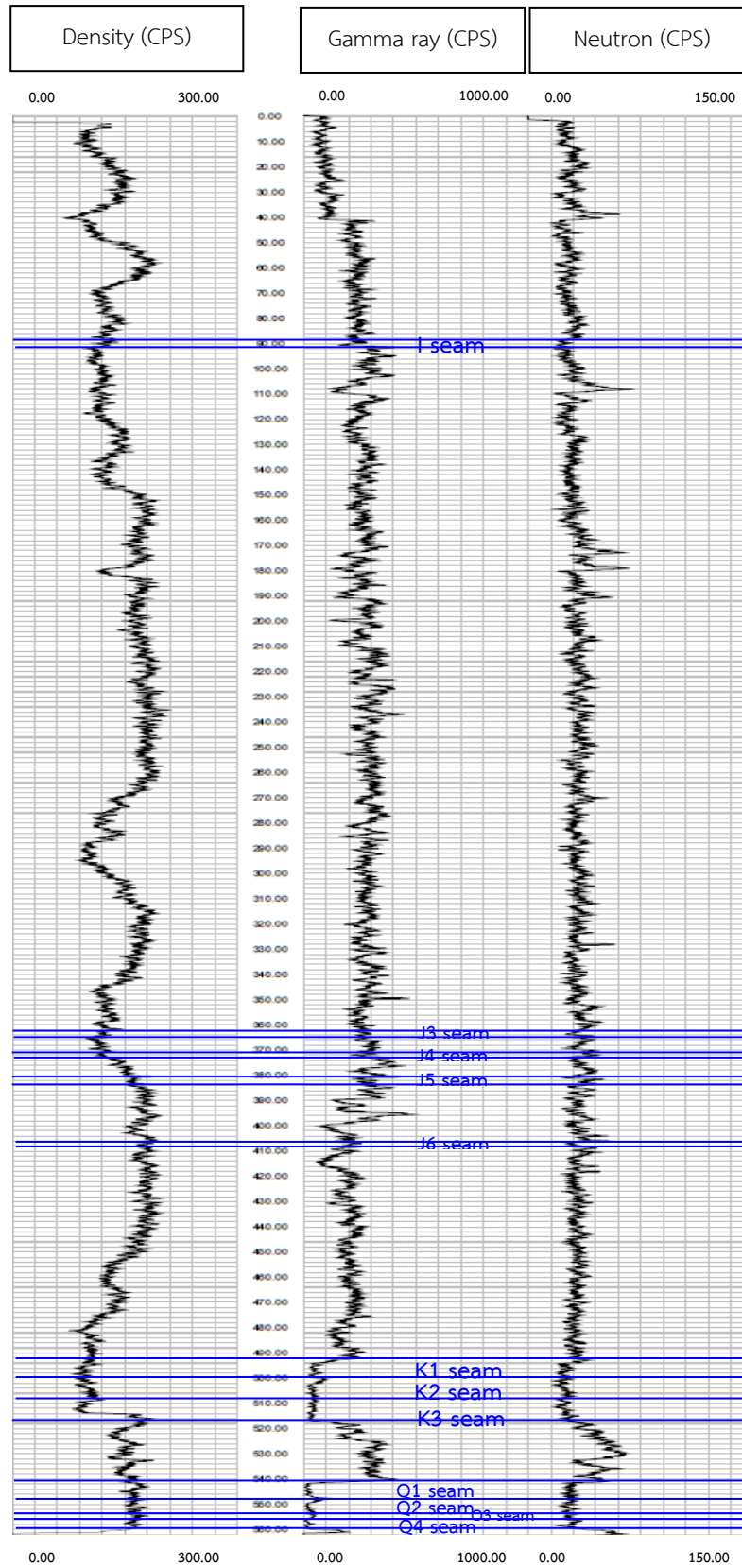


Figure 3.5 The geophysical responses of borehole no. MMC-2.

Bore Hole No :MMC-2		Location : North 7.83, West 17.03	
Total Depth Drilled :565 m.		Elevation :+310.98 m.	
Log by :Kunwato Rittidate			
Depth (meters)	Lithology	Sample descriptions	Sample id.
		Alluvium deposits: top soils, clays, silts, sands, gravels, vary color: yellow, red, light to medium brown.	
50		Claystone, siltstone and mudstone: red to brownish-red, with lenses of sandstone, no macrofossils, abundant gypsums and pyrites with rare plant roots.	
100		Coal (I seam): brownish black, dull, crumbly, gypsum and pyrite disseminated, gastropod fossils (<i>Margaya</i> sp.).	MMC-2-1-I
150			
200			
250		Claystone, siltstone and mudstone: red to brownish-red, with lenses of sandstone, no macrofossils, abundant gypsums and pyrites with rare plant roots and flame structure, gray claystone and silty claystone, with red-brown mottled in the bottom part.	
300			
350		Coal (J3 subseam): brownish black, dull, crumbly, gypsum and pyrite disseminated, plants remain.	MMC-2-2-J3
		Coal (J4 subseam): brownish black, dull, crumbly, gastropod fossils (<i>Melanoides</i> sp.), gypsum and pyrite disseminated.	MMC-2-3-J4
		Coal (J5 subseam): brownish black, dull, soft to brittle, siliceous white spots, pyrite disseminated.	MMC-2-4-J5
400		Coal (J6 subseam): brownish black to black, dull, soft to brittle, gastropod fossils (<i>Melanoides</i> sp.).	MMC-2-5-J6
450		Overburden: claystone and mudstone with occasional siltstone, brownish gray, highly calcareous, coal flakes, pyritic in part.	
		Coal (K1 subseam): grayish black, dull to brighten banded, brittle to hard, pyrite disseminated, plants remain.	MMC-2-6-K1
		Coal (K2 subseam): brownish black to grayish black, dull, brittle to slightly hard, pyrite disseminated and gastropod fossils (<i>Planorbis</i> sp.)	MMC-2-7-K2
500		Coal (K3 subseam): grayish black to black banded, dull to slightly bright, brittle to hard, pyrite disseminated, gastropod fossils (<i>Planorbidae</i> sp.), plants remain.	MMC-2-8-K3
		Interburden: claystone: brown, brownish gray, gray, green and greenish gray containing common coal flakes, plants remain, rare ostracods.	
550		Coal (Q1 subseam): grayish black, dull to brighten banded, brittle to hard, and plants remain.	MMC-2-9-Q1
		Coal (Q2 subseam): grayish black, dull to brighten banded, brittle, and plants remain.	MMC-2-10-Q2
		Coal (Q3 subseam): grayish black to black, dull to brighten banded, brittle to hard, plants remain.	MMC-2-11-Q3
		Coal (Q4 subseam): grayish black to black, dull to brighten banded, soft in a top part, brittle to hard in a bottom part, plants remain.	MMC-2-12-Q4
600		Underburden: claystone, mudstone and silty claystone, grey to greenish grey, calcareous, gastropod bedded (<i>Paludina</i> sp.).	
650			

● location of selected sample

Figure 3.6 The sample descriptions of borehole no. MMC-2.

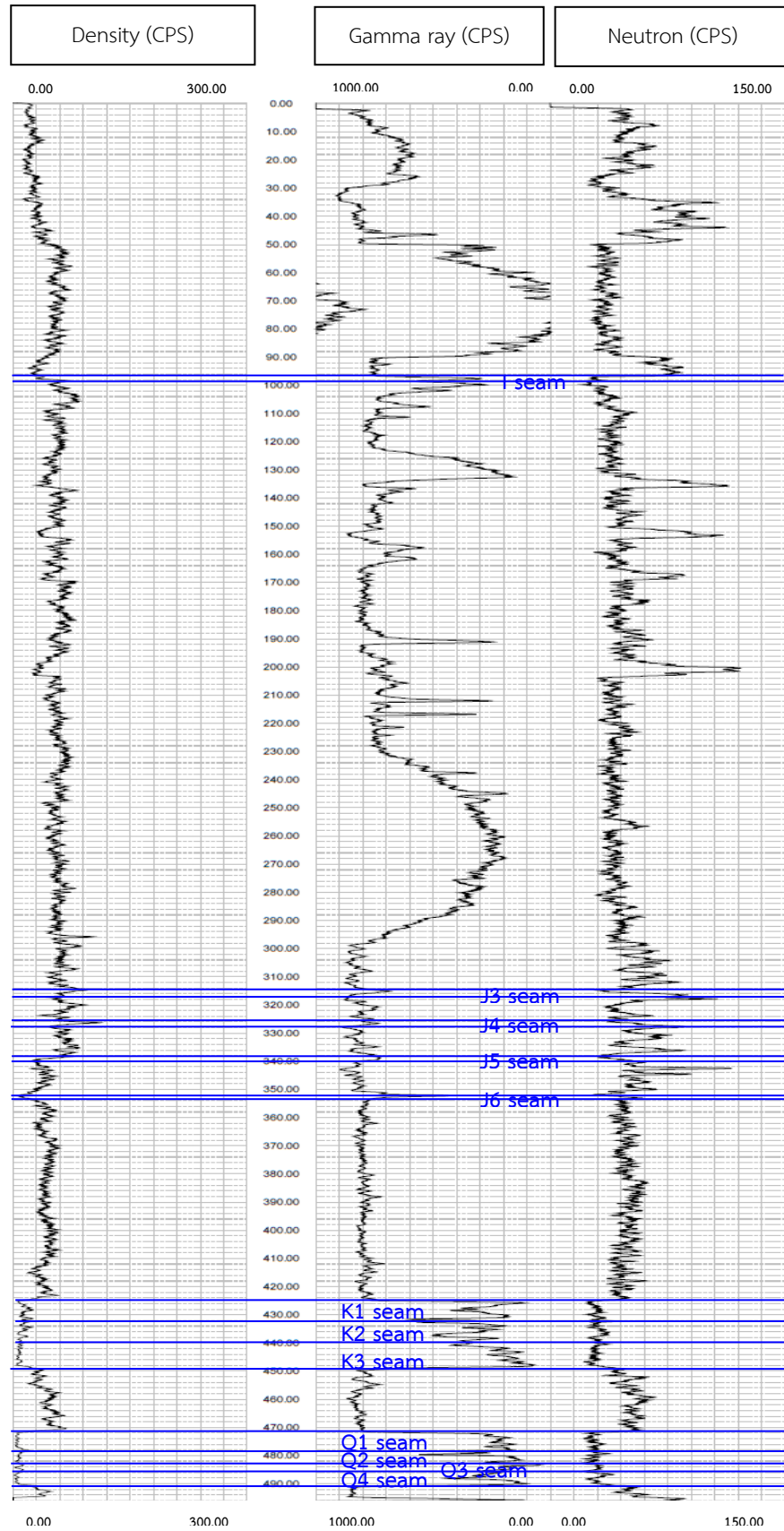


Figure 3.7 The geophysical responses of borehole no. MMC-3.

Bore Hole No: MMC-3		Location : North 0.048, West 19.71	
Total Depth Drilled :500 m.		Elevation:+310 m.	
Log by :Kurwatoo Rittidate			
Depth (meters)	Symbol	Description	Sample id
50		Claystone, siltstone and mudstone: red to brownish-red, with lenses of sandstone, no macrofossils, abundant gypsums and pyrites with rare plant roots.	
100		Coal (I seam) : brownish black, dull, crumbly, gypsum and pyrite disseminated.	MMC-3-1-I
150			
200		Claystone, siltstone and mudstone: red to brownish-red, with lenses of sandstone, no macrofossils, abundant gypsums and pyrites with rare plant roots, and gray claystone and silty claystone, with red-brown mottled in the bottom part.	
250			
300		Coal (J3 subseam): brownish black, dull, crumbly, gypsum and pyrite disseminated, with silty claystone, plants remain.	MMC-3-2-J3
		Coal (J4 subseam): brownish black, dull, crumbly, white spots of calcareous and siliceous, gastropod fragments, gypsum and pyrite disseminated.	MMC-3-3-J4
		Coal (J5 subseam): brownish black, dull, brittle, gypsum and pyrite disseminated.	MMC-3-4-J5
350		Coal (J6 subseam): brownish black, dull, brittle, pyrite disseminated, gastropods and plants remain.	MMC-3-5-J6
		Overburden: claystone and mudstone with occasional siltstone, brownish gray, highly calcareous, coal flakes, and pyritic in part.	
400		Coal (K1 subseam): grayish black, dull to brighten banded, brittle to hard, sub-conchoidal to conchoidal fracture, pyrite disseminated, plants remain.	MMC-3-6-K1
		Coal (K2 subseam): brownish black, dull, brittle to slightly hard, pyrite disseminated, gastropod fossils (<i>Planorbis sp.</i>)	MMC-3-7-K2
450		Coal (K3 subseam): grayish black, dull to brighten banded, brittle to slightly hard, pyrite disseminated and gastropod fossils (<i>Planorbis sp.</i>)	MMC-3-8-K3
		Interburden: claystone: brown, brownish gray, gray, green and greenish gray containing common coal flakes, plant remains, rare ostracods.	
		Coal (Q1 subseam): grayish black, dull to brighten banded, brittle to slightly hard, pyrite disseminated and silty claystone interbedded, and plants remain.	MMC-3-9-Q1
500		Coal (Q2 subseam): grayish black, dull to brighten banded, brittle to slightly hard, pyrite disseminated and silty claystone interbedded.	MMC-3-10-Q2
		Coal (Q3 subseam): grayish black, dull to brighten banded, brittle to hard, pyrite disseminate, plants remain.	MMC-3-11-Q3
550		Coal (Q4 subseam): grayish black to black, dull, soft in a top part and brittle to hard in a bottom part, plants remain.	MMC-3-12-Q4
		Underburden: claystone, mudstone and silty claystone, grey to greenish grey, calcareous, gastropod bedded (<i>Paludina sp.</i>) in the upper part.	
600			

● location of selected sample

Figure 3.8 The sample descriptions of borehole no. MMC-3.





3.1.1 Sample description

The coal Q seam, 12 samples were collected from borehole no. MMC1, MMC2 and MMC3. Q seam is divided into 4 subseams as Q4-, Q3-, Q2- and Q1 subseam in the study area, which identified by their geophysical responses and lithological features. The lower part of this sequence is Q4 subseam is grayish black to black, dull to bright in part, soft to brittle in a top part and hard in a bottom part, sub-conchoidal to conchoidal fracture, and plants remain. Q3 subseam is grayish black to black, dull, brittle to hard, sub-conchoidal to conchoidal fracture, pyrites disseminate, and plants remain. Q2 subseam is brownish black to grayish black, dull, brittle to slightly hard, sub-conchoidal fracture, carbonaceous mudstone and silty claystone interbedded, white spots of siliceous and calcareous and plants remain. The upper part of this sequence is Q1 subseam is grayish black to black, dull to bright in part, brittle to hard, sub-conchoidal to conchoidal fracture, carbonaceous mudstone and silty claystone interbedded, plants remain.

The coal K seam, 9 samples were collected from borehole no.MMC-1, no.MMC-2 and no.MMC-3. K seam is divided into 3 subseams as K3-, K2- and K1 subseam in the study area, which identified by their geophysical responses and lithological features. The lower part of this sequence is K3 subseam is grayish black to black, black band interbedded, dull to slight bright, brittle to hard, sub-conchoidal to conchoidal fracture, gastropod fossils (*Planorbis sp.*), and white spots of calcareous and siliceous, plants remain. K2 subseam is brownish black to grayish black, dull, brittle to slightly hard, sub-conchoidal to conchoidal fracture, carbonaceous mudstone and silty claystone interbedded; white spots of siliceous and carbonaceous, diatomite layer, pyrite disseminated, gastropod fossils (*Planorbis sp.*) and plants remain. The upper part of this sequence is K1 subseam is grayish black to black band interbedded, dull to slight bright in black band, brittle to slightly hard, sub-conchoidal to conchoidal fracture, white spots of calcareous and siliceous, pyrite disseminated and plant remains.



The coal J seam is divided into six subseams; J6, J5, J4 and J3 subseam were deposited in the study area, which classified subseam by their geophysical responses and lithological features, 12 samples were collected from borehole no.MMC1, no.MMC-2 and no.MMC-3. The lower part of this sequence is J6 subseam, brownish black to grayish black, dull, brittle, gastropod fragments (*Melanoides sp.*), pyrite disseminated and plants remain. J5 subseam is brownish black to grayish black, dull, white spots of calcareous and siliceous, gypsum and pyrite disseminated, diatomite layer, carbonaceous mudstone interbedded. J4 sub-seam is brownish black, dull, crumbly, white spots of calcareous and siliceous, gastropod fragments (*Melanoides sp.*), gypsum and pyrite disseminated. The upper part of this sequence is J3 sub-seam is brownish black, dull, crumbly, white spots of calcareous and siliceous, gypsum and pyrite disseminated, with carbonaceous mudstone.

The upper coal seam is I seam, 2 samples were collected from boreholes no.MMC2 and no.MMC3. I seam is divided into 2 subseams as I2 and I1 subseam in the study area (from upper to lower deposition), which identified by their geophysical responses and lithological features. I seam is brownish black, dull, mostly crumbly, abundant gypsums and pyrites disseminated, and gastropod fossils (*Margaya sp.*)

Coal seam	Coal subseam	Description	Core sample
Q	Q4	Grayish black to black, dull to brighten banded luster in part, soft to brittle and hard, sub-conchoidal to conchoidal fracture, and plant remains.	
	Q3	Grayish black to black, dull luster, brittle to hard, sub-conchoidal to conchoidal fracture, pyrites disseminate, and plant remains.	
	Q2	Brownish black to grayish black, dull luster, brittle to slightly hard, sub-conchoidal fracture, intraclast of carbonaceous mudstone, and plant remains.	
	Q1	Grayish black to black, dull to brighten banded luster in part, brittle to hard, sub-conchoidal to conchoidal fracture, intraclast of carbonaceous mudstone, plant remains.	

0 m 5 m

Figure 3.9 Sample descriptions of Q seam coal.

Coal seam	Coal subseam	Description	Core sample
K	K3	Grayish black to black, dull to slight bright luster, brittle to hard, sub-conchoidal to conchoidal fracture, gastropod fossils (<i>Planorbis sp.</i>), and white spots of calcareous and siliceous, plants remain.	
	K2	Brownish black to grayish black, dull luster, brittle to slightly hard, sub-conchoidal to conchoidal fracture, carbonaceous mudstone interbedded, white spots of siliceous and carbonaceous, diatomite layer, pyrite disseminated, gastropod fossils (<i>Planorbis sp.</i>), and plants remain.	
	K1	Grayish black to black, dull to slight bright luster in black banded, brittle to slightly hard, sub-conchoidal to conchoidal fracture, pyrite disseminated and plants remain.	

0 m  5 m

Figure 3.10 Sample descriptions of K seam coal.

Coal seam	Coal subseam	Description	Core sample
J	J6	Brownish black to grayish black, dull, brittle, gastropod fragments (<i>Melanoidea sp.</i>), pyrite disseminated and plants remain.	
	J5	Brownish black to grayish black, dull, white spots of calcareous and siliceous, gypsum and pyrite disseminated, diatomite, carbonaceous mudstone interbedded.	
	J4	Brownish black, dull, crumbly, white spots of calcareous and siliceous, gastropod fragments (<i>Melanoidea sp.</i>), gypsum and pyrite disseminated.	
	J3	Brownish black, dull, white spots of calcareous and siliceous, gypsum and pyrite disseminated, with carbonaceous mudstone interbedded.	



Figure 3.11 Sample descriptions of J seam coal.



Coal seam	Coal subseam	Description	Core sample
I	I2	Brownish black, dull, crumbly, abundant gypsums and pyrites disseminated, and gastropod fossils (<i>Margaya sp.</i>).	
	I1	Brownish black, dull, mostly crumbly, abundant gypsums and pyrites disseminated, and gastropod fossils (<i>Margaya sp.</i>).	



Figure 3.12 Sample descriptions of I seam coal.

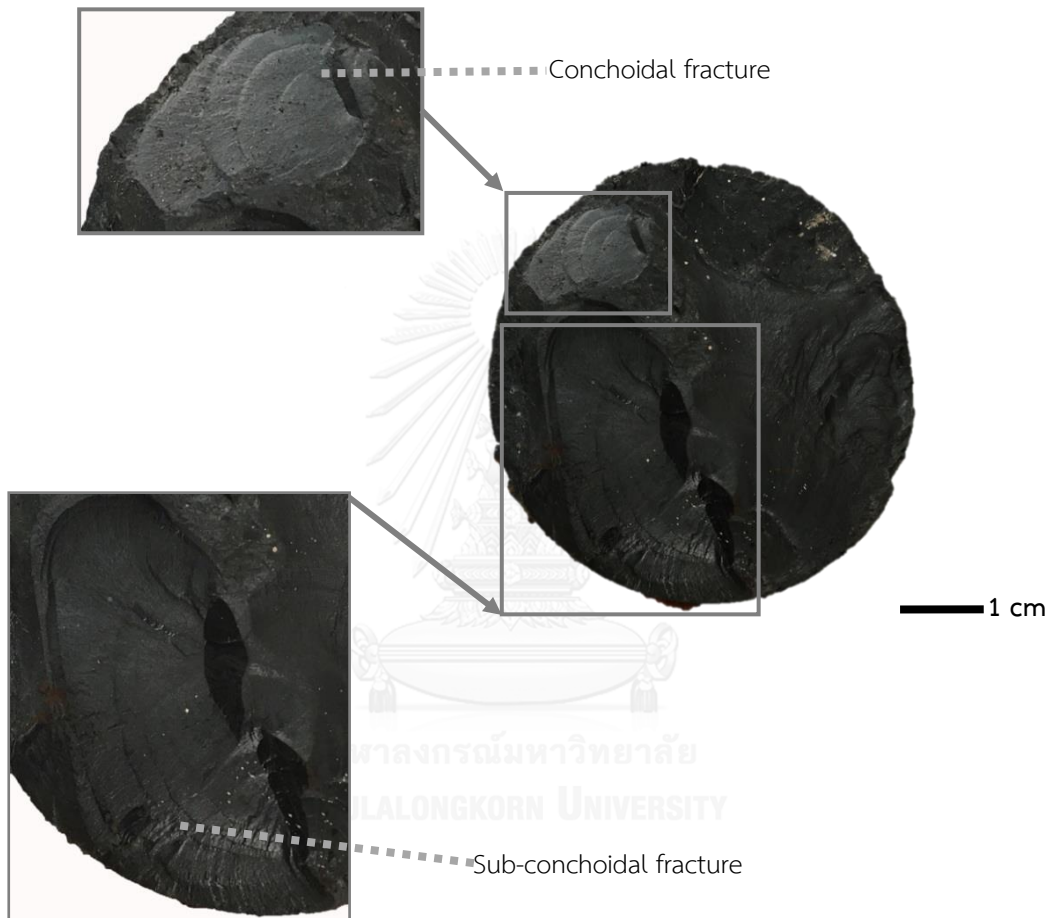


Figure 3.13 Mesoscopic of Q4 subseam - grayish black to black, dull, brittle to hard, sub-conchoidal to conchoidal fracture.



Figure 3.14 Mesoscopic of Q3 subseam - grayish black to black, dull, brittle to hard, sub-conchoidal to conchoidal fracture and plant remains.

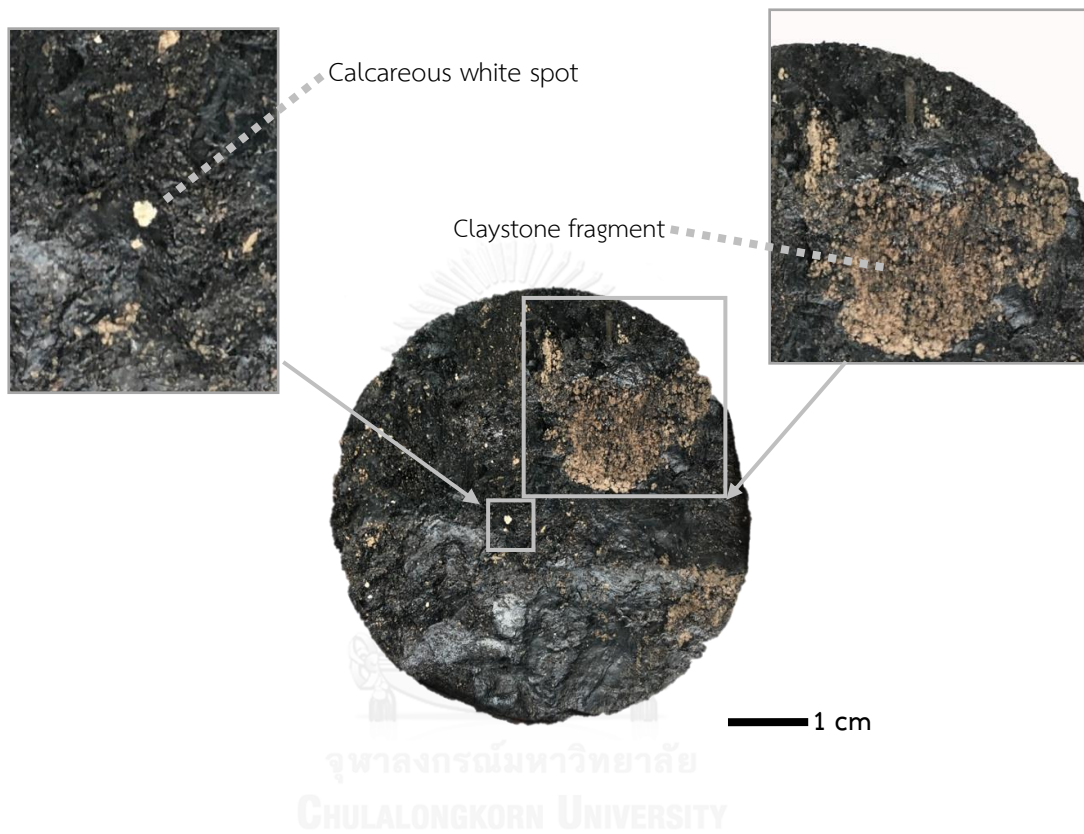


Figure 3.15 Mesoscopic of Q2 subseam - brownish black to grayish black, dull, brittle to slightly hard, sub-conchoidal fracture, claystone fragments, calcareous white spot and plant remains.

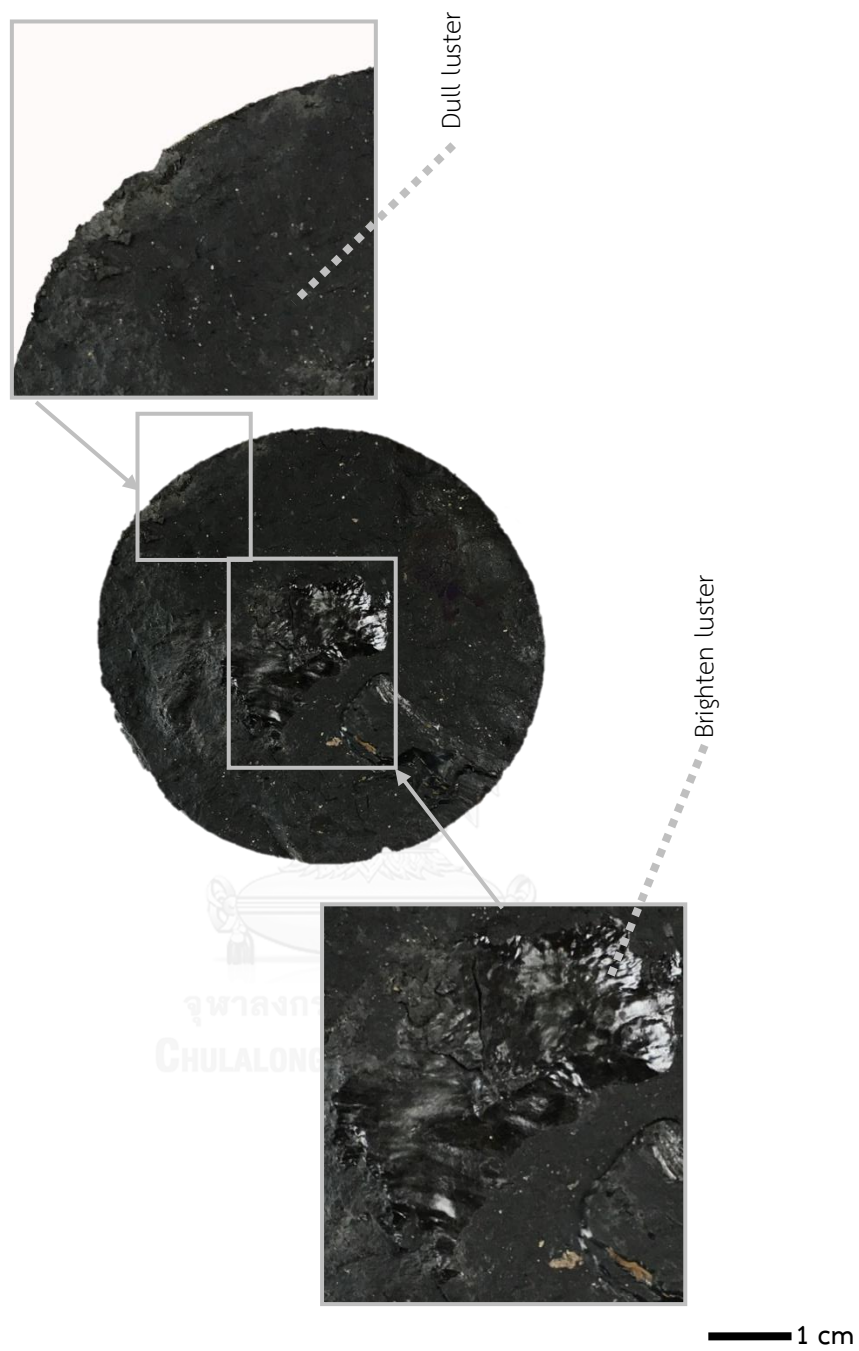


Figure 3.16 Mesoscopic of Q1 subseam - grayish black to black, dull to brighten banded, brittle to hard, sub-conchoidal to conchoidal fracture.

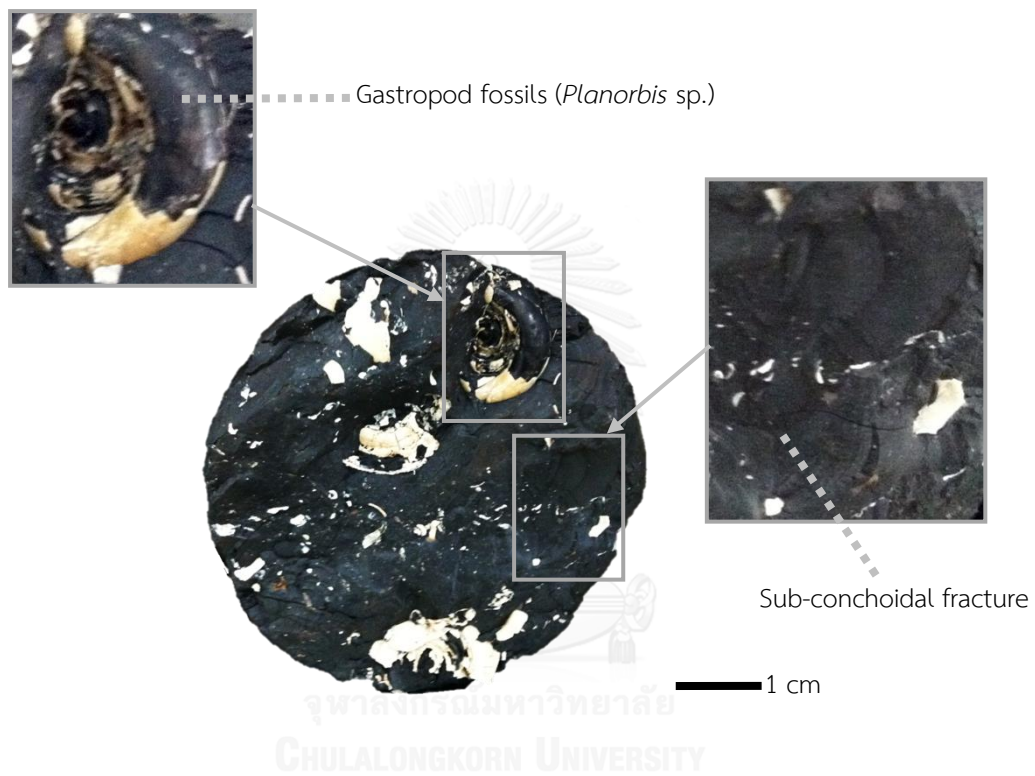


Figure 3.17 Mesoscopic of K3 subseam - grayish black to black, dull to slight bright in part, brittle to hard, sub-conchoidal to conchoidal fracture, gastropod fossils (*Planorbis* sp.), and white spots of calcareous.

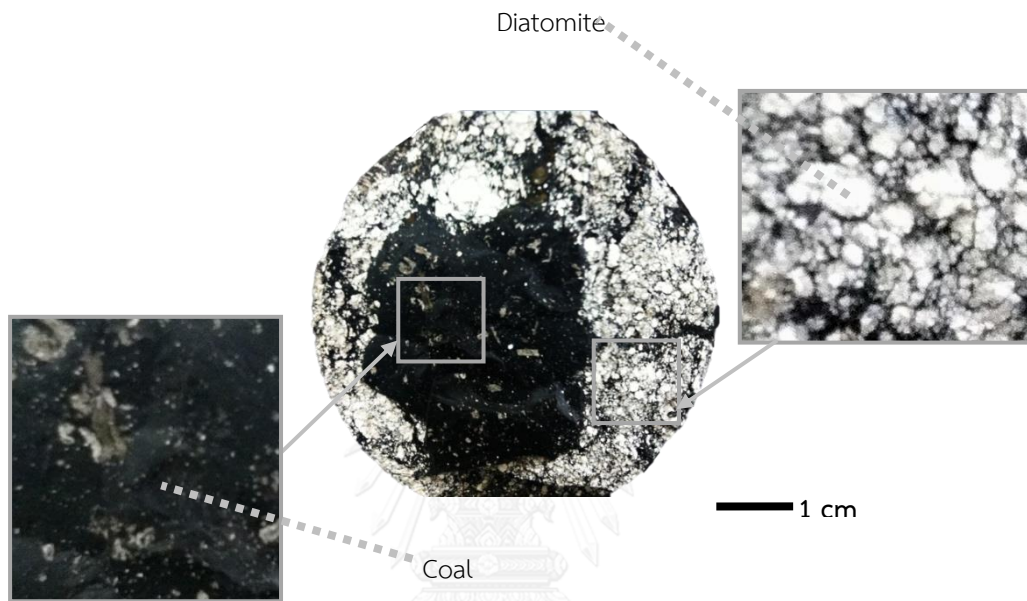


Figure 3.18 Mesoscopic of K2 subseam - grayish black, dull, brittle to slightly hard, sub-conchoidal to conchoidal fracture, layers of diatomite and plant remains.

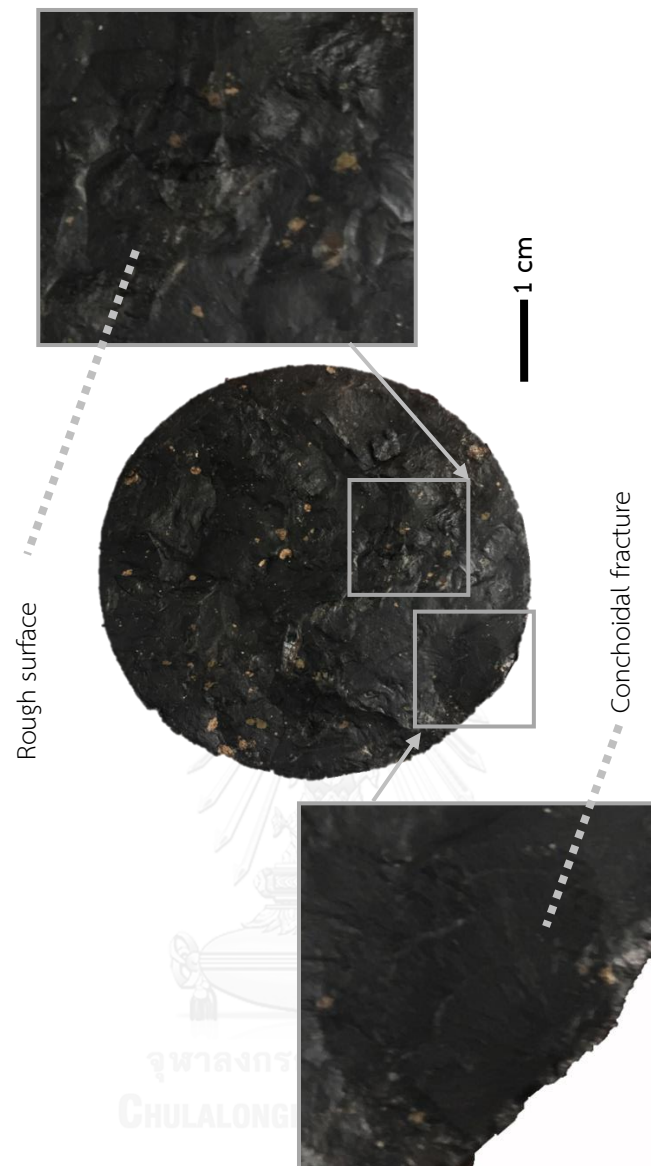


Figure 3.19 Mesoscopic of K1 subseam - grayish black to black dull to slight bright in black band, brittle to slightly hard, sub-conchoidal to conchoidal fracture, rough core surface.



Figure 3.20 Mesoscopic of J6 subseam - brownish black to grayish black, dull, brittle, and gastropods remain (*Melanoides sp.*).

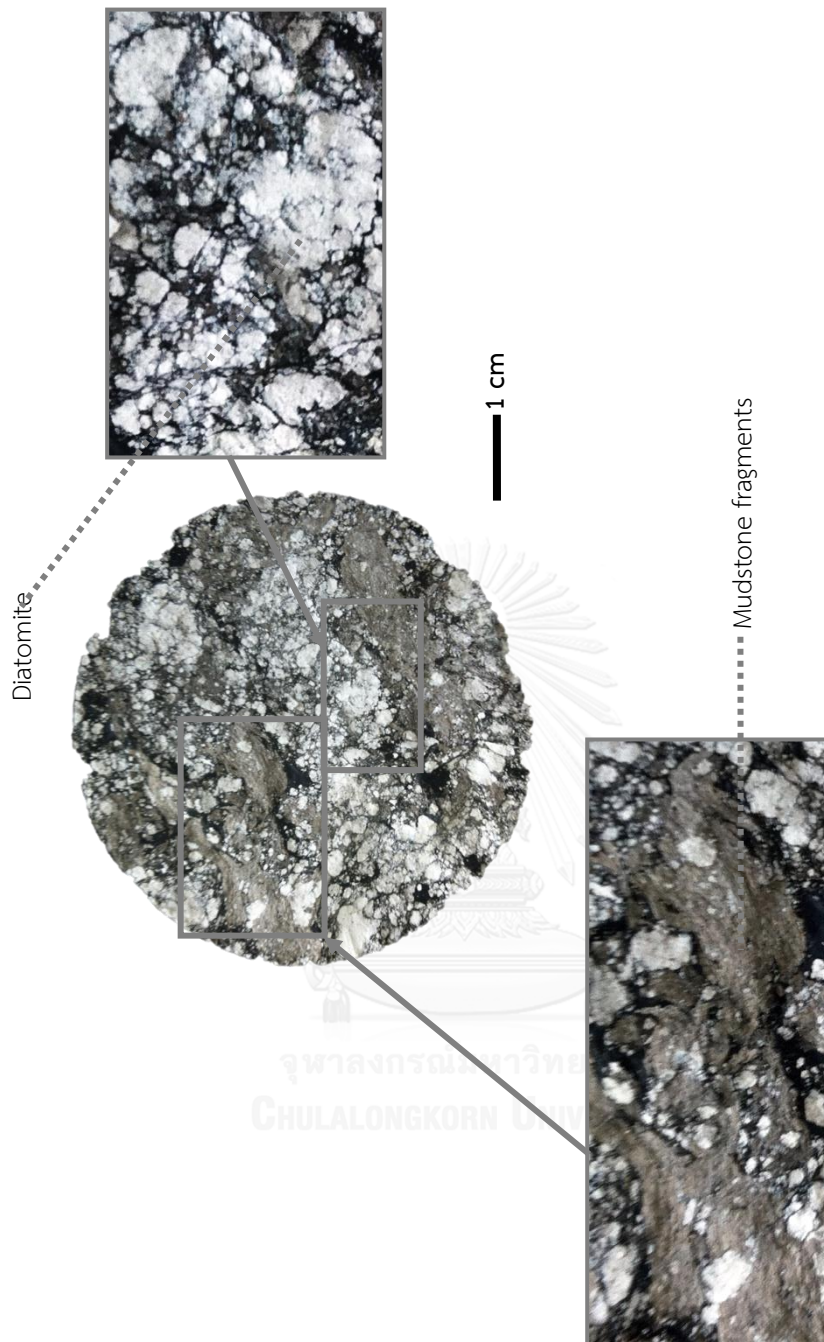


Figure 3.21 Mesoscopic of J5 subseam - brownish black to grayish black, dull, white spots of fossil fragments, mudstone fragments and volcanic debris?

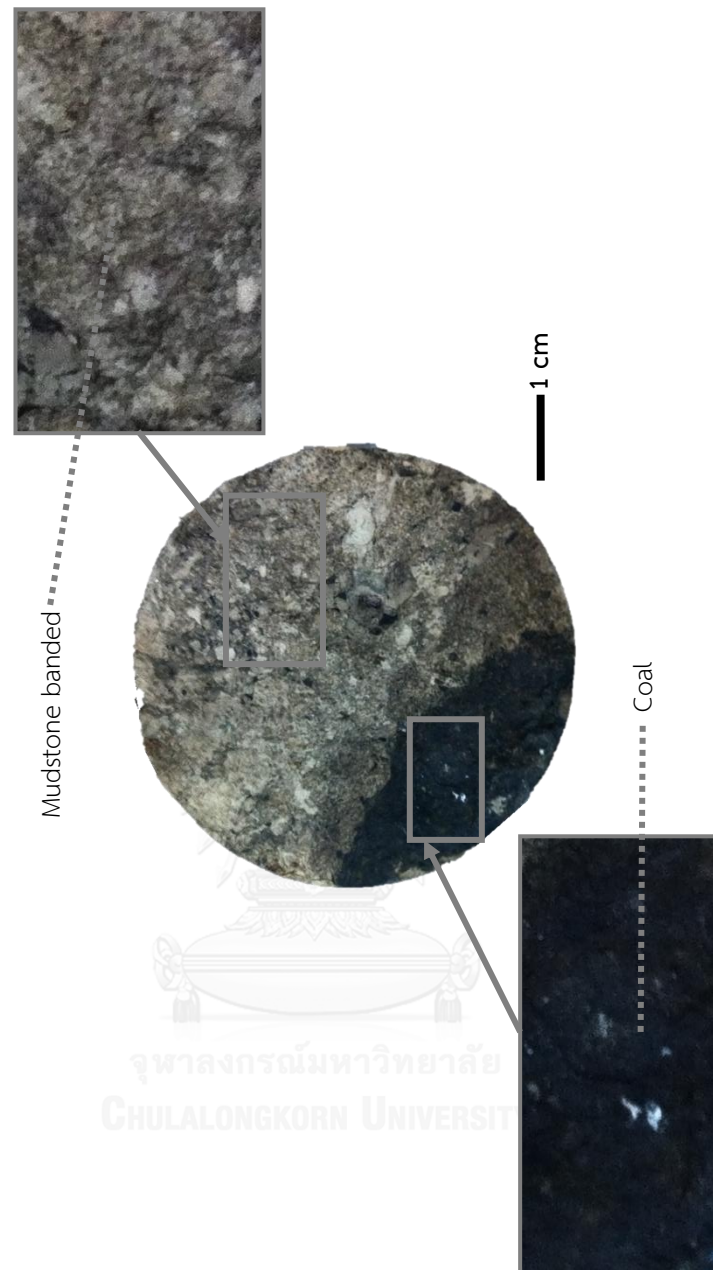


Figure 3.22 Mesoscopic of J4 subseam - brownish black, dull, white spots of calcareous and siliceous, mudstone banded and volcanic debris?.

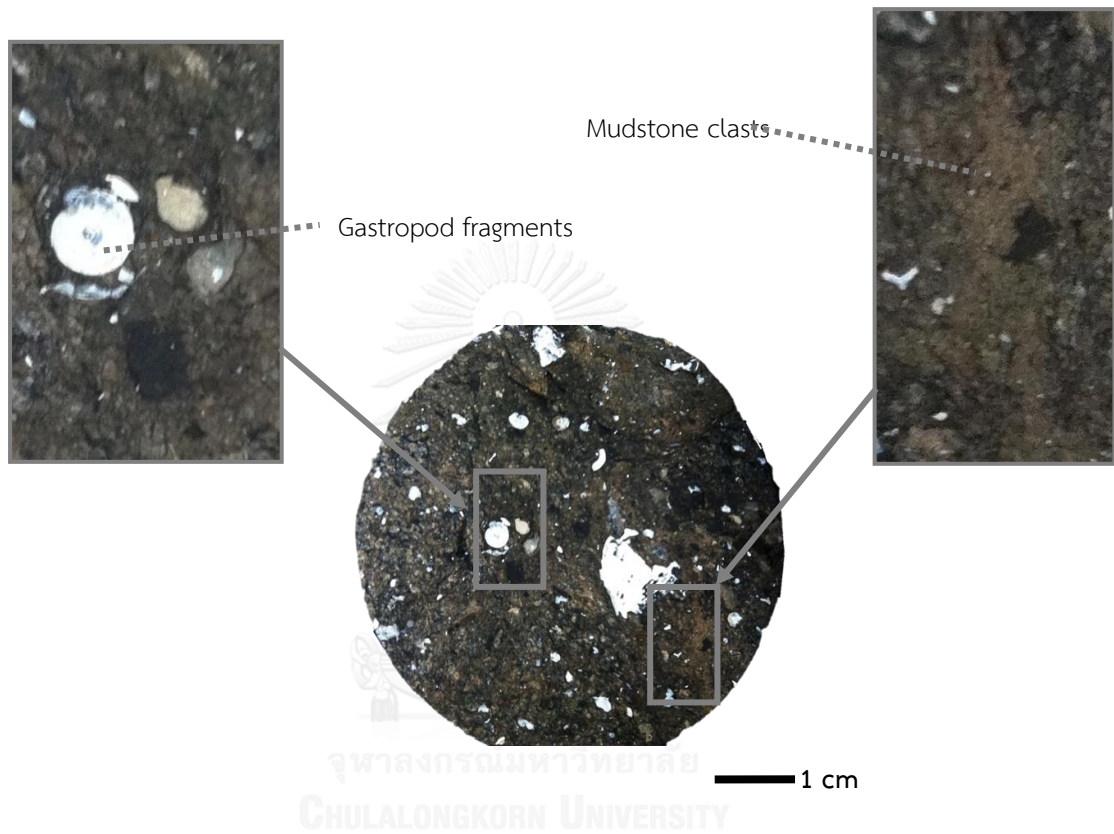


Figure 3.23 Mesoscopic of J3 subseam - brownish black, dull, white spots of fossils fragments, with mudstone clasts.

3.2 Analytical method

3.2.1 Petrographic analysis

Petrographic study of coal is different from petrographic study of other rock because shape and internal structure of macerals (organic material) are more visible under the fluorescence mode. Therefore, the samples were prepared as polished section (figure 3.24). The polished section procedures are as follows;

- (1) The samples were cut to blocks (maximum size approximately 8-9 cm in length). Each sample was perpendicular and parallel with bedding by cutting.
Brittle material was impregnated with epoxy resin.
- (2) Polished the sample on the high speed polishing machine using silicon carbide powder (grit 200) until the sample were smooth.
- (3) Polished the sample on the polishing mirror using silicon carbide powder (grit 400, 600 and 1000) by hand until the sample were very smooth. Then, cleaned the sample with water.
- (4) Polished the sample using chromium oxide approximately 20 minutes and micropolish (0.05 μm gamma alumina) approximately 20 minutes as well.
- (5) Cleaned the sample by water and to rub gently on a polishing cloth while water is flowing.



Figure 3.24 The polished section of coal for petrographic microscope study.

Coal sample were studied under polarizing microscope with UV. Excitation (figure 3.25). Macerals were identified and counted. Vitrinite, liptinite, inertinite, and maceral matter were calculated to percentage. It can imply to depositional environment and relate to coalification rank.



Figure 3.25 Polarizing microscope with UV Excitation at Geology department, Chiangmai University.

3.2.2 Geochemical analysis

3.2.2.1 Proximate analysis

Proximate geochemical analysis was used to evaluate the percentage by weight of the fixed carbon, volatiles matters, ash and moisture content in sample. Sample preparation for proximate analysis is as follows;

Coal samples were crushed to size 250 μm and were split. Then, each sample is weighed approximately 1 g in crucible.

Proximate analysis procedures

(1) The crushed samples were weighed 1 g in crucibles. The crucibles were taken to the oven at $108\pm 2^\circ\text{C}$ with the lids for 1 hour. The samples were cooled in desiccator.

(2) The sample were weighed again and were calculated the loss in weight. The loss of weight is moisture value. Then, the moisture values were made to percentage.

(3) The samples from step 1 and 2 were heated at $900\pm 15^\circ\text{C}$ in furnace without lids for 1 hour and 30 minutes until the carbon was burned. The residue remaining was weighed as ash.

(4) The flash crushed samples were weighed approximately 1 g in crucibles with lid. Then, the crucibles were taken to the furnace and were heated at $900\pm 15^\circ\text{C}$ for 7 minutes. The samples were cooled in desiccator.

(5) Weighed the sample and calculated the loss in weigh. Then, the volatile matter was calculated from % volatile matter = % the loss in weight - %moisture.

(6) From step 1-5, there are 3 values: %moisture, %ash, and %volatile matter. Then, Fixed carbon value was calculated from this equation: % fixed carbon = 100 - (%moisture - %ash - %volatile matter) (ASTM D4182-97, 2004).

Moreover, the mixed samples were weighed 1 g and were analyzed proximate analysis in the proximate analyzer (LECO TGA-701) (figure 3.26) for moisture content, ash content, volatile matter content and fixed carbon content of mixed sample.



Figure 3.26 Proximate analyzer (LECO TGA-701) at Laboratory Section, Mae Moh Mine.

3.2.2.2 Ultimate analysis

Ultimate geochemical analysis was used to indicate various elemental chemical constituents include carbon, hydrogen, nitrogen, oxygen and sulphur.

The crushed samples were weighed approximately 1 g in consumable aluminum or tin capsules and were taken to the CHN determinator (LECO TRuSpec CHN) for carbon, hydrogen and nitrogen content (Figure 3.27) and S determinator (LECO SC632) for sulphur content (figure 3.28). The samples were injected into

combustion chamber. The combustion products were change into N_2 , CO_2 , H_2O and SO_2 (D4239-12, 2012)(ASTM D4239-12, 2012). Each element was measured in several stages and oxygen was calculated.



Figure 3.27 CHN determinator (LECO TRuSpec CHN) for carbon, hydrogen and nitrogen contents at Laboratory Section, Mae Moh Mine.



Figure 3.28 S determinator (LECO SC632) for sulphur contents at Laboratory Section, Mae Moh Mine.

3.2.2.3 Calorific value analysis

The crushed samples were weighed approximately 1 g and were taken to the bomb calorimeters (LECO AC600) (figure 3.29). The water temperature increase surrounding the vessel. Then, the gross calorific value was calculated (ASTM D5865-11a, 2011).



Figure 3.29 Bomb calorimeters (LECO AC600) at Laboratory Section, Mae Moh Mine.

Chapter 4

4. Results

The scope of this study is coal petrography and associated stratigraphy in central part of Mae Moh basin. The study 3 boreholes are used to interpret the lithostratigraphy. 35 coal samples were collected from 3 boreholes for petrographic and geochemical analysis. They were collected from main coal seams in Mae Moh group as J-, K- and Q seam of the Na Khaem formation, and minor coal seam is I seam in Huai Luang formation. The resulting can be used to determine for coal quality, coalification rank and depositional paleo environment as well.

4.1 Lithostratigraphy

The Mae Moh group lies unconformably on the Triassic Lamphang group. It also underlies unconformably the coarse grained terrigenous sediments of Quaternary fluvial deposits. Focusing on Tertiary sequence of the Mae Moh basin has been named the Mae Moh group were investigated by the detailed lithostratigraphic logs of these 3 study boreholes along with pervious stratigraphy. Mae Moh group is divided into 3 formations. The lower sequence is Huai King formation (0 –300 m, thick), overall is a finding upwards sequence that culminates in a dominantly silty clay facies interbedded fluvial and alluvial sandstone, partially oxidized sandy claystone, and siltstone with calcrete layers at the base of the Mae Moh basin, no macrofossils, abundant gastropods (*Viviparus* sp.) are present in the lower part of the formation. The middle sequence is Na Khaem formation (300–400 m, thick) which deposited fine-grained grey sediments with the coal bearing from bottom to top as S-, R-, Q-, K-, and J- seams. The upper sequence is Huai Luang formation (0-400 m, thick) which is also commonly referred to Red Beds, consists of red to brownish-red, claystone, siltstone and mudstone with lenses of sandstone, no macrofossils, abundant gypsums and pyrites with rare plant roots. This formation

contains the minor coal seam namely I seam, which abundant partly pyritized gastropods (*Margaya* sp.). The Tertiary sediment is overlain by unconsolidated Quaternary fluvial deposits consist of materials up to 30 m thick: top soils, clays, silts, sands and gravels, vary color: yellow, red, light to medium brown, extend across much of the area. The stratigraphy of study area can be explained by lithostratigraphy studied are as follows;

4.1.1 Borehole no. MMC-1

Borehole no. MMC-1 located in central part of Mae Moh basin at mine grids; north 17.04, west 13.96, and 317 m thick. Sedimentary sequence composed of Huai Luang formation in the upper and Na Khaem formation in the lower. The geological cross section of mine grid line North 17 (figure 4.1) and sedimentary log is described from the bottom to top (figure 4.2).

The lower sequence is underburden of member III in Na Khaem formation, represented by claystone, mudstone and silty claystone, grey to greenish grey, highly calcareous, abundant gastropod fossils (*Paludina* sp.) in the upper bedded. This sequence is overlaid by Q seam of member II in Na Khaem formation.

The Q seam is divided into 4 subseams as Q4, Q3, Q2 and Q1 from bottom to top, which identified by their geophysical responses and lithological features. The thickness of Q seam is 19.4 m. Lower subseam is Q4; grayish black to black, dull to slightly bright in black banded, soft to brittle in a top part and hard in a bottom part, sub-conchoidal to conchoidal fracture, pyrites disseminate and plants remain, 5.15 m thick. Q3 is grayish black to black, dull to brighten in black banded, brittle to hard, sub-conchoidal to conchoidal fracture, pyrites disseminate, and plants remain, 1.85 m thick. Middle subseam is Q2; brownish black to grayish black, dull, brittle to slightly hard, sub-conchoidal fracture, carbonaceous mudstone and silty claystone interbedded, siliceous and calcareous white spots, pyrites disseminate, and plants remain, 5.65 m thick. Upper subseam is Q1; brownish black to grayish black, dull,

brittle to hard, sub-conchoidal to conchoidal fracture, carbonaceous mudstone and silty claystone interbedded, pyrites disseminate, and plants remain, 6.75 m thick.

Over the Q seam is represented by brown, brownish gray, gray, green and greenish gray claystone is containing common coal flakes, plants remain, rare ostracods. This sequence is named interburden (23.65 m, thick) of member II in Na Khaem formation.

Interberden is overlaid by K seam. K seam is upper part of member II in Na Khem formation, divided into 3 subseams as K3, K2, and K1 from bottom to top which identified by their geophysical responses and lithological features. The thickness of K seam is 22.75 m. Lower subseam is K3; grayish black to black, dull, brittle to hard, sub-conchoidal to conchoidal fracture, gastropod fossils (*Planorbis sp.*), calcareous and siliceous white spots, pyrite disseminated and plants remain, 8.8 m thick. Middle subseam is K2; brownish black to grayish black, dull, brittle to slightly hard, sub-conchoidal to conchoidal fracture, carbonaceous mudstone and silty claystone interbedded, siliceous and carbonaceous white spots, pyrite disseminated, diatom layers, gastropod fossils (*Planorbis sp.*) and plants remain, 7.65 m thick. Upper subseam is K1; grayish black to black, dull to brighten in black banded, brittle to hard, sub-conchoidal to conchoidal fracture, calcareous and siliceous white spots, pyrite disseminated and plants remain, 6.3 m thick.

Over K seam is represented by claystone and mudstone with occasional siltstone, brownish gray, highly calcareous, pyritic in part, coal flakes, gastropod (*Melanoides sp.*) interbedded. This sequence is named overburden (78.75 m, thick) of member I in Na Khaem formation. In this sequence is consisting of J seam. In study area remains 4 subseams as J6, J5, J4 and J3 from bottom to top which identified by their geophysical response and lithological features. The J seam is interbedded by thin to thick bedded of fine grained grey sediments. Lower subseam is J6; brownish black to grayish black, dull, brittle, pyrite disseminated, gastropod fossils (*Melanoides*

sp.) and plants remain, 1.7m thick. J5 is brownish black to grayish black, dull, calcareous and siliceous white spots, gypsum and pyrite disseminated, thin carbonaceous mudstone interbedded, 4.1 m thick. J4 is brownish black, dull, crumble, calcareous and siliceous white spots, gastropod fragments, gypsum and pyrite disseminated, 0.7 m thick. J3 is brownish black, dull, calcareous and siliceous white spots, carbonaceous mudstone fragments, gypsum and pyrite disseminated, 0.7 m thick.

The Na Khaem formation is overlaid by Huai Luang formation represented by claystone, siltstone and mudstone are red to brownish red, with lenses of sandstone, no macrofossils, abundant gypsums and pyrites disseminated with rare plant roots, gray silty claystone with red brown mottled in the bottom part.



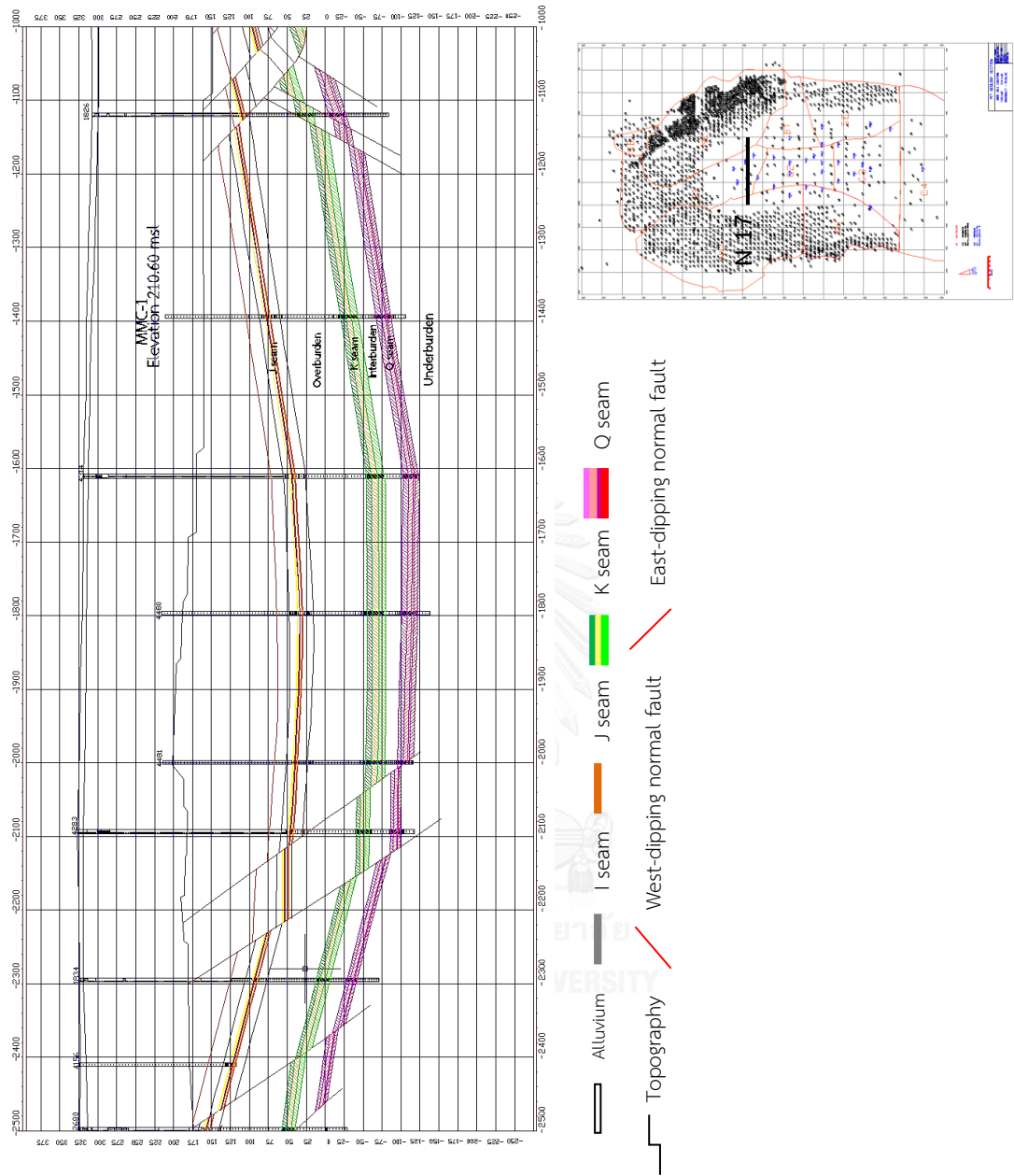


Figure 4.1 Geological cross section of mine grid line N17 in central part of Mae Moh basin (unpublished cross section from EGAT, 2016).

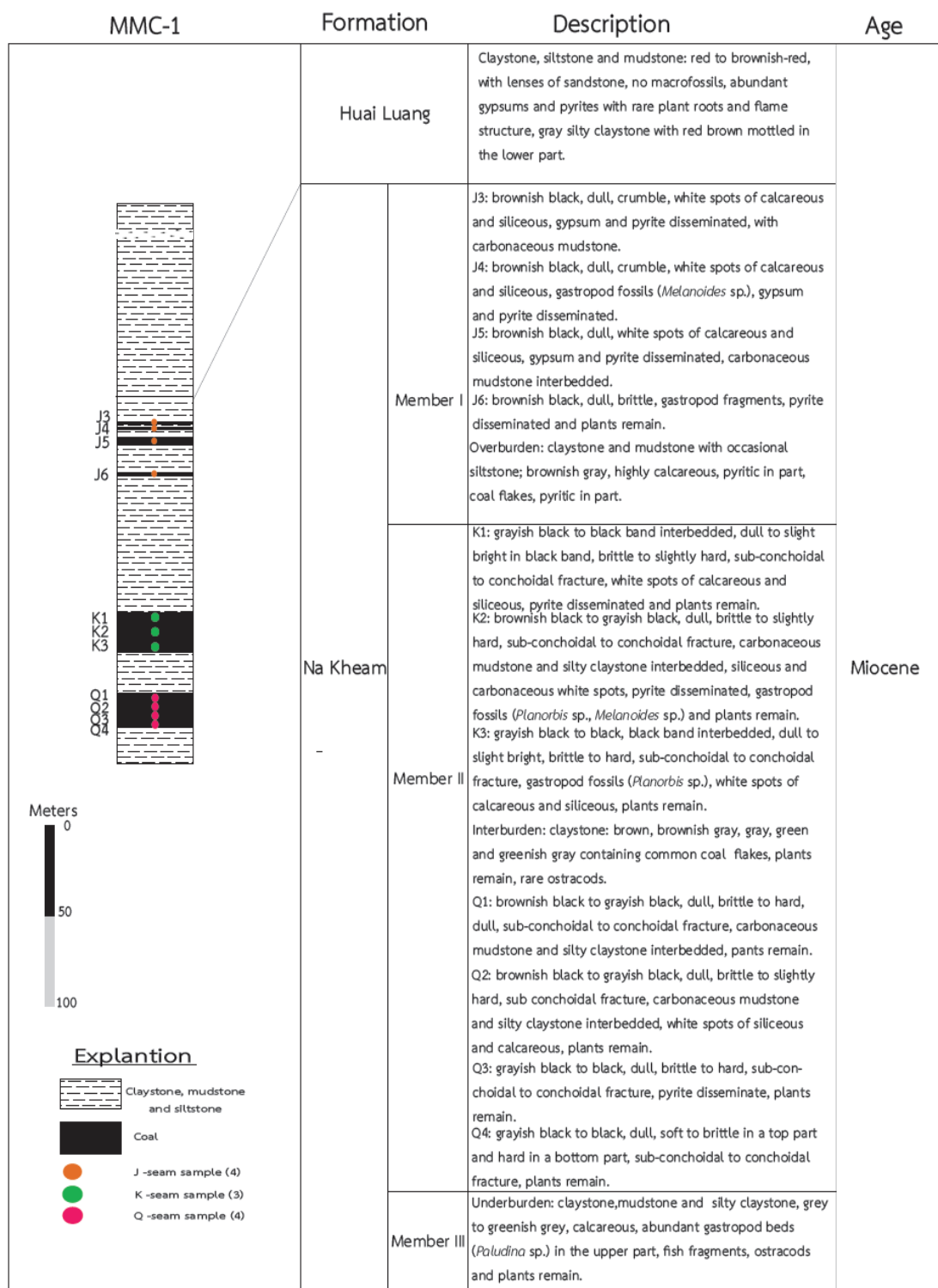


Figure 4.2 Lithostratigraphic column of borehole no. MMC-1

4.1.2 Borehole no. MMC-2

Borehole no. MMC-2 located in central area of Mae Moh basin at mine grids; north 7.83, west 17.03 and 565 m thick. Sedimentary sequence composed of Quaternary deposited in the upper, Huai Luang formation in the middle, and Na Khaem formation in the lower. The geological cross section of mine grid line North 8 (figure 4.3) and sedimentary log is described from the bottom to top (figure 4.4).

The lower sequence is underburden of member III in Na Khaem formation which represented by claystone, mudstone and silty claystone, grey to greenish grey, highly calcareous, abundant gastropod fossils (*Paludina* sp.) in the upper bedded, ostracods and plants remain. This sequence is overlaid by Q seam of member II in Na Khaem formation.

The Q seam is divided into 4 subseams as Q4, Q3, Q2 and Q1 from bottom to top, which identified by their geophysical responses and lithological features. The thickness of Q seam is 19 m. Lower subseam is Q4; grayish black to black, dull, soft in a top part and brittle to hard in a bottom part, sub-conchoidal to conchoidal fracture, pyrites disseminate and plants remain, 4.2 m thick. Q3 is grayish black to black, dull to brighten in black banded, brittle to hard, sub-conchoidal to conchoidal fracture, pyrites disseminate, and plants remain, 2.5 m thick. Middle subseam is Q2; grayish black, dull, brittle to slightly hard, sub-conchoidal fracture, carbonaceous mudstone and silty claystone interbedded, siliceous and calcareous white spots, pyrites disseminate, and plants remain, 6.1 m thick. Upper subseam is Q1; grayish black, dull, brittle to hard, sub-conchoidal to conchoidal fracture, carbonaceous and siliceous white spots, mudstone and silty claystone interbedded, pyrites disseminate, and plants remain, 6.2 m thick.

Over the Q seam is represented by brown, brownish gray, gray, green and greenish gray claystone is containing common coal flakes, plants remain, rare ostracods. This sequence is named interburden (23.9 m, thick) of member II in Na Khaem formation.

Interberden is overlaid by K seam. K seam is upper part of member II in Na Khaem formation, divided into three subseams as K3, K2, and K1 from bottom to top, which identified by their geophysical responses and lithological features. The thickness of K seam is 24.3 m. Lower subseam is K3; grayish black to black, dull to brighten in black banded, brittle to slightly hard, sub-conchoidal to conchoidal fracture, calcareous and siliceous white spots, pyrite disseminated, gastropod fossils (*Planorbis* sp.) and plants remain, 6.8 m thick. Middle subseam is K2; brownish black, dull, brittle to slightly hard, sub-conchoidal to conchoidal fracture, siliceous and carbonaceous white spots, mudstone and silty claystone interbedded, pyrite disseminated, gastropod fossils (*Planorbis* sp.) and plant remains, 11 m thick. Upper subseam is K1; grayish black to black, dull to brighten in black banded, brittle to hard, sub-conchoidal to conchoidal fracture, pyrite disseminated and plant remains, 6.5 m thick.

Over K seam is represented by claystone and mudstone with occasional siltstone, brownish gray, highly calcareous, pyritic in part, coal flakes, gastropod (*Planorbis* sp.) interbedded. This sequence is named overburden (83.4 m thick) of member I in Na Khaem formation. In this sequence is consisting of J seam. In study area remains 4 subseams as J6, J5, J4 and J3 from bottom to top which identified by their geophysical response and lithological features. The J seam is interbedded by thin to thick bedded of fine grained grey sediments. Lower subseam is J6; brownish black to black, dull, brittle, pyrite disseminated, gastropod fossils (*Melanoides* sp.) and plant fragments, 2.1 m thick. J5 is brownish black; dull, soft to brittle, calcareous and siliceous white spots, gypsum and pyrite disseminated, carbonaceous mudstone interbedded, 3 m thick. J4 is brownish black, dull, calcareous and siliceous white spots, gastropod fragments, gypsum and pyrite disseminated, 0.7 m thick. J3 is brownish black, dull, crumble, calcareous and siliceous white spots, silty claystone fragments, gypsum and pyrite disseminated, 0.8 m thick.

The Na Khaem formation is overlaid by Huai Luang formation is represented by claystone, siltstone and mudstone are red to brownish-red, with lenses of sandstone, no macrofossils, abundant gypsums and pyrites with rare plant roots and

flame structure and minor coal seam namely I seam. I seam is brownish black, dull, mostly crumble, gypsum and pyrite disseminated, and gastropod fragments (*Margaya* sp.), 2 m thick. The Huai Luang formation is the upper sequence of Mae Moh group, which underlies unconformably the coarse grained terrigenous sediments of Quaternary fluvial deposits.

The uppermost Quaternary deposited is represented by alluvium which composed of top soils, clays, silts, sands, gravels, vary color: yellow, red, and light to medium brown.



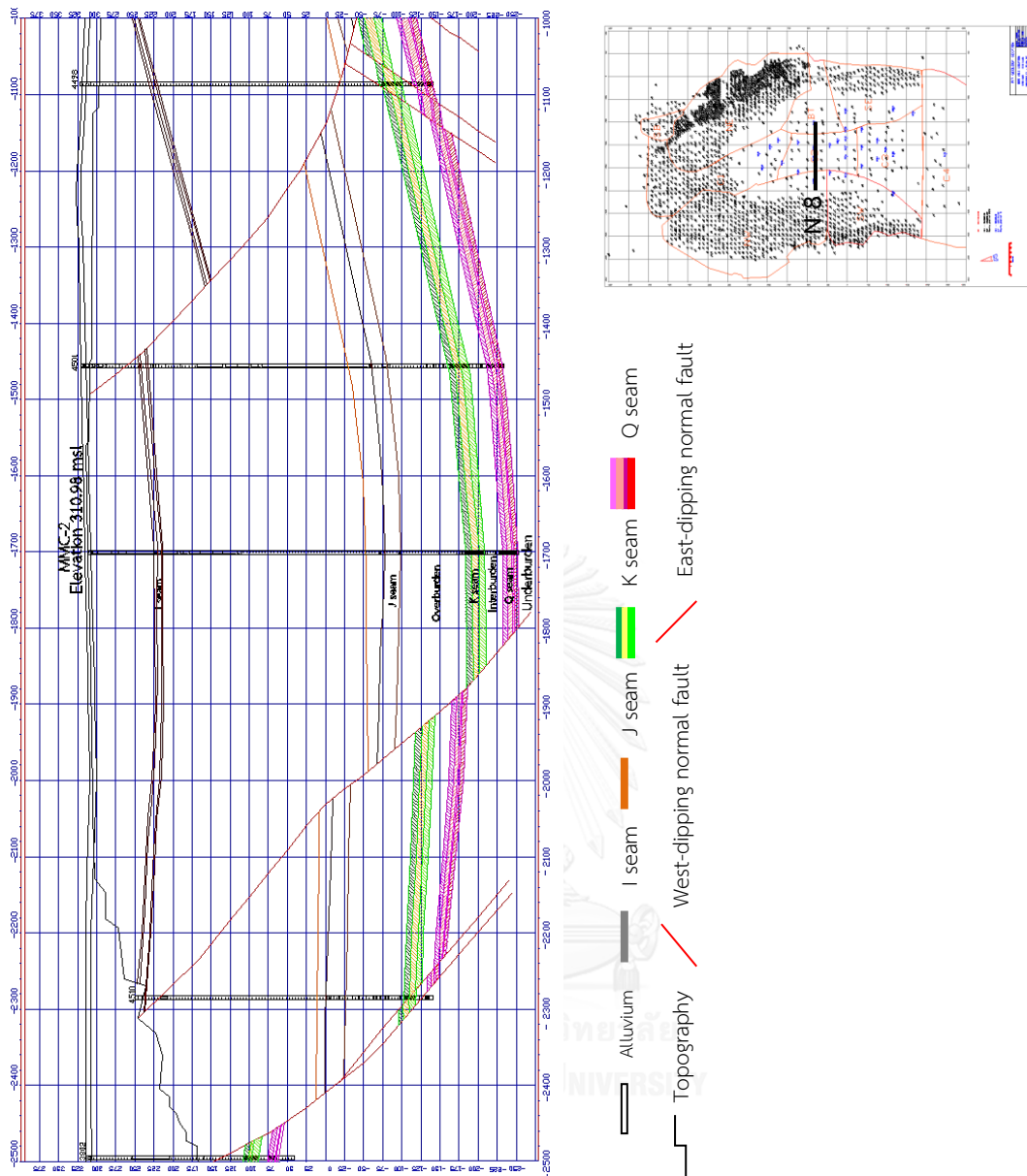


Figure 4.3 Geological cross section of mine grid line N8 in central part of Mae Moh basin (unpublished cross section from EGAT, 2016).

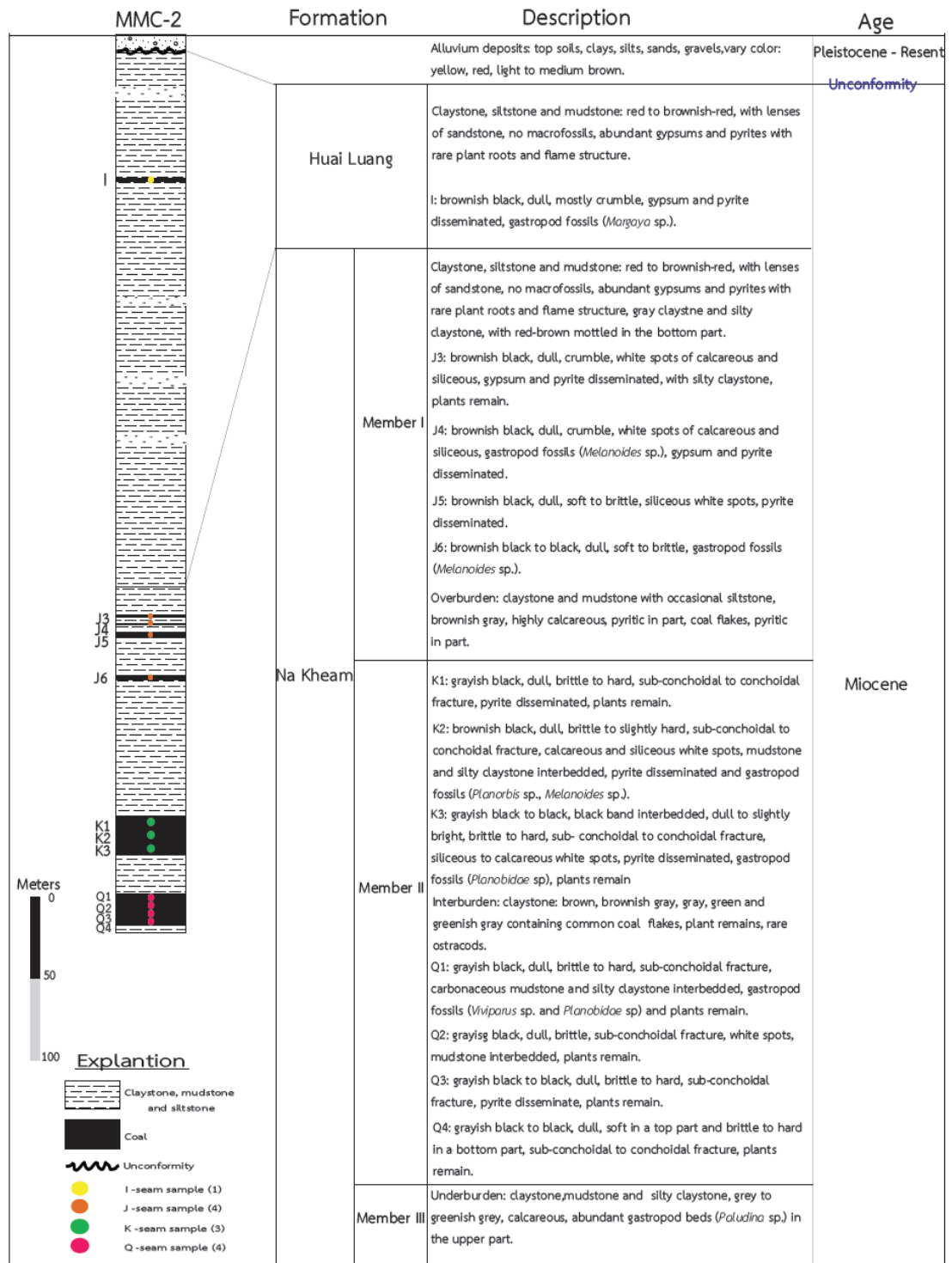


Figure 4.4 Lithostratigraphic column of borehole no. MMC-2.

4.1.3 Borehole no. MMC-3

Borehole no. MMC-3 located in central area of Mae Moh basin at mine grids; north 0.048, west 19.71 and 500 m thick. Sedimentary sequence composed of Quaternary deposited in the upper, Huai Luang formation in the middle, and Na Khaem formation in the lower. The geological cross section of mine grid line North 8 (figure 4.5) and sedimentary log is described from the bottom to top (figure 4.6).

The lower sequence is underburden of member III in Na Khaem formation which represented by claystone, mudstone and silty claystone, grey to greenish grey, highly calcareous, abundant gastropod fossils (*Paludina* sp.) in the upper part, ostracods and plants remain. This sequence is overlaid by Q seam of member II in Na Khaem formation.

The Q seam is divided into 4 subseams as Q4, Q3, Q2 and Q1 from bottom to top, which identified by their geophysical response and lithological features. The thickness of Q seam is 18.5 m. Lower subseam is Q4; grayish black to black, dull, soft in a top part and brittle to hard in a bottom part, sub-conchoidal to conchoidal fracture, pyrites disseminate and plants remain, 4.1 m thick. Q3 is grayish black to black, dull to brighten in black banded, brittle to hard, sub-conchoidal to conchoidal fracture, pyrites disseminate, and plants remain, 1.8 m thick. Middle subseam is Q2; grayish black, dull, brittle to slightly hard, sub-conchoidal fracture, carbonaceous mudstone and silty claystone interbedded, siliceous and calcareous white spots, pyrites disseminate, and plants remain, 5.6 m thick. Upper subseam is Q1; grayish black, dull, brittle to slightly hard, sub-conchoidal to conchoidal fracture, carbonaceous and siliceous white spots, mudstone and silty claystone interbedded, pyrites disseminate, gastropod fossils and plants remain, 7 m thick.

Over the Q seam is represented by brown, brownish gray, gray, green and greenish gray claystone is containing common coal flakes, plants remain, rare ostracods. This sequence is named interburden (23 m thick) of member II in Na Khaem formation.

Interberden is overlaid by K seam. K seam is upper part of member II in Na Khaem formation, divided into three subseams as K3, K2, and K1 from bottom to top which identified by their geophysical responses and lithological features. The thickness of K seam is 24 m. Lower subseam is K3; grayish black, dull, brittle to slightly hard, sub-conchoidal to conchoidal fracture, calcareous and siliceous white spots, pyrite disseminated, gastropod fossils (*Planorbis* sp.) and plants remain, 8 m thick. Middle subseam is K2; brownish black, dull, brittle to slightly hard, sub-conchoidal to conchoidal fracture, siliceous and carbonaceous white spots, carbonaceous mudstone and silty claystone interbedded, pyrite disseminated, gastropod fossils (*Planorbis* sp.) and plants remain, 10.2 m thick. Upper subseam is K1; grayish black to black, dull to bright in black banded, brittle to hard, sub-conchoidal to conchoidal fracture, pyrite disseminated and plants remain, 5.8 m thick.

Over K seam is represented by claystone and mudstone with occasional siltstone, brownish gray, highly calcareous, pyritic in part, coal flakes, gastropod (*Melanoidea* sp.) interbedded. This sequence is named overburden (72 m thick) of member I in Na Khaem formation. In this sequence is consisting of J seam. In study area 4 remains subseams as J6, J5, J4 and J3 from bottom to top which identified by their geophysical response and lithological features. The J seam is interbedded by thin to thick bedded of fine grained grey sediments. Lower subseam is J6; brownish black, dull, brittle, pyrite disseminated, gastropod fossils (*Melanoidea* sp.) and plant fragments, 1 m thick. J5 is brownish black, dull, white spots of calcareous and siliceous, gypsum and pyrite disseminated, carbonaceous mudstone interbedded, 2 m thick. J4 is brownish black, dull, crumble, calcareous and siliceous white spots, gastropod fragments, gypsum and pyrite disseminated, 1 m thick. J3 is brownish black, dull, crumble, gypsum and pyrite disseminated, with silty claystone fragments, 1 m thick.

The Na Khaem formation is overlaid by Huai Luang formation is represented by claystone, siltstone and mudstone are red to brownish-red, with lenses of sandstone and conglomerate, no macrofossils, abundant gypsums and pyrites with

rare plant roots and flame structure and minor coal seam namely I seam. I seam is brownish black, dull, mostly crumble, gypsum and pyrite disseminated, 2 m thick.

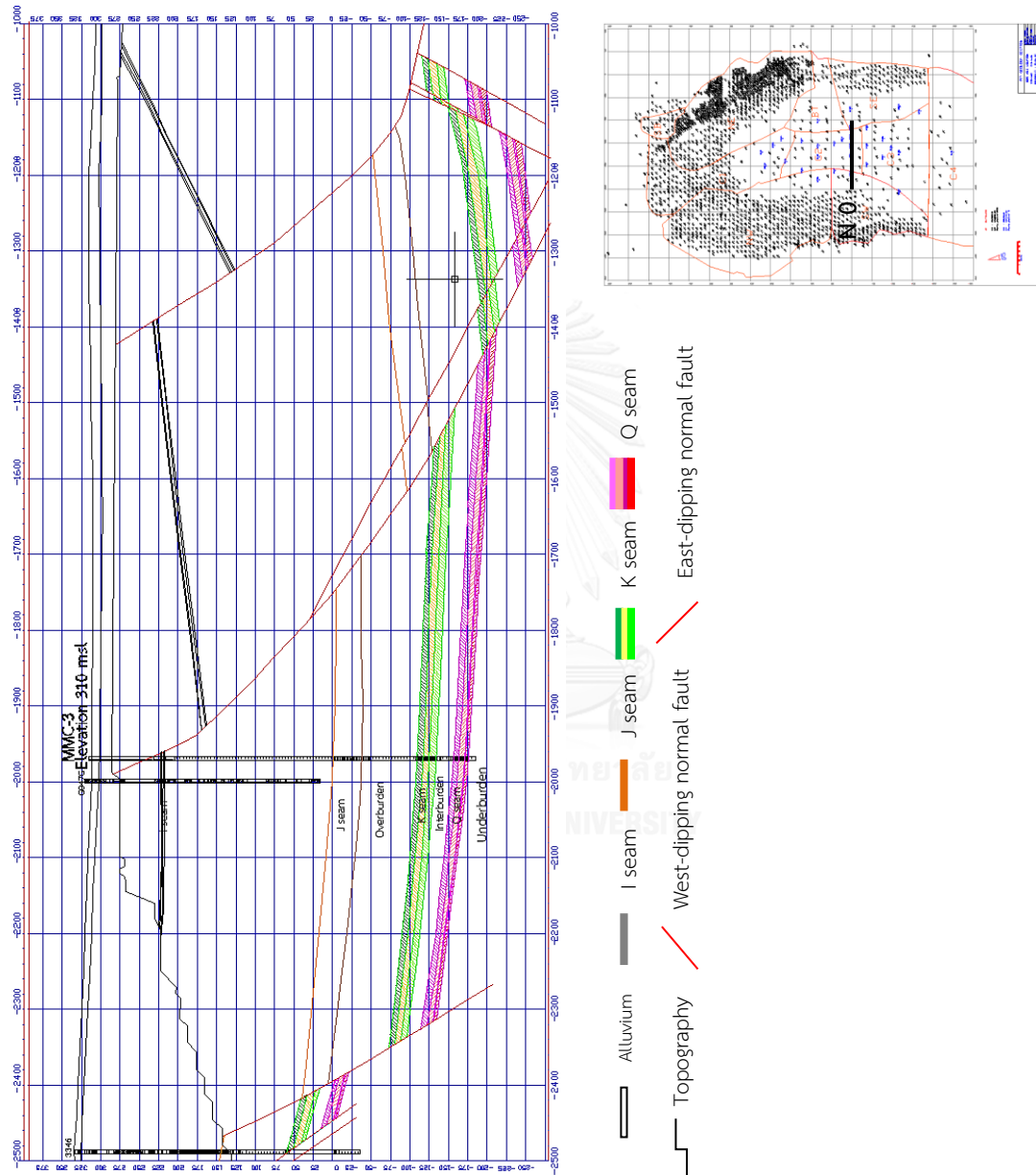


Figure 4.5 Geological cross section of mine grid line N0 in central part of Mae Moh basin (unpublished cross section from EGAT, 2016).

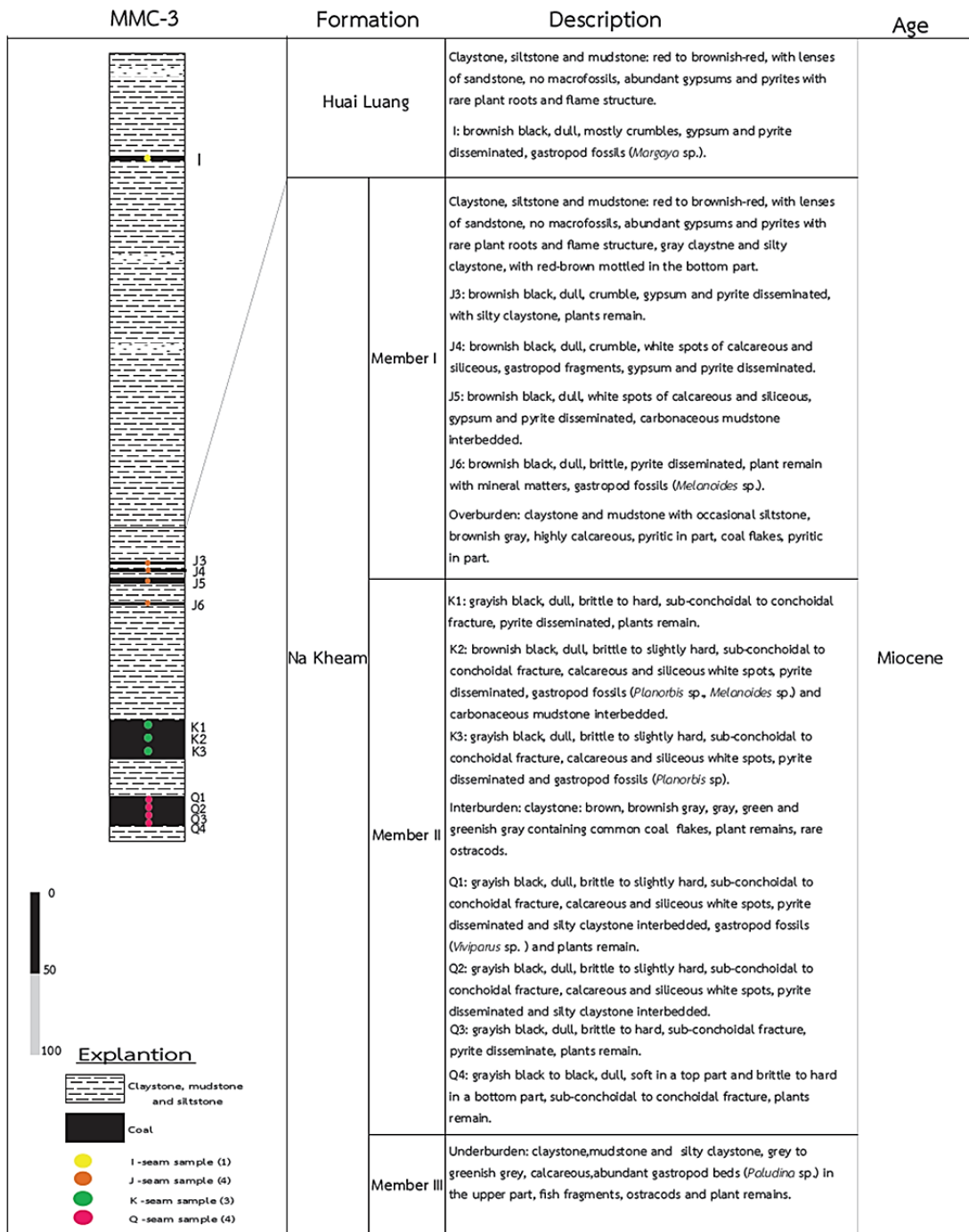


Figure 4.6 Lithostratigraphic column of borehole no. MMC-3.

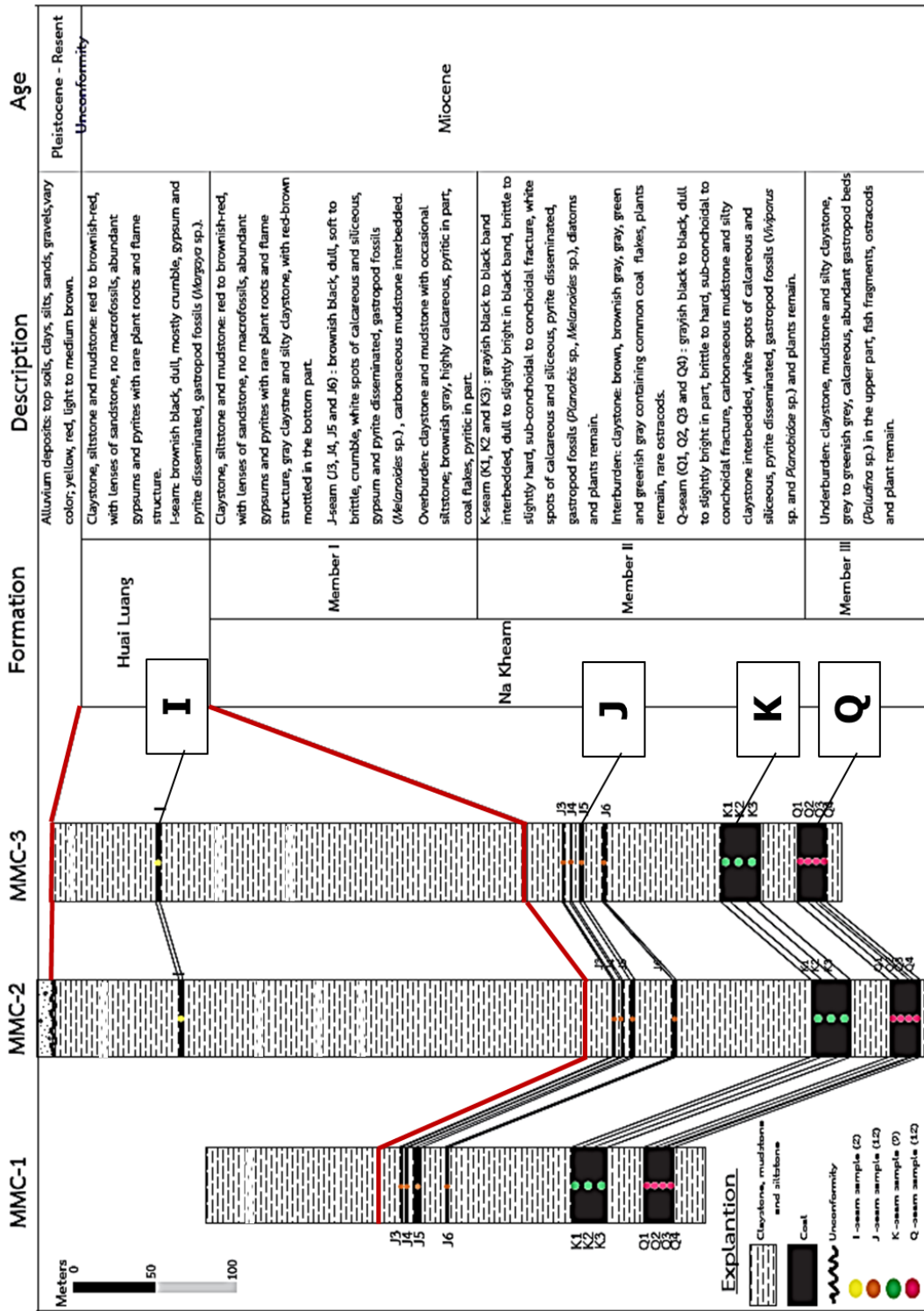


Figure 4.7 Composite stratigraphy of study area.

4.2 Geochemical results

Geochemical analysis was described the chemical variations within the coal sequence from the bottom to top of deposition. Coal samples were measured the proximate analysis, ultimate analysis, and calorific value analysis.

The proximate analyses of the lower sequence Q seam shows the weight *on as received basis* of fixed carbon ranges from 23.38 to 29.32%, volatile matter ranges from 30.06 to 31.34%, ash ranges from 12.13 to 16.08%, and moisture ranges from 28.49 to 29.48%.

K seam shows the weight of fixed carbon ranges from 21.96 to 27.11%, volatile matter ranges from 29.87 to 31.13%, ash ranges from 11.66 to 16.41%, and moisture ranges from 30.50 to 30.81%.

J seam shows the weight of fixed carbon ranges from 15.82 to 21.16%, volatile matter ranges from 28.52 to 29.51%, ash ranges from 17.96 to 23.18%, and moisture ranges from 31.37 to 32.70%.

I seam shows the weight of fixed carbon ranges from 16.00 to 17.40%, volatile matter ranges from 24.61 to 25.41%, ash ranges from 24.19 to 26.39%, and moisture is 33%.

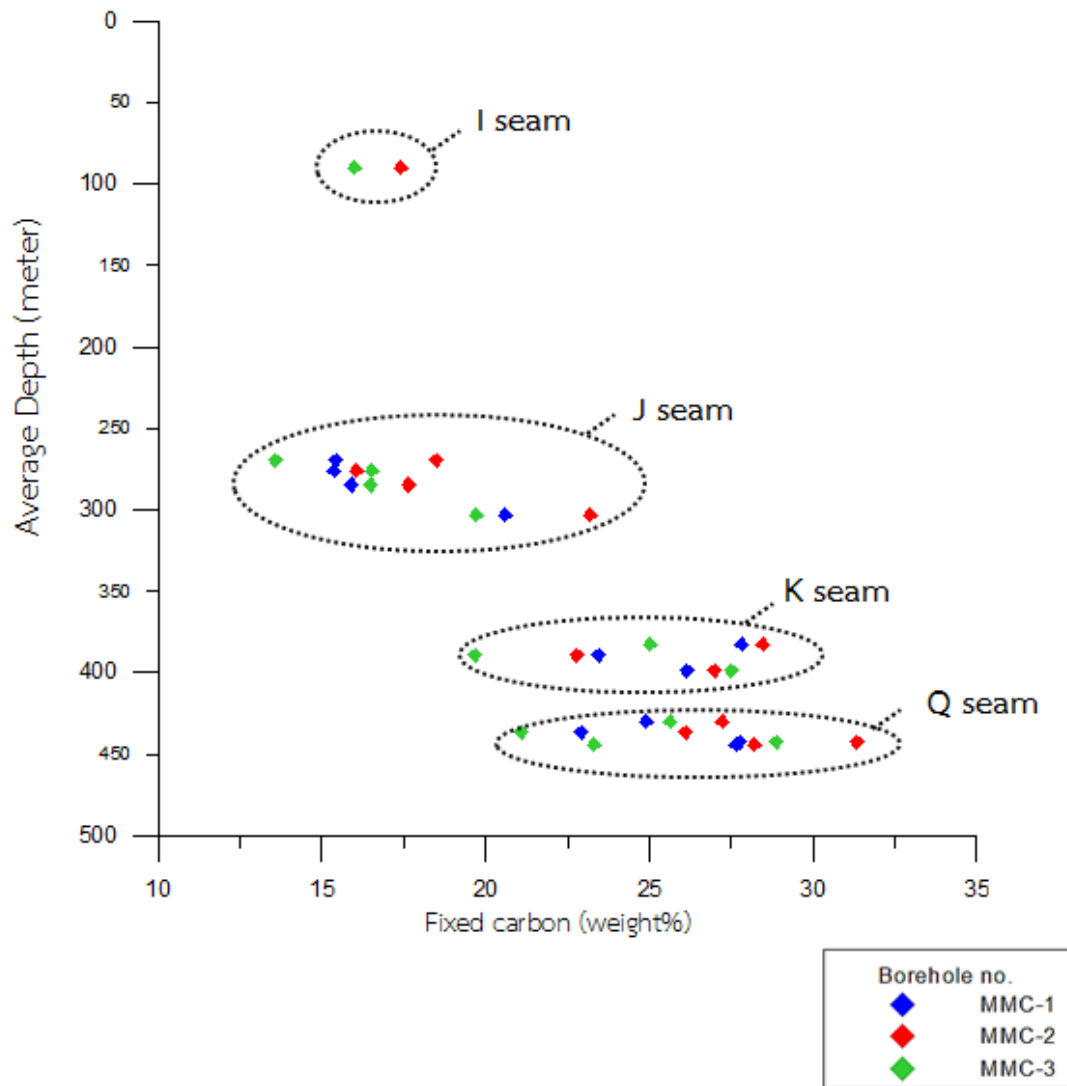


Figure 4.8 Graph showing fixed carbon variations (*on as received basis*, weight %) within the coal sequence, in central part of Mae Moh basin.

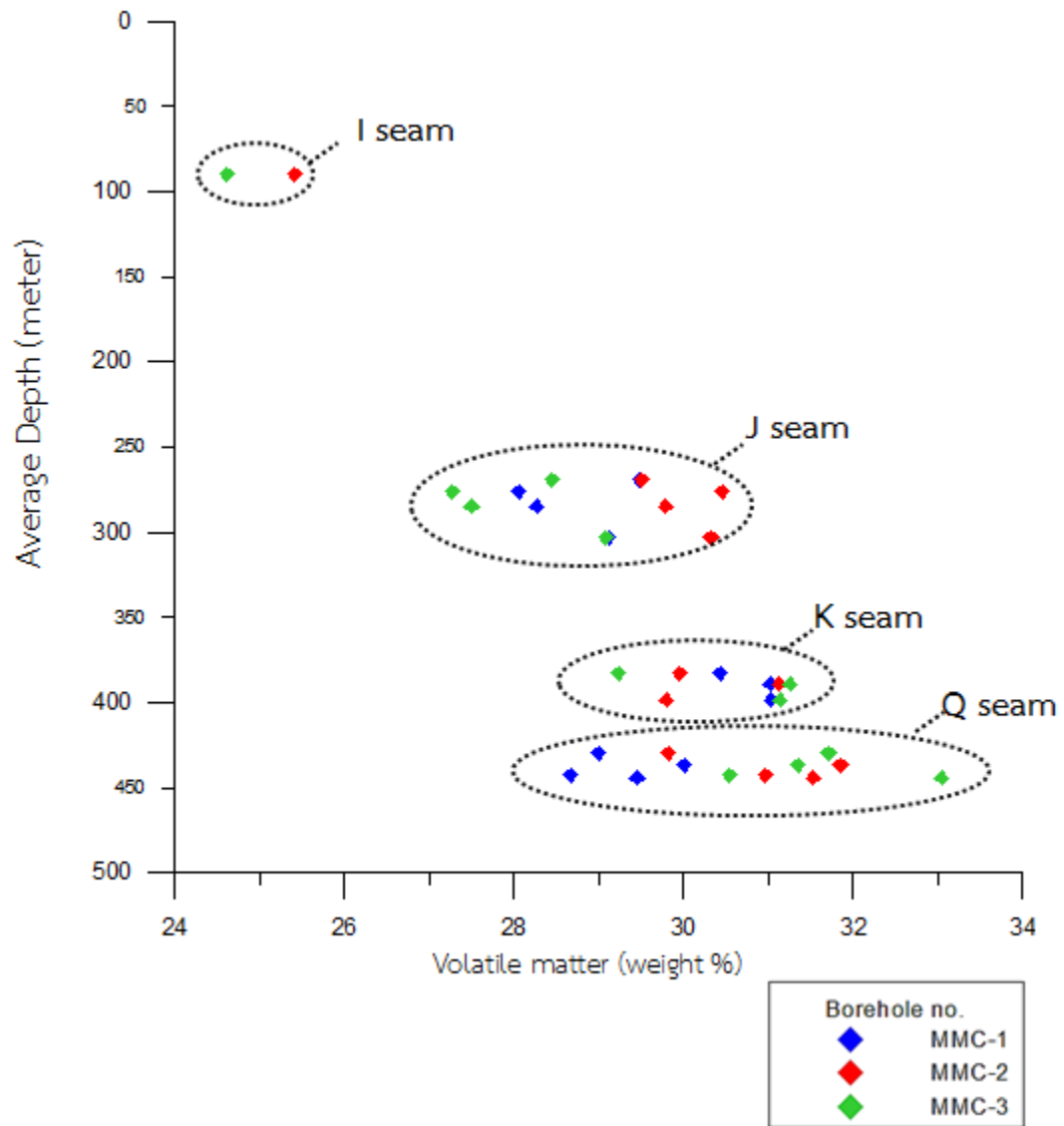


Figure 4.9 Graph showing volatile matter variations (*on as received basis*, weight %) within the coal sequence, in central part of Mae Moh basin.

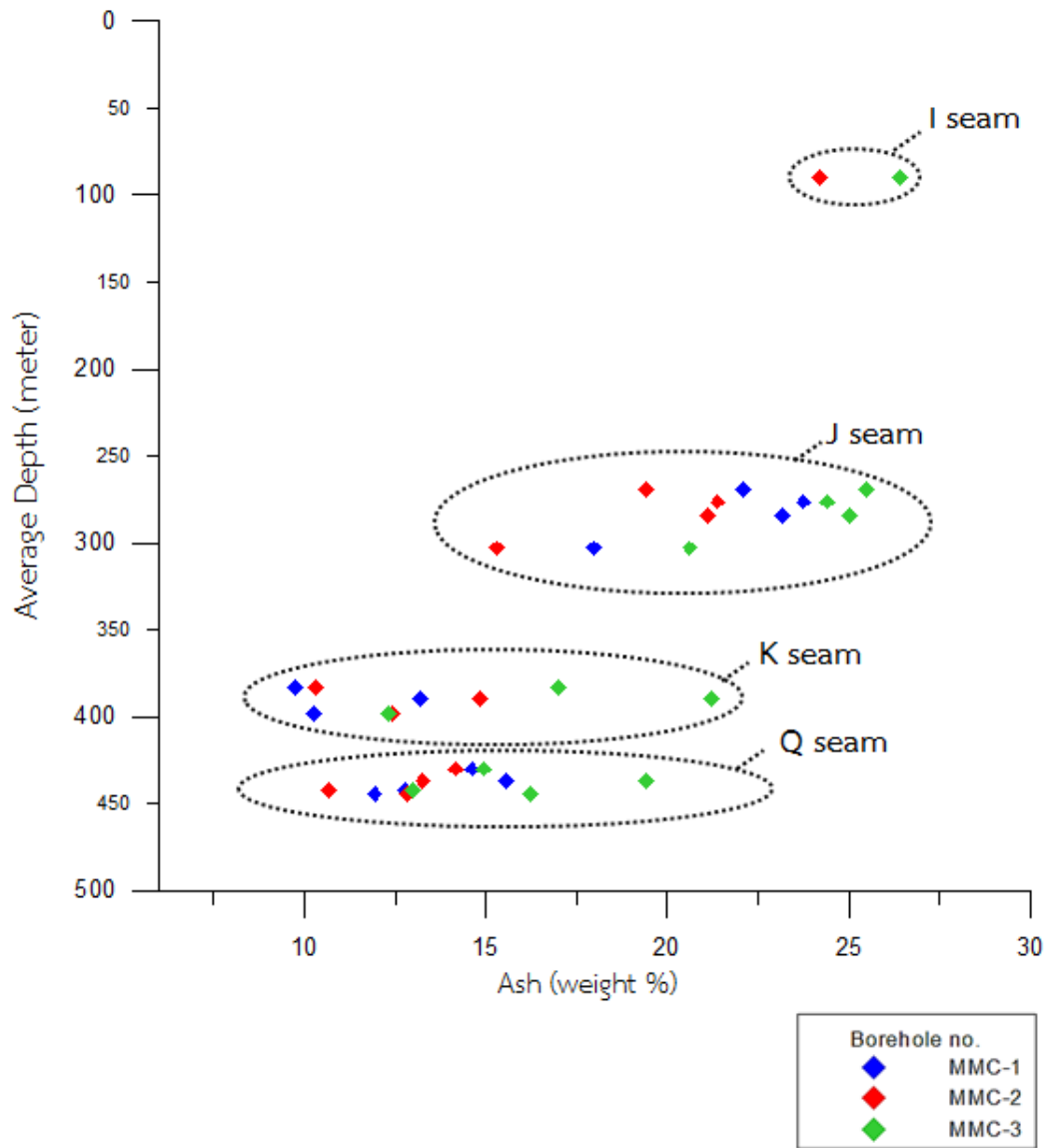


Figure 4.10 Graph showing ash variations (*on as received basis*, weight %) within the coal sequence, in central part of Mae Moh basin.

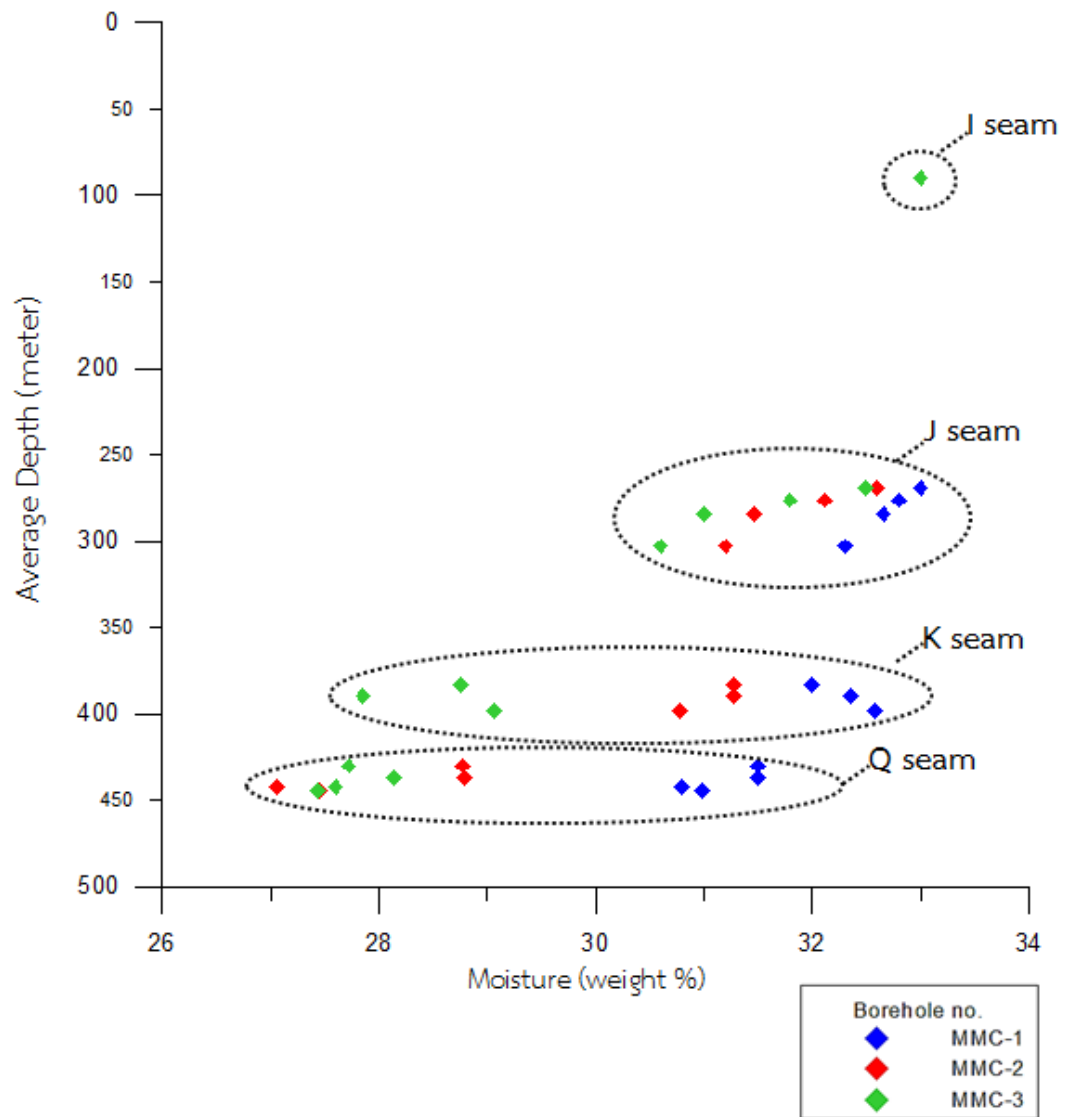


Figure 4.11 Graph showing moisture variations (*on as received basis*, weight %) within the coal sequence, in central part of Mae Moh basin.

The samples were analyzed by ultimate analysis method. Ultimate analysis gives carbon (C), hydrogen (H), nitrogen (N), oxygen (O), and also sulphur (S) elemental contents. Oxygen is then obtained by calculation.

The ultimate analyses of Q seam shows the weight *on dry basis* of carbon content ranges from 71.92 to 73.16%, hydrogen content ranges from 5.06 to 5.26%, nitrogen content ranges from 2.24 to 2.38%, oxygen content ranges from 13.57 to 14.74% and sulphur content ranges from 5.07 to 6.41%.

K seam shows the weight of carbon content ranges from 69.93 to 70.75%, hydrogen content ranges from 4.96 to 5.10%, nitrogen content ranges from 2.48 to 2.57%, oxygen content ranges from 17.59 to 19.24% and sulphur content ranges from 2.58 to 4.68%.

J seam shows the weight of carbon content ranges from 65.24 to 68.32%, hydrogen content ranges from 5.03 to 5.30%, nitrogen content ranges from 1.79 to 2.20%, oxygen content ranges from 19.69 to 20.84% and sulphur content ranges from 3.90 to 7.21%.

I seam shows the weight of carbon content ranges from 63.57 to 63.64%, hydrogen content ranges from 5.08 to 5.21%, nitrogen content ranges from 1.73 to 1.81%, oxygen content ranges from 23.20 to 23.69% and sulphur content ranges from 5.93 to 6.14%.

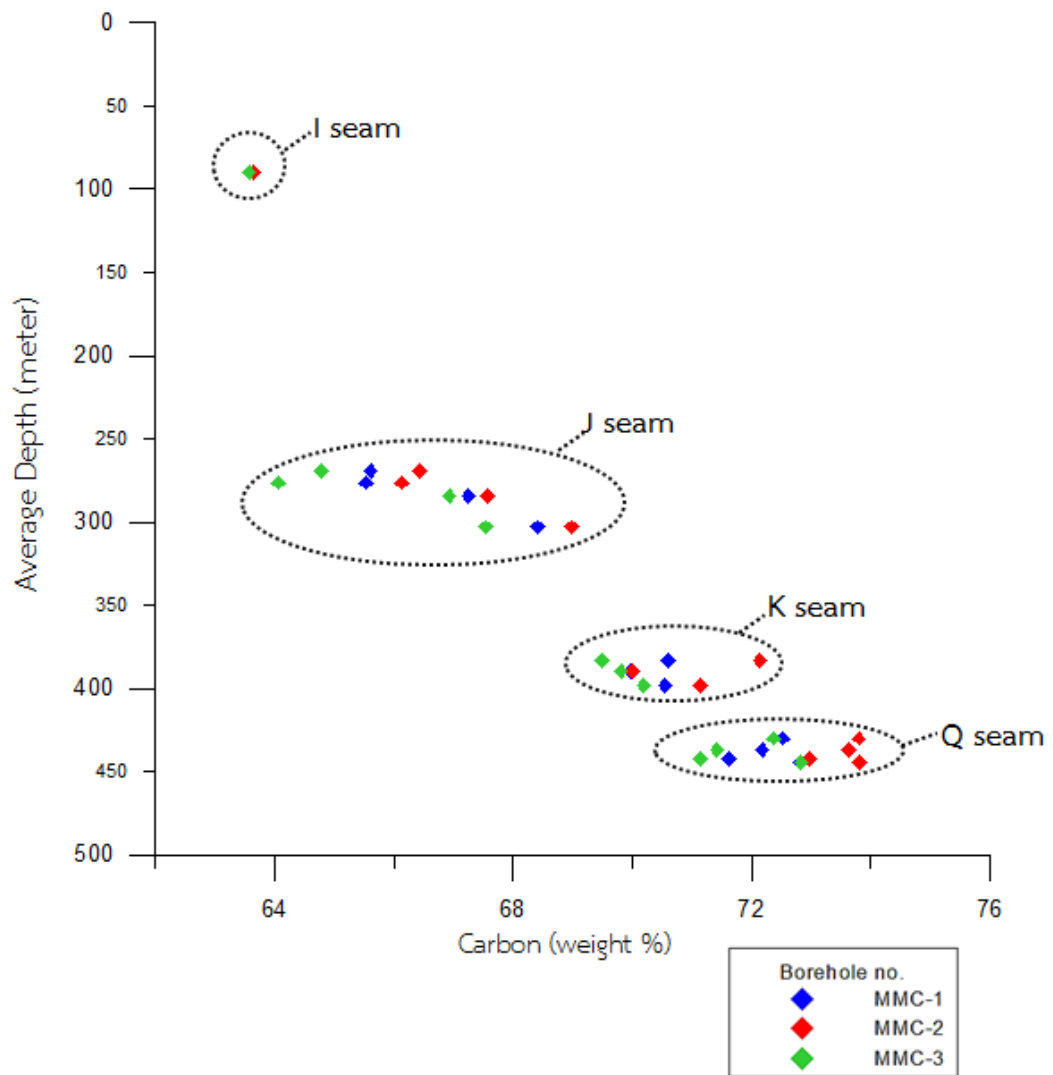


Figure 4.12 Graph showing carbon content variations (*on dry basis*, weight %) within the coal sequence, in central part of Mae Moh basin.

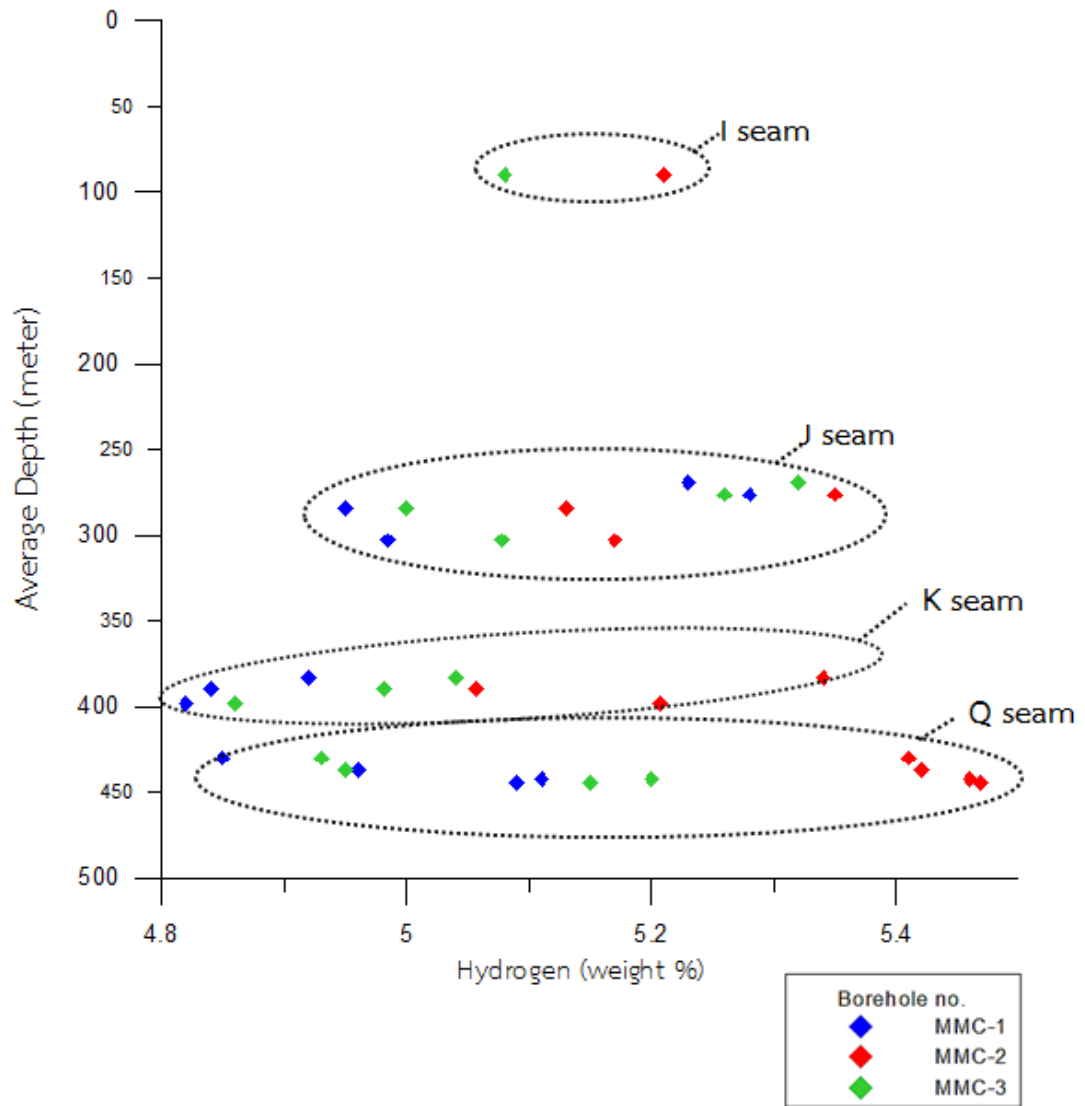
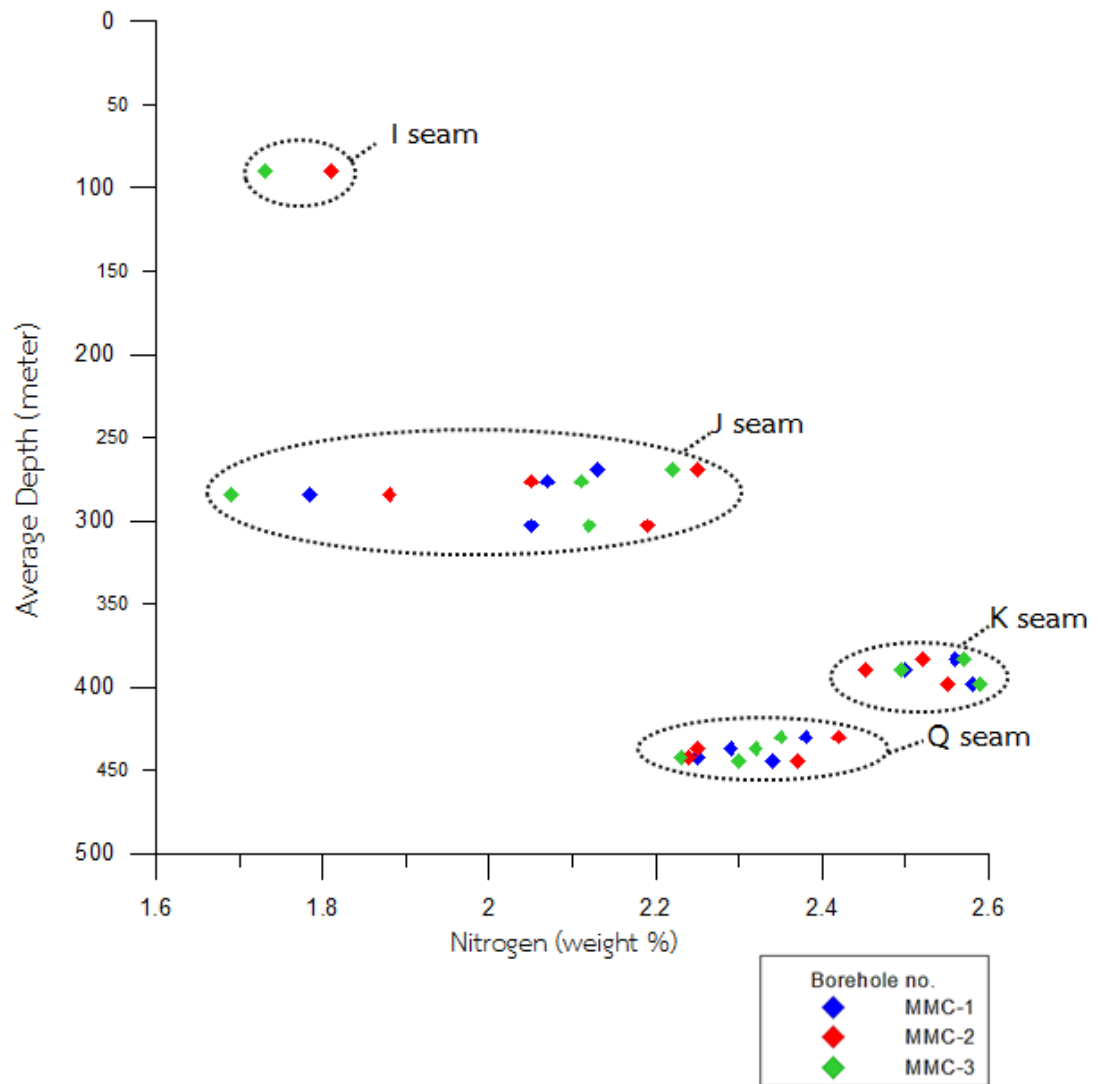


Figure 4.13 Graph showing hydrogen content variations (*on dry basis*, weight %) within the coal sequence, in central part of Mae Moh basin.



CHULALONGKORN UNIVERSITY

Figure 4.14 Graph showing nitrogen content variations (*on dry basis, weight %*) within the coal sequence, in central part of Mae Moh basin.

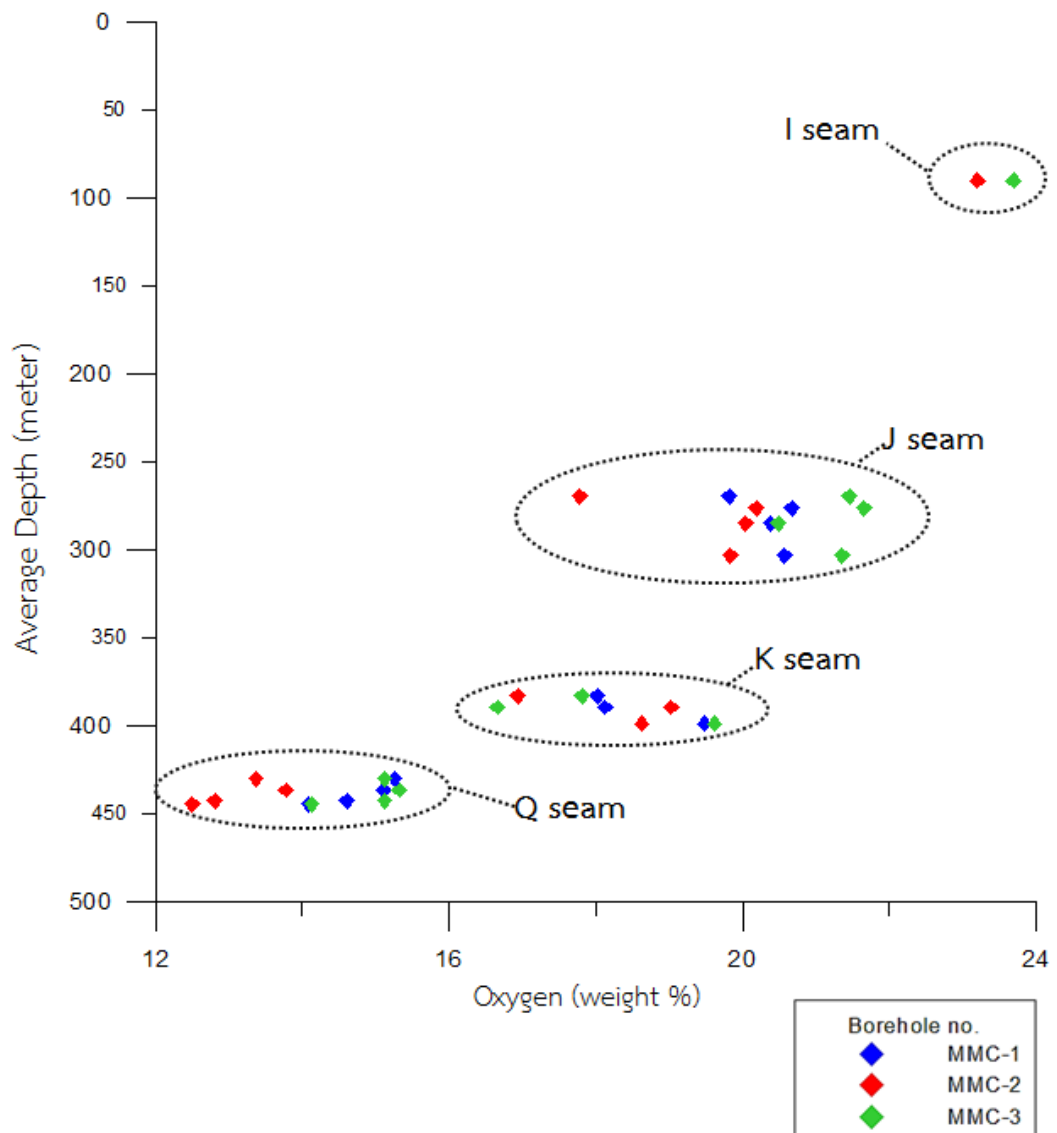


Figure 4.15 Graph showing oxygen content variations (*on dry basis*, weight %) within the coal sequence, in central part of Mae Moh basin.

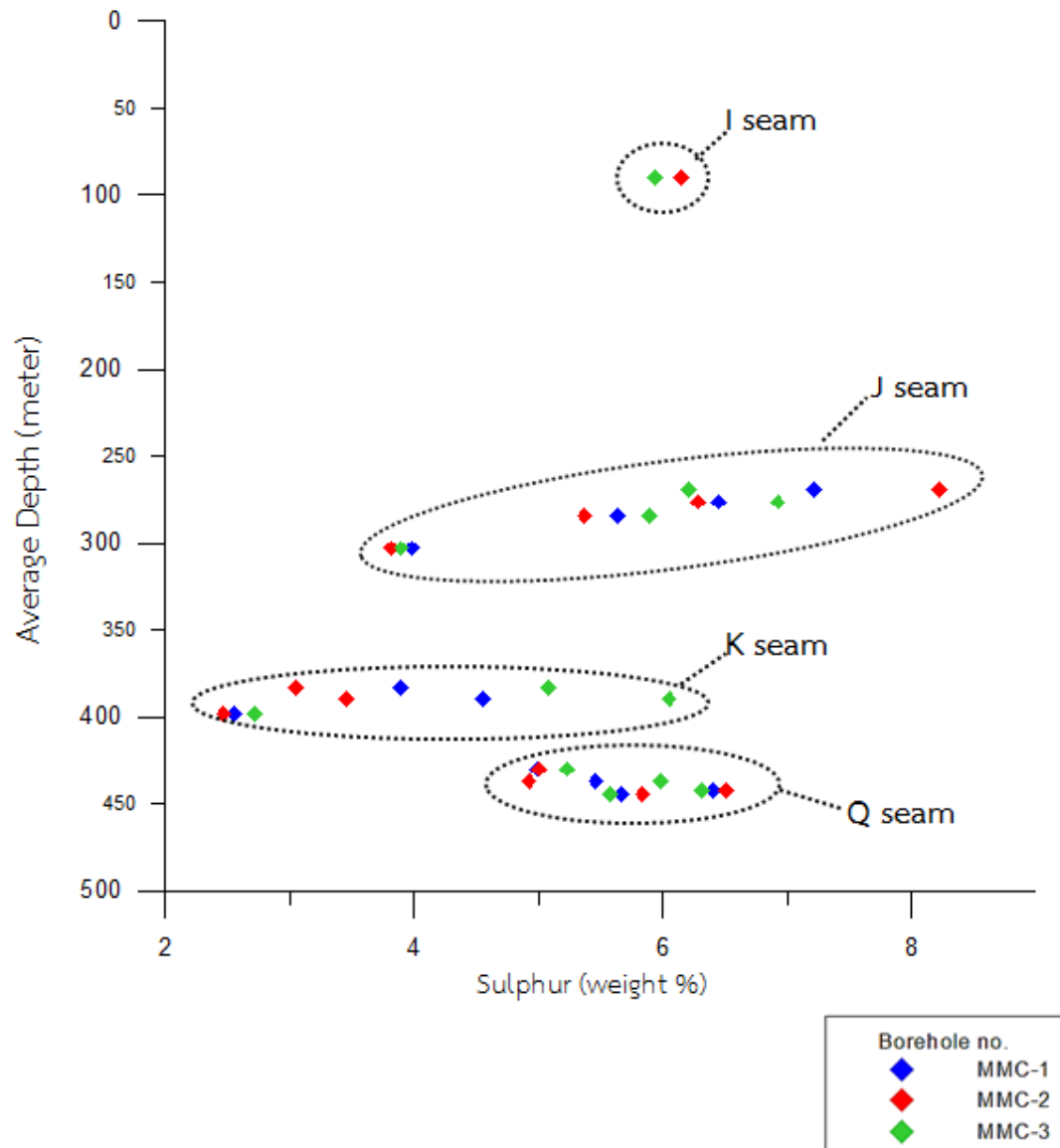


Figure 4.16 Graph showing sulphur content variations (*on dry basis*, weight %) within the coal sequence, in central part of Mae Moh basin.

Calorific value (Kcal/kg.)

Calorific value is the chemical energy which is released as thermal energy under combustion condition. For coal, calorific value indicates rank. The calorific value *on as received basis* of Q seam ranges from 3,737 to 4,054 Kcal/kg., K seam ranges from 3,476 to 3,839 Kcal/kg. J seam ranges from 2,440 to 3,203 Kcal/kg. I seam ranges 2,123-2,243 Kcal/kg.

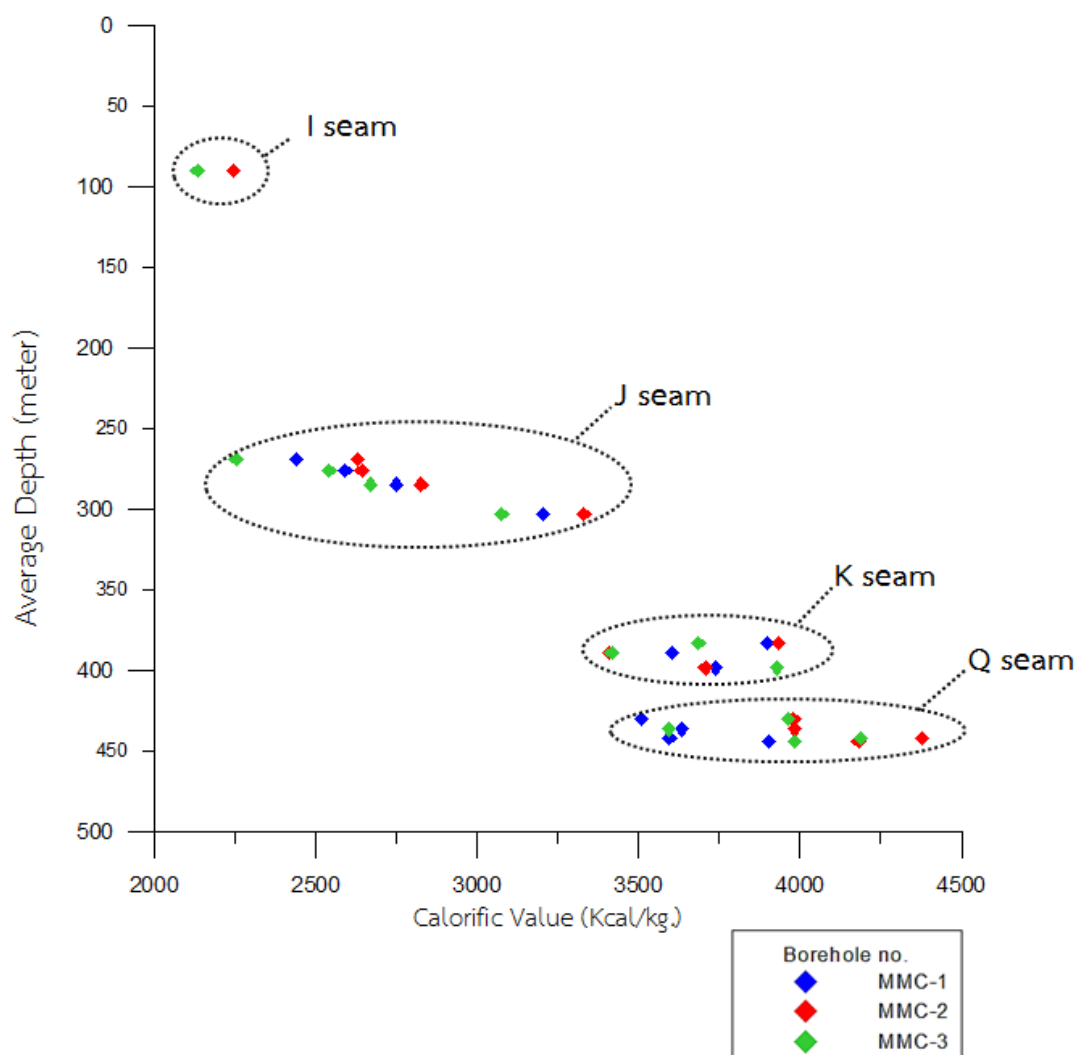


Figure 4.17 Graph showing calorific value variations (*on as received basis*, Kcal/kg.) within the coal sequence, in central part of Mae Moh basin.

4.3 Petrographic results

4.3.1 Petrographic determination

The smallest microscopically recognizable organic entities in coal and sedimentary rocks are called macerals. They are analogous to minerals in rocks. Whereas minerals are inorganic and have a homogeneous chemistry and an orderly internal structure, macerals consist of a mixture of organic compounds. The chemical and physical properties of macerals vary with coal rank or effects of metamorphism (coalification) as well as with the starting material. Macerals in coal are distinguished microscopically by color, relief in a polished surface, morphology, size, reflectance and fluorescence. Macerals can be classified and subdivided because they represent different parts of the original plant material and microorganisms that contributed to the peat. The degree of degradation, fragmentation, and oxidation of the organic plant material prior to preservation are also considered in the classification of macerals. The quantity of each maceral group varies both between and within coal beds. The 3 major groups of macerals are vitrinite (huminites), liptinite and Inertinite. These maceral groups are each subdivided into maceral subgroups and macerals. Several standardized systems of nomenclature exist worldwide. The Australian Standard, AS3856-1986 (Australian Standards, 1995) and the ASTM Standard, D2799 (ASTM, 1996) are variations of the system used by the International Committee for Coal and Organic Petrology (1998 and 2001), which is continually reviewing their terminology and classification. These classifications are shown in table 4.1. This study was using the classification and properties of macerals, following the Australian Standard, AS3856-1986.

Table 4.1 Classification of macerals into subgroups and groups, based on the International Committee for Coal and Organic Petrology (1998 and 2001), the Australian Standard system of nomenclature (AS, 1995), and the American Society for Testing and Materials (ASTM, 1996).

Maceral Group	Maceral Subgroup	Maceral (ICCP, 1995)	Maceral (AS 3856-1986)	Maceral (ASTM D 2799)
Vitrinite (Huminite)	Telovitrinite	Telinite	Textinite*	Vitrinite
		Collotelinite	Texto-Ulminite*	
			Eu-Ulminite* Telocollinite	
	Detrovitrinite	Vitrodetrinite	Attrinite*	
		Collodetrinite	Densinite*	
			Desmocollinite	
	Gelovitrinite	Gelinite	Corpogelinite	
		Corpogelinite	Porigelinite*	
			Eugelinite	
Liptinite			Sporinite	Sporinite
			Cutinite	Cutinite
			Fluorinite	Resinite
			Resinite	Alginate
			Suberinite	
			Alginate	
			Liptodetrinite	
			Exsudatinite	
			Bituminite	
Inertinite	Telo-Inertinite		Fusinite	Fusinite
			Semifusinite	Semifusinite
			Funginite (Sclerotinite)	Sclerotinite
	Detro-Inertinite		Inertodetrinite	Inertodetrinite
			Micrinite	Micrinite
	Gelo-Inertinite		Macrinite	Macrinite

*Refers to brown coal (low rank) macerals, otherwise the vitrinite classification is for medium and high rank coals.

In this study, the coal samples are collected from 4 coal seams namely Q, K and J seams of the Na Khaem formation and minor coal seam as I seam of Huai Luang formation, were taken from the 3 boreholes in central part of Mae Moh basin. The 35 pellets are prepared for coal petrographic study, using point counting method under polarizing microscope with normal reflected light, crossed-polarized light and fluorescence light. Generally, the characteristics of the coal within the Mae Moh basin under the reflected light, compared with rocks, is that the huminite likes groundmass and the inertinite likes grains scatter in the groundmass. The inertinite is dark, while huminite is medium bright. The liptinite is clearly characterized by grain, very bright under the reflected light.

Petrographic investigation of individual coal seams reveal the studied coals consist largely of macerals >70% with small amount of inorganic materials <30%. Huminite maceral group is the highest percentage followed by liptinite and inertinite. Moreover, there are mineral matters in all samples. The results of coal petrography in this study are summarized in table 4.2.

Huminite tends to increase from I seam to Q seam (figure 4.18) similar to liptinite and inertinite group (figure 4.19 and 4.20). Conversely the mineral matter tends to decrease from I seam to Q seam (figure 4.21).

Table 4.2 The average percentage of maceral and mineral matter and calculated facies indices of coals in central part of Mae Moh basin.

Coal seam	Coal subseam	Huminite		Liptinite		Inertinite		Mineral matter		Ternary plot			Diesel diagram	
		(average %)	(average %)	(average %)	(average %)	(average %)	(average %)	vertex A	vertex B	vertex C	TPI value	GI value		
I	I1	54	15	4	27	10	48	4	0.11	13.50				
	I2	55	10	4	29	8	47	5	0.14	11.00				
	I3	55	13	4	28	9	48	5	0.12	12.25				
J	J3	57	13	6	24	10	34	6	0.20	8.90				
	J4	46	25	5	24	14	31	5	0.29	8.64				
	J5	48	24	5	23	15	25	5	0.36	8.96				
	J6	59	15	7	19	15	26	7	0.40	8.02				
	J7	53	19	6	23	13	29	6	0.31	8.63				
	J8	57	16	14	14	23	33	14	0.47	4.19				
K	K2	57	16	13	14	24	31	13	0.45	4.54				
	K3	59	16	13	12	26	32	13	0.50	4.69				
	K4	58	16	13	13	24	32	13	0.47	4.47				
	K5	58	19	13	11	28	29	13	0.50	4.56				
Q	Q2	63	11	12	15	20	29	12	0.49	5.26				
	Q3	58	18	14	10	27	35	14	0.45	4.18				
	Q4	57	17	13	13	27	35	13	0.47	4.55				
	Q5	59	16	13	12	26	32	13	0.48	4.64				

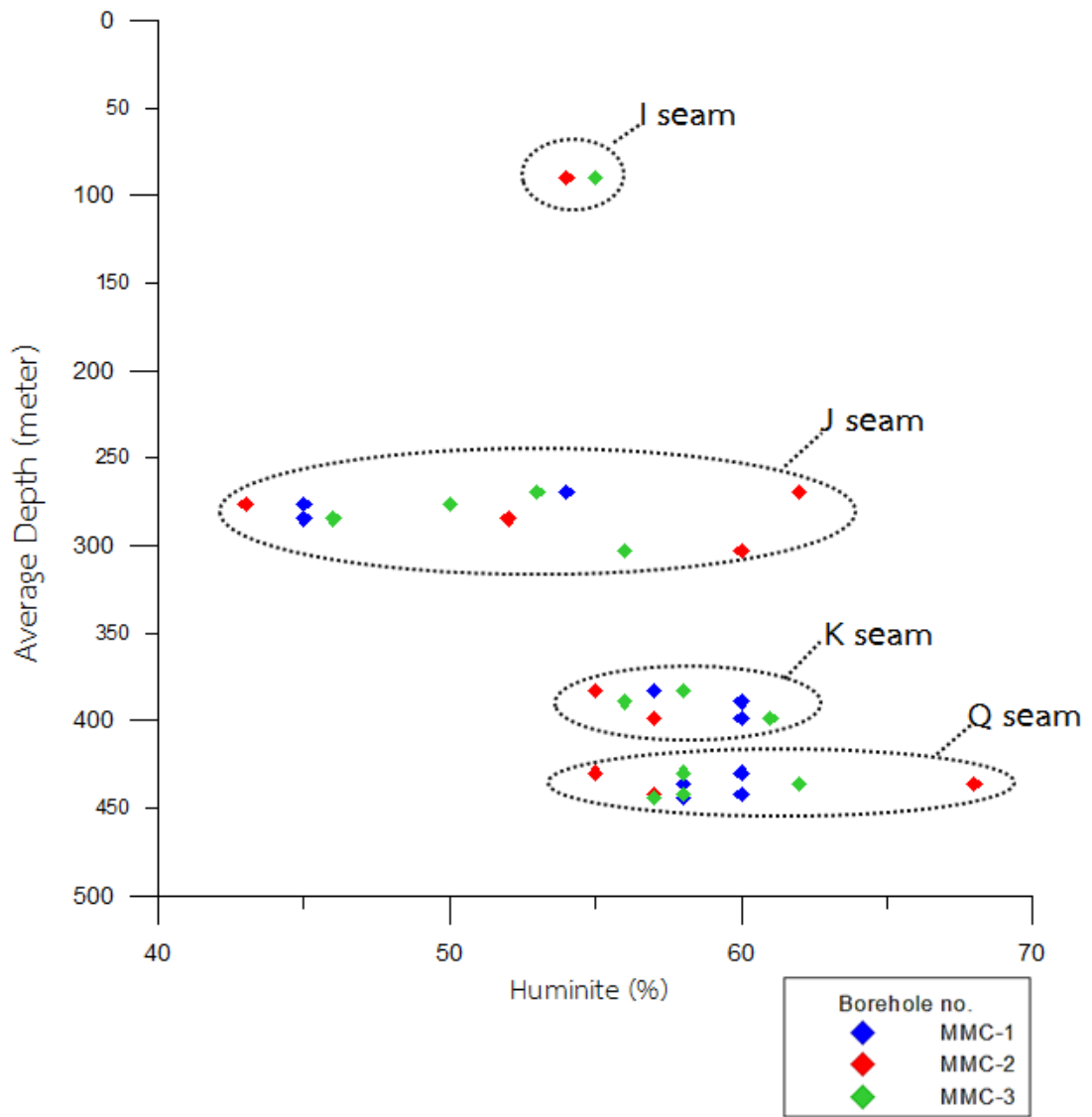


Figure 4.18 Graph showing huminite contents (%) within the coal sequence, in central part of Mae Moh basin.

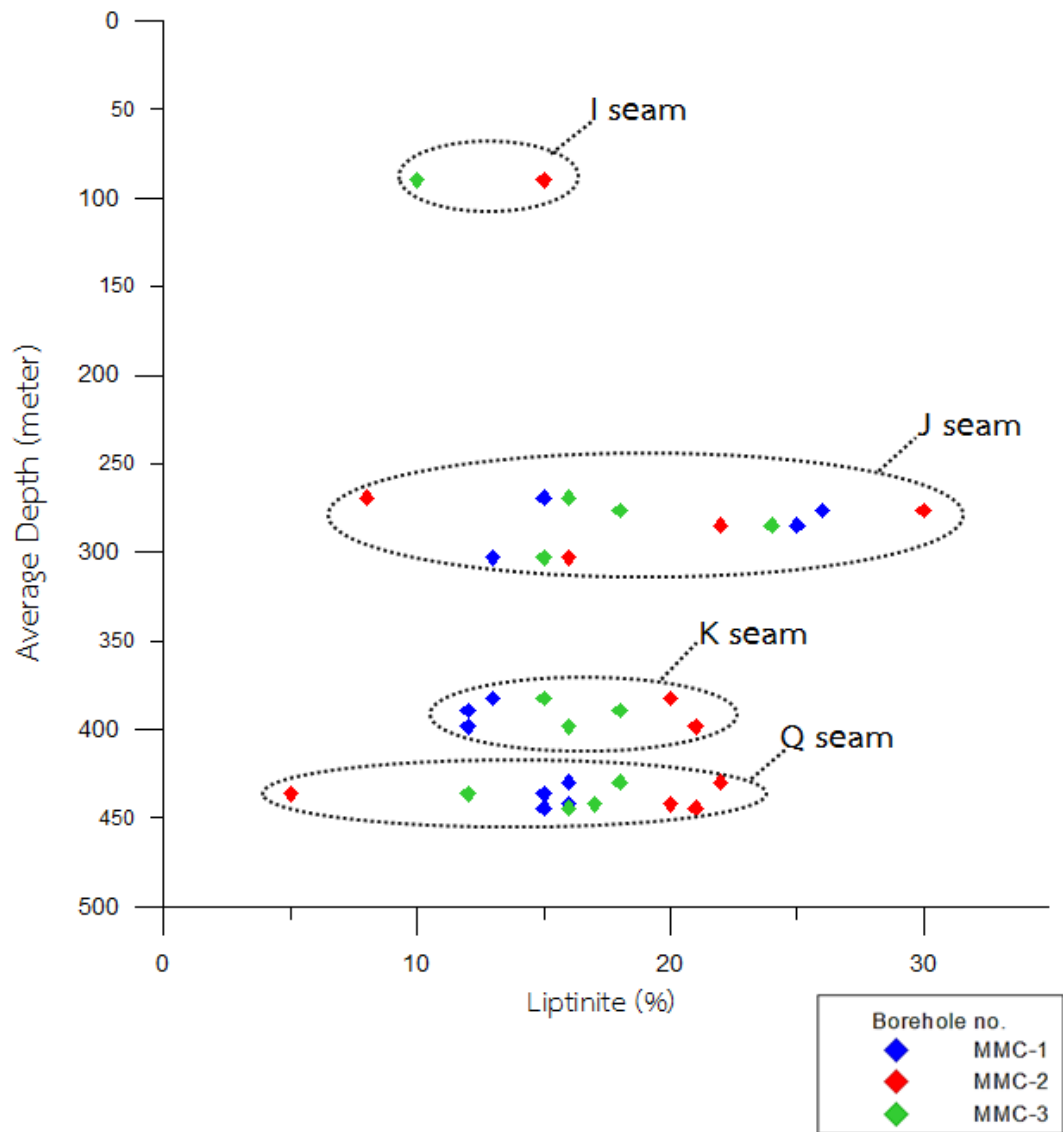


Figure 4.19 Graph showing liptinite contents (%) within the coal sequence, in central part of Mae Moh basin.

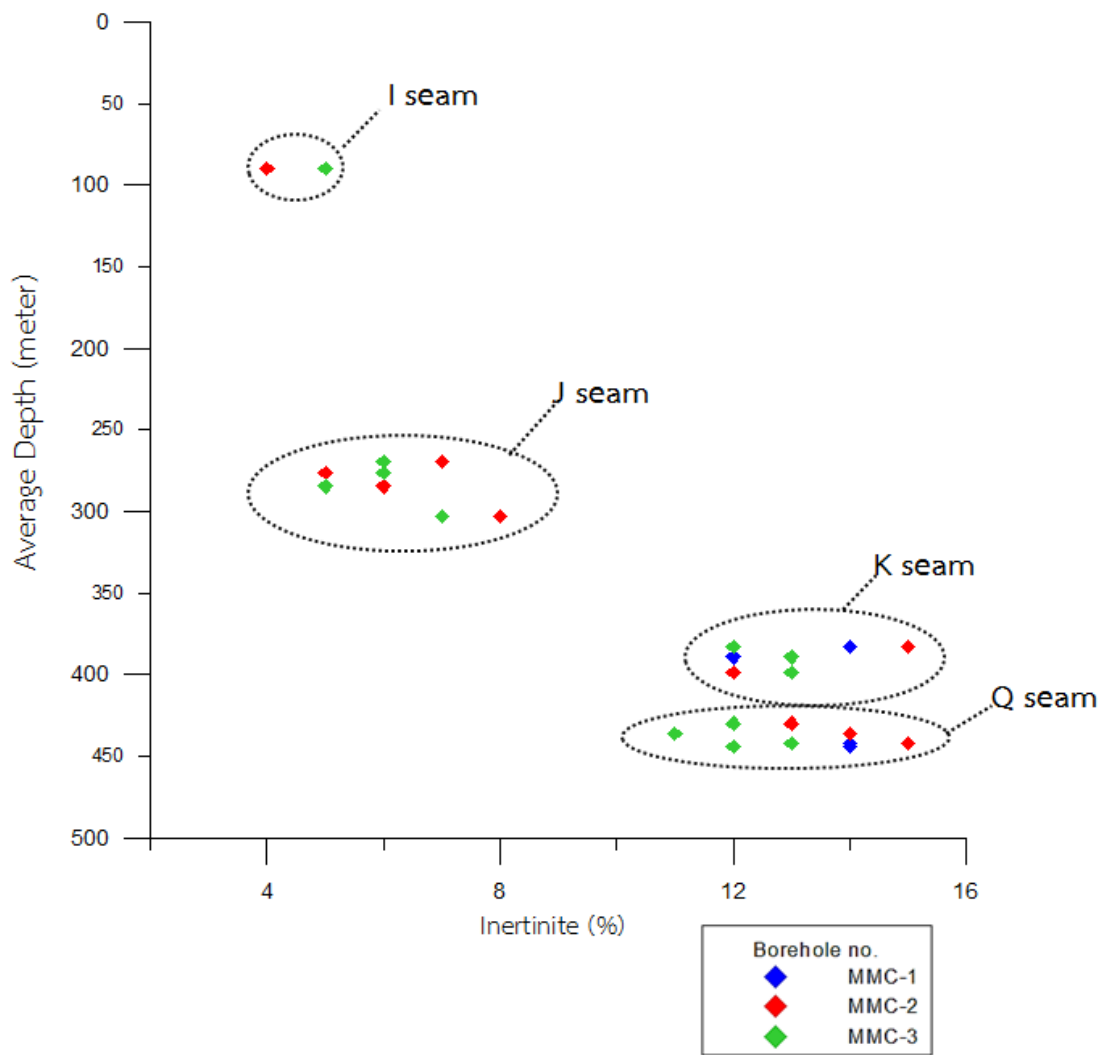


Figure 4.20 Graph showing inertinite contents (%) within the coal sequence, in central part of Mae Moh basin.

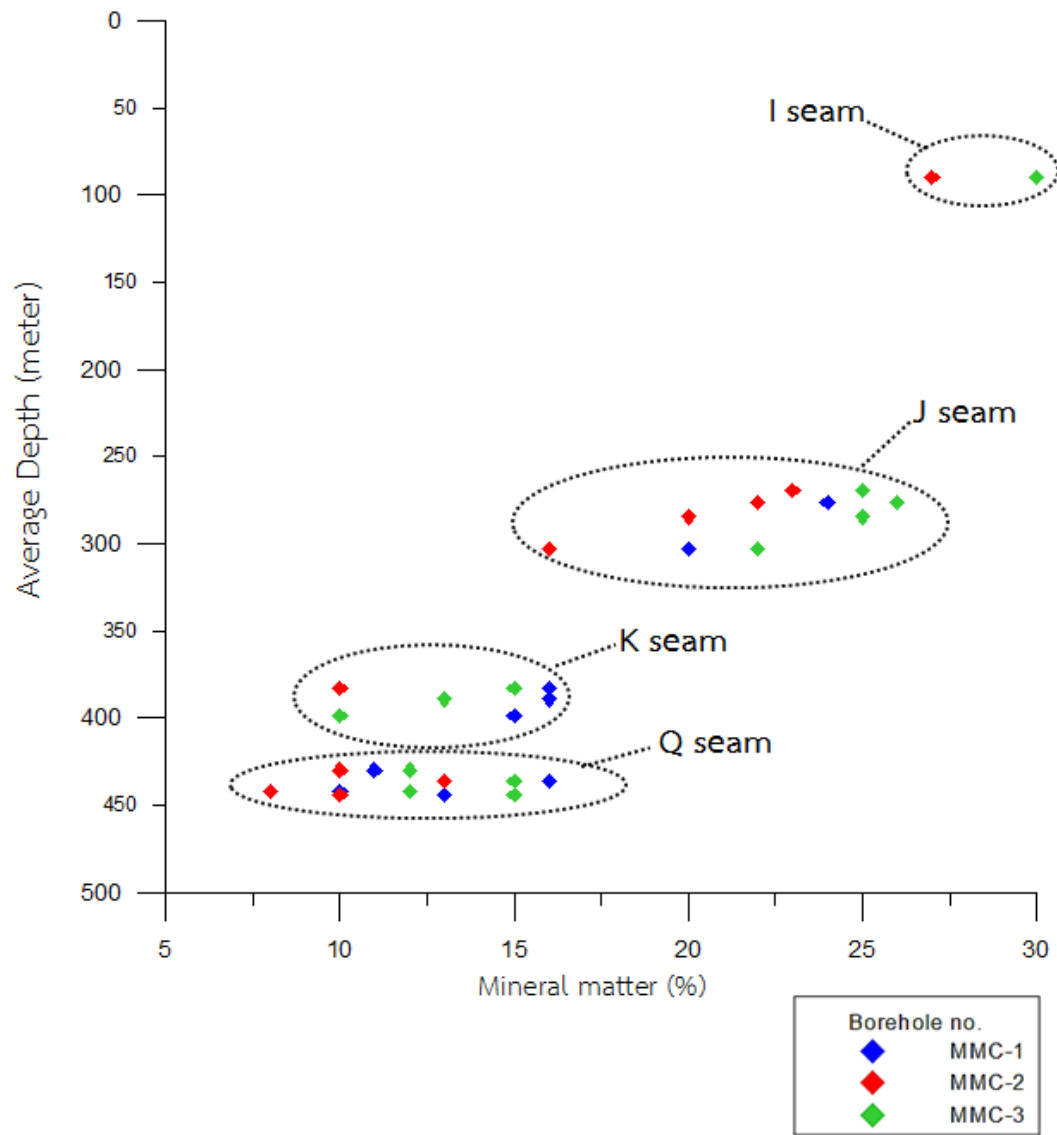


Figure 4.21 Graph showing mineral matter contents (%) within the coal sequence, in central part of Mae Moh basin.

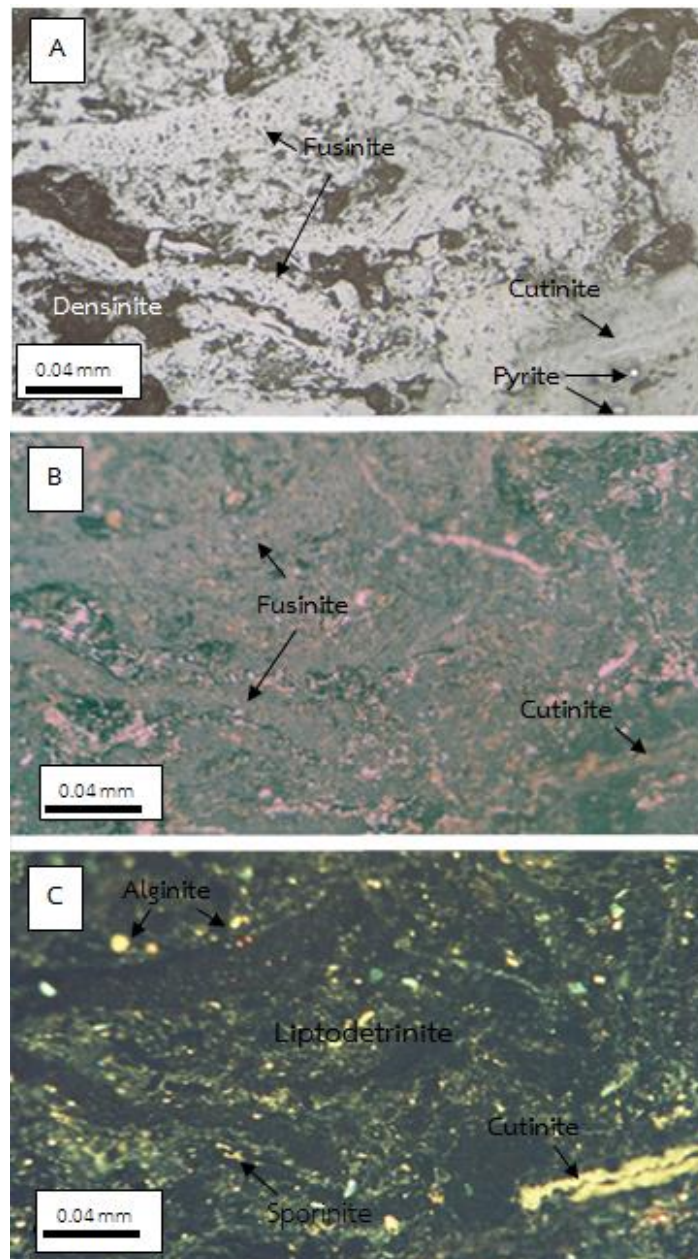
The Q seam, 12 samples were collected from borehole no.MMC1, no.MMC2 and no.MMC3. Q seam is divided into 4 subseams as Q4, Q3, Q2 and Q1 subseam from bottom to top.

Q4 subseam consists of 57 to 58% huminite group are dominated by gelinite and densinite. 15 to 21% of liptinite group are dominated by liptodetrinite, cutinite, sporinite, and amorphinite. 12 to 14% of inertinite group are dominated by fusinite, semifusinite, sclerotinite. 10 to 15% of mineral matters are dominated by clay mineral, quartz, and pyrite dominantly in form of framboidal.

Q3 subseam consists of 57 to 60% huminite group are dominated by gelinite, densinite and some textolinite. 16 to 20% of liptinite group are dominated by sporinite, amorphinite, liptodetrinite and cutinite. 13 to 15% of inertinite group are dominated by semifusinite, fusinite and sclerotinite. 8 to 12% of mineral matters are dominated by clay mineral, quartz, and pyrite dominantly in form of framboidal.

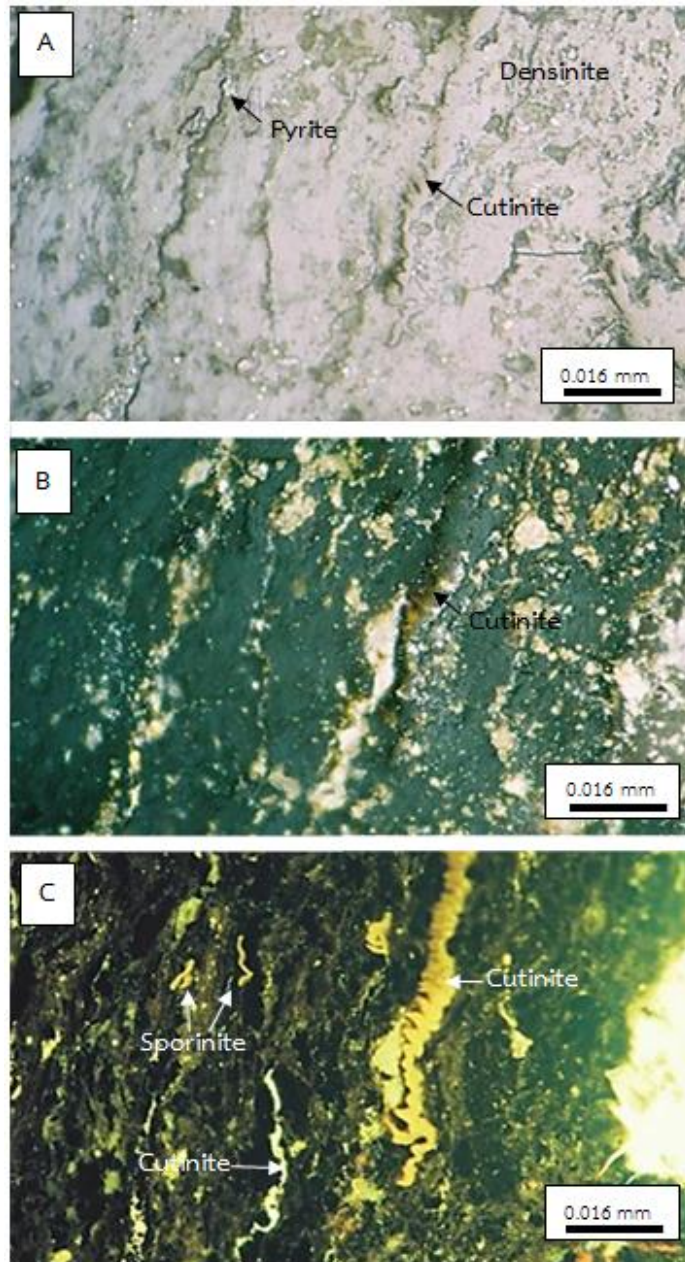
Q2 subseam consists of 58 to 68% huminite group are dominated by gelinite densinite, and some textolinite. 5 to 15% of liptinite group are dominated by cutinite, sporinite, liptodetrinite, amorphinite, and exsudatinite. 13 to 16% of inertinite group are dominated by fusinite and sclerotinite. 13 to 16% of mineral matters are clay mineral, quartz, and pyrite dominantly in form of framboidal.

Q1 subseam consists of 55 to 60% huminite group are dominated by gelinite and gelinite. 16 to 22% of liptinite group are dominated by sporinite, liptodetrinite, cutinite, amorphinite, and alginite. 12 to 13% of inertinite group are dominated by semifusinite, fusinite and sclerotinite. 10 to 12% of mineral matters are clay mineral, quartz, and pyrite dominantly in form of framboidal.



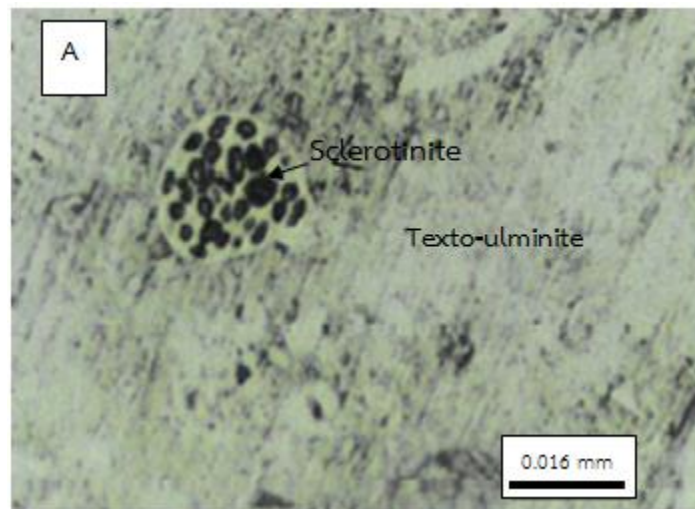
(A) PPL = Plane Polarize light, (B) XPL = Cross Polarized light, (C) FL = Fluorescence light

Figure 4.22 photomicrographs of highly reflecting fusinite band under plane polarize light (A), bright yellow serrated linear of cutinite, bright yellow various shape of sporinite, bright yellowish green of alginite stand out in the groundmass, and common pale yellow to pale green small fragment of liptodetrinite under fluorescence light (C) in groundmass of densinite; Q4 subseam.



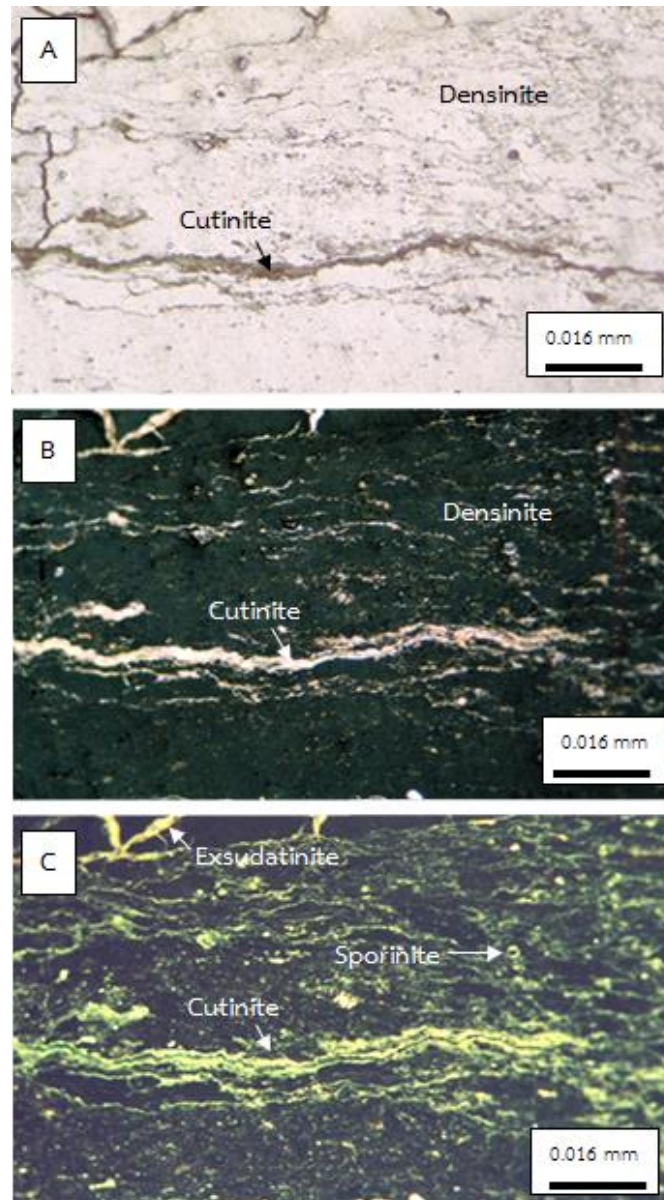
(A) PPL = Plane Polarize light, (B) XPL = Cross Polarized light, (C) FL = Fluorescence light

Figure 4.23 photomicrographs of bright yellow serrated linear of cutinite, bright yellow various shape of sporinite under fluorescence light (C) in the groundmass of densinite with abundant pyrite; Q4 subseam.



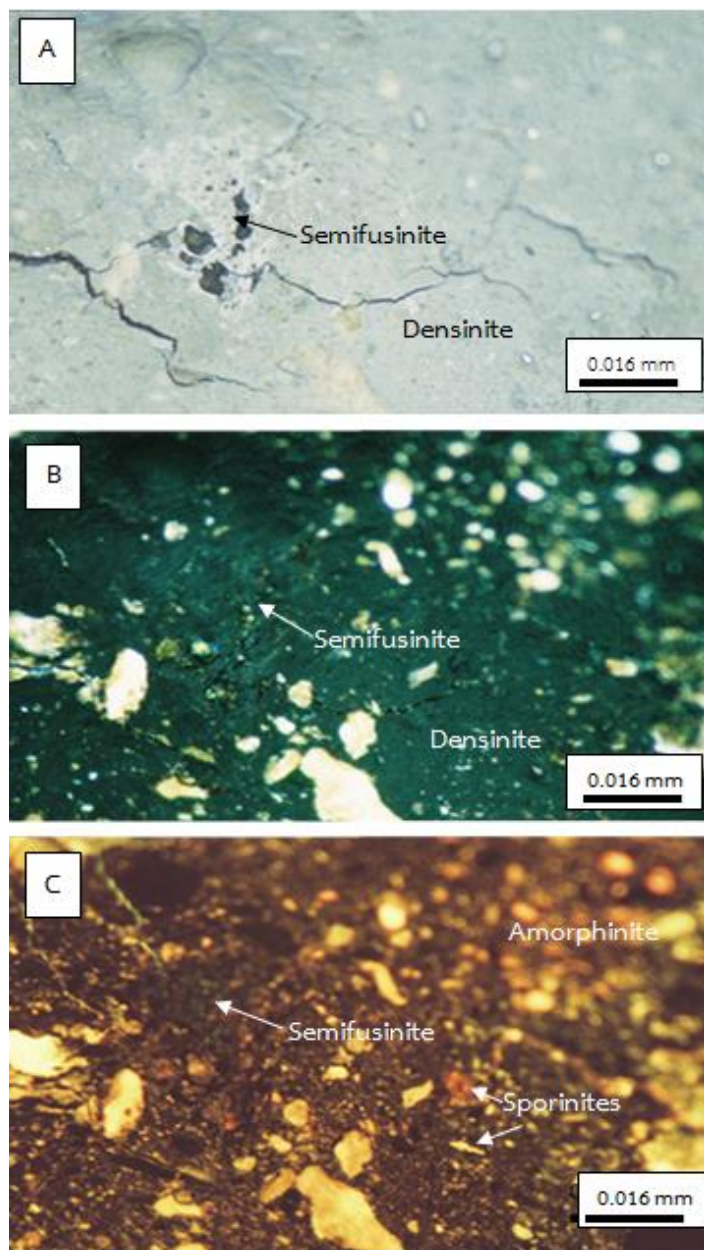
(A) PPL = Plane Polarize light

Figure 4.24 photomicrographs of texto-ulminite including highly reflecting round shape of sclerotinite which derived from fungal material and considered being an oxidation product of resin; Q3 subseam.



(A) PPL = Plane Polarize light, (B) XPL = Cross Polarized light, (C) FL = Fluorescence light

Figure 4.25 photomicrographs of dark stringer cutinite, which running across (thin-walled cutinite) under plane polarize light (A), bright yellowish green round shape of sporinite and some exsudatinite filled into crack in groundmass of densinite, under cross polarized light (C); Q2 subseam.



(A) PPL = Plane Polarize light, (B) XPL = Cross Polarized light, (C) FL = Fluorescence light

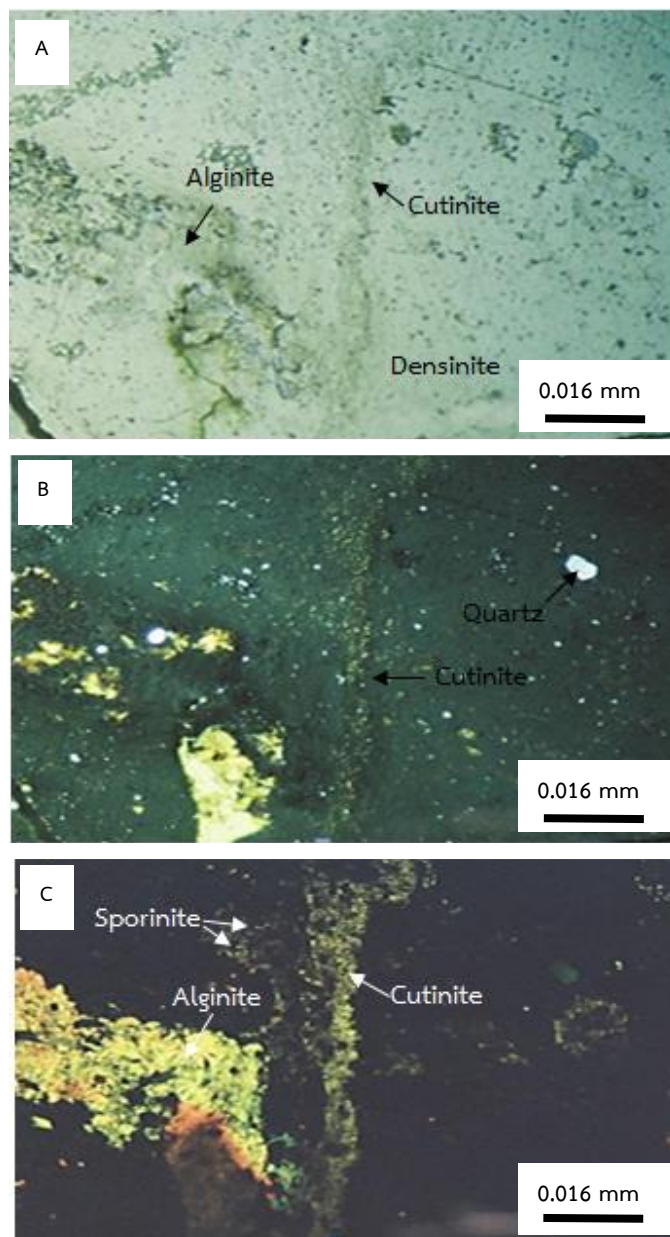
Figure 4.26 photomicrographs of intermediate reflecting of semifusinite, which partially visible cellular structure under plane polarize light (A), discrete small fragment of liptodetrinite, amorphous shape of amorphinite under fluorescence light (C) in the groundmass of densinite; Q1 subseam.

The K seam, 9 samples were collected from borehole no.MMC-1, no.MMC-2 and no.MMC-3. K seam is divided into 3 subseams as K3, K2 and K1 subseam from bottom to top.

K3 subseam consists of 57 to 61% huminite group are dominated by gelinite, densinite and some texto-ulminite. 12 to 21% of liptinite group are dominated by amorphinite, sporinite, cutinite, liptodetrinite, alginite, and some exsudatinite. 12 to 13% of inertinite group are dominated by sclerotinite and fusinite. 10 to 15% of mineral matters are clay mineral, and quartz, pyrite dominantly in form of framboidal.

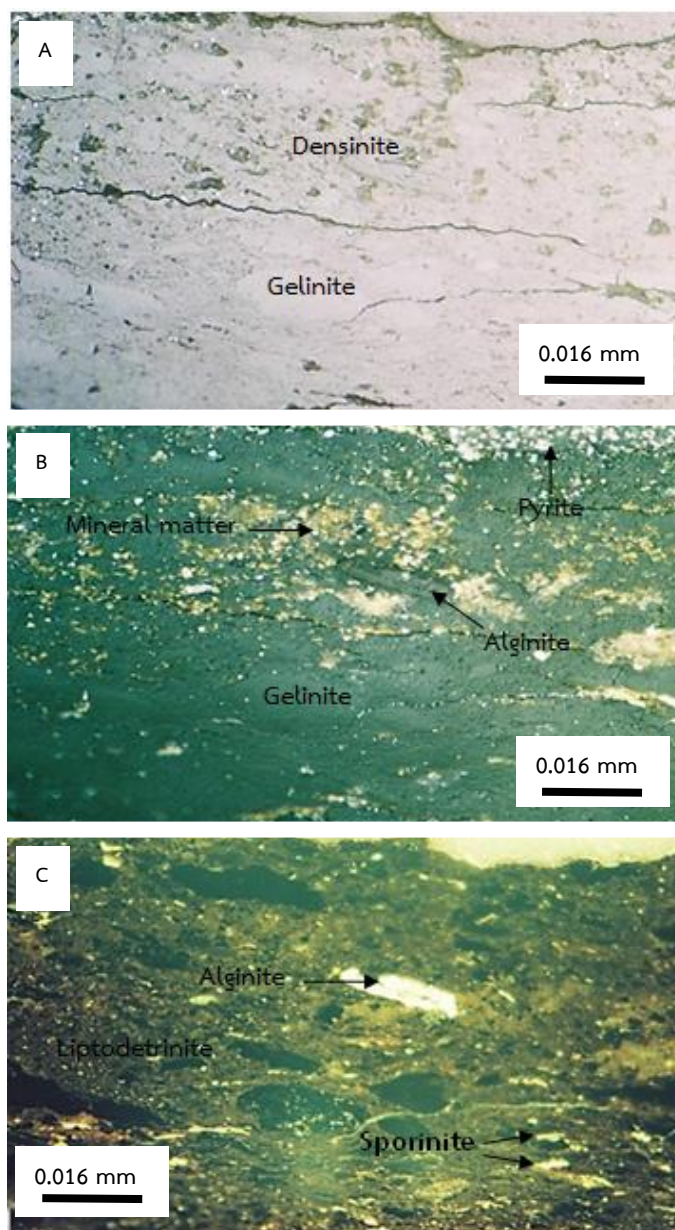
K2 subseam consists of 56 to 60% huminite group are dominated by densinite, gelinite and some texto-ulminite. 12 to 18% of liptinite group are dominated by liptodetrinite, amorphinite, sporinite, cutinite, alginite and some exsudatinite. 12 to 13% of inertinite group are dominated by semifusinite, fusinite and sclerotinite. 13 to 16% of mineral matters are as clay mineral, quartz, pyrite dominantly in form of framboidal and layers of diatomite association.

K1 subseam consists of 55 to 58% huminite group are dominated by gelinite and densinite and some texto-ulminite. 13 to 20% of liptinite group are dominated by sporinite, cutinite, liptodetrinite, amorphinite, alginite and exsudatinite. 12 to 15% of inertinite group are dominated by fusinite and sclerotinite. 10 to 16% of mineral matters are clay mineral, quartz, pyrite dominantly in form of framboidal and diatomite.



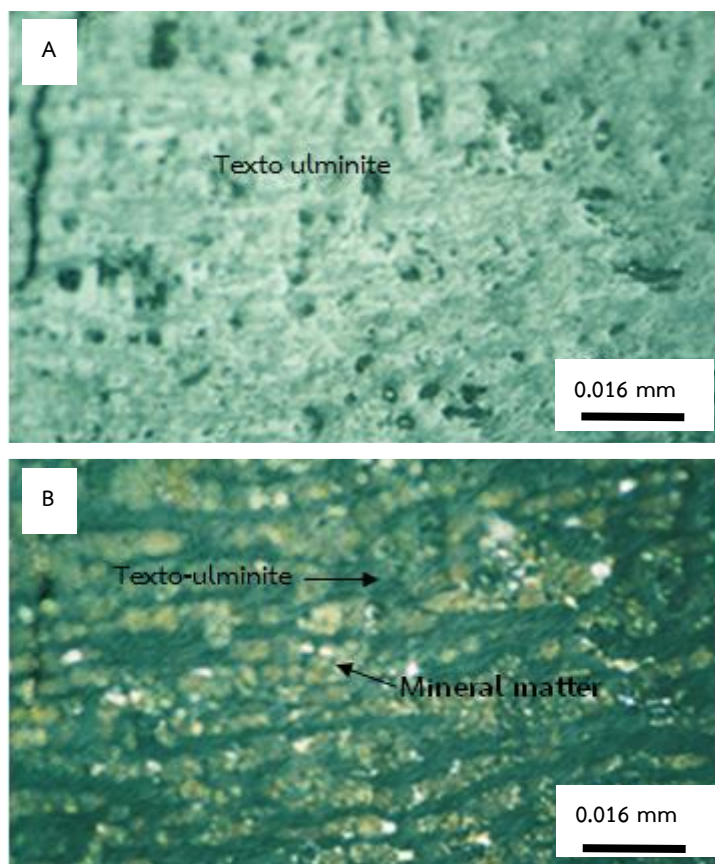
(A) PPL = Plane Polarize light, (B) XPL = Cross Polarized light, (C) FL = Fluorescence light

Figure 4.27 photomicrographs of yellowish green fluorescing of alginite, yellowish brown fluorescing of sporinite, associated with yellowish green serrated linear fluorescing of cutinite in groundmass of densinite; K3 subseam.



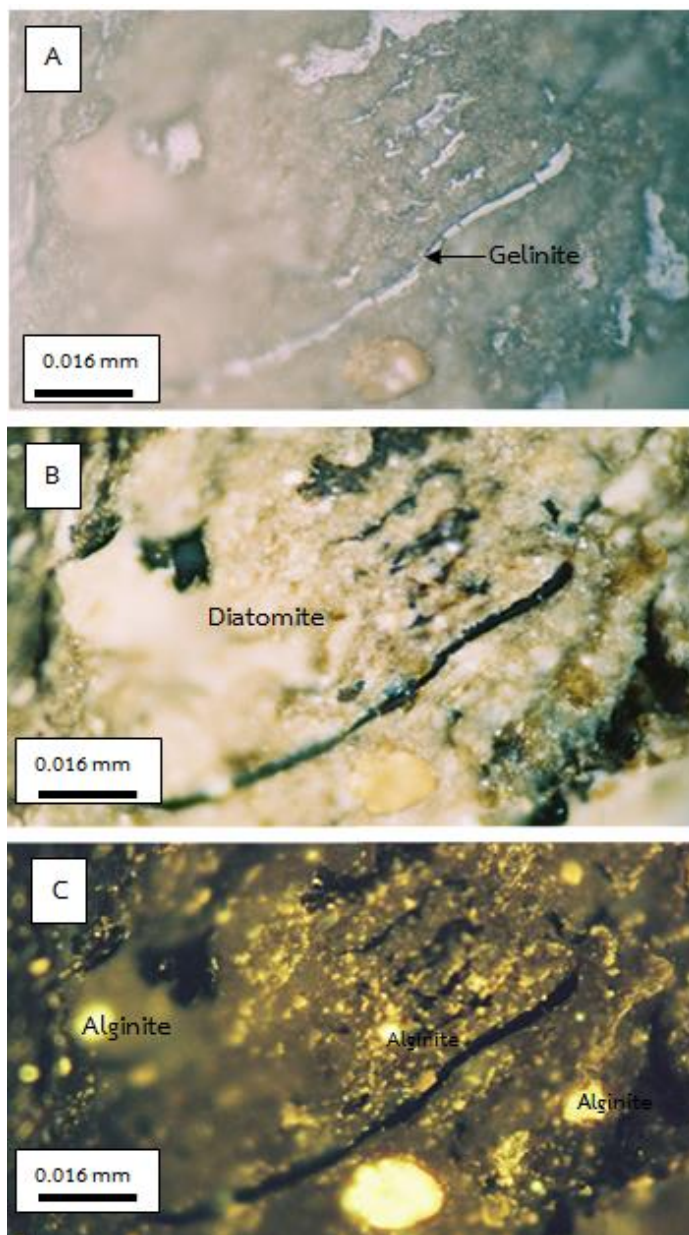
(A) PPL = Plane Polarize light, (B) XPL = Cross Polarized light, (C) FL = Fluorescence light

Figure 4.28 photomicrographs of bright linear yellow fluorescing of alginite in type of *Lamalginite?*, abundant yellowish green various shape of sporinite under fluorescence light (C) in the groundmass of densinite with abundant pyrite; K3 subseam.



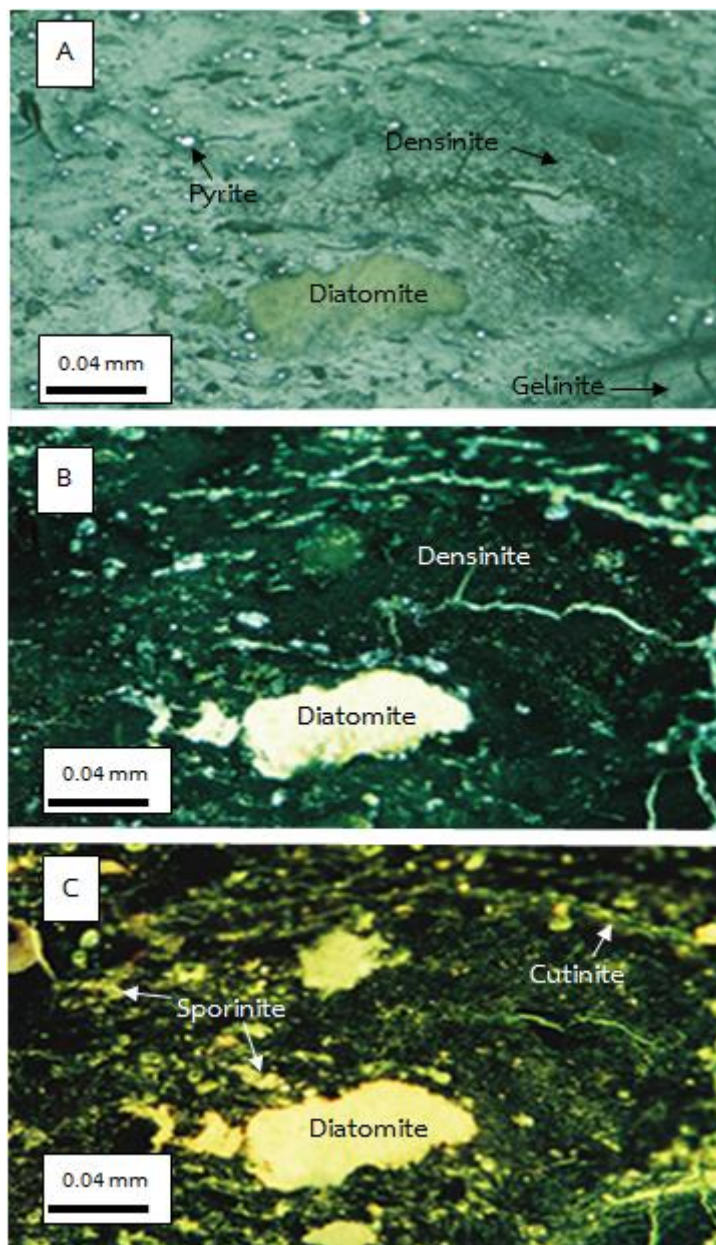
(A) PPL = Plane Polarize light, (B) XPL = Cross Polarized light

Figure 4.29 photomicrographs of texto-ulminite, represent intact fragments of plant matter; presence of remnant cell structure, filled with mineral matter under cross polarized light (B); K2 subseam.



(A) PPL = Plane Polarize light, (B) XPL = Cross Polarized light, (C) FL = Fluorescence light

Figure 4.30 photomicrographs of bright yellow to yellowish green round shape of alginite in type of *Botryococcus sp.?* stand out under fluorescence light (C), associated with diatomite and mineral matter; K2 subseam.



(A) PPL = Plane Polarize light, (B) XPL = Cross Polarized light, (C) FL = Fluorescence light

Figure 4.31 photomicrographs of diatomite, yellow various shapes of sporinite, associated with yellowish green serrated linear fluorescing of cutinite under fluorescence light (C) in the groundmass of densinite and gelinite; K1 subseam.

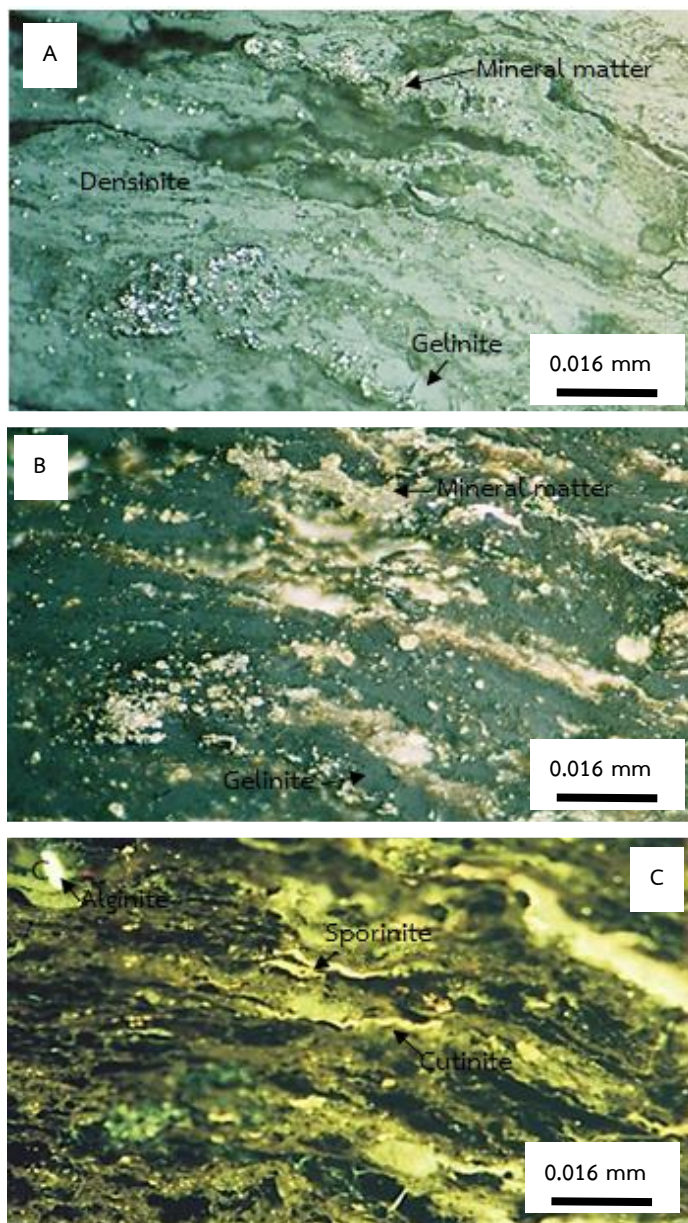
The J seam is divided into 4 subseams; J6, J5, J4 and J3 subseam were deposited in study area, 12 samples were collected from borehole no.MMC1, no.MMC-2 and no.MMC-3.

J6 subseam consists of 56 to 60% huminite group are dominated by gelinite and densinite, 13 to 16% of liptinite group are dominated by liptodetrinite, amorphinite, sporinite, alginite and cutinite. 7 to 8% of inertinite group are dominated by semifusinite, fusinite and sclerotinite. 16 to 22% of mineral matters are clay mineral, quartz, pyrite dominantly in form of framboidal and diatomite.

J5 subseam consists of 45 to 52% huminite group are dominated by densinite and gelinite. 22 to 25% of liptinite group are dominated by sporinite, liptodetrinite, cutinite and amorphinite. 5 to 6% of inertinite group are dominated by fusinite, and 20 to 25% of mineral matters are clay mineral, quartz, and pyrite dominantly in form of framboidal, diatomite and volcanic ash in place.

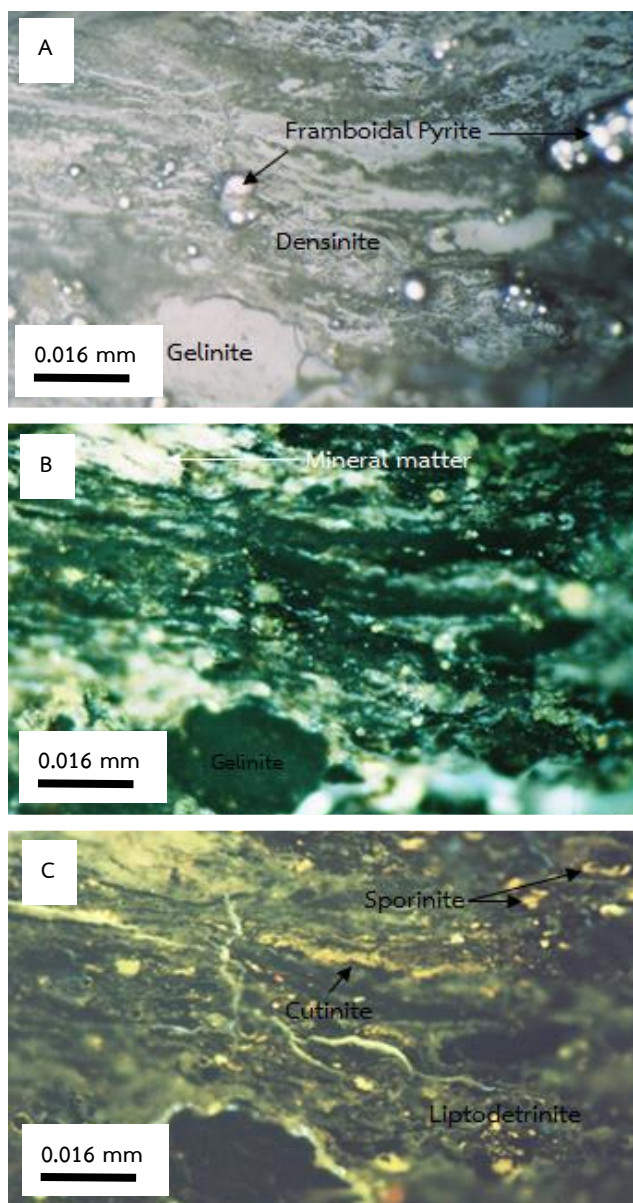
J4 subseam consists of 43 to 50% huminite group are dominated by gelinite and densinite. 18 to 30% of liptinite group are dominated by liptodetrinite, alginite, sporinite and amorphinite. 5 to 6% of inertinite group are dominated by semifusinite, fusinite and sclerotinite. 22 to 26% of mineral matters are clay mineral, quartz, pyrite dominantly in form of framboidal and volcanic ash in place.

J3 subseam consists of 53 to 62% huminite group are dominated by gelinite and densinite. 8 to 16% of liptinite group are dominated by sporinite, liptodetrinite, amorphinite, alginite and cutinite. 6 to 7% of inertinite group are dominated by fusinite, semifusinite and sclerotinite. 23 to 25% of mineral matters are clay mineral, quartz, pyrite dominantly in form of framboidal.



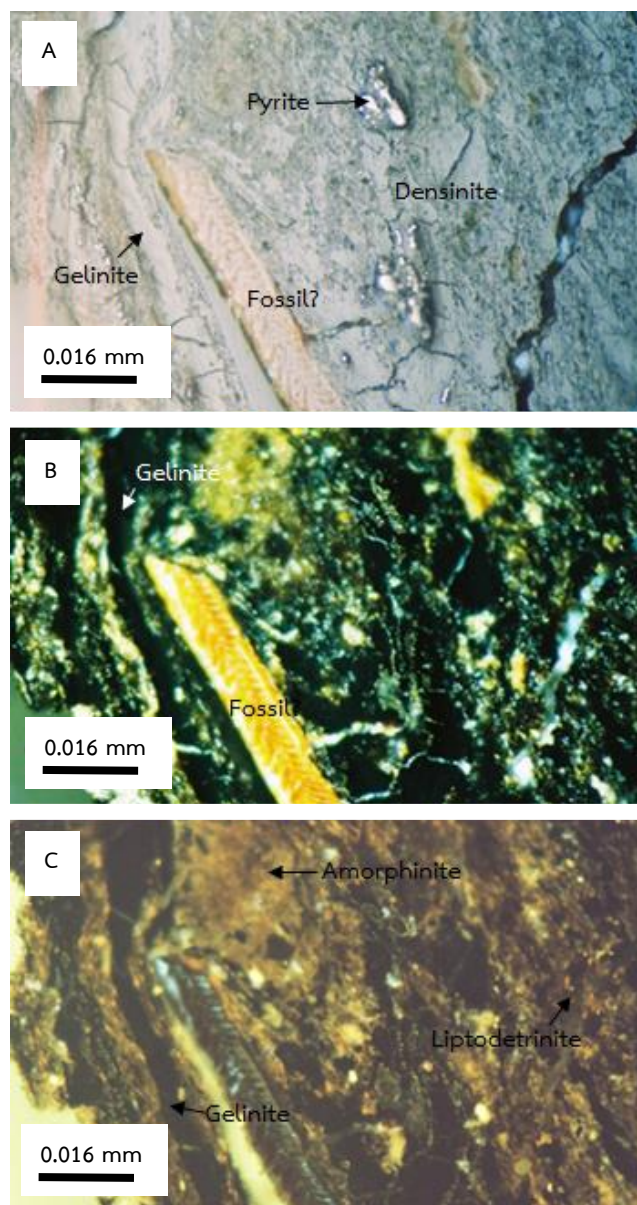
(A) PPL = Plane Polarize light, (B) XPL = Cross Polarized light, (C) FL = Fluorescence light

Figure 4.32 photomicrographs of gelified material of gelinite and individual small fragment of densinite, including yellow fluorescing crenulation on some surface of cutinite, bright yellow of alginite stand out under fluorescence light (C), associated with mass of mineral matters mainly pyrite; J6 subseam.



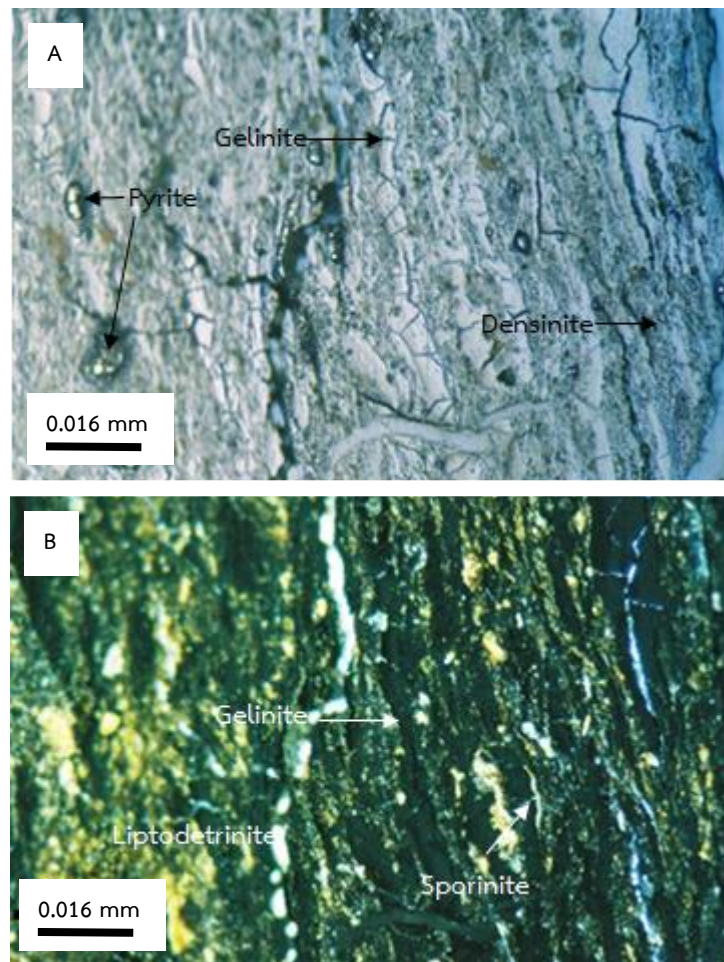
(A) PPL = Plane Polarize light, (B) XPL = Cross Polarized light, (C) FL = Fluorescence light

Figure 4.33 photomicrographs of bright yellow appendage of cutinite, bright yellowish green various shapes of sporinite, yellow discrete small fragment of liptodetrinite under fluorescence light (C), associated with pyrite in form of framboidal pyrite (round shape) brighten under plane polarize light (A) in groundmass of densinite and gelinite; J5 subseam.



(A) PPL = Plane Polarize light, (B) XPL = Cross Polarized light, (C) FL = Fluorescence light

Figure 4.34 photomicrographs of gelified material layer of gelinite and individual small fragment of densinite, associated with discrete small fragment of liptodetrinite, amorphous shape of amorphinite, and fossil remains (fish fragments?); J4 subseam.



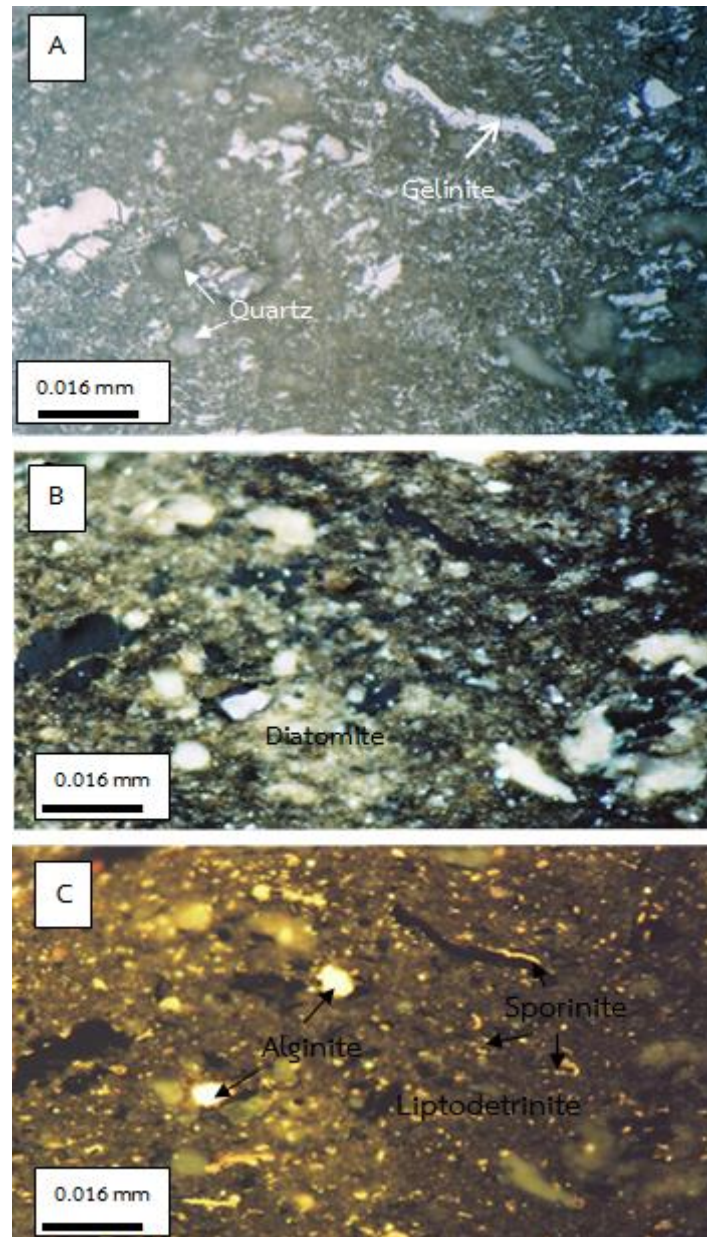
(A) PPL = Plane Polarize light, (B) XPL = Cross Polarized light

Figure 4.35 photomicrographs of gelified material layer of gelinite and individual small fragments of densinites, including bright yellowish green various shape of sporinite, discrete small fragment of liptodetrinite under fluorescence light (C), associated with brighten pyrite in form of framboidal pyrite (round shape) under plane polarize light (A); J3 subseam.

The upper coal seam is I seam, 2 samples were collected from borehole no.MMC2 and no.MMC3. I seam is divided into 2 subseams as I2 and I1 subseam from bottom to top, in the study area.

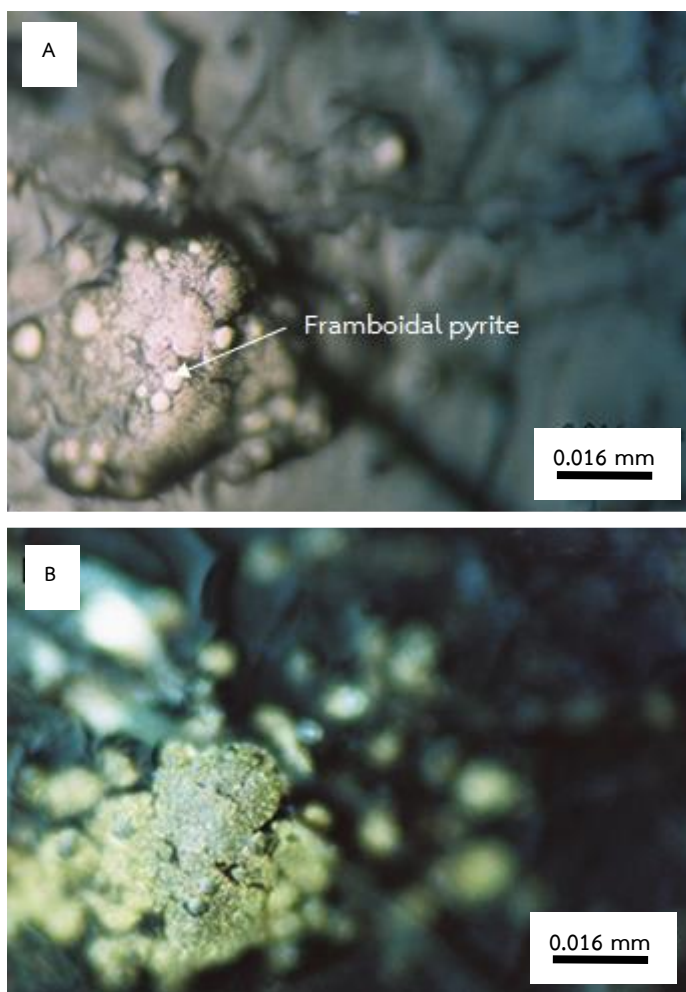
I seam consists of 54 to 55% huminite group are dominated by gelinite and densinite. 10 to 15% of liptinite group are dominated by alginite, sporinite, amorphinite and litodetrinite. 4 to 5% of inertinite group are dominated by fusinite, semifusinite and sclerotinite. 27 to 30% of mineral matters are clay mineral, quartz, and pyrite dominantly in form of framboidal.





(A) PPL = Plane Polarize light, (B) XPL = Cross Polarized light, (C) FL = Fluorescence light

Figure 4.36 photomicrographs of gelified material layer of gelinite, including bright yellow fluorescing alginite, bright yellow various shape of sporinite, yellow discrete small fragment of liptodetrinite under fluorescence light (C), associated with mass of mineral matter mainly quartz and pyrite; I seam.



(A) PPL = Plane Polarize light, (B) XPL = Cross Polarized light

Figure 4.37 photomicrographs of brighten pyrite in form of framboidal pyrite (round shape) under plane polarize light (A) and bright yellow under cross polarized light (B) in the groundmass of gelinite; I seam.

Huminite group is the main group in study coals. Major type is gelinite, following by densinite, and some texto-ulminite.

Gelinite is derived from the contents of plant cells or from humic fluids from plant tissue which may occur during decay and diagenesis. Therefore, gelinite shows structureless, compact and homogeneous. It is formed as groundmass. It apparently shows shrinkage cracks because of desiccation. It was found in almost all coal seams. Fluorescence color is none and shows colourless in normal reflected light.

Densinite is individual particular fragments. It is formed as groundmass with gelinite. It was found in all coal seams. It displays colorless in normal reflected light and fluorescence is none.

Texto-ulminite is plant tissue. The tissue is gelified but it still displays cellular structure (cell walls). Texto-ulminite is found in Q and K seam. It displays colorless in normal reflected light and fluorescence color is none.

Liptinite group is the material that forms the outer layer of spores and pollens. They are generally more resistant to degradation. They are dominated by liptodetrinite, sporinite, cutinite, alginite and some exsudatinite. All mecerals of this group are fluorescent.

Liptodetrinite is fragments of liptinites which occurs from oxidized liptinite in oxidized condition. It is found in all coal seams. It has a small size. The fluorescence color is yellow or the color can change depending on its origin.

Sporinite derives from spore or pollen. It was found in all coal seams. Sporinite shows different shapes because it is from different types of plant. There are round shape and long shape. They show colorless but some show yellow to golden yellow under normal reflected light. Some samples show brown color and high relief under crossed-polarized light. They appear orange, yellow to yellowish brown color under fluorescence light. It was dominated in Q and K seam.

Cutinite is cutin which forms the outer layers of leaves or cuticles. The physical properties of cutinite are similar to sporinite. It shows long shape and ridge shape. It is colorless under normal reflected light and shows brown color under crossed-polarized light. The Fluorescence color is yellowish green. It was dominated in Q and K seam.

Alginite is derived from algae, divided into 2 groups: telalginite and lamalginite. Lamalginite is abundant. It shows small, thin and long shape. It has high relief, colorless under normal reflected light and shows brown color under crossed-polarized light. The fluorescence color of lamalginite is yellowish brown to yellowish green. Telalginite is *Botryococcus* sp. *Botryococcus* shows a thick mass and similar to flowers. It is colorless, has high relief under normal reflected light and has brown color, high relief under crossed-polarized light. The fluorescence color shows yellow and some show yellowish green. It was dominated in J and I seam.

Exsudatinite is a secondary resinite which fills in vein, crack, the empty cell lumens or any space available. Exsudatinite is found in Q and K seam. It has colorless under normal reflected light. The fluorescence color is yellowish green.

Inertinite group is derived from tissue of fungi and fine detrital fragment which are called sclerotinite/funginite and fusinite, respectively.

Fusinite is well preserved cellular structure of parenchyma, collenchyma or sclerenchyma which occur from fire, in situ burning or tectonic activities. It shows very bright and strong relief under normal reflected light and black under UV Excitation. Fusinite is found in almost all samples, dominated in Q and K seam.

Sclerotinite is derived from fungal. It is rare in this basin. Its color under normal reflected light is colorless and brighter than huminite and liptinite but some show pale grey. The fluorescence color is none. It was rare in I seam.

Moreover, there are mineral matters in all samples. Quartz, clay mineral, pyrite and layer of diatomite and volcanic ash are found. Mineral matters have no

fluorescence color. Some pyrite and diatomite are fluorescent because they are filled by hydrocarbon. Under normal reflected light, quartz shows colorless, clay mineral shows brown or colorless, pyrite shows yellow or golden yellow and layer of diatomite shows yellow as well.

4.3.2 Vitrinite reflectance measurement

The degree to which the vitrinite in a coal reflects light in polished section studies can readily be seen to increase as the rank of the coal increases. Using standardized techniques, with green light (wavelength 5250\AA) and immersion oil with an R.I. of 1.515, the amount of light reflected from a well-polished vitrinite particle can be determined using a suitable photo-multiplier and appropriate reference standards.

If polarized light is used, a variation in reflectance will be noted as the microscope stage is rotated, since vitrinite usually behaves as the microscope stage is rotated, since vitrinite usually behaves as a uniaxial negative mineral. In such a case, the maximum reflectance, or the average of the two maxima 180° apart is determined for each grain in the crushed maceral mount. When such maximum reflectance readings have been obtained from a suitable number of vitrinite grains (usually 50) the mean maximum reflectance, $R_{o_{\max}}$ is calculated for the coal sample.

The mean maximum reflectance of vitrinite varies from around 0.3% for brown coals to over 2.3% for anthracites. It varies most significantly in material of bituminous rank, and as a result is applicable as a rank indicator for many commercial coals, where rank is related to coking or liquefaction characteristics. In combination with an index of coal type it can be used to characterize coal samples on a petrographic, rather than a chemical basis (Bennett and Taylor, 1970). The development from peat through the stages of the different brown coals (lignite), sub-bituminous and bituminous coals to anthracites and meta-anthracites is termed coalification.

This study was measured their mean maximum vitrinite reflectances of 4 coal seams as I-, J-, K- and Q seam by SGS (THAILAND) LIMITED. They have the $R_{o_{max}}$ of 0.53, 0.60, 0.57 and 0.58%, respectively. The highest vitrinite reflectance is sample from J seam, with $R_{o_{max}}$ 0.60% and lowest vitrinite reflectance is sample from I seam, with $R_{o_{max}}$ 0.53%. They can be classified to subbituminous A ranks, according to the German (DIN) and North American (ASTM) classifications.



Chapter 5

5. Discussion

5.1 Depositional paleo environment

In this study, 3 boreholes in the central part of Mae Moh basin were selected for lithostratigraphy studied and 35 coal samples selected for petrography study, which collected from main coal seams in Mae Moh group as J-, K- and Q seam of the Na Khaem formation, and minor coal seam as I seam of Huai Luang formation. Composite stratigraphy has been made by 3 boreholes correlation. It can be used to interpret the depositional environment by appearance characters of each sequence along with the coal petrography study.

Coal petrographic study is dominated by huminite, followed by liptinite and inertinite group. Huminite group is characterized by gelinite followed by densinite and some textu-ulminite. Liptinite group is composed of liptodetrinite, sporinite, cutinite, alginite, amorphinite and some exsudatinitite. Inertinite group is fusinite, semifusinite and funginite in sclerotinitite type. Moreover, there are mineral matters in all samples, characterized by diatomite, clay mineral, pyrite dominantly in form of framboidal, silicate, carbonate, and some volcanic ash in place. Details of depositional sequence are described from the lower to upper deposition following paragraphs.

The underburden is the lowest part, consists of fine grained sediment as claystone, mudstone and silty claystone, indicated that low energy of floodwater had been transported into the basin. These large amounts of sediments were transported into the basin which made the basin shallow enough for plant deposit lead to coal formation (Q seam). This petrographic study is revealed depositional environment of Q seam is alternation of lacustrine to forest swamp environments. In the lacustrine environments, the major macerals are dominated by huminite group

mainly disintegrate types such as gelinites and densinites. Liptinites are dominated by liptodetrinite indicated highly oxidation of plant materials before deposition and exsudatinite is common even at early levels of maturation. Rare alginite is indicated waterlog was not common. In the forest swamp environments are characterized by the presence of dissolved texto-ulminite, sporinite, cutinite and macerals in the inertinite consist of fusinite and funginite in form of sclerotinite. Fusinite is indicated dried up condition. Pyrites in form of framboidal are disseminated throughout the coals.

The Q seam was terminated by floodwater which resulted in thick bed of fine grained sediment (interburden) above coal seam. Interburden is a persistent sequence of the fine grained sediments of brown, brownish gray, gray, green and greenish gray claystone, and containing common coal flakes, fish remains, plant roots, rare ostracods and gastropods (*Viviparus sp.*), indicated freshwater lacustrine deposited. A large amount of interburden was transported into the basin continuously which made the basin shallow enough for plant accumulation lead to coal formation (K seam) again. The depositional environment of K seam is alternation of lacustrine to forest swamp environments. In the lacustrine environments, the major macerals are dominated by huminite group mainly of high disintegrate types such as gelinite, densinite. Liptinites represented by alginite. The major of alginites in Mae Moh is thin-wall lamarginite which dominant in late middle Miocene time (Ratanasthien et al., 1999). Liptodetrinite indicated highly oxidation of plant materials before deposition. The tree trunks association indicated the forest swamp environments are characterized by the macerals composed of highly dissolved texto-ulminite, sporinite and cutinite. Exsudatinites indicated early levels of maturation. The diatomite association indicated there was a volcanic eruption occurred during the deposition period and contributed high silica volcanic ash into the basin. Gastropod fossils (*Planorbis sp.*, *Melanooides sp.*) associated in coal indicated shallow water lacustrine and mastodon remains associated in K1 subseam could be infer the possibility catastrophism and terminated the K seam (Ginsberg, 1983).

Piwkam (2012) reported two palynological zones found in K and Q seams. The first zone is the *Laevigatosporites ovatus* zone found in all of sequences, consists mainly of *Laevigatosporites ovatus*, *Cyathidites minor* and *Foveotriletes margaritae* which interpreted to be in a subtropical to tropical climate. The second zone is the *Magnastriatites grandiosus* zone found in the upper sequences, represents as a fresh water lacustrine deposit that is the evidence of the freshwater spores of *Magnastriatites grandiosus* in abundance. The spores compared with the genus *Ceratopteris*, freshwater floating ferns strongly indicate spores living in swamp.

The next sequence consists of thick bed of fine grained sediments (overburden) again. Overburden is brownish gray claystone and mudstone with occasional siltstone, highly calcareous and gastropod (*Melanoides sp.*) which indicated a long time of floodwater deposit. The upper sequence is coal formation (J seam). The depositional environment of J seam is alternation of lacustrine to forest swamp environments similar to Q and K seam. In the lacustrine environments, the major macerals are dominated by huminite group mainly of disintegrate types as gelinite, densinite. Liptinites dominated by alginite and liptodrinite. The forest swamp deposits are characterized by cutinite, and sporinite along with fusinite are included. Mineral matters are dominated by pyrites in form of framboidal pyrites, diatomite, and some volcanic ash. The high percentage of sulphur, and diatomite throughout the J seam could be the effect of this volcanic eruption and terminated the J seam. During the deposition of J seam short time coal accumulation indicated highly tectonic disturbance during the deposition (Ratanasthien et al., 1997).

Tankaya (2001) reported the coals deposited in northern part of Mae Moh basin, the mineral matters are dominated by silica in form of quartz, kaolinite, calcite, gypsum and siderite. The result of sulphur's isotope from gypsum is low value ($^{34}\text{S} +0.5$ to $+4.3\%$) indicated effect from volcanic eruption during coal accumulation.

The upper most of top J seam is dominant of claystone, siltstone and silty claystone, with vary color. It marks the transition from the reducing environment of

lacustrine deposition typical of the Na Khaem formation to the oxidizing conditions characteristic of the alluvium deposits of the Huai Luang formation, which is also commonly referred to as Red Bed, consists of red to brownish red claystone, siltstone and mudstone with lenses of sandstone. The brownish red to red colors due to the oxidation of fine grained pyrite to hematite disseminated throughout certain layers of the formation (Sompong et al., 1996). No macrofossils have been found but there are abundant gypsums and pyrites with rare roots and flame structures which indicated fluvial lacustrine deposited.

The red bed sequence is thick fine to coarse grained sediments indicated that floodwater had been transported into the basin for a long time, which made the basin shallow enough for plant deposit lead to coal formation (I seam). The depositional environment of I seam is mainly of lacustrine environments is characterized by the macerals composed mainly of gelinite and densinite. Liptinite dominated by alginite and liptodetrinite. The presence of abundant pyrites in form of framboidal pyrites and gypsums are distributed throughout the mass of coals. Framboidal pyrites indicated the source of mainly aquatic plants which underwent huminization under the influence of aerobic bacteria first, followed by anaerobic bacteria (Ratanasthien and Kandharosa, 1987) and the presence of gypsum in this sequence suggests high pH conditions. This coal deposit was terminated by floodwater deposit again which resulted in thick sediment above the coal seam. And the last sequence is alluvium deposits represented by clays, silts, sands, gravels with vary color indicated fluviatile depositional environment.

Their depositional of studied coal deposited in central part of Mae Moh basin similarity in northwest part of Mae Moh basin, 70 coals samples show a relatively high huminite (60 to 90%) and liptinite (5 to 25%) contents, a low inertinite contents (less than 5 %) and no recorded in percentage of mineral matters. The petrographic results could indicate typical depositional environment is lacustrine swampy peat bearing formation (Ratanasthien et al., 1997). In the Li basin, the two sections (Ban Pa Kha and Ban Pu) of Li formation which is believed deposit during upper Oligocene

have in common on some lithofacies which did not occur in Mae Moh basin. There is carbonaceous shale, oil shale, mudstone, fining upward and coarsening upward sandstone lithofacies. Some planar and trough cross-bedded sandstone are also present in the Li basin. From lithofacies association of two sections, It can be indicated the depositional environment of this basin are dominantly fluvial- alluvial system which some minor lacustrine deposits associated in Ban Pa Kha. According to Promkotra, 1994, petrography results of 24 coal samples from Ban Pa Kha in Li basin are mostly of huminite (85 to 95%) dominated by textinite and less of liptinite (2 to 7%) presented by cutinite and resinite, rare of Inertinite (0 to 3 %) consists of sclerotinite only. The percentage of mineral matter is varying from 2 to 10%. The coal beds are associated with dark gray mudstone, greenish grey mudstone and thin beds of fine-grained sandstone. This association may represent the changing of depositional environment from low energy flood plain and forest swamp to shallow lacustrine-deltaic environment. The fine grained sand bed may deposit during the high flooding period. The lacustrine deposits are carbonaceous shale, oil shale and dark grey mudstone. The well preserved organic matter suggests an accumulation under anoxic conditions probably in a stratified lacustrine (Reading, 1996). The coarsening upward sandstone at Ban Pu commonly associated with dark grey mudstone and coal. Therefore, the suitable interpreted depositional environments for this sand facies would be a crevasse splay deposit. Another support this interpretation is that these two sections association occurred near the braided channel and overbank deposit (Uttamo, 1998).

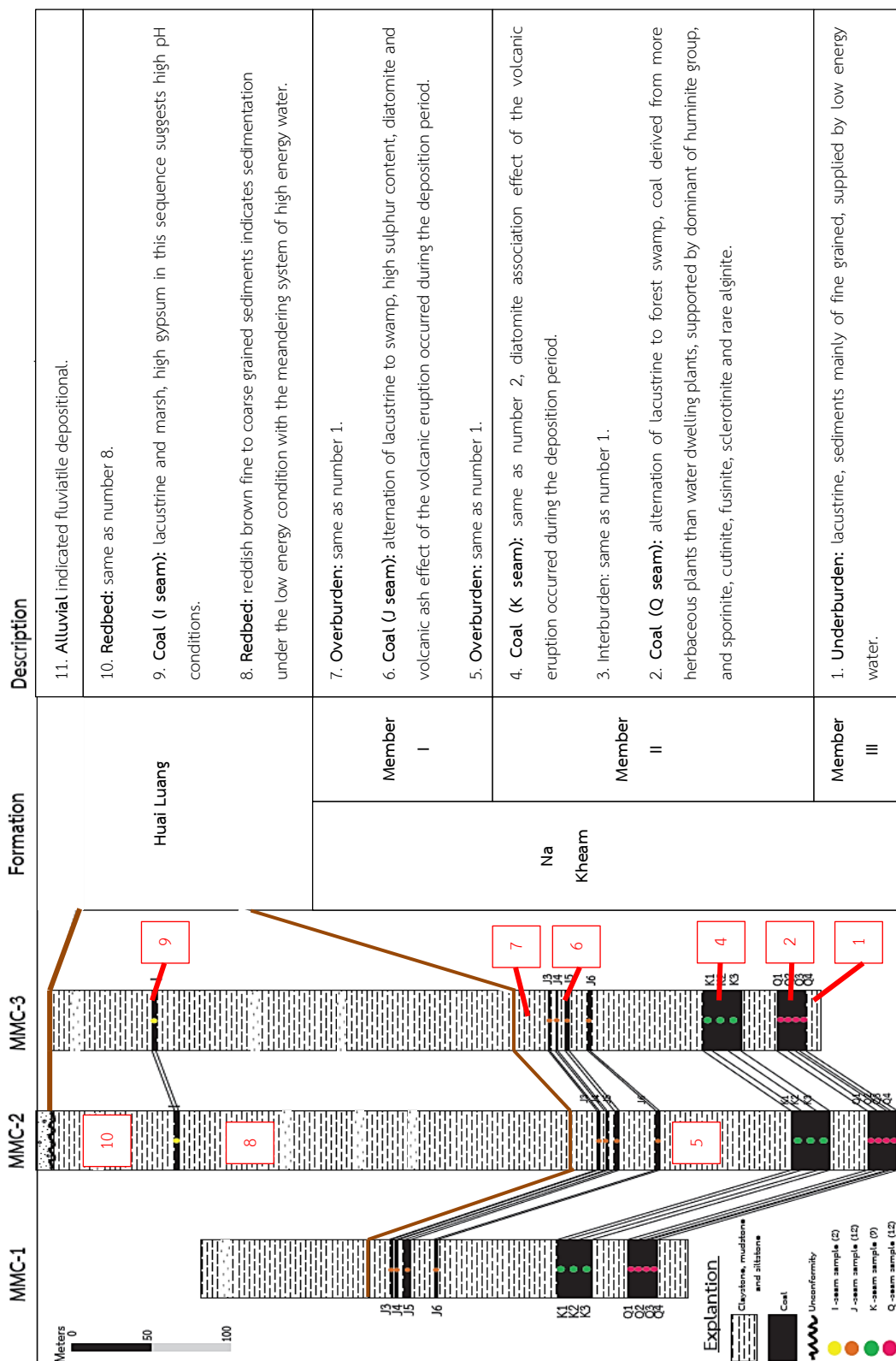
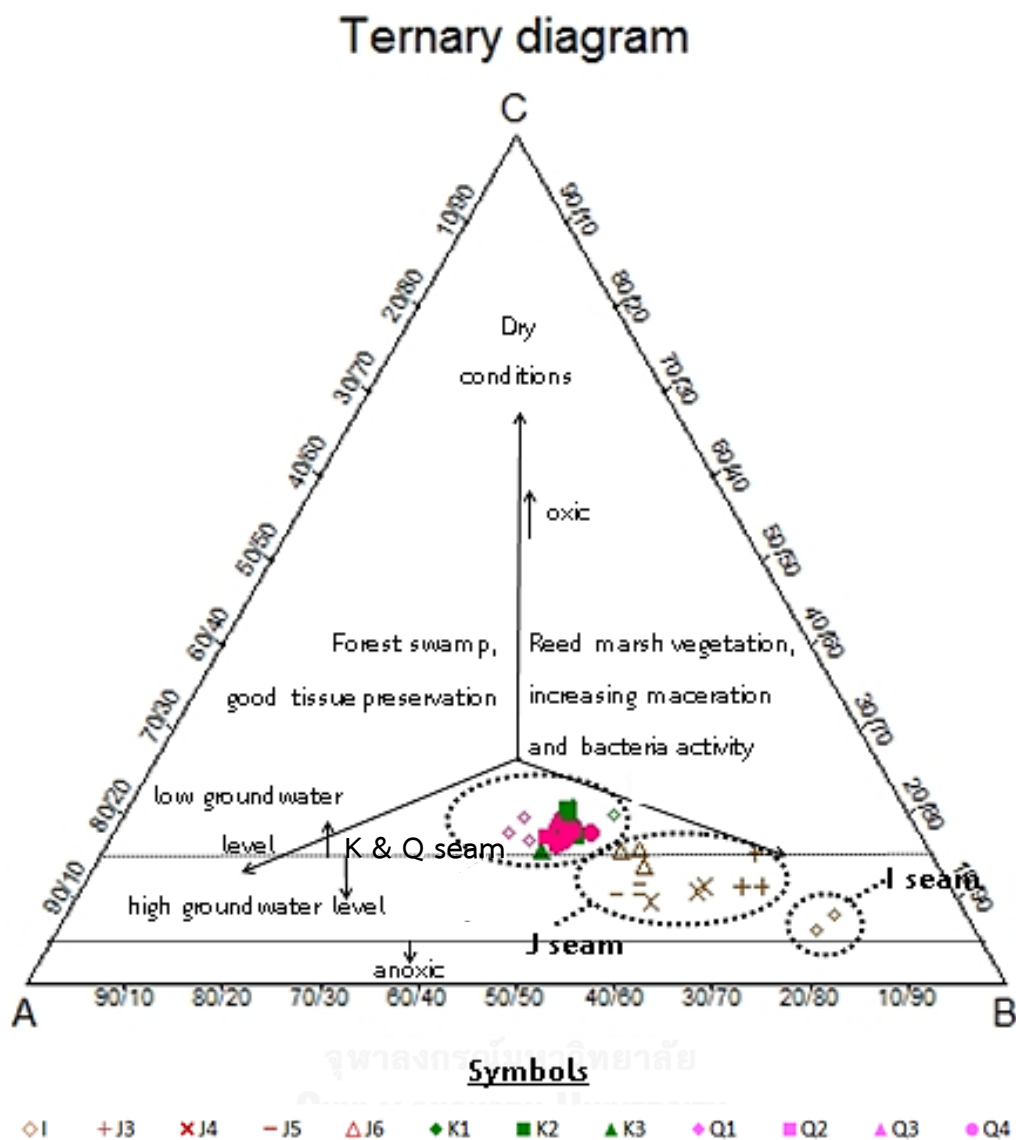


Figure 5.1 Depositional environment interpretation of study area in central part of Mae Moh basin.

The ternary diagram of maceral assemblages is used for evaluation of depositional environment. (Hower, 1990; Mukhopadhyay, 1986) defined the vertices of a ternary diagram, later modified by Kalkreuth et al. (1991) as: vertex a) parameter that considers gelified tissues and liptinite from terrestrial plants in forest swamps with good tissue preservation; vertex b) parameter that includes gelified detritus, gelinite, and liptinite related to aquatic environments such as a reed marsh dominated by herbaceous plants with a high level of tissue maceration and high bacterial activity; and vertex c) parameter that comprises the inertinite content, related to oxidizing environments, including wildfire (Scott, 1989). This interpretive ternary diagram was used for facies determination based on maceral assemblages.

The study coal samples were plotted into the ternary diagram, showing a peat-forming environment is not definitely ascribed to forest swamp or a reed marsh environment. I and J seam suggest high groundwater level during peat formation, while K and Q seam suggest low groundwater level during peat formation which can be inferred peat originated from higher plants.



A= humotelinite+ corpohuminite+phlobaphinite
+terrestrial liptinite

Equation 1

Terrestrial liptinite = sporinite+cutinite+resinite+fluorinite

B= humodetrinite+ gelinite+liptodetrinite+alginate

Equation 2

C= inertinite

Equation 3

Figure 5.2 Ternary diagram suggesting peat-forming environments for Mae Moh coals, based on maceral assemblages (modified after (Mukhopadhyay, 1986)).

Furthermore, Diessel (1986) has introduced two petrographic indices, the Gelification Index (GI) and Tissue Preservation Index (TPI). These indices were used to characterize the depositional environments of Australian Permian coals. For low rank Miocene and Jurassic coals, these indices have been modified by Kalkreuth et al. (1991) and Petersen (1993), respectively. TPI is mainly governed by water depth and the frequency of dry periods and is modified by pH and trophic level, but the botanical composition plays also a role. GI is a measure of groundwater table and/or pH indicator, because gelification requires the continuous presence of water and because microbial activity requires low acidity (Kolcon and Sachsenhofer, 1999). A fluctuating water table caused by drier periods may increase the wildfire frequency, which also will influence the GI due to the formation of inertinite during burning of the plants. The coals were plotted in the Diessel's diagram with TPI and GI base on maceral assemblage. The Tissue Preservation Index (TPI) and Gelification Index (GI) are calculated as shown in equation 4 and equation 5.

$$\text{TPI} = \frac{\text{humotelinite} + \text{semifusinite} + \text{fusinite}}{\text{humodetrinite} + \text{humocollinite} + \text{inertodetrinite}} \quad \text{Equation 4}$$

$$\text{GI} = \frac{\text{huminite}}{\text{inertinite}} \quad \text{Equation 5}$$

The TPI is a ratio of tissue derived structured macerals (gelified and oxidized) versus tissue-derived unstructured macerals (detritus and gels). This petrographic index also gives an indication of the vegetation which has contributed to the peat biomass and its preservation. High TPI values indicate well-preserved plant tissues balanced by the ratio of plant growth and peat accumulation versus rise in groundwater table controlled by basin subsidence. Low TPI suggests either predominance of herbaceous plants or poor preservation of wood material. The GI relates macerals of the huminite/vitrinite group plus macrinite to oxidized tissues and

detritus to quantify the gelification degree of the organic matter. Thus the GI reflects the relative water level during peat formation, indicating the relative dryness or wetness of the peat forming conditions. It is a measure not only of the degree of tissue gelification but also the rates of peat accumulation and basin subsidence. Wet conditions of peat formation are predicted to have high GI and TPI indices, whereas drier conditions lead to low GI and low TPI indices (Diessel, 1992).

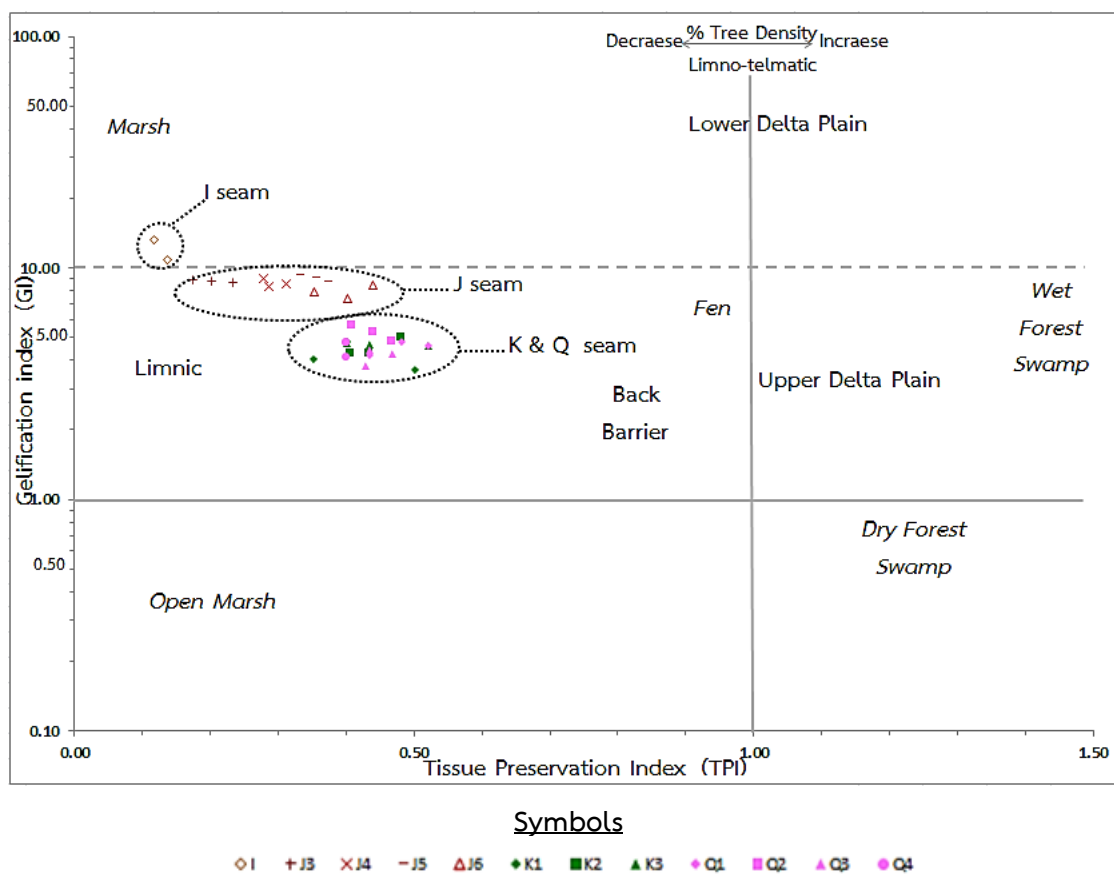


Figure 5.3 The study coal facies depicted from the Gelification Index (GI) and Tissue Preservation Index (TPI) in relation to depositional setting and type of mire (modified after (Diessel, 1986)).

Mae Moh coals were plotted in the Diessel's diagram (Diessel, 1986) with TPI and GI base on maceral assemblage. The study samples are characterized by low TPI values (0.11 to 0.52) and moderate to high GI values (3.67 to 13.50). Accordingly

deciphered these study coals have originated under limnic(lacustrine) condition of peat formation with vegetation characteristics of marsh and wet forest swamp type, which was also supported by dominance of huminite macerals (e.g., gelinite, densinite, and some textolinite) following by liptinite macerals (e.g., litodetrinite, sporinite, cutinite, and alginite) and less of inertinite macerals (e.g., fusinite, semifusinite and sclerotinite). The low TPI values suggest high bacterial activity, and high pH conditions, and preservation of gastropod shells. High alkalinity and reducing conditions may be inferred from the presence of syngenetic (framboidal) pyrites, which in turn destroys cellular and thus the poor tissue preservation. Low TPI values can be either the result of the vegetation type (e.g. high angiosperm/gymnosperm ratio) or due to less favorable conditions of tissue preservation (Kolcon and Sachsenhofer, 1999). The high GI values suggest a constant influx of calcium-rich water into the basin (Markic and Sachsenhofer, 1997; Singh and Singh, 2000).

Similarly to Pliocene lignites from Apofysis mine, Amynteo basin, Northwestern Greece, the huminite is the most abundant maceral group (47 to 84%) and consists mostly of humodetrinite, while liptinite (2 to 11%) and inertinite (3 to 17%) has relatively low percentage, associated with mineral matters 7 to 34%. Pyrite content is relatively high (1.5 to 3.5%), found mostly in the form of framboidal pyrite and suggests enhanced activity of sulphate-reducing bacteria, probably related to carbonate and sulphate-rich waters in the basin. The presence of high amounts of pyrites thus indicates a marine influence on the precursor mires. Low TPI and high GI values are observed. TPI less than 0.6 and GI higher than 6 suggest a topogenous mire. GI>10 reveals a marsh-reed environment or a forest with high degrees of degradation, permanently flooded (Iordanidis and Georgakopoulos, 2003).

Sia and Abdullah (2012) recorded the petrographic of Pliocene Balingian coal from Sarawak, Malaysia is dominated by huminite (56.7 to 94.7%), with low to moderate amounts of liptinite (1.1 to 40.8%) and low amounts of inertinite (0.8 to 8.9%), pointing to predominantly anaerobic deposition conditions in the paleomires, with limited thermal and oxidative tissue destruction. Most of the studies samples

are characterized by low TPI and high GI values, and are plotted on the marsh field of the Diessel's diagram.

By contrast, Permian Gondwana coals from Barapukuria basin, northwest part of Bangladesh, the eight coal samples have that maceral composition is dominated by the inertinite group (30 to 69%). Semifusinite, fusinite and inertinite were the most common macerals of the inertinite group. Following by vitrinite group (2 to 50%) is collotelinite, collodetrinite and vitrodetrinite were the most frequently found macerals of the vitrinite group. Liptinite groups (15 to 25%) are most common sporinite and cutinite. Mineral matter is low percent (2 to 15%). Clay mineral occurred in higher than the other minerals. Low GI (0.03 to 1.72) versus low TPI (0.25 to 29.50) cross-plot and dominance of inertinite macerals clearly demonstrate that the organic matter has been derived from terrestrial inputs and the condition of deposition was oxic (dry forest swamp) which was also supported by the absence of alginite. It is most likely that the coals were deposited within a peat swamp flood basin environmental setting (Farhaduzzaman et al., 2012).

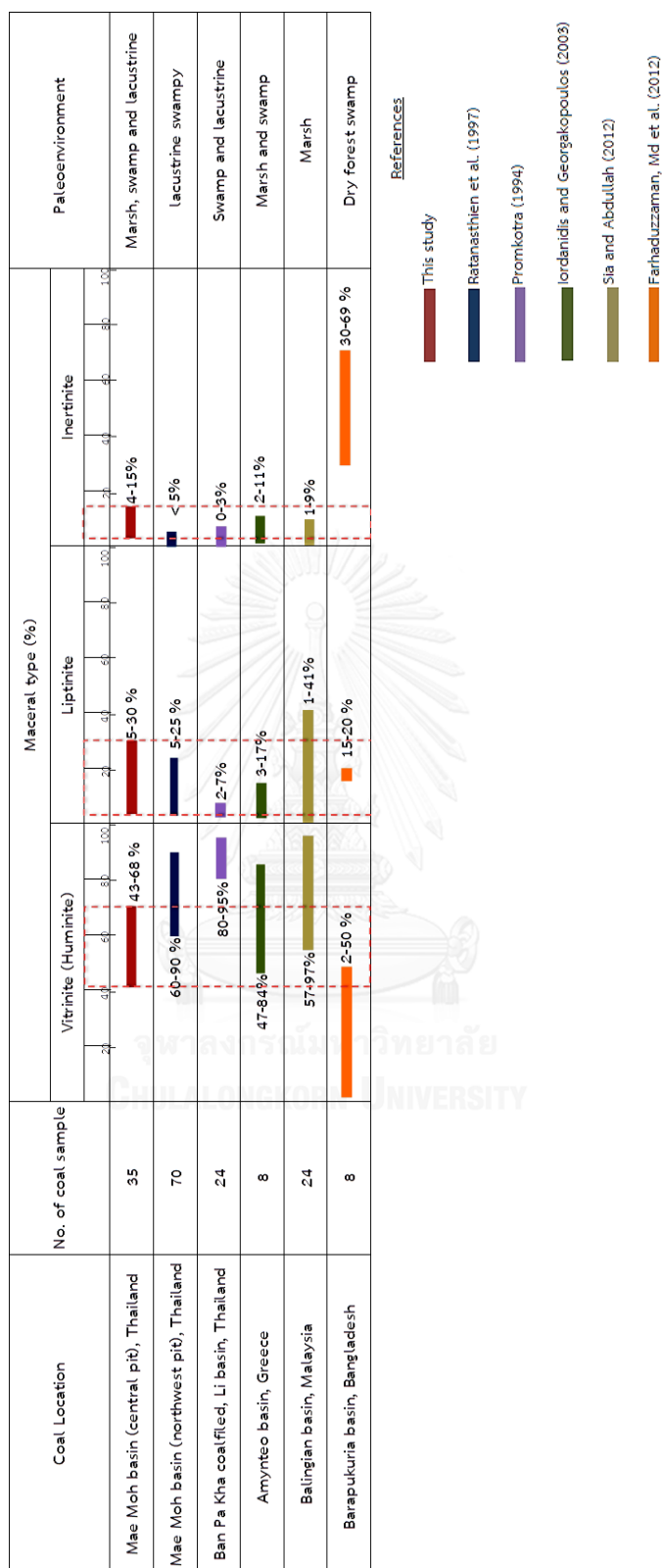


Figure 5.4 Comparisons of maceral contents (%) related to depositional environment of the study coals in Mae Moh basin and other basins.

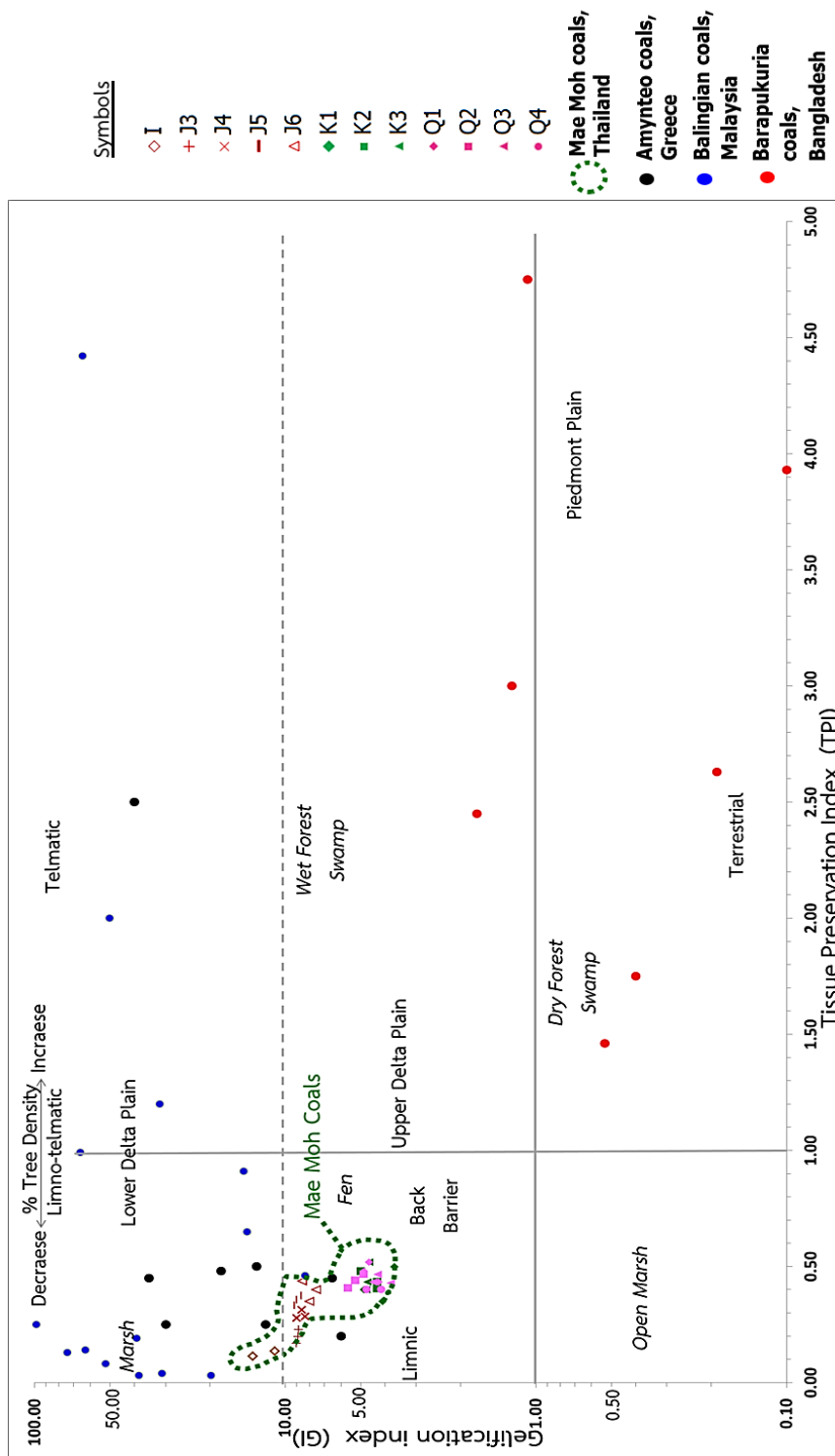


Figure 5.5 Diagram of TPI versus GI showing the depositional paleo environment of the peat mires (modified after (Diessel, 1986)), compare between the study coals in Mae Moh basin and oversea coals basin.

5.2 Coalification rank

The categorization of coals by degree of metamorphism is known as rank classification. The changes in rank result mainly from the weight of overlaying sedimentary rock, the heat produced by depth of burial, time, structural deformation, chemistry of the water and biochemical actions, all of which contribute to progressive compaction.

There are 3 analyses to classify the coal; proximate analysis, ultimate analysis and calorific determination. The results of proximate and calorific value analysis can assess the coalification rank by using the ASTM stand D388 (2005), and ultimate analysis also used to assess the coal rank by Van Krevelen diagram (Krevelen, 1993).

Proximate analysis; fixed carbon and volatile matter contents tend to increase from I seam to Q seam (figure 4.8 and 4.9). Conversely, ash and moisture decrease toward from I seam to Q seam (figure 4.10 and 4.11).

The relationship of proximate analysis indicates that increasing of fixed carbon content shows decreased of ash and moisture contents. The ash content is considered to be an approximation for mineral matters. Likewise, increasing of fixed carbon shows increased of volatile matter. Therefore, coals of this study area have high volatile matter, carbon and hydrogen contents that can be generated hydrocarbon such as methane.

Ultimate analysis; carbon, hydrogen, nitrogen, oxygen and sulphur contents are derived from organic compound. Therefore, carbon from ultimate analysis is higher than fixed carbon from proximate analysis. Carbon, hydrogen and nitrogen contents tend to increase, but in some points are not always the same because there are different in type of peats (figure 4.12, 4.13 and 4.14). Conversely, oxygen contents decrease toward from I seam to Q seam (figure 4.15). Trend of sulphur content decrease but some points are not the same, depending on reduced

condition or element supply (figure 4.16). Most of coal seams quite contain high sulphur could be resulted from volcanic ash contribution.

Calorific value tends to increase from I seam to Q seam (figure 4.17). This value relates to volatile matter content from proximate analysis and carbon and hydrogen content from ultimate analysis. Therefore, high volatile matter, carbon and hydrogen content relate to high calorific value.

Besides, the atomic ratio of hydrogen and carbon (H/C ratio) and oxygen and carbon ratio (O/C ratio) were described the coalification rank by using Krevelen diagram (Krevelen, 1993). Carbon, hydrogen, and oxygen content from ultimate analysis are divided by the atomic weight, and then they are calculated the ratio of H/C and O/C. The study coals were plotted within the coalification band of Van Krevelen diagram (Krevelen, 1993). They show trend of coal rank increasing from I seam to Q seam which are lignite/subbituminous, and some samples of Q seam fell within the rank of bituminous, probably due to its high carbon contents. Similar to the H/C and O/C atomic ratios of the coal from northeast part of Mae Moh basin were plotted within the Van Krevelen diagram. They fell within the lignite/subbituminous band (Sompong et al., 1996).

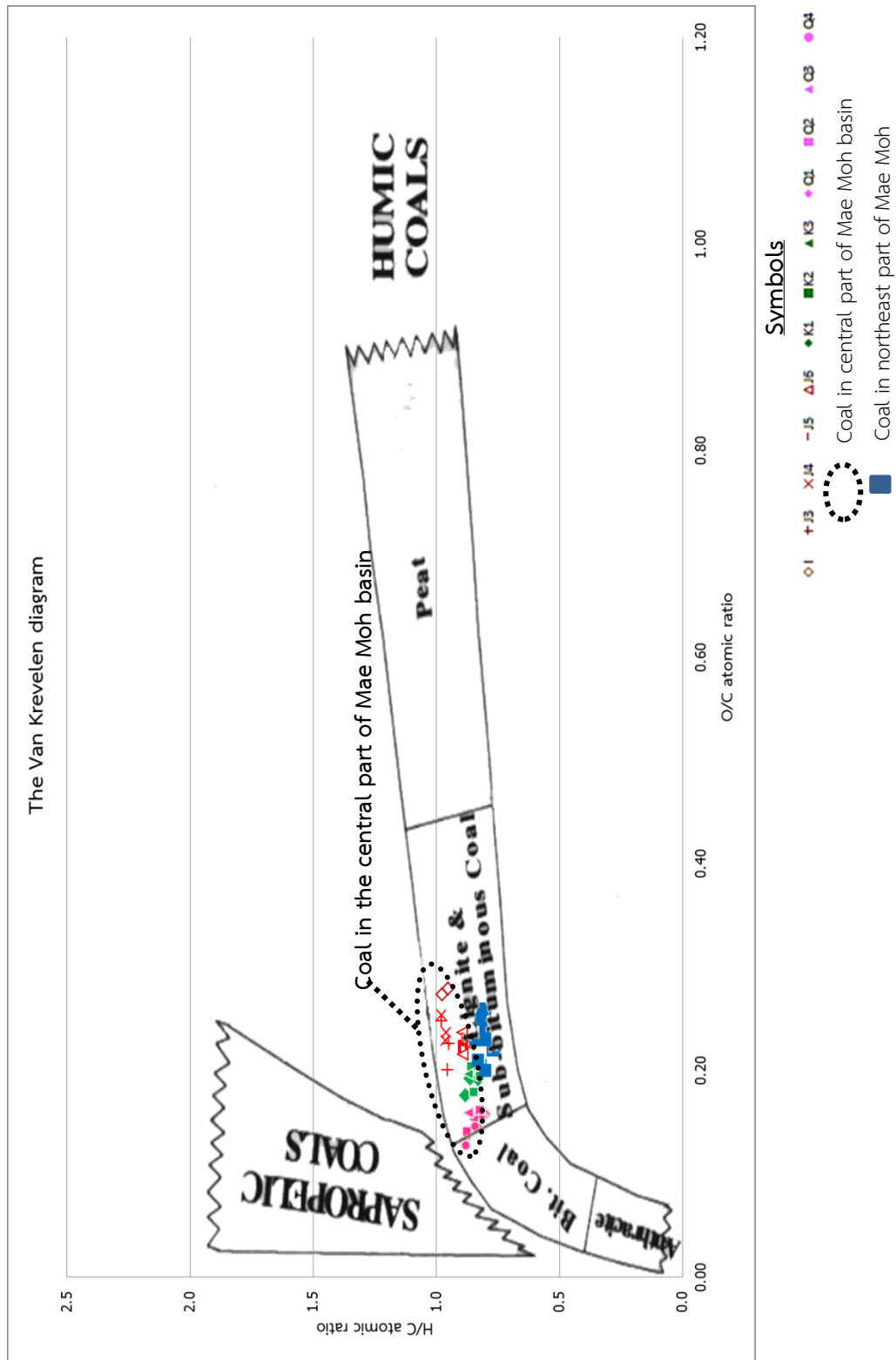


Figure 5.6 The Mae Moh coal samples plotted on H/C versus O/C atomic ratio diagram (modified after (Krevelen, 1993)).

According to the ASTM classification of coal by rank considering percent fixed carbon and volatiles matter on dry, mineral-matter-free basis along with calorific value on moist, mineral matter free basis. For coal, the calorific value has to be changed to unit of Btu/lb (British Thermal Units per pound). The results show the fixed carbon is less than 69%, volatiles matter is more than 31%, and calorific value is from 6,828-10,207 Btu/lb. They can be classified to lignite A to subbituminous B ranks. Coalification rank tends to increase from I seam to Q seam.

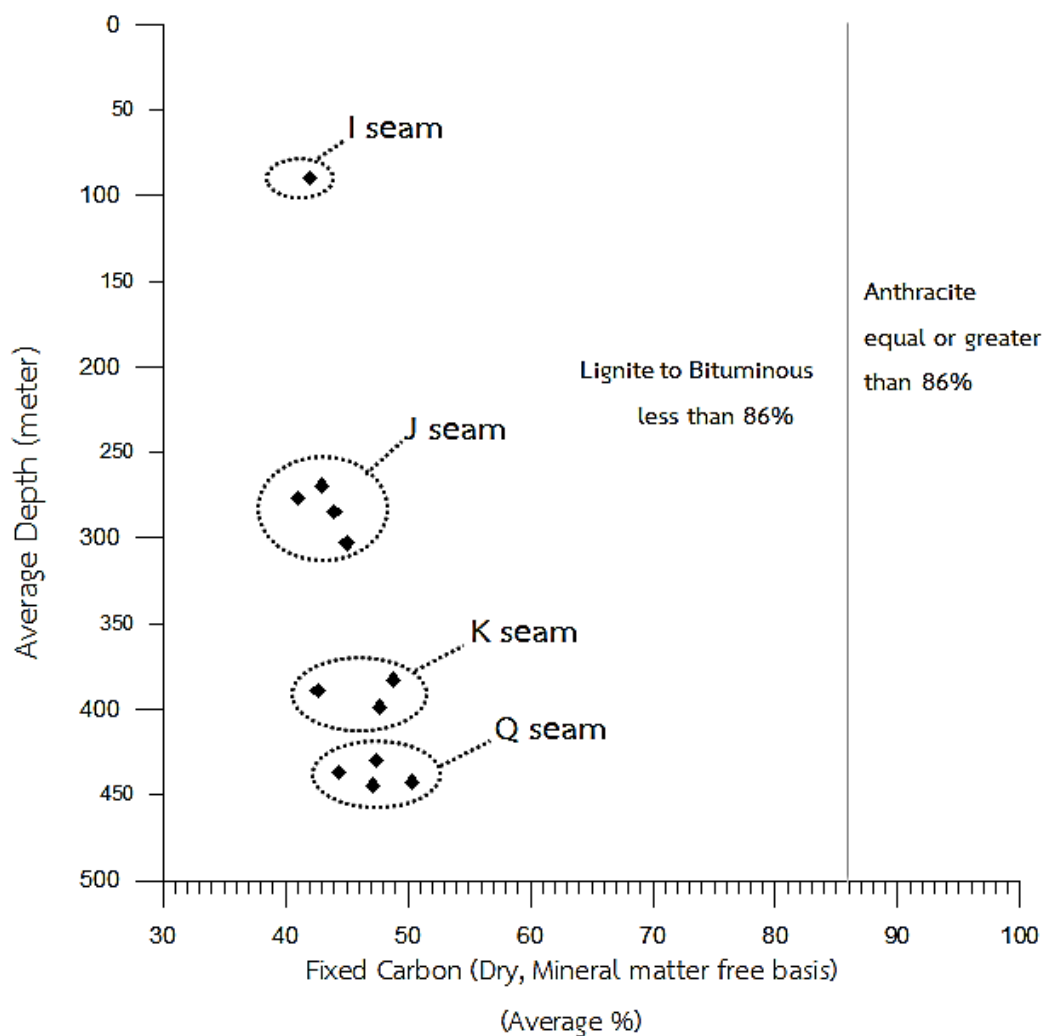


Figure 5.7 Graph showing coal rank related to coal seams by using the ASTM standard (D388), which described by the fixed carbon on dry, mineral matter free basis.

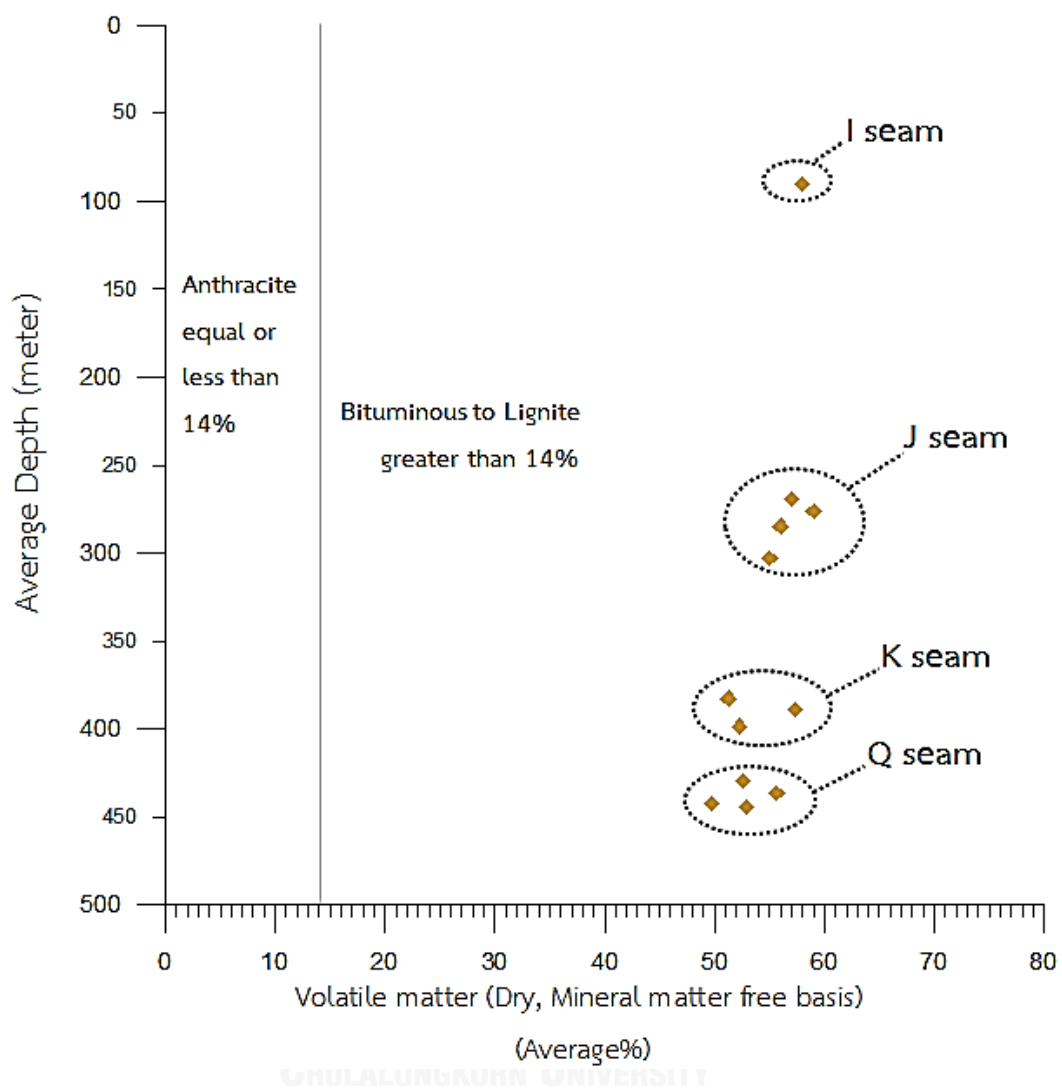


Figure 5.8 Graph showing coal rank related to coal seams by the ASTM standard (D388), which described by the volatile matter on dry, mineral matter free basis.

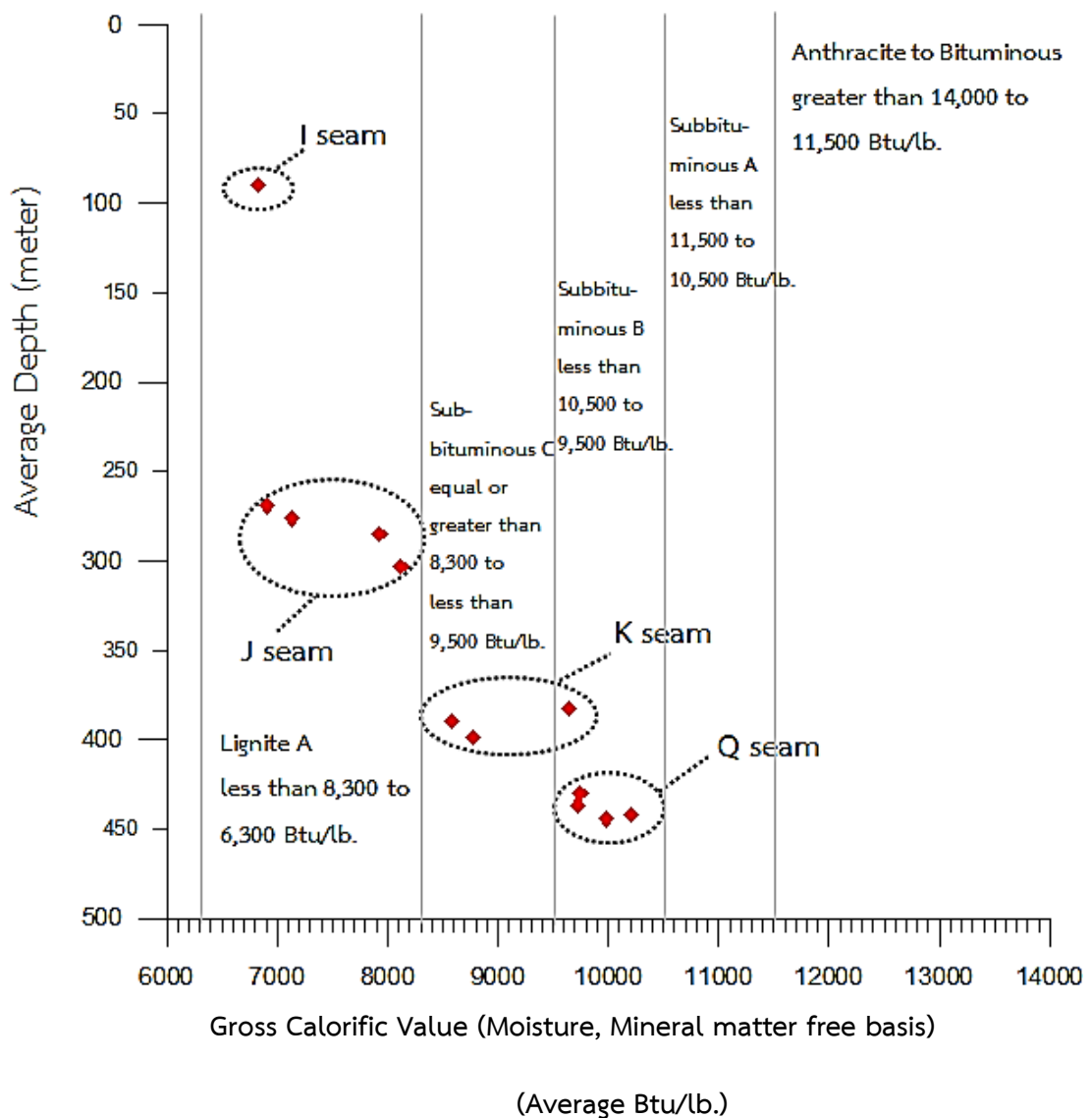


Figure 5.9 Graph showing coal rank related to coal seams by using the the ASTM standard (D388), which described by calorific value on moist, mineral matter free basis.

Coals in study area are classified as low rank coal varies from lignite A to subbituminous B. Trend of coalification rank increases from I seam to Q seam, which related to depth of burial.

Sompong et al. (1996) reported the coal samples (J-, K- and Q seam) were collected from northeast part, which shallower than central part of Mae Moh basin

.Their coal quality in fixed carbon and volatiles matter on dry, mineral matter free basis along with calorific value on moist, mineral matter free basis are 33 to 42%, 58 to 67% and 6,755 to 7,579 Btu/lb respectively, classify the coals are lignite A rank.

The comparison between the studied coals in central part and northeast part of Mae Moh basin by Sompong et al. (1996) following ASTM (D388) show coals deposit in central part is higher rank than coals deposit in northeast part, which related to depth to depth of burial (figure 5.10, 5.11 and 5.12).

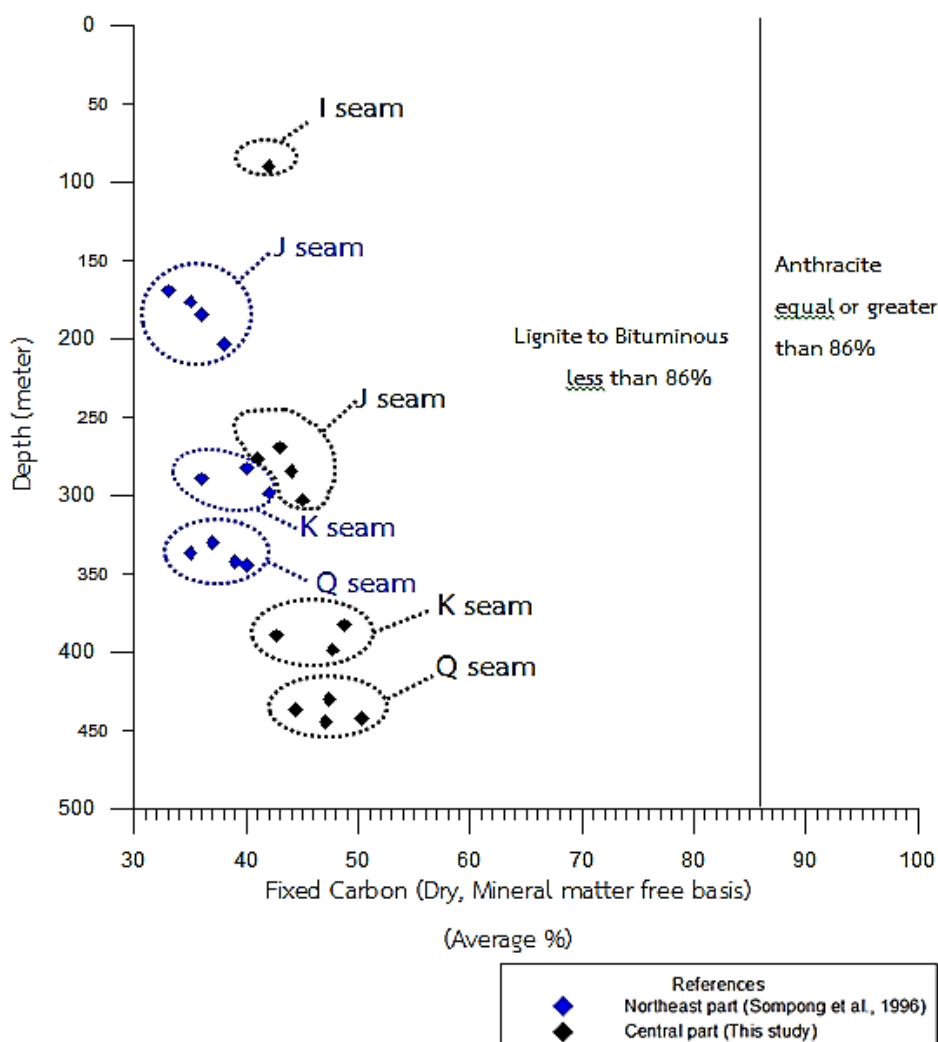


Figure 5.10 Graph showing fixed carbon (on dry, mineral matter free basis, avg. %) compared between central part by this study and northeast part by Sompong et al. (1996) following ASTM D388.

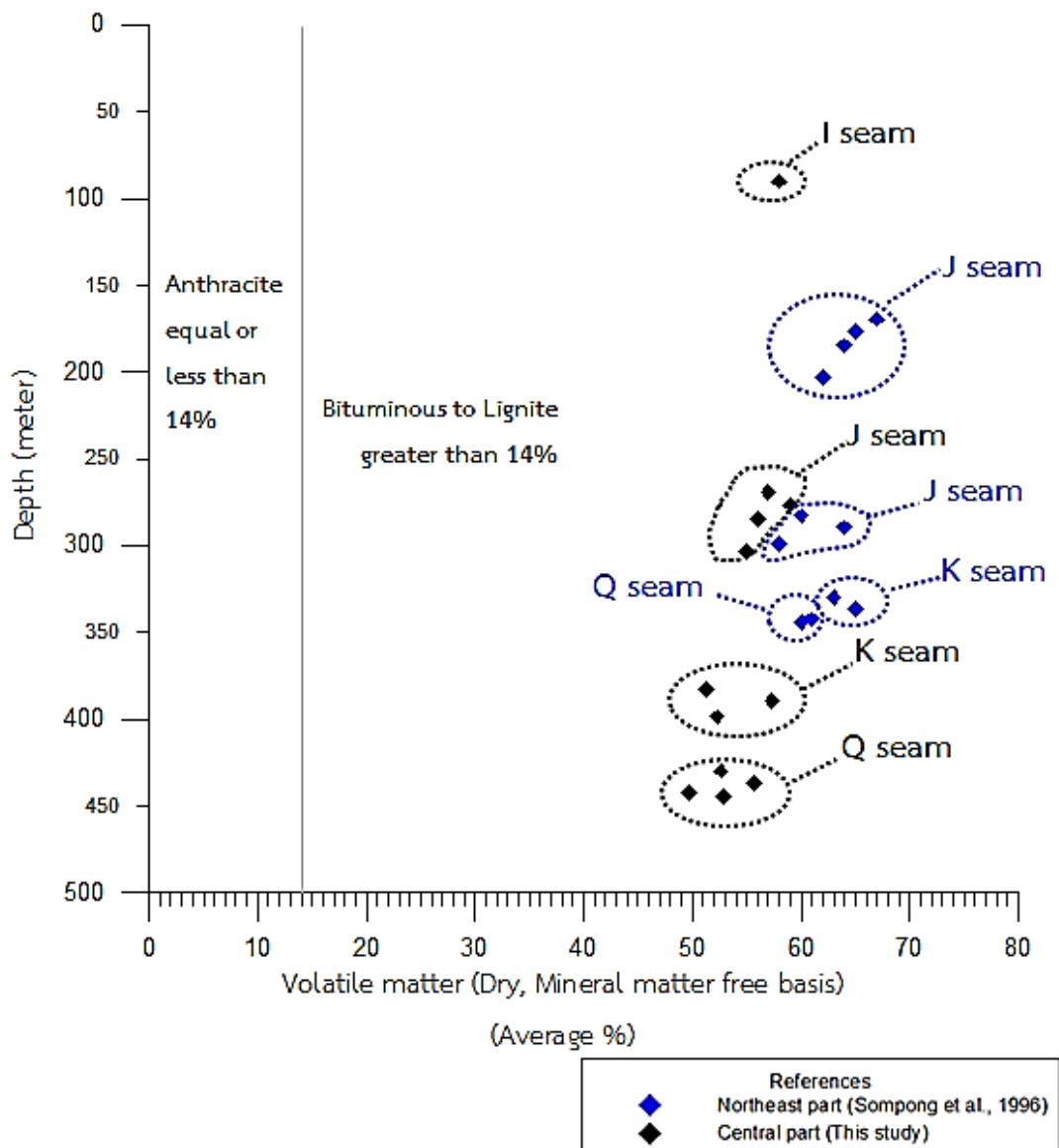


Figure 5.11 Graph showing volatile matter (on dry, mineral matter free basis, avg. %) compared between central part by this study and northeast part by Sompong et al. (1996) following ASTM D388.

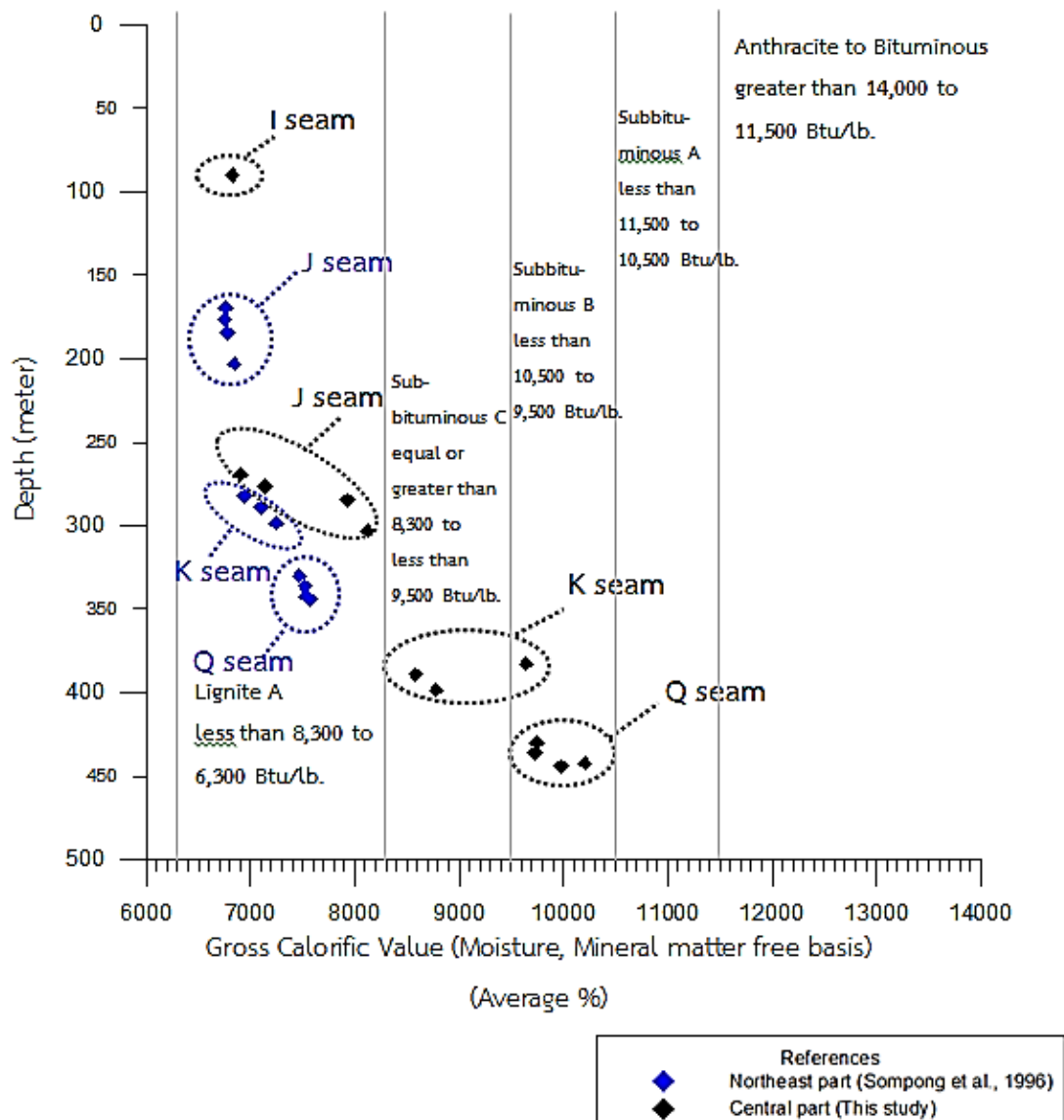


Figure 5.12 Graph showing gross calorific value (on moist, mineral matter free basis, avg. Btu/lb.) compared between central part by this study and northeast part by Sompong et al. (1996) following ASTM D388.

Moreover, petrographic study can also use to imply coalification rank of coal.

The study coals have a mean maximum vitrinite reflectances between 0.53 to 0.60%, with the average of 0.57%, suggesting a subbituminous A rank. The highest percentage vitrinite reflectances of J seam is 0.60%, may be affected from heat by volcanism process. The coal rank was determined by using the vitrinite reflectance is higher than the coal rank from geochemical determination.

Singharajwarapan et al. (2014) recorded the vitrinite reflectance of K and Q seams were also collected from central part are relative low, varying from R0 0.32 to 0.53%, with the average of 0.42%, suggesting a subbituminous C to subbituminous B ranks. Sompong et al. (1996) reported the vitrinite reflectance of the coals was collected from northeast part of Mae Moh basin has a mean random vitrinite reflectance between 0.23 to 0.44% with the average 0.33%, suggesting a lignite rank.

All the studies can be implied the vitrinite reflectance of Mae Moh coals are regarded low rank as lignite to subbituminous rank, indicating immature stage. This is consistent with the lithology of coal, which considering as the lower rank or soft brown coal.

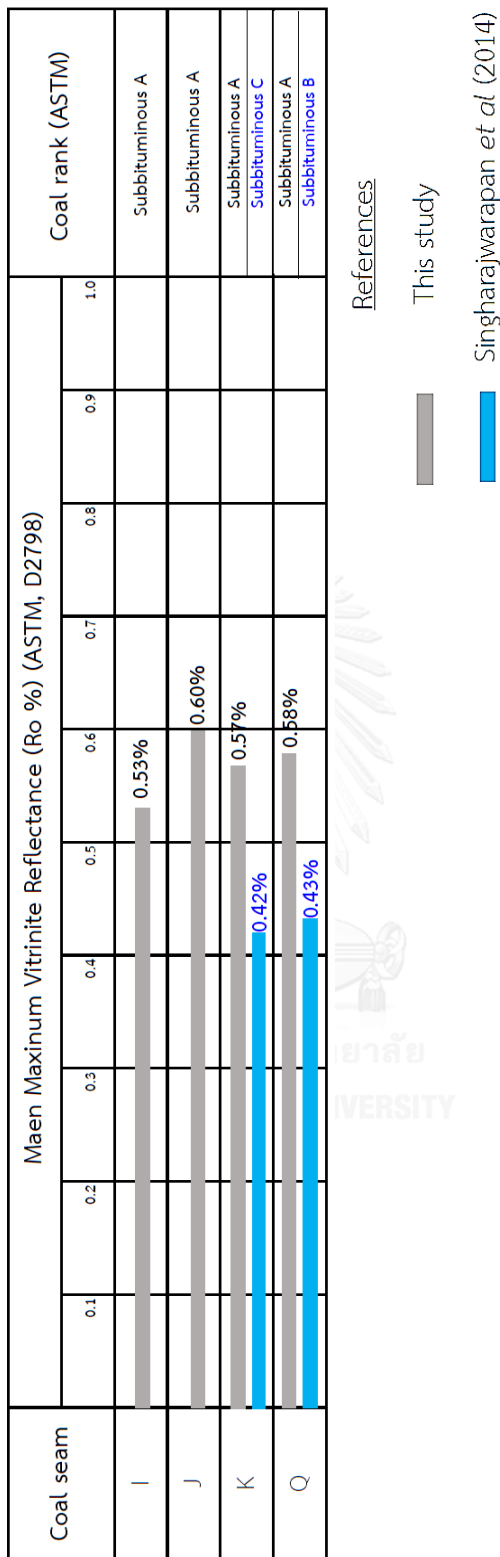


Figure 5.13 Comparisons of the vitrinite reflectance (Ro %) of coals in central part of Mae Moh basin by this study and Singharajwarapan et al. (2014).

The low rank of Mae Moh coals similarity in the Pliocene lignites from Apofysis mine, Amynteo basin, Northwestern Greece in term of their high ash contents and sulphur content, the high ash contents could indicate of a topogenous setting. They have vitrinite reflectance 0.20-0.24% (avg.0.22%), indicated lignite ranks and immature stage (Iordanidis and Georgakopoulos, 2003). The Pliocene Balingian coals from Sarawak, Malaysia have a mean random huminite reflectance between 0.26 and 0.35%, suggesting a lignite coal rank. Nevertheless, geochemical classification based on total moisture and calorific value suggests a subbituminous C rank (Sia and Abdullah, 2012).

According to Ratanasthien (1987), petrographical characteristics of Thai coal by reported major coal deposits in Thailand occur in Tertiary basin while traces of thin coal beds have been found associated with Jurassic and Carboniferous rocks. The Carboniferous coals were subjected to intensive tectonic activities and produced highest rank with R_{Omax} 6.72 %. Jurassic coals show greater rank of coalification with R_{Omax} varying between 0.5 and 4.14 % whereas Tertiary coals are almost immature, R_{Omax} varying between 0.27 and 0.68 %. By contrast, the Permian Gondwana coals from Barapukuria basin, northwest part of Bangladesh, geochemical study has been measured moisture (10%), ash (12.4%), volatile matter (29.2%), fixed carbon (48.4%), sulphur (0.53%) and calorific value 10,450 Btu/lb (6,604 Kcal/kg.), suggest the coal is high volatile bituminous which is in the good agreement with the measured vitrinite reflectance values ranged from 0.72 to 0.81, indicating a high volatile bituminous B rank indicating initial mature stage (Farhaduzzaman et al., 2012).

Table 5.1 Comparison the vitrinite reflectance measurements between the study coals and oversea coals.

Coal Location	Vitrinite reflectance (Vol. %)		Coal rank	Age	Reference
	Min-Max% Ro	Mean % Ro			
Central part	0.53-0.60	0.57	Subbituminous A, immature stage	Miocene	This study
	0.32-0.53	0.42	Subbituminous C, immature stage	Miocene	Singharajwarapan <i>et al</i> (2014)
Northwest part	0.23-0.44	0.33	Lignite, immature stage	Miocene	Sompong <i>et al</i> (1996)
Amynteo basin, Greece	0.20-0.24	0.22	Lignite, immature stage	Pliocene	Iordanidis and Georgakopoulos (2003)
Balingian basin, Malaysia	0.26-0.35	0.32	Lignite, immature stage	Pliocene	Sia and Abdullah (2012)
Barapukuria basin, Bangladesh	0.72-0.81	0.77	High volatile bituminous B, initial mature stage	Permian	Farhaduzzaman <i>et al</i> (2012)

5.3 Evolution

The Mae Moh basin was formed during the middle Miocene, then strongly faulted, uplifted and eroded. The basin passed through a transgressive-regressive, fluvial-lacustrine-fluvial depositional cycle that partly reflected regional changes in the base level of erosion created by changing distant sea levels, and was partly a response to the changing tectonic regime.

Phase I: Depositional environment of Huai King formation.

Deposition began with the fluvial facies of the Huai King formation. The bulk of this formation was supplied by braided stream. The coarse grained sediment was dumped close to the edge of the highland, while the fine grained spread across the valley floor. The characteristic fining upward trend of the Huai King formation implies that the gradient diminished with time. As movement on the faults slowed and sediments filled the topography, the region became one of slow moving streams flood plains and ephemeral lacustrine and peat swamps occurred around the area, which became S seam coal.

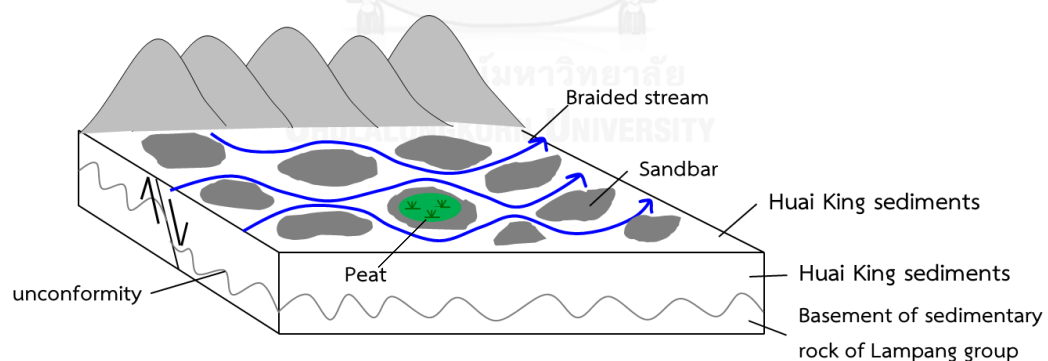


Figure 5.14 Depositional environment of coal S seam.

Phase II: Depositional environment of Na Khaem formation.

The second phase of deposition was marked by widespread inundation and establishment of lacustrine conditions. The change was rapid, so that extensive fine

grained sediments such as clays and muds with some silty muds were deposited across most of the basin (underburden). The margins of the lacustrine were vegetated. The tectonic processes similar to those controlling deposition during phase I persisted during phase II. There is no indication there was a significant change in the rate of subsidence, and the flooding is likely to have been due to a change in the base level of erosion by a rise in level of the distant sea (Sompong et al., 1996). A slowing of the processes enabled deltaic facies to advance into a shallow lacustrine so that swamps became established, and generating the peats that became R seam coal.

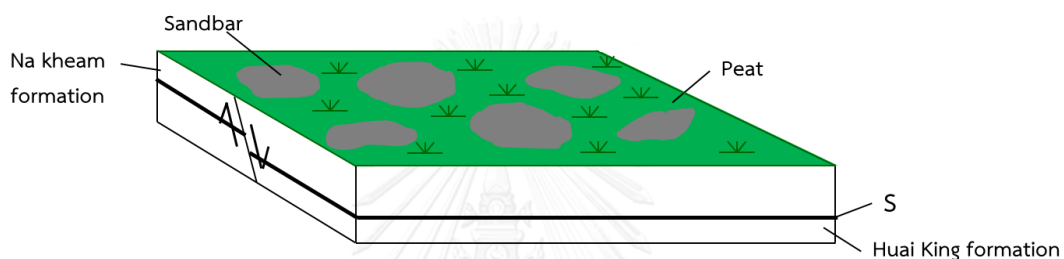


Figure 5.15 Depositional environment of coal R seam.

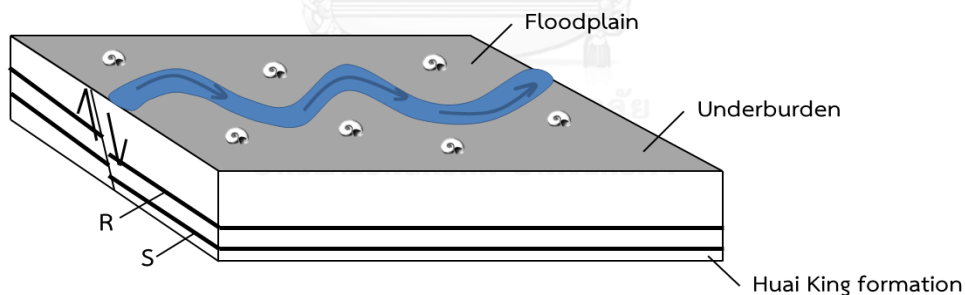


Figure 5.16 Depositional environment of underburden.

In the lacustrine- deltaic environment, if the rate of sediment input remains constant, but there is a reduction in the rate regional subsidence and changing base level of erosion, the delta top became to shallower water and then swampy environment. The spread of the swamp that generated the Q seam coal.

The highest percentage of huminite dominated by textolinite, cutinite, sporinite and rare alginite in the Q seam, indicates peat originated from higher plants in low groundwater level condition. Some liptodetrinite and fusinite indicates high oxidation of plant material before deposition.

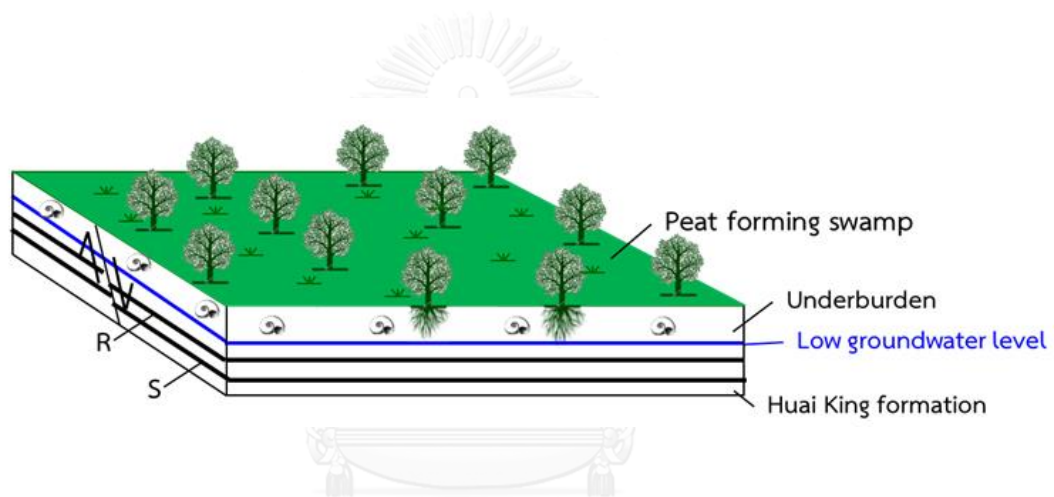


Figure 5.17 Depositional environment of coal Q seam.

The top of Q seam is sharp and records a flooding surface created by rapid flooding of the coal forming swamps that brought lacustrine conditions across the basin. Most noticeable is the interburden, fine grained sediments that resulted from a major flooding accompanied by occurring plant and animal communities. The interburden contains gastropods (*Viviparus sp.*), indicated freshwater environment (Songtham et al., 2005; Ugai et al., 2006).

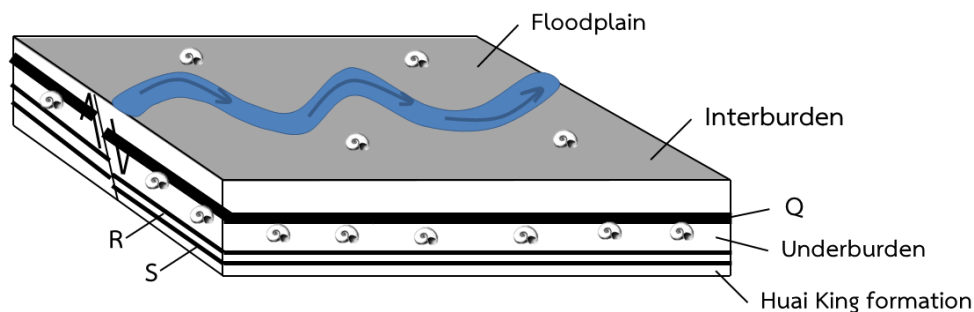


Figure 5.18 Depositional environment of interburden.

Termination of the Q seam, swamp enables sediments to be fed into the lacustrine. Another characteristic pause in the raise of relative water level enabled re-establishment of widespread swamps, and the peat of K seam growth. Conditions returned more or less those that prevailed during the growth of the Q seam peats.

The highest percentage of huminite dominated by textolminite, sporinite cutinite and some alginite in the K seam indicates peat originated from higher plants in low groundwater level condition. Some liptodetrinite and fusinite indicates high oxidation of plant material before deposition. Abundant gastropod (*Planobris sp*, *Viviparus sp.*) indicated freshwater environment (Songtham et al., 2005; Ugai et al., 2006). Moreover, the diatomite and volcanic ashes association can be inferred volcanic eruption occurred during the deposition.

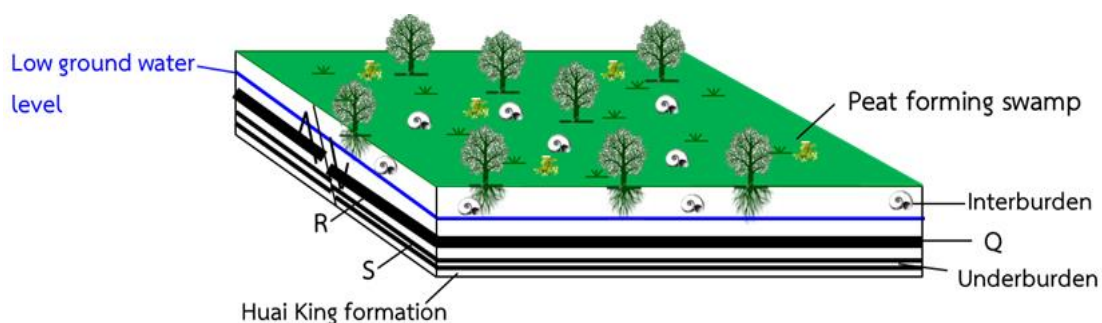


Figure 5.19 Depositional environment of coal K seam.

Another flood, probably the most widespread, end of the K seam peats and distributed thick fine grained sediments of overburden (base of member I). However, the peat formation was occurring to a close as a new tectonic regime began to influence deposition. The change from the one regime to the other was gradual, its influence not becoming apparent until once again sedimentation exceeded the rate of subsidence or raise in water level and the swamps that generated the J seam coal.

The dominant of gelinite, sporinite and alginite, without textolinite suggests lack of higher plants under high groundwater level condition. Abundant gastropod (*Melanoides sp.*) indicated poor water quality (Songtham et al., 2005; Ugai et al., 2006). Diatomite and volcanic ashes association can be inferred volcanic eruption occurred during the deposition.

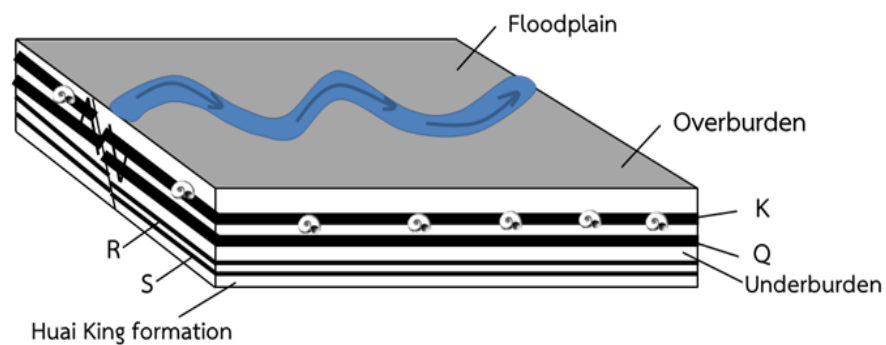


Figure 5.20 Depositional environment of overburden.

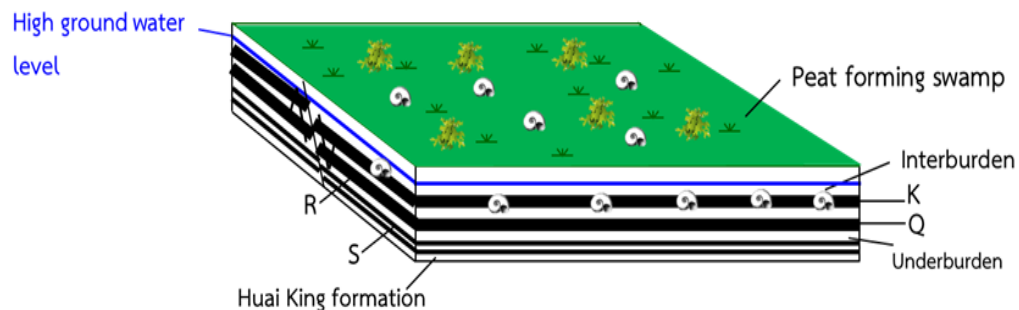


Figure 5.21 Depositional environment of coal J seam.

The change from the one environment to the other are recorded in the sequence of top J, a transitional zone from essentially reducing to oxidizing condition. The abundant of gypsum is also indicative of the transformation. These depositional changes are expressions of the end of the old tectonic regime and the beginning of the new that resulted in the shaping of the basin as it today (Sompong et al., 1996).

Phase III: Depositional environment of Huai Luang formation.

The new tectonic regime results in the deposition of the Huai Luang formation (Red bed). Deposition kept up with subsidence. The fluctuating lacustrine level was suitable for peat swamps to be generated I seam coal. Most of gelinite and rich alginite, without textolinite suggests lack of higher plants under high groundwater level condition. Abundant gastropod (*Margaya sp.*) indicated brackish water (Songtham et al., 2005; Ugai et al., 2006). Pyrite and gypsum are abundant in I seam. Isotope of pyrite (^{34}S -13.6 to - 7.8%) and gypsum (^{34}S +16.4 to 20.0%) from the red bed zone indicated marine incursion (Silaratana et al., 2004; Tankaya, 2001).

Lacustrine conditions were largely replaced by streams. However, overall there was no major tectonism. The bulk of this formation is fine to coarse grained.

Structuring of the basin was succeeded by a period uplift and consequent erosion. The uplift was part of a late Neogene regional movement that raised northern Thailand (Bunopas, 1981).

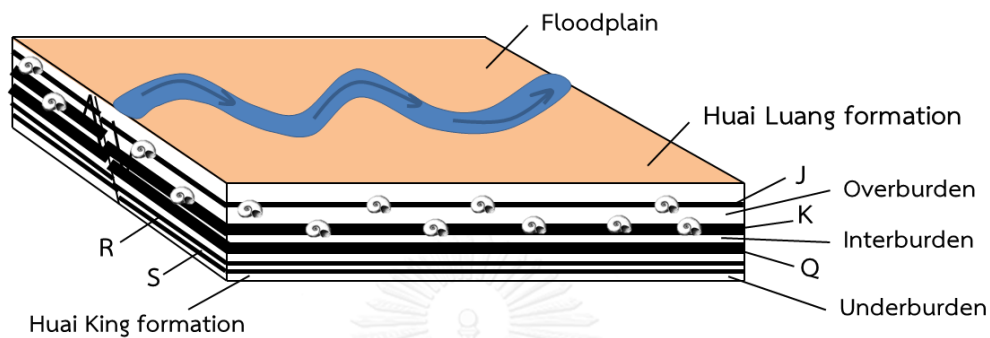


Figure 5.22 Depositional environment of red bed.

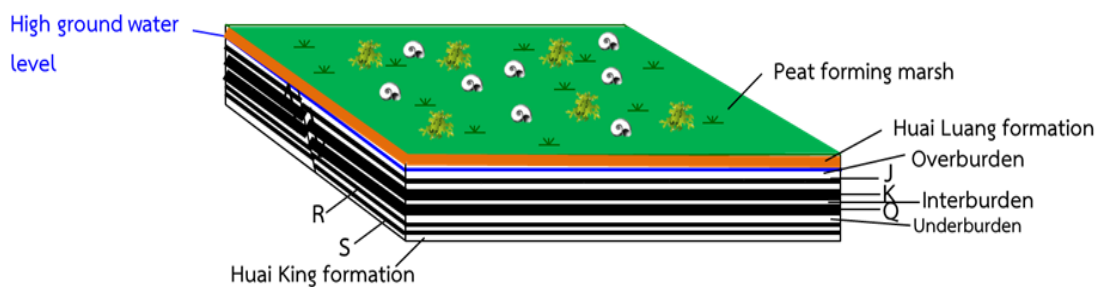


Figure 5.23 Depositional environment of coal I seam.

Chapter 6

6. Conclusion

The Mae Moh basin is one of the important intermontane basins located in northern Thailand. The basin is well known for its largest coal deposit in the country. 3 boreholes in the central part of Mae Moh basin have been investigated for lithostratigraphy study, and 35 coal samples were collected for petrographic and geochemistry analyses. The resulting can be used to determine for coalification rank and depositional paleo environment.

Composite stratigraphy has been made by 3 boreholes correlation and pervious stratigraphy has been used to interpret the sedimentary sequence. The Lampang group and unconformably underlie the Quaternary terrigenous sediments. The Mae Moh sediments are grouped into 3 major sequences. The lower sequence belongs to the Huai King formation with fining upward sequences (claystone to gravel), indicates sediment deposition in the braided system of the fluvial environment. The middle sequence is the Na Khaem formation which is characterized by fine grained sediment with thick to thin coal seams from bottom to top as S-, R-, Q-, K and J seam. The Na Khaem formation has been formed by the sedimentation under the alternation of lacustrine and swamp. The upper sequence is Huai Luang formation mainly the fine to coarse grained red sediments (claystone to sandstone) with thin coal as I seam interbedded, indicated fluvial depositional environment.

Detailed petrographic investigation have been focused on polished sections of coal samples in main coal seams as J-, K-, Q seam of the Na Khaem formation, and minor coal seam as I seam in Huai Luang formation, in the central part of Mae Moh basin, reveal that studied coals consist largely of macerals >70% with small amount of inorganic materials <30%. Huminite maceral group is the highest

percentage followed by liptinite and inertinite. Huminite group (43 to 68%, avg. 56%) is characterized by gellinite, densinite, and some texto-ulminite. Liptinite group (5 to 30%, avg. 17%) is composed of liptodetrinite, sporinite, cutinite, alginite, amorphinite and exsudatinite. Inertinite group (4 to 15%, avg. 10%) is fusinite, semifusinite and funginite in sclerotinite type. The inorganic materials (8 to 30%, avg. 17%) is characterized by diatomite, clay mineral, pyrites dominantly in form of framboidal, silicates as quartz and some volcanic ash in place.

The results from macerals and mineral matters along with appearance characteristic of sediments are used to interpret depositional environment. The depositional environments of this study area always changed from bottom to tops depend on their accumulated in different condition.

The fine grained claystone, mudstone indicated that the sediments were transported from low energy of flooding current.

Coal deposit alternations of lacustrine to forest swamp environments.

In the lacustrine environments, the major macerals are dominated by huminite group mainly of highly disintegrate types such as gellinite and densinite. Liptinites are dominated by liptodetrinite, alginite, and exsudatinite.

In the forest swamp environments are characterized by the presence of dissolved texto-ulminite, sporinite, cutinite and macerals in the inertinites consist of fusinite and funginite in form of sclerotinite. Moreover, the diatom association could imply that there was a volcanic eruption during the depositional period that contributed high silica volcanic ash and pyrite to the basin.

Mae Moh coals were plotted in the Diessel's diagram (Diessel, 1986) with TPI (Tissue Preservation Index) and GI (Gelification Index) base on maceral assemblage. The studied samples are characterized by low TPI values (0.11 to 0.52) and moderate to high GI values (3.67 to 13.50). These study coals have originated under limnic

condition (lacustrine) of peat formation with vegetation characteristics of marsh and wet forest swamp type.

Proximate and ultimate analyses along with calorific value analyses have been used for classifying in coalification rank and quality of coal. The result shows that the weight% on as received basis of fixed carbon is between 16.70 and 26.25%, volatiles matter is between 25.01 and 30.66%, ash is between 13.47 and 25.29%, moisture is between 28.98 and 33.00%, and the weight% on dry basis of carbon content is between 63.61 and 72.60%, oxygen content is between 14.27 and 23.45%, hydrogen content is between 5.01 and 5.18%, sulphur content is between 3.76 and 6.04%, nitrogen content is between 1.77 and 2.53%, and gross calorific values on as received basis is almost constant varying from 2,188 to 3,908 Kcal/kg. According to the ASTM (D388) classification, the percentages of the fixed carbon and volatiles matter on dry, mineral-matter-free basis along with calorific values on moist, mineral-matter-free basis are 41-50%, 50-59% and 6,828-10,207 Btu/lb, respectively. The results lead to classify the Mae Moh coal rank as lignite A to subbituminous B. The Mae Moh coal seams in the study area are classified as the low quality and low rank with high ash and sulphur contents.

The relation of petrographic study and geochemical analysis of study coals in central part of Mae Moh basin are shown in the figure 6.1.

Coal seam	Appearance characters	Macerals and minerals (%)				Proximate analysis (wt%, on asreceived basis)					Ultimate analysis (wt%, on dry basis)					Calorific value (Kcal/kg, on as-received basis)	Coal rank Class/Group ASTM (D388)	depositional paleo environment
		H	L	I	MM	M	A	VM	FC	C	H	N	O	S				
I	Brownish black, dull, crumbly, abundant gypsums and pyrites disseminated, and gastropods remain.	55	13	4	28	33.00	25.29	25.01	16.70	63.61	5.15	1.77	23.45	6.04	2188	Lignite A	lacustrine and marsh	
J	Brownish black to grayish black, dull, brittle, gastropods remain, fine-grained sediments interbedded, gypsum and pyrites remain.	53	19	6	23	32.01	21.64	28.95	17.41	66.61	5.18	2.05	20.36	5.82	2746	Lignite A	lacustrine and swamp	
K	Brownish black to grayish black, dull to bright banded, brittle to hard, pyrite disseminated gastropod and plants remain.	58	16	13	13	30.66	13.47	30.55	25.31	70.44	5.01	2.53	18.26	3.76	3702	Subbituminous C to B	lacustrine and swamp	
Q	Grayish black to black, dull to bright banded, brittle to hard pyrite disseminated and plants remain.	59	16	13	12	28.98	14.11	30.66	26.25	72.60	5.17	2.31	14.27	5.66	3908	Subbituminous B	lacustrine and swamp	

H: huminite, L: liptinite, I: inertinite, MM: mineral matter, M: moisture content, A: ash content, VM: volatile matter content, FC: fixed carbon, C: carbon content, H: hydrogen content, N: nitrogen content, O: oxygen content, S: sulphur content

Figure 6.1 The relation of petrographic study, geochemical analysis and depositional paleo environment.

REFERENCES

- Australian Standards, A.-. 1995. Methods for microscopical determination of the reflectance of coal macerals, Standards Association of Australia Trans.). In (Ed.),^(Eds.), (ed., Vol. pp.). North Sydney, NSW, Australia. (Reprinted from. Barr, S., Macdonald, A., Haile, N., and Reynolds, P. 1976. Paleomagnetism and the age of the Lampang basalt (northern Thailand) and the age of the underlying pebble tools. Journal of the Geological Society of Thailand 2: 1-10.
- Bennett, A., and Taylor, G. 1970. A petrographic basis for classifying Australian coals. in Proc. Australas. Inst. Min. Metall. pp. 1-5.
- Bunopas, S. 1981. Paleogeographic history of Western Thailand and adjacent parts of South-East Asia: a plate tectonics interpretation [Ph. D. thesis]. Victoria Univ. of Wellington, New Zealand., 1983. Paleozoic succession in Thailand. in Workshop on Stratigraphic Correlation of Thailand and Malaysia. pp. 39-76.
- Chaodumrong, P. 1985. Sedimentological studies of some Tertiary deposits of Mae Moh basin, Changwat Lampang. Unpublished MSc Thesis. Chulalongkorn University, Thailand.
- Charoenprawat, A., Chuaviroj, S., Hinthong, C., and Chonglakmani, C. 1995. Geological Map of Thailand, Sheet Lampang (NE47-7), scale 1: 250,000. Geological Survey Division, Department of Mineral Resources, Bangkok, Thailand.
- Charusiri, P., and Pum-Im, S. 2009. Cenozoic Tectonic Evolution of Major Sedimentary Basins in Central, Northern, and the Gulf of Thailand. Bulletin of Earth Science Technology 2: 40-61.
- Chinbunchorn, N., Pradidtan, S., and Sattayarak, N. 1989. Petroleum potential of Tertiary intermontane basins in Thailand. in International Symposium on Intermontane Basins: Geology and Resources, Chiang Mai, Thailand. pp. 29-41.
- Corsiri, R., and Crouch, A. 1985. Mae Moh coal deposit: geologic report. Thailand/Australia Lignite Mines Development Project, Electricity Generating Authority of Thailand 1: 1-448.

- Dame, and Moore. 1996. Mae Moh Mine. Geohydrology studies. Phase 2-groundwater investigations Trans.). In ed., R. (Ed.),^(Eds.), (ed., Vol. pp.). (Reprinted from.
- Diessel, C. 1986. On the correlation between coal facies and depositional environments. in Proceeding 20th Symposium of Department Geology, University of New Castle, New South Wales. pp. 19-22.
- Diessel, C.F.K. 1992. Coal-bearing Depositional System, Springer-Verlag, New York, Berlin 3 540 52516 5. 721.
- Engineers, L.-C. 1981. Mae Moh lignite assessment. Report to Elec. Generating Auth. of Thailand.
- Farhaduzzaman, M., Abdullah, W.H., and Islam, M.A. 2012. Depositional environment and hydrocarbon source potential of the Permian Gondwana coals from the Barapukuria Basin, Northwest Bangladesh. International Journal of Coal Geology 90–91: 162-179.
- Galloway, W.E. 1989. Genetic stratigraphic sequences in basin analysis I: architecture and genesis of flooding-surface bounded depositional units. AAPG bulletin 73: 125-142.
- Germeraad, J.H., Hopping, C., and Muller, J. 1968. Palynology of Tertiary sediments from tropical areas. Review of palaeobotany and palynology 6: 189-348.
- Ginsberg, L., Ingavat, R., and Tassy, P., 1983. Siamongale thailandica nouveau Mustelidae,(Canivera mammalia) neogene du Sud_ est asiatique. 7e ser., no. 25: 953-956.
- Hower, J.C. 1990. Organic petrography and organic geochemistry of Texas tertiary coals in relation to depositional environment and hydrocarbon generation: by Prasanta K. Mukhopadhyay. Report of Investigations No. 188, Bureau of Economic Geology, University of Texas at Austin. 118pp. \$9.00 Trans.). In (Ed.),^(Eds.), (ed., Vol. pp.). Pergamon. (Reprinted from.
- Iordanidis, A., and Georgakopoulos, A. 2003. Pliocene lignites from Apofysis mine, Amynteo basin, Northwestern Greece: petrographical characteristics and depositional environment. International Journal of Coal Geology 54: 57-68.

- Jitapankul, S., Charussuriyong, P., and Jantanachotivot, S. 1985. Geology of Tertiary deposits of Mae Moh basin. Proc. Confer. Lignite Indust. in Thailand, Elec. Generating Auth. of Thailand, Thailand 1: 16-16.
- Jungyusuk, N., and Sirinawin, T. 1983. Cenozoic basalts of Thailand. in Conference on Geology and Mineral Resources of Thailand. pp.
- Kalkreuth, W., Marchioni, D., Calder, J., Lamberson, M., Naylor, R., and Paul, J. 1991. The relationship between coal petrography and depositional environments from selected coal basins in Canada. International Journal of Coal Geology 19: 21-76.
- Kolcon, I., and Sachsenhofer, R.F. 1999. Petrography, palynology and depositional environments of the early Miocene Oberdorf lignite seam (Styrian Basin, Austria). International Journal of Coal Geology 41: 275-308.
- Krevelen, D.W. 1993. Coal--typology, physics, chemistry, constitution. Elsevier Science.
- Le Dain, A.Y., Tapponnier, P., and Molnar, P. 1984. Active faulting and tectonics of Burma and surrounding regions. Journal of Geophysical Research: Solid Earth 89: 453-472.
- Map.google.com. [Online]. Available from:
- Markic, M., and Sachsenhofer, R. 1997. Petrographic composition and depositional environments of the Pliocene Velenje lignite seam (Slovenia). International Journal of Coal Geology 33: 229-254.
- Metcalf, I. 1993. Southeast Asian terranes: Gondwanaland origins and evolution. Gondwana 8: 181-200.
- Mukhopadhyay, P.K. 1986. Petrography of selected Wilcox and Jackson Group lignites from the Tertiary of Texas. In Geology of Gulf Coast Lignites, pp. 126-145. Ann. Meet. Geol. Soc. Am., Coal Geology Div., Field Trip.
- Petersen, H. 1993. Petrographic facies analysis of Lower and Middle Jurassic coal seams on the island of Bornholm, Denmark. International Journal of Coal Geology 22: 189-216.
- Piwkam, S. 2012. Palynology of lignite and Claystone (K and O Zone) in the Mae Moh Basin: Implication for the Paleo-climate and Paleo-environment. M.S. thesis, Mahidol university.

- Ratanasthien, B. 1987. Petrographical characteristics of Thai coals. Coal science and technology 11: 155-158.
- Ratanasthien, B., Chompoosri, S., and Mathatthanachai, T. 1997. Deposition environment of Mae Moh Basin as indicated by coal petrography. in Proceedings of the International Conference on Stratigraphy and Tectonic Evolution of Southeast Asia and the South Pacific. Department of Mineral Resources, Bangkok. pp. 596-605.
- Ratanasthien, B., and Kandharosa, W. 1987. Coal-, oil-, oil shale bearing formations intermontane basins of Thailand. in Proc. Sixth GEOSEA Congress, Jakarta Indonesia. pp.
- Ratanasthien, B., Kandharosa, W., Chompusri, S., and Chartprasert, S. 1999. Liptinite in coal and oil source rocks in northern Thailand. Journal of Asian Earth Sciences 17: 301-306.
- Reading, H. 1996. Sedimentary environments: processes, facies and stratigraphy. Blackwell Publishing.
- Sasada, M., Ratanasthien, B., and Soponpongpipat, P. 1987. New K-Ar Ages from the Lampang Basalt Northern Thailand. publisher not identified.
- Scott, A.C. 1989. Observations on the nature and origin of fusain. International Journal of Coal Geology 12: 443-475.
- Sia, S.G., and Abdullah, W.H. 2012. Geochemical and petrographical characteristics of low-rank Balingian coal from Sarawak, Malaysia: Its implications on depositional conditions and thermal maturity. International Journal of Coal Geology 96-97: 22-38.
- Silaratana, T. 2005. Effects of environmental factors on accumulation of fossil fuel deposits in Northern Thailand= ผล ของ ปัจจัย สิ่งแวดล้อม ต่อ การ สะสม ด้วย ของ แหล่ง เชื้อเพลิง ธรรมชาติ ใน ภาค เหนือ ของ ประเทศไทย. Chiang Mai: Graduate School, Chiang Mai University, 2005.
- Silaratana, T., et al. 2004. Sulfur isotopic implication of Middle Miocene marine incursion in Northern Thailand. Science Asia 30: 43-58.

- Singh, M.P., and Singh, A.K. 2000. Petrographic characteristics and depositional conditions of Eocene coals of platform basins, Meghalaya, India. International journal of coal geology 42: 315-356.
- Sompong, W., Springbelt, G., and Evans, P. 1996. Lignite mine development project. Mae Moh coal deposit: Geological Report, prepared by the Australian Agency for International Development (AusAID)/Electricity Generating Authority of Thailand (EGAT)/Landslide Mitigation Demonstration Project (LM DP) Phase III.
- Songtham, W., et al. 2005. Middle miocene molluscan assemblages in mae moh basin, lampang province, Northern Thailand. ScienceAsia 31: 183-191.
- Sotirov, A., and Kortenski, J. 2004. Petrography of the coal from the Oranovo–Simitli basin, Bulgaria and indices of the coal facies. International Journal of Coal Geology 57: 71-76.
- Sotirov, A., and Sokolov, D. 1998. Major elements in the coal from the Oranovo–Simitli basin. Review of the Bulgarian Geological Society 59: 165-175.
- Tankaya, W. 2001. Implication of geochemistry on depositional environments in Mae Moh coal field Changwat Lampang. Chiang Mai: Graduate School, Chiang Mai University, 2001.
- Tapponnier, P., Peltzer, G., and Armijo, R. 1986. On the mechanics of the collision between India and Asia. Geological Society, London, Special Publications 19: 113-157.
- Ugai, H., Ratanasthien, B., and Silaratana, T. 2006. Cenozoic freshwater molluscan fossils of Thailand. Journal of the Geological Society of Thailand 1: 67-82.
- Uttamo, W. 1998. Lithofacies of Mae Moh and Li basins, Northern Thailand, Southeast Asia Research. Department of Geology, Royal Holloway, University of London.



Appendix A

Geochemical results

Table 1A Proximate analysis (as receive basis) of Borehole no. MMC-1.

Hole id.	Depth_From (meter)	Depth_To (meter)	Thickness (meters)	Sample id.	Moisture ASTM D3302-02a	Ash ASTM D5142-09	Volatile ASTM D5142-09	Fixed Carbon ASTM D5142-09
				MMC1-1-I	N/A			
	126.20	126.90	0.70	MMC1-2-J3	33.00	22.10	29.48	15.42
	129.20	129.90	0.70	MMC1-3-J4	32.80	23.76	28.06	15.38
	135.10	139.20	4.10	MMC1-4-J5	32.66	23.18	28.27	15.89
	149.50	151.25	1.75	MMC1-5-J6	32.30	17.98	29.12	20.60
	230.00	236.30	6.30	MMC1-6-K1	32.00	9.74	30.43	27.83
	236.85	243.95	7.10	MMC1-7-K2	32.36	13.18	31.02	23.44
	243.95	252.75	8.70	MMC1-8-K3	32.58	10.25	31.03	26.14
	276.40	283.15	6.75	MMC1-9-Q1	31.50	14.60	29.00	24.90
	283.15	288.80	5.65	MMC1-10-Q2	31.50	15.56	30.01	22.93
	288.80	290.65	1.85	MMC1-11-Q3	30.80	12.77	28.67	27.76
	290.65	295.80	5.15	MMC1-12-Q4	30.98	11.93	29.45	27.64

Table 2A Proximate analysis (as receive basis) of Borehole no. MMC-2.

Hole id.	Depth_From (meter)	Depth_To (meter)	Thickness (meters)	Sample id.	Moisture ASTM D3302-02a	Ash ASTM D5142-09	Volatile ASTM D5142-09	Fixed Carbon ASTM D5142-09
MMC-2	86.00	91.00	5.00	MMC2-1-I	33.00	24.19	25.41	17.40
	365.70	366.50	0.80	MMC2-2-J3	32.60	19.40	29.51	18.49
	372.70	373.40	0.70	MMC2-3-J4	32.11	21.39	30.46	16.04
	381.00	384.00	3.00	MMC2-4-J5	31.46	21.11	29.79	17.64
	407.50	409.60	2.10	MMC2-5-J6	31.20	15.29	30.32	23.19
	493.00	499.50	6.50	MMC2-6-K1	31.28	10.29	29.95	28.48
	499.95	510.50	10.30	MMC2-7-K2	31.27	14.84	31.13	22.76
	510.50	517.30	6.60	MMC2-8-K3	30.78	12.42	29.80	27.00
	541.20	547.40	6.20	MMC2-9-Q1	28.77	14.18	29.82	27.23
	547.40	553.50	6.10	MMC2-10-Q2	28.79	13.26	31.85	26.10
	553.50	556.00	2.50	MMC2-11-Q3	27.06	10.66	30.96	31.32
	556.00	560.20	4.20	MMC2-12-Q4	27.46	12.82	31.52	28.21

Table 3A Proximate analysis (as receive basis) of Borehole no. MMC-3.

Hole id.	Depth_From (meter)	Depth_To (meter)	Thickness (meters)	Sample id.	Moisture ASTM D3302-02a	Ash ASTM D5142-09	Volatile ASTM D5142-09	Fixed Carbon ASTM D5142-09
MMC-3	94.00	96.00	2.00	MMC3-1-I	33.00	26.39	24.61	16.00
	316.00	317.00	1.00	MMC3-2-J3	32.50	25.49	28.45	13.56
	327.00	328.00	1.00	MMC3-3-J4	31.80	24.40	27.27	16.53
	338.00	340.00	2.00	MMC3-4-J5	31.00	25.02	27.50	16.48
	352.00	353.00	1.00	MMC3-5-J6	30.60	20.62	29.08	19.70
	425.00	430.80	5.80	MMC3-6-K1	28.76	17.00	29.23	25.01
	431.30	441.00	9.40	MMC3-7-K2	27.85	21.21	31.25	19.68
	441.00	449.00	7.90	MMC3-8-K3	29.06	12.32	31.13	27.49
	472.00	479.00	7.00	MMC3-9-Q1	27.72	14.93	31.71	25.64
	479.00	484.60	5.60	MMC3-10-Q2	28.14	19.41	31.35	21.10
	484.60	486.40	1.80	MMC3-11-Q3	27.60	12.97	30.54	28.89
	486.40	490.50	4.10	MMC3-12-Q4	27.44	16.22	33.04	23.30

Table 4A Ultimate analysis (dry basis) of Borehole no. MMC-1.

Hole id.	Depth_From (meter)	Depth_To (meter)	Thickness (meters)	Sample_name	Carbon	Hydrogen	Nitrogen	Oxygen	Sulphur	H/C Atomic Ratio	O/C Atomic Ratio
MMC-1				MMC1-1-I			N/A			N/A	N/A
	126.20	126.90	0.70	MMC1-2-J3	65.61	5.23	2.13	19.82	7.21	0.98	0.27
	129.20	129.90	0.70	MMC1-3-J4	65.54	5.28	2.07	20.67	6.44	0.95	0.28
	135.10	139.20	4.10	MMC1-4-J5	67.26	4.95	1.79	20.38	5.63	0.95	0.23
	149.50	151.25	1.75	MMC1-5-J6	68.42	4.99	2.05	20.57	3.98	0.95	0.20
	230.00	236.30	6.30	MMC1-6-K1	70.61	4.92	2.56	18.02	3.89	0.98	0.25
	236.85	243.95	7.10	MMC1-7-K2	69.97	4.84	2.50	18.13	4.55	0.96	0.24
	243.95	252.75	8.70	MMC1-8-K3	70.56	4.82	2.58	19.48	2.55	0.96	0.23
	276.40	283.15	6.75	MMC1-9-Q1	72.53	4.85	2.38	15.26	4.98	0.98	0.25
	283.15	288.80	5.65	MMC1-10-Q2	72.18	4.96	2.29	15.11	5.46	0.88	0.23
	288.80	290.65	1.85	MMC1-11-Q3	71.63	5.11	2.25	14.61	6.40	0.90	0.22
	290.65	295.80	5.15	MMC1-12-Q4	72.81	5.09	2.34	14.09	5.67	0.89	0.23

Table 5A Ultimate analysis (dry basis) of Borehole no. MMC-2.

Hole id.	Depth_From (meter)	Depth_To (meter)	Thickness (meters)	Sample_name	Carbon	Hydrogen	Nitrogen	Oxygen	Sulphur	H/C Atomic Ratio	O/C Atomic Ratio
MMC-2	86.00	91.00	5.00	MMC2-1-I	63.64	5.21	1.81	23.20	6.14	0.87	0.23
	365.70	366.50	0.80	MMC2-2-J3	66.43	5.32	2.25	17.78	8.22	0.89	0.22
	372.70	373.40	0.70	MMC2-3-J4	66.13	5.35	2.05	20.19	6.28	0.90	0.24
	381.00	384.00	3.00	MMC2-4-J5	67.58	5.13	1.88	20.04	5.37	0.83	0.19
	407.50	409.60	2.10	MMC2-5-J6	68.99	5.17	2.19	19.83	3.82	0.88	0.18
	493.00	499.50	6.50	MMC2-6-K1	72.15	5.34	2.52	16.94	3.05	0.86	0.19
	499.95	510.50	10.30	MMC2-7-K2	70.01	5.06	2.45	19.03	3.46	0.82	0.19
	510.50	517.30	6.60	MMC2-8-K3	71.14	5.21	2.55	18.63	2.47	0.86	0.20
	541.20	547.40	6.20	MMC2-9-Q1	73.80	5.41	2.42	13.37	5.00	0.85	0.18
	547.40	553.50	6.10	MMC2-10-Q2	73.63	5.42	2.25	13.78	4.92	0.81	0.21
	553.50	556.00	2.50	MMC2-11-Q3	72.98	5.46	2.24	12.81	6.51	0.87	0.20
	556.00	560.20	4.20	MMC2-12-Q4	73.82	5.47	2.37	12.50	5.84	0.82	0.21

Table 6A Ultimate analysis (dry basis) of Borehole no. MMC-3.

Hole id.	Depth_From (meter)	Depth_To (meter)	Thickness (meters)	Sample_name	Carbon	Hydrogen	Nitrogen	Oxygen	Sulphur	H/C Atomic Ratio	O/C Atomic Ratio
MM C-3	94.00	96.00	2.00	MMC3-1-I	63.57	5.08	1.73	23.69	5.93	0.80	0.16
	316.00	317.00	1.00	MMC3-2-J3	64.79	5.32	2.22	21.46	6.21	0.87	0.14
	327.00	328.00	1.00	MMC3-3-J4	64.05	5.26	2.11	21.66	6.92	0.81	0.16
	338.00	340.00	2.00	MMC3-4-J5	66.93	5.00	1.69	20.49	5.89	0.82	0.16
	352.00	353.00	1.00	MMC3-5-J6	67.54	5.08	2.12	21.36	3.90	0.88	0.14
	425.00	430.80	5.80	MMC3-6-K1	69.50	5.04	2.57	17.81	5.08	0.83	0.16
	431.30	441.00	9.40	MMC3-7-K2	69.81	4.98	2.50	16.66	6.05	0.85	0.15
	441.00	449.00	7.90	MMC3-8-K3	70.20	4.86	2.59	19.62	2.72	0.89	0.13
	472.00	479.00	7.00	MMC3-9-Q1	72.37	4.93	2.35	15.12	5.23	0.87	0.16
	479.00	484.60	5.60	MMC3-10-Q2	71.43	4.95	2.32	15.32	5.98	0.83	0.15
	484.60	486.40	1.80	MMC3-11-Q3	71.14	5.20	2.23	15.12	6.31	0.88	0.13
	486.40	490.50	4.10	MMC3-12-Q4	72.84	5.15	2.30	14.13	5.57	0.84	0.15

Table 7A Calorific Value analysis (as receive basis) of Borehole no. MMC-1.

Hole id.	Depth_From (meter)	Depth_To (meter)	Thickness (meters)	Sample id.	Gross Calorific Value		Net Calorific Value	
					ASTM D586510 a (Kcal/Kg.)	ASTM D586510 a	(Kcal/Kg.)	(Btu/lb.)
MMC-1				MMC1-1-I	N/A	N/A	N/A	N/A
	126.20	126.90	0.70	MMC1-2-J3	2440	2085	4392	3752
	129.20	129.90	0.70	MMC1-3-J4	2592	2229	4665	4012
	135.10	139.20	4.10	MMC1-4-J5	2748	2381	4946	4286
	149.50	151.25	1.75	MMC1-5-J6	3203	2839	5765	5109
	230.00	236.30	6.30	MMC1-6-K1	3897	3534	7015	6361
	236.85	243.95	7.10	MMC1-7-K2	3603	3239	6485	5830
	243.95	252.75	8.70	MMC1-8-K3	3737	3375	6726	6075
	276.40	283.15	6.75	MMC1-9-Q1	3509	3148	6316	5666
	283.15	288.80	5.65	MMC1-10-Q2	3634	3271	6541	5888
	288.80	290.65	1.85	MMC1-11-Q3	3596	3234	6473	5821
	290.65	295.80	5.15	MMC1-12-Q4	3902	3552	7024	6394

Table 8A Calorific Value analysis (as receive basis) of Borehole no. MMC-2.

Hole id.	Depth_From (meter)	Depth_To (meter)	Thickness (meters)	Sample id.	Gross Calorific Value ASTM D586510 a (Kcal/Kg.)		Net Calorific Value ASTM D586510 a (Kcal/Kg.)		Gross Calorific Value (Btu/lb.)	Net Calorific Value (Btu/lb.)
MM C-2	86.00	91.00	5.00	MMC2-1-I	2243	1897	4037	3415	4037	3415
	365.70	366.50	0.80	MMC2-2-J3	2628	2276	4730	4097	4730	4097
	372.70	373.40	0.70	MMC2-3-J4	2642	2268	4756	4082	4756	4082
	381.00	384.00	3.00	MMC2-4-J5	2826	2478	5087	4460	5087	4460
	407.50	409.60	2.10	MMC2-5-J6	3330	2964	5994	5335	5994	5335
	493.00	499.50	6.50	MMC2-6-K1	3933	3576	7079	6437	7079	6437
	499.95	510.50	10.30	MMC2-7-K2	3409	3052	6137	5494	6137	5494
	510.50	517.30	6.60	MMC2-8-K3	3706	3350	6671	6029	6671	6029
	541.20	547.40	6.20	MMC2-9-Q1	3980	3630	7164	6534	7164	6534
	547.40	553.50	6.10	MMC2-10-Q2	3984	3635	7171	6543	7171	6543
	553.50	556.00	2.50	MMC2-11-Q3	4378	4035	7880	7263	7880	7263
	556.00	560.20	4.20	MMC2-12-O4	4181	3800	7525	6840	7525	6840

Table 9A Calorific Value analysis (as receive basis) of Borehole no. MMC-3.

Hole id.	Depth_From (meter)	Depth_To (meter)	Thickness (meters)	Sample id.	Gross Calorific Value ASTM D586510 a (Kcal/Kg.)		Net Calorific Value ASTM D586510 a (Kcal/Kg.)		Gross Calorific Value (Btu/lb.)	Net Calorific Value (Btu/lb.)
MMC C-3	94.00	96.00	2.00	MMC3-1-I	2132	1767	3838	3181		
	316.00	317.00	1.00	MMC3-2-J3	2252	1893	4054	3407		
	327.00	328.00	1.00	MMC3-3-J4	2541	2190	4574	3942		
	338.00	340.00	2.00	MMC3-4-J5	2669	2284	4804	4111		
	352.00	353.00	1.00	MMC3-5-J6	3076	2713	5537	4883		
	425.00	430.80	5.80	MMC3-6-K1	3686	3336	6635	6005		
	431.30	441.00	9.40	MMC3-7-K2	3416	3070	6148	5526		
	441.00	449.00	7.90	MMC3-8-K3	3927	3577	7069	6439		
	472.00	479.00	7.00	MMC3-9-Q1	3962	3616	7132	6509		
	479.00	484.60	5.60	MMC3-10-Q2	3593	3245	6467	5841		
	484.60	486.40	1.80	MMC3-11-O3	4187	3842	7537	6916		
	486.40	490.50	4.10	MMC3-12-Q4	3984	3639	7171	6550		

Table 10A Coalification rank analysis of Borehole no. MMC-1.

Hole id.	Depth_From (meter)	Depth_To (meter)	Thickness (meters)	Sample id	Moisture, Mineral Matter Free Basis_Gross Calorific Value (Btu/lb.)	Dry, Mineral Matter Free Basis_Fixed Carbon (%)	Dry, Mineral Matter Free Basis_Volatile Matter (%)	Class/Group ASTM (D388)
MMC-1	126.20	126.90	0.70	MMC1-1-J3	7044	78	22	Lignite A
	129.20	129.90	0.70	MMC1-2-J4	7311	6	94	Lignite A
	135.10	139.20	4.10	MMC1-3-J5	7364	8	92	Lignite A
	149.50	151.25	1.75	MMC1-4-J6	8209	46	54	Lignite A
	230.00	236.30	6.30	MMC1-5-K1	8599	49	51	Subbituminous C
	236.85	243.95	7.10	MMC1-6-K2	8150	44	56	Subbituminous C
	243.95	252.75	8.70	MMC1-7-K3	8111	47	53	Subbituminous C
	276.40	283.15	6.75	MMC1-8-Q1	8519	47	53	Subbituminous C
	283.15	288.80	5.65	MMC1-9-Q2	8931	45	55	Subbituminous C
	288.80	290.65	1.85	MMC1-10-Q3	8831	49	51	Subbituminous C
	290.65	295.80	5.15	MMC1-11-Q4	9086	50	50	Subbituminous C

Table 11A Coalification rank analysis of Borehole no. MMC-2.

Hole id.	Depth_From (meter)	Depth_To (meter)	Thickness (meters)	Sample id	Moisture, Mineral Matter Free Basis_Gross Calorific Value (Btu/lb.)	Dry, Mineral Matter Free Basis_Fixed Carbon (%)	Dry, Mineral Matter Free Basis_Volatile Matter (%)	Class/Group ASTM (D388)
MMC-2	86.00	91.00	5.00	MMC2-1-I	7180	42	58	Lignite A
	381.00	384.00	3.00	MMC2-2-J5	8462	46	54	Lignite A
	407.50	409.60	2.10	MMC2-3-J6	9046	42	58	Subbituminous C
	493.00	499.50	6.50	MMC2-4-K1	9884	50	50	Subbituminous B
	499.95	510.50	10.30	MMC2-5-K2	8284	44	56	Subbituminous C
	510.50	517.30	6.60	MMC2-6-K3	8929	49	51	Subbituminous B
	541.20	547.40	6.20	MMC2-7-Q1	10027	49	51	Subbituminous B
	547.40	553.50	6.10	MMC2-8-Q2	10032	46	54	Subbituminous B
	553.50	556.00	2.50	MMC2-9-Q3	10472	52	48	Subbituminous B
	556.00	560.20	4.20	MMC2-10-Q4	10305	49	51	Subbituminous B

Table 12A Coalification rank analysis of Borehole no. MMC-3.

Hole id.	Depth_From (meter)	Depth_To (meter)	Thickness (meters)	Sample id	Moisture, Mineral Matter Free Basis_Gross Caloric Value (Btu/lb.)	Dry, Mineral Matter Free Basis_Fixed Carbon (%)	Dry, Mineral Matter Free Basis_Volatile Matter (%)	Class/Group ASTM (D388)
MMC-3	94.00	96.00	2.00	MMC3-1-I	6475	72	28	Lignite A
	316.00	317.00	1.00	MMC3-2-J3	6761	47	53	Lignite A
	327.00	328.00	1.00	MMC3-3-J4	6964	43	57	Lignite A
	338.00	340.00	2.00	MMC3-4-J5	7963	50	50	Lignite A
	352.00	353.00	1.00	MMC3-5-J6	8611	42	58	Subbituminous C
	425.00	430.80	5.80	MMC3-6-K1	10449	48	52	Subbituminous B
	431.30	441.00	9.40	MMC3-7-K2	9315	40	60	Subbituminous B
	441.00	449.00	7.90	MMC3-8-K3	9294	48	52	Subbituminous B
	472.00	479.00	7.00	MMC3-9-Q1	10689	46	54	Subbituminous A
	479.00	484.60	5.60	MMC3-10-Q2	10206	42	58	Subbituminous B
	484.60	486.40	1.80	MMC3-11-Q3	11319	50	50	Subbituminous A
	486.40	490.50	4.10	MMC3-12-Q4	10537	43	57	Subbituminous A

Appendix B

Classification of coal

Table 1B ASTM classification of coals by rank (after ASTM D388, 2005).

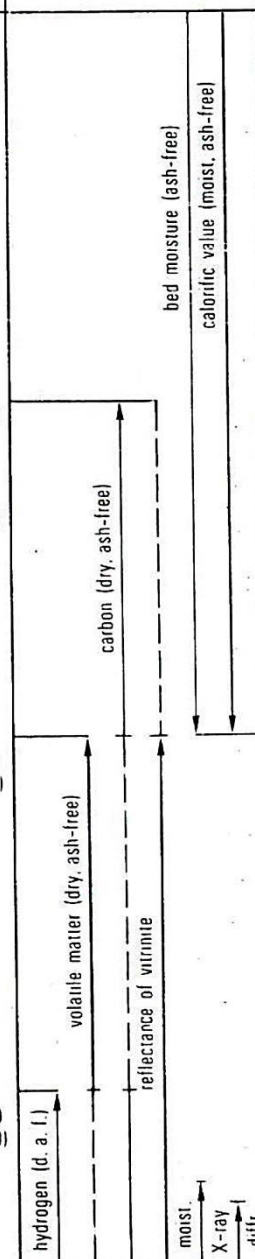
Class/Group	Fixed carbon limits (%) (dry mineral matter Free basis)		Volatile matter limits (%) (dry mineral matter)		Calorific value limits (Btu/lb/ MJ/kg) (Moist* mineral matter free)		Agglomerating character
	= or >	<	=	= or <	= or >	<	
Anthracite							
Meta-anthracite	98	-	-	2	-	-	Nonagglomerating
Anthracite	92	98	2	8	-	-	
Semianthracite	86	92	8	14	-	-	
Bituminous							
Low volatile	78	86	14	14	-	-	Commonly agglomerating (there may be nonagglomerating varieties with notable exceptions in the high
Medium volatile	69	78	22	22	-	-	
High volatile A	-	69	31	31	14000**/32.6	-	
High volatile B	-	-	-	-	1300**/30.2	14000/32.6	
High Volatile c	-	-	-	-	11500/26.7 10500/24.4	13000/30.2 11500/26.7	
Subbituminous							
Subbituminous A	-	-	-	-	10500/24.4	11500/26.7	Nonagglomerating
Subbituminous B	-	-	-	-	9500/22.1	10500/24.4	
Subbituminous C	-	-	-	-	8300/19.3	9500/22.1	
Lignite							
Lignite A	-	-	-	-	6300/14.7	8300/19.3	
Lignite B	-	-	-	-	-	6300/14.7	

*Moist refers to coal containing its natural inherent moisture but not including visible water of the surface of the coal.

**Coals having 69% or more fixed carbon on the dry mineral matter free basis shall be classified according to the fixed carbon, regardless of calorific value.

Table 2B The different stages of coalification according to the German (DIN) and North American (ASTM) classifications and their distinction on the basis of different physical and chemical rank parameters. The last column shows the applicability of various rank parameters to the different coalification stage.

Rank		Refl. Rm _{Oil}	Vol. M. d. a. f. %	Carbon d. a. f. Vitrite	Bed Moisture	Cal. Value Btu/lb (kcal/kg)	Applicability of Different Rank Parameters	
German	USA						bed moisture (ash-free)	calorific value (moist. ash-free)
Torf	Peat	0.2	68					
			64	ca. 60	ca. 75			
Weich-	Lignite	0.3	60			7200 (4000)		
			56		ca. 35			
Matt-	Sub-Bit.	C	0.4	52				
		B		48	ca. 71	ca. 25	9900 (5500)	
Glanz-	C	A	0.5	44				
			0.6	44	ca. 77	ca. 8-10	12600 (7000)	
Flamm-	High Vol. Bituminous	B	0.7	40				
Gasflamm-			0.8	36				
Gas-		A	1.0	32				
Fett-	Medium Volatile Bituminous		1.2	28	ca. 87	15500 (8650)		
			1.4	24				
Ess-	Low Volatile Bituminous		1.6	20				
			1.8	16				
Mager-	Semi-Anthracite	2.0	12					
Anthrazit	Anthracite		8	ca. 91		15500 (8650)		
			3.0	4				
Meta-Anthr.	Meta-A.	4.0	4					



Coals are classified according to their fixed carbon and volatile matter contents calculated to a “dry” and “mineral matter free” basis, or according to their Btu/lb calculated to a “moist” and “mineral matter free” basis. Moist refers to the coal’s inherent moisture (or equivalent). Mineral matter is calculated from the coal’s ash and sulfur contents.

$$\text{Dry, Mineral Matter Free Basis FC} = \frac{\text{FC} - 0.15\text{S}}{100 - (\text{M} + 1.08\text{A} + 0.55\text{S})} \times 100$$

$$\text{FC} = 100 - \text{Dry, Mineral Matter Free VM}$$

$$\text{Moist, Mineral Matter Free Basis BTU} = \frac{\text{BTU} - 50\text{S}}{100 - (1.08\text{A} + 0.55\text{S})} \times 100$$

M = percentage of Inherent Moisture

VM = percentage of Volatile Matter calculated to the inherent moisture basis;

FC = percentage of Fixed Carbon calculated to the inherent moisture basis;

S = percentage of Sulfur calculated to the inherent moisture basis;

A = percentage of Ash calculated to the inherent moisture basis; and

BTU = BTU per pound calculated to the inherent moisture basis.

Inherent moisture basis data

$$= (\text{As Received basis data}) \times \frac{(100 - \text{Inherent moisture})}{(100 - \text{As Received moisture})}$$

VITA

Name: Miss Kunwattoo Rittidate

Date of Birth: 27th. April, 1985

Educational Background:

Name of the University: Chulalongkorn University

Date of attendance: May 2003 -May 2007

Certificate, degree and academic distinction obtained:

Bachelor of Science Program in Geology

Employment: May 2007 - December 2009

Geologist, Akara Minig Limited

January 2010 - present

Geologist, Electricity Generating Authority of

Thailand

Address: 36, Soi 2, Newniwate village, Prachuapsiri road

Amphoe Muang, Prachuapkirikhun province

77000

E-mail: kunwattoo.r@egat.co.th